U.S. DEPARTMENT OF COMMERCE
National Technical Information Service

PB-297 755

Fabric Filter Model Sensitivity Analysis

GCA Corp, Bedford, MA GCA Technology Div

Prepared for

Industrial Environmental Research Lab, Research Triangle Park, NC

Apr 79

PB 297755

United States
Environmental Protection
Agency

Industrial Environmental Research
Laboratory
Research Triangle Park NC 27711

EPA-600/7-79-043c
April 1979

EPA

Fabric Filter Model Sensitivity Analysis

Interagency Energy/Environment R&D Program Report

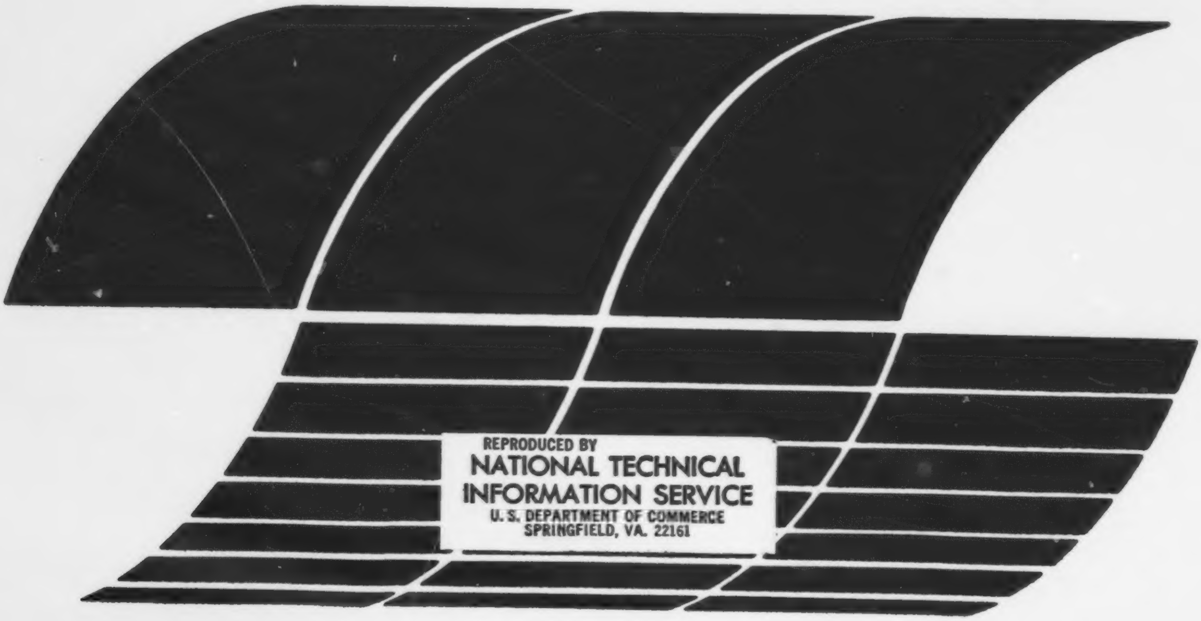

REPRODUCED BY
NATIONAL TECHNICAL
INFORMATION SERVICE
U. S. DEPARTMENT OF COMMERCE
SPRINGFIELD, VA. 22161

RESEARCH REPORTING SERIES

Research reports of the Office of Research and Development, U.S. Environmental Protection Agency, have been grouped into nine series. These nine broad categories were established to facilitate further development and application of environmental technology. Elimination of traditional grouping was consciously planned to foster technology transfer and a maximum interface in related fields. The nine series are:

1. Environmental Health Effects Research
2. Environmental Protection Technology
3. Ecological Research
4. Environmental Monitoring
5. Socioeconomic Environmental Studies
6. Scientific and Technical Assessment Reports (STAR)
7. Interagency Energy-Environment Research and Development
8. "Special" Reports
9. Miscellaneous Reports

This report has been assigned to the INTERAGENCY ENERGY-ENVIRONMENT RESEARCH AND DEVELOPMENT series. Reports in this series result from the effort funded under the 17-agency Federal Energy/Environment Research and Development Program. These studies relate to EPA's mission to protect the public health and welfare from adverse effects of pollutants associated with energy systems. The goal of the Program is to assure the rapid development of domestic energy supplies in an environmentally-compatible manner by providing the necessary environmental data and control technology. Investigations include analyses of the transport of energy-related pollutants and their health and ecological effects; assessments of, and development of, control technologies for energy systems; and integrated assessments of a wide range of energy-related environmental issues.

EPA REVIEW NOTICE

This report has been reviewed by the participating Federal Agencies, and approved for publication. Approval does not signify that the contents necessarily reflect the views and policies of the Government, nor does mention of trade names or commercial products constitute endorsement or recommendation for use.

This document is available to the public through the National Technical Information Service, Springfield, Virginia 22161.

TECHNICAL REPORT DATA
(Please read Instructions on the reverse before completing)

1. REPORT NO.
EPA-600/7-79-043c

2.

3. RECIPIENT'S ACCESSION NO.

4. TITLE AND SUBTITLE
Fabric Filter Model Sensitivity Analysis

5. REPORT DATE
April 1979

6. PERFORMING ORGANIZATION CODE

7. AUTHOR(S)
Richard Dennis, H.A. Klemm, and William Battye

8. PERFORMING ORGANIZATION REPORT NO.
GCA-TR-78-26-G

9. PERFORMING ORGANIZATION NAME AND ADDRESS
GCA/Technology Division
Burlington Road
Bedford, Massachusetts 01730

10. PROGRAM ELEMENT NO.
EHE624

11. CONTRACT/GRANT NO.
68-02-2607, Task 7

12. SPONSORING AGENCY NAME AND ADDRESS
EPA, Office of Research and Development
Industrial Environmental Research Laboratory
Research Triangle Park, NC 27711

13. TYPE OF REPORT AND PERIOD COVERED
Task Final; 6/78 - 2/79

14. SPONSORING AGENCY CODE
EPA/600/13

15. SUPPLEMENTARY NOTES IERL-RTP project officer is James H. Turner, MD-61, 919/541-2925.

16. ABSTRACT
The report gives results of a series of sensitivity tests of a GCA fabric filter model, as a precursor to further laboratory and/or field tests. Preliminary tests had shown good agreement with field data. However, the apparent agreement between predicted and actual values was based on limited comparisons: validation was carried out without regard to optimization of the data inputs selected by the filter users or manufacturers. The sensitivity tests involved introducing into the model several hypothetical data inputs that reflect the expected ranges in the principal filter system variables. Such factors as air/cloth ratio, cleaning frequency, amount of cleaning, specific resistence coefficient K2, the number of compartments, and inlet concentration were examined in various permutations. A key objective of the tests was to determine the variables that require the greatest accuracy in estimation based on their overall impact on model output. For K2 variations, the system resistance and emission properties showed little change; but the cleaning requirement changed drastically. On the other hand, considerable difference in outlet dust concentration was indicated when the degree of fabric cleaning was varied. To make the findings more useful to persons assessing the probable success of proposed or existing filter systems, much of the data output is presented in graphs or charts.

17. KEY WORDS AND DOCUMENT ANALYSIS

a. DESCRIPTORS	b. IDENTIFIERS/OPEN ENDED TERMS	c. COSATI Field/Group
Pollution	Pollution Control	13B
Filtration	Stationary Sources	07D
Fabrics	Fabric Filters	11E
Mathematical Models	Bag Houses	12A
Sensitivity		14B
Analyzing		

18. DISTRIBUTION STATEMENT Unlimited	19. SECURITY CLASS *(This Report)* Unclassified	21. NO. OF PAGES 214
	20. SECURITY CLASS *(This page)* Unclassified	22. PRICE A10 - A01

EPA Form 2220-1 (9-73)

EPA-600/7-79-043c
April 1979

Fabric Filter Model Sensitivity Analysis

by

Richard Dennis, H.A. Klemm, and William Battye

GCA/Technology Division
Burlington Road
Bedford, Massachusetts 01730

Contract No. 68-02-2607
Task No. 7
Program Element No. EHE624

EPA Project Officer: James H. Turner

Industrial Environmental Research Laboratory
Office of Energy, Minerals, and Industry
Research Triangle Park, NC 27711

Prepared for

U.S. ENVIRONMENTAL PROTECTION AGENCY
Office of Research and Development
Washington, DC 20460

i.a

ABSTRACT

Preliminary testing of the GCA filtration model has shown good agreement with field data. However, the apparent agreement between predicted and actual values is based upon limited comparisons and the validation processes were carried out without regard to optimization of the data inputs selected by the filter users or manufactureres. As a precursor activity to further laboratory and/or field tests, a series of sensitivity tests have been performed. The procedure has been to introduce into the model several hypothetical data inputs that reflect the expected ranges in the principal filter system variables. Such factors as air/cloth ratio, cleaning frequency, amount of cleaning, specific resistance coefficient (K_2) number of compartments and inlet concentration were examined in various permutations. A key objective of these tests was to determine which variables would require the greatest accuracy in estimation based upon their overall impact on model output. In the case of K_2 variations, the system resistance and emission properties showed little change but the cleaning requirement was drastically changed. On the other hand, considerable difference in outlet dust concentration was indicated when the degree of fabric cleaning was varied. To make the findings more useful to those persons assessing the probable success of proposed or existing filter systems, much of the data output has been presented in the form of graphs or charts. This procedure enables control personnel, for example, to make rapid decisions as to whether a given filter system can perform according to specifications.

Preceding page blank

CONTENTS

Abstract iii
Figures vi
Tables xi
Acknowledgment xiii

1. Summary 1
2. Introduction 4
   2.1 Program Scope 4
   2.2 Background for Filtration Model 9
   2.3 Dust Penetration With Woven Glass Fabrics 15
   2.4 Model Applications 18
   2.5 Summation 23
3. Critique of Major System Variables, Theory and Practice 26
   3.1 Dust Dislodgement and Adhesion 26
   3.2 Specific Resistance Coefficient 40
   3.3 Effect of Filtration Velocity on K_2 48
4. Sensitivity Analyses 53
   4.1 Preliminary Screening Tests 53
   4.2 Multivariable Sensitivity Tests 62
   4.3 Use of the Sensitivity Test Data 107

References 120

Appendices

A. Equations for Estimating Dust Penetration 122
B. Results of Sensitivity Tests 123
C. Sensitivity Analysis Graphical Presentations for Multivariable Systems 133
D. Derivation of Relationships Between Average System Pressure Drop and System Design Parameters 188

Preceding page blank

FIGURES

Number Page

1 Typical drag versus loading curves for filters with different degrees of cleaning and a maximum allowable level for terminal drag, S_T, and terminal fabric loading, W_T 11

2 Predicted and observed outlet concentrations for bench scale tests. GCA fly ash and Sunbury fabric 16

3 System breakdown for I bags and J areas per bag 19

4 Nucla baghouse simulation, resistance versus time 21

5 Estimated cleaned area fraction, a_c, based upon dust removal by (a) gravity and/or shaking acceleration forces or (b) aerodynamic drag forces caused by reverse air flow. Coal fly ash and twill weaves glass fabrics 28

6 Cleaned bag surface with inside illumination by fluorescent tube 29

7 Schematic, hoop stressing during reverse flow for depressed region, collapsed bag with clean side (external) pressure exceeding dirty side (internal) pressure, $P_c > P_d$ 39

8 Ratio of K_2 values predicted by Happel and Kozeny-Carman equations versus dust cake porosity 42

9 Variations in porosity functions with porosity 46

10 Variation in porosity function with bulk density and discrete particle density 47

11 Drag versus fabric loading curves typifying abrupt cake collapse and gradual cake and/or fabric compression 50

12 K_2 versus velocity for wet ground mica. From Spaite and Walsh . 52

13 Effect of face velocity and limiting pressure drop on average pressure loss 65

14 Effect of face velocity and limiting pressure drop on average pressure loss 66

15 Effect of face velocity and limiting pressure drop on average pressure loss 67

16 Effect of face velocity and limiting pressure drop on average pressure loss 68

17 Effect of face velocity and limiting pressure drop on average pressure loss 69

FIGURES (continued)

Number Page

18 Effect of face velocity and limiting pressure drop on average pressure loss 70

19 Effect of face velocity and limiting pressure drop on average pressure loss 71

20 Effect of face velocity and limiting pressure drop on average penetration 72

21 Effect of face velocity and limiting pressure drop on average penetration 73

22 Effect of face velocity and average pressure drop on average penetration 74

23 Effect of face velocity and limiting pressure drop on average penetration 75

24 Effect of face velocity and limiting pressure drop on average penetration 76

25 Effect of face velocity and limiting pressure drop on average penetration 77

26 Effect of face velocity and limiting pressure drop on average penetration 78

27 Relationship between time between cleaning cycles, limiting pressure loss and face velocity 79

28 Relationship between time between cleaning cycles, limiting pressure loss and face velocity 80

29 Relationship between time between cleaning cycles, limiting pressure loss and face velocity 81

30 Relationship between time between cleaning cycles, limiting pressure loss and face velocity 82

31 Relationship between time between cleaning cycles, limiting pressure loss and face velocity 83

32 Relationship between time between cleaning cycles, limiting pressure loss and face velocity 84

33 Relationship between time between cleaning cycles, limiting pressure loss and face velocity 85

34 Effect of velocity on average pressure loss for timed cleaning cycle system 86

35 Effect of time between cleaning cycles, t_f, on average penetration 93

36 Effect of variations in cleaning intensity on average pressure drop 94

37 Effect of variations on inlet concentration on average pressure drop 95

FIGURES (continued)

Number Page

38 Effect of cleaning intensity on average penetration 96

39 Effect of inlet concentration on average penetration 97

40 Effect of K_2 and C_i on average pressure loss 100

41 Effect of K_2 and C_i on time between cleaning cycles 101

42 Effect of K_2 and C_i on average penetration 102

43 $\overline{P}$ versus a_c and P_L 134

44 $\overline{P}$ versus a_c and P_L 135

45 $\overline{P}$ versus a_c and P_L 136

46 $\overline{P}$ versus a_c and P_L 137

47 $\overline{P}$ versus a_c and P_L 138

48 $\overline{P}$ versus a_c and P_L 139

49 $\overline{P}$ versus a_c and P_L 140

50 $\overline{P}$ versus a_c and P_L 141

51 $\overline{P}$ versus a_c and P_L 142

52 $\overline{P}$ versus a_c and P_L 143

53 $\overline{P}$ versus C_i and P_L 144

54 $\overline{P}$ versus C_i and P_L 145

55 $\overline{P}$ versus C_i and P_L 146

56 $\overline{P}$ versus C_i and P_L 147

57 $\overline{P}$ versus C_i and P_L 148

58 $\overline{P}$ versus C_i and P_L 149

59 $\overline{P}$ versus C_i and P_L 150

60 $\overline{P}$ versus C_i and P_L 151

61 $\overline{P}$ versus C_i and P_L 152

62 $\overline{Pn}$ versus a_c and P_L 153

63 $\overline{Pn}$ versus a_c and P_L 154

64 $\overline{Pn}$ versus a_c and P_L 155

65 $\overline{Pn}$ versus a_c and P_L 156

66 $\overline{Pn}$ versus a_c and P_L 157

67 $\overline{Pn}$ versus a_c and P_L 158

68 $\overline{Pn}$ versus a_c and P_L 159

FIGURES (continued)

Number Page

69 $\overline{Pn}$ versus a_c and P_L 160
70 $\overline{Pn}$ versus a_c and P_L 161
71 $\overline{Pn}$ versus a_c and P_L 162
72 $\overline{Pn}$ versus a_c and P_L 163
73 $\overline{Pn}$ versus a_c and P_L 164
74 $\overline{Pn}$ versus C_i and P_L 165
75 $\overline{Pn}$ versus C_i and P_L 166
76 $\overline{Pn}$ versus C_i and P_L 167
77 $\overline{Pn}$ versus C_i and P_L 168
78 $\overline{Pn}$ versus C_i and P_L 169
79 $\overline{Pn}$ versus C_i and P_L 170
80 $\overline{Pn}$ versus C_i and P_L 171
81 $\overline{Pn}$ versus C_i and P_L 172
82 $\overline{Pn}$ versus C_i and P_L 173
83 t_f versus a_c and P_L 174
84 t_f versus a_c and P_L 175
85 t_f versus a_c and P_L 176
86 t_f versus a_c and P_L 177
87 t_f versus a_c and P_L 178
88 $\overline{Pn}$ versus a_c and P_L 179
89 t_f versus a_c and P_L 180
90 t_f versus C_i and P_L 181
91 t_f versus C_i and P_L 182
92 t_f versus C_i and P_L 183
93 t_f versus C_i and P_L 184
94 t_f versus C_i and P_L 185
95 t_f versus C_i and P_L 186
96 t_f versus C_i and P_L 187
97 Example of pressure-time trace for limiting pressure or time controlled cleaning systems 189
98 Example of pressure-time trace for continuously cleaned systems . 189

FIGURES (continued)

Number Page

99 Estimation of average pressure drop by computer model and simplified equations 194

100 Estimation of average pressure drop by computer model and simplified equations 197

101 Estimation of average pressure drop by computer model and simplified equations 198

TABLES

Number Page

1 Required Data Inputs for Specific Model Application 6

2 Measured and Predicted Performance for Woven Glass Bags with Coal Fly Ash 22

3 Variables Scheduled for Sensitivity Analysis 24

4 Estimates of Maximum Aerodynamic Drag Forces During Reverse Flow Cleaning 34

5 Instantaneous and Final Aerodynamic Drag During Reverse Flow Cleaning, Fly Ash Filtration with Woven Glass Bags 37

6 Predicted and Measured K_2 Values for Various Dust/Fabric Combinations, Size Properties and Operating Parameters 43

7 Input Parameters Selected for Baseline Tests 54

8 Effect of Variations in Input Parameters on System Performance . 56

9 Values of Key Parameters Used in Sensitivity Analyses 63

10 Data Inputs Required for Estimation of the Cleaning Parameters, a_c 109

11 Figure Key for Estimating Major Filter Performance Parameters Average Pressure Loss, $(\overline{P}_L)$, Average Penetration $(\overline{P}_n)$, Time Between Cleanings (t_f) 112

12 Operating Data for Sample Field Problem 115

13 Corrected Input Parameters for Estimating Effect of K_2 Variability on Filter System Performance 117

14 Sensitivity Curve Selections for Estimating Effect of K_2 Variability on Filter System Performance 118

15 Sensitivity Data Summary for Tables 16 through 22 124

16 Predicted System Performance with $a_c = 0.1$ and $C_i = 2.29$ g/m^3 as Fixed Inputs and V_i (m/min) and P_L (N/m^2) as Independent Variables 125

17 Predicted System Performance with $a_c = 0.1$ and $C_i = 6.87$ g/m^3 as Fixed Inputs and V_i (m/min) and P_L (N/m^2) as Independent Variables 126

18 Predicted System Performance with $a_c = 0.1$ and $C_i = 2.29$ g/m^3 as Fixed Inputs and V_i (m/min) and P_L (N/m^2) as Independent Variables 127

TABLES (continued)

Number Page

19 Predicted System Performance with $a_c = 0.4$ and $C_i = 2.29\ g/m^3$ as Fixed Inputs and V_i (m/min) and P_L (N/m^2) as Independent Variables 128

20 Predicted System Performance with $a_c = 0.4$ and $C_i = 6.87\ g/m^3$ as Fixed Inputs and V_i (m/min) and P_L (N/m^2) as Independent Variables 129

21 Predicted System Performance with $a_c = 0.4$ and $C_i = 22.9\ g/m^3$ as Fixed Inputs and V_i (m/min) and P_L (N/m^2) as Independent Variables 130

22 Predicted System Performance with $a_c = 1.0$ and $C_i = 6.87\ g/m^3$ as Fixed Inputs and V_i (m/min) and P_L (N/m^2) as Independent Variables 131

23 Predicted System Performance for Fixed and Variable Data Input Combinations Not Specified in Tables 16 through 22 132

24 Values of Parameters Used to Generate Average Pressure Drop Versus Velocity Curves 196

ACKNOWLEDGMENT

The authors express their most sincere appreciation to Dr. James H. Turner, EPA Project Officer, for his advice, discerning technical reviews and encouragement throughout the present and related modeling studies. We also wish to acknowledge the capable support of Ms. Patrice A. Svetaka in the preparation of the many graphs and tables developed for the sensitivity analyses.

1.0 SUMMARY

Validation procedures for the original GCA filtration model have been based mainly upon comparisons of resistance and emission levels predicted by the model and the actual values measured at two field installations. The data inputs for the model consisted of those parameters describing the collection system operating parameters and certain properties of the dust and gas. In the latter case, data indicating dust adhesion properties, specific resistance coefficient for the dust, and unique relationships (and constants) for a specified dust/fabric combination were determined in the field or laboratory prior to testing the model.

Despite the apparent good agreement between predicted and actual values, the data base for the model was still very limited. Many recognized variables such as the number of individual compartments undergoing sequential cleaning, the time intervals between successive cleaning cycles or the average collector resistance could not be changed during the validation tests. Thus, there was no opportunity to determine what impact the many possible permutations and combinations of such variables might have had on filter performance. Therefore, it is recommended that additional field and laboratory measurements be carried out as soon as practicable to determine what variability must be expected in field behavior or in the filtration properties of commercially available fabrics. As a precursor activity, a sequence of sensitivity analyses were performed that are intended to play a major role in defining the relative importance of many system variables and hence to provide useful guidelines for determining the future direction of both field and laboratory investigations.

An immediate objective, however, was to generate supporting data for an improved fabric filter model under development in a concurrent study.*

The results of model sensitivity testing as presented in a series of working tables and graphs are intended to assist the filtration model user in several decision making processes. First, data inputs supplied by the filter user and/or manufacturer can be screened to determine whether they are compatible with practical field operations. Second, the degree of accuracy (or margin of error) associated with variations in any data input can be estimated beforehand. Third, in the event that an immediate (~ few hours) estimate of a proposed filter system's performance is needed and computer access is delayed by a day, the available sensitivity graphs and tables can provide rough approximations.

In Section 2 of this report, the several mathematical relationships among the variables defining overall filter system performance have been reviewed. In addition, the capabilities of the former and revised models and the unique treatment given fabric cleaning processes and their impact on both particulate emissions and fabric pressure loss are also discussed.

Because of the critical roles played by dust dislodgement and adhesion phenomona, several mechanisms involved in the separation of dust from woven fabric were examined, Section 3, to determine their relative contributions. It appeared that the magnitude of reverse flow velocities had minor impact on fabric cleaning insofar as aerodynamic drag effects or hoop stresses were concerned. Modifications in the computation of the specific resistance coefficient for the dust, K_2, were also introduced by using a flow field concept developed for higher porosity dust cakes; i.e., > 0.70.

---

*Dennis, R. and H. A. Klemm. Fabric Filter Model, Format Change. Vol. I Detailed Technical Report, Vol. II User's Guide. U.S. Environmental Protection Agency, Industrial Environmental Research Laboratory, Research Triangle Park, North Carolina. EPA-600/7-79-043a, EPA-600/7-79-043b. February 1979.

The basic procedure for conducting the sensitivity tests described in Section 4 was to first assume a set of input parameters satisfying the criteria for proper filter model operation. Then the specific impact of different data input combinations on performance (particulate emission rates and pressure loss were noted for systems in which key variables were varied singly or in pairs. Key parameters involved in these computer simulations were air-to-cloth ratio, limiting pressure drop, inlet dust concentration, fabric cleaning parameter, number of compartments, time increment for iterations, compartment cleaning time and reverse flow velocity. To keep the number of tests within practical boundaries, provision was made for interpolations in many of the model systems.

Because of the large number of graphs and tables involved, a special key or index has been prepared so that premodeling assessments of estimated filter system performance can be made. Given a fixed set of input parameters along with the condition that one variable may undergo considerable change; e.g., filtration velocity, one can select the family of curves most closely bracketing the input parameters and by appropriate interpolation (or extrapolation) make rough estimates of system performance.

2.0 INTRODUCTION

2.1 PROGRAM SCOPE

GCA/Technology Division has developed a mathematical model to describe the performance of woven glass fabrics used for the filtration of fly ash from coal burning combustion facilities.[1-4] Because of the limited number of such filter systems now used at major power plants, the preliminary validation of modeling concepts was necessarily confined to a few systems. Therefore, the Environmental Protection Agency requested that the model be tested under many simulated field conditions to better assess its capabilities and, in particular, to determine the overall strengths and weaknesses of the existing model structure and methods of application.

The program discussed in this report describes the results of sensitivity analyses whose major role has been to ascertain which variables have the greatest impact upon model performance, and as a corollary, what degree of precision and accuracy should be expected with presently available data and/or field measurements. A given sensitivity test involves no more than allowing a specified system variable to range within fixed percentiles of its estimated average value when functioning as a basic data input to the model.

In Section 4, the results of the sensitivity tests are presented in both graphical and tabular form. The model user is instructed as to how these data can be used to assist him in assessing the importance of certain data inputs to the model and the degree of confidence to be placed in the model output.

Supporting data to acquaint the reader with the basic operation of the model and the unique relationships among the many variables entering into the model are described in the following paragraphs. Typical field situations are discussed where sensitivity analyses are expected to aid in the modelling process.

At this time, the role of most variables constituting an input to the fabric filter model can be identified with respect to how they affect the performance of a single filter element; i.e., any part of the fabric surface for which the approaching dust concentration, local drag, filtration velocity and surface loading can be defined at a specified time.

These relationships, however, become very complex when the performance of several filter elements operating in parallel and sequentially cleaned is to be estimated. Although one can infer correctly that a higher K_2 value will lead to increased filter resistance unless the fabric is cleaned more frequently, the precise effect of variations in K_2 (the specific resistance coefficient for the dust) can only be tested in the model. The same may be said with respect to filtration velocity, number of compartments, duration and frequency of cleaning, the adhesive characteristics of the dust, and other numerous system variables.

Therefore, the insertion of several representative sets of trial data into the model provides a very practical and inexpensive way (a) to determine which variables exert the controlling influence and (b) to establish permissible ranges for input data estimates. The required data inputs for a specific model application are listed in Table 1.

TABLE 1. REQUIRED DATA INPUTS FOR SPECIFIC MODEL APPLICATION[*]

Item	Variable	Description	Comments
1	Number of compartments	6	System design parameter
2	Complete cleaning cycle	24 minutes	Time to sequentially clean six compartments
3	Cleaning time per compartment	4 minutes	Indicates total compartment off-line time
4	Minimum time increment for iterative computations[†]	2 minutes	Provides data points for maximum, minimum and average resistance and penetration during off-line period for on-line compartments
5	Average face velocity (V)	0.824 m/min	Based on total flow and total fabric area
6	Reverse flow velocity (V_R)	0.0415 m/min	Weighted average velocity over total (4 min) cleaning interval
7	Inlet dust concentration (C_i)	2.6 g/m^3	
8	Temperature	$412^{o}K$	Average baghouse temperature
9	Effective (clean) fabric drag (S_E)	434 $N \cdot min/m^3$	Based on linear extrapolation of drag versus fabric loading measurements with uniform dust deposit
10	Specific resistance coefficient (K_2)	0.76 $N \cdot min/g \cdot m$	Value determined at 0.61 m/min and $25^{o}C$
11	Residual dust loading (W_R)	50 g/m^2	Refers to surface loading on freshly cleaned area only
12	Maximum allowable pressure P_L	1160 N/m^2	Fabric pressure loss at which cleaning cycle is to be actuated
13	Cleaned fabric area fraction (a_c)[†]	0.375	Fraction of cleaned surface exposed when cleaning is initiated with a fabric loading corresponding to a resistance of 1160 N/m^2

---

[*] Modeling of actual field performance of stoker-fired boilers at Nucla, Colorado, Colorado UTE Electric Association.[1,6]

[†] Items 4 and 13 computed outside the program to provide necessary data inputs. This procedure used for original model (Reference 1) and also for sensitivity tests described in this report.

The sensitivity testing should make the model more versatile as well as simplifying its use. From the point of view of state or federal control personnel, the model should allow them to use the relevant system, fabric and dust parameters to determine whether the filter system will provide acceptable emissions at a resistance level within the working range of the induced or forced draft fans or any supplemental gas moving capability.

If experienced filter design personnel are using the model, a detailed series of sensitivity tests should enable the selection of operating and cleaning parameters that afford the best compromise between allowable emission levels and overall power requirements.

As stated previously, preliminary validations of the GCA filtration model were based mainly upon comparisons of resistance and emission levels predicted by the model and the actual values measured at two field installations. The data inputs for the model consisted of those parameters describing the collection system operating parameters and certain properties of the dust and gas. In the latter case, data indicating dust adhesion properties, specific resistance coefficient for the dust, and unique relationships (and constants) for a specified dust/fabric combination were determined in the field or laboratory prior to testing the model.

Two important items were considered in developing the present program; first, despite the apparent good agreement between predicted and actual values for the Nucla, Colorado and Sunbury, Pennsylvania, filter installations, the data bases for the model were still very limited. Second, the validation process operates upon the specified input parameters without regard to whether they represent optimum selections. For example, the number of individual compartments undergoing sequential cleaning, the time intervals between successive cleaning cycles or the average collector resistance as specified by the user or manufacturer may not have been optimum choices. Similarly, by restricting average face velocities to less than 0.92 m/min it is usually assumed by the designer that overall average system emissions will not exceed permissible levels.

With respect to the first item, it is strongly recommended that additional field and laboratory measurements be carried out as soon as practicable to determine what variability must be expected in field behavior or in the filtration properties of commercially available fabrics. The sensitivity testing described in this report represents a logical precursor activity to any formal laboratory or field experimentation for improving the model in that many critical areas for future study can be readily identified.

If the input parameters for the filtration system are to be selected for optimum performance in terms of minimum power requirements alone (excluding emission values), Table 1, item 2, increased or more intense cleaning is suggested as a solution provided that some estimate of bag service life versus replacement cost is available. However, if strict adherence to emission levels is to be maintained, the impact of overcleaning on total emissions must be ascertained. Here two possibilities may be examined as possible controlling factors; the frequency and/or intensity of cleaning and the number of separate compartments constituting the complete collection system.

Generally, increasing the number of compartments will reduce the range between maximum and minimum effluent concentrations and, in many cases, reduce the average effluent concentration. A similar reduction in the range between maximum and minimum operating pressures will also take place.

If the size and capital cost of fabric filters is reduced by increasing the face velocity, one must ascertain whether the resultant increases in operating costs due to higher resistance and more frequent fabric replacement may override the capital cost advantage. Even when increased air-to-cloth ratios appear to indicate an overall cost reduction, it is important to note that effluent concentrations are strongly dependent on face velocity, increasing approximately as the 2.2 power of velocity.

2.2 BACKGROUND FOR FILTRATION MODEL

2.2.1 Capabilities

The model that has been subjected to sensitivity testing is intended for use with coal fly ash/glass fabric systems or with other dusts and fabrics possessing similar physical properties. Within the above framework, the model provides the following capabilities:

- The model is adaptable to constant flow conditions.
- The model can describe equally well a continuous or intermittent cleaning regimen.
- The present model can be used either with collapse and reverse flow systems or mechanical shaking systems, but not in combination. It is not intended for use with pulse jet or high velocity reverse jet cleaning systems.
- The model can be used equally well with pressure or time-controlled cleaning.
- The model provides estimates of average and point values of filter resistance for the selected set of operating conditions.
- The model provides estimates of average and point values for penetration and mass effluent concentration for the selected set of operating conditions.

It is emphasized that in conjunction with the sensitivity analyses discussed in this report, a separate study was conducted whose objective was to simplify the original model by performing supplementary calculations and data checking routines within the program.[7]

2.2.2 Filter Drag Relationship

In this section, we have outlined briefly the basic structure and development of the original GCA model and its preliminary trial runs. A very detailed description of all aspects of the model is given in a recent EPA report[1] while various aspects of its design and applications appear in the open literature.[2] The central building block for the model is the classical filter drag-fabric loading relationship that has been discussed extensively in the literature.[8]

The equation:

$$S = S_E + K_2 W \tag{1}$$

in which S is the total filter drag, S_E the effective residual drag, K_2 the specific resistance coefficient for the dust, and W the fabric dust loading in mass per unit area describes the drag for any element of the filter for which the dust loading is uniformly distributed and the local filtration velocity is known.

Deposition of a uniformly distributed dust layer at a constant rate upon an unused or completely cleaned fabric produces the characteristic relationship shown in Curve 1, Figure 1. The origin for the curved section of Curve 1 depicts the true residual drag, S_R, at the minimal residual loading, W_R, which, for a cleaned glass fabric is approximately 50 grams/m^2.

The effective residual drag, S_E, which appears in Equation (1) is usually employed to estimate filter drag or resistance properties. It is determined by the linear extrapolation of Curve 1 to the zero fabric loading level, Figure 1.

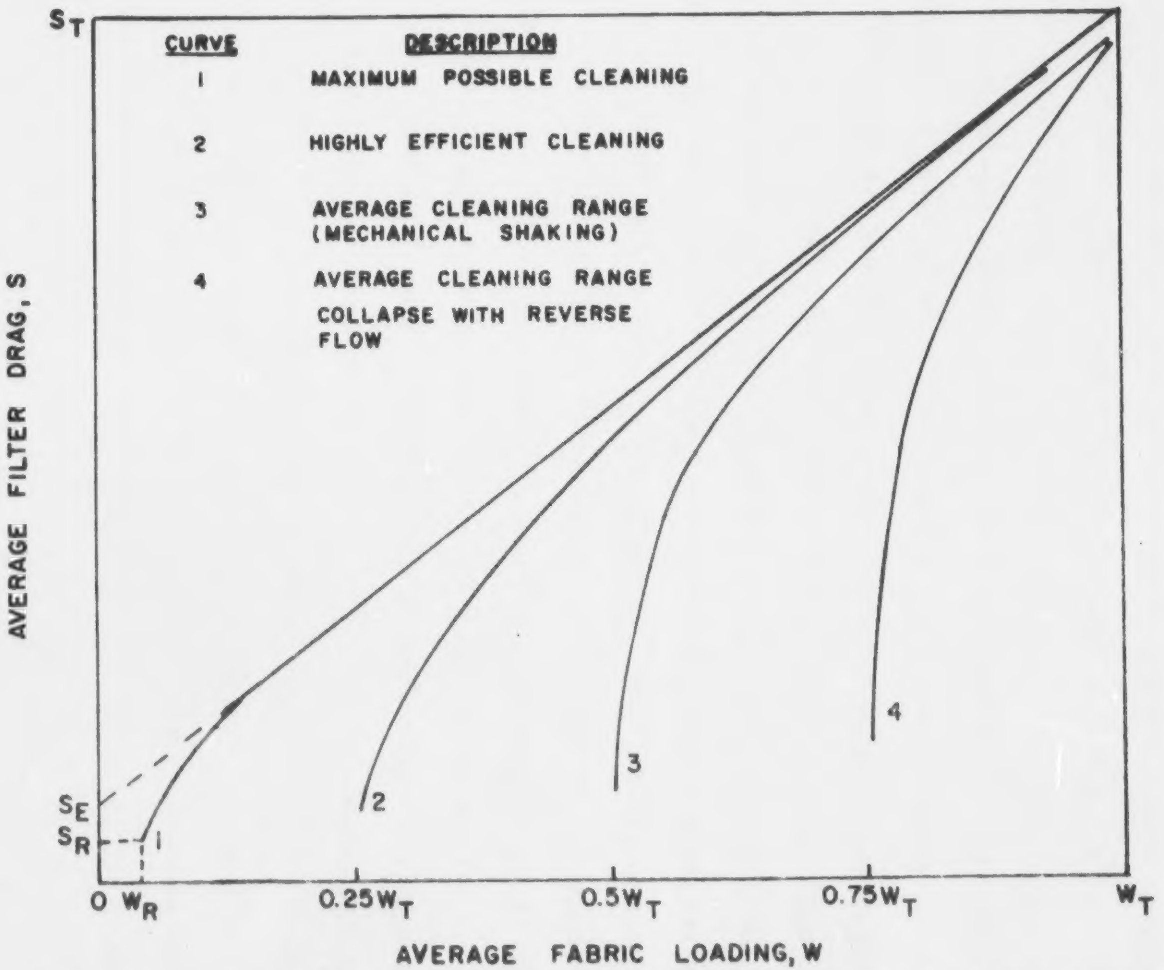

Figure 1. Typical drag versus loading curves for filters with different degrees of cleaning and a maximum allowable level for terminal drag, S_T, and terminal fabric loading, W_T.

The slope of Curve 1; i.e., $K_2 = (S-S_E)/W$, defines correctly the K_2 value for the dust at the specified gas velocity and viscosity provided that the dust is distributed uniformly over the filtration surface. In practice, however, typical drag curves for steady-state field operation usually assume the form of Curves 2 through 4 because (a) most fabric cleaning seldom reduces the average filter loading by more than 50 percent and often as little as 10 percent and (b) dust is dislodged as slabs or flakes with the separation taking place at the interface between the dust layer and the fabric surface. As a result, *unequal* and *changing* flows take place through cleaned and uncleaned regions so that a true K_2 value cannot be determined directly.[2]

The reason for this form of dust detachment is that there are far fewer adhesive bonds between the dust surface and fabric yarns than there are cohesive bonds within the dust cake itself. The result of this bonding phenomenon, which applies to the filters cleaned by reverse flow and/or mechanical shaking, is that a *cleaned* fabric surface is always characterized by at least two regions: (a) the actual cleaned area for which residual drag and dust holdings are uniquely defined and (b) the uncleaned region from which no dust is removed. Resumption of filtration upon filter surfaces such as described above leads to the various curve forms shown in Figure 1.

The form of these curves is governed by several parallel flow paths in which the approaching gas stream is apportioned according to the local drag values at any specified time for *cleaned* and *uncleaned* surfaces:

$$S = \left[\sum_{i=1}^{n} \frac{a_c}{S_c} + \frac{a_{u_1}}{S_{u_1}} \cdots \frac{a_{u_i}}{S_{u_i}} \right]^{-1} A \qquad (2)$$

In Equation (2), S and A refer to overall drag and filter area, respectively, a indicates any area fraction on the filter surface, i designates the i^{th} fractional area and its associated properties, n is the total number of filter areas making up the whole surface, and the subscripts c and u refer to the cleaned and uncleaned filter areas, respectively.

The resultant pressure losses, P, at time $t + \Delta t$, for cleaned and uncleaned filter surfaces are equal and expressable by the following relationship:

$$P_{t + \Delta t} = (S_E V)_{t + \Delta t} + (K_2 \ V \ W)_{t + \Delta t} \qquad (3)$$

Equations (2) and (3) are the building blocks for the iteration process from which local and average drag and resistance may be estimated for any time and/or average filter dust loading during a filtration cycle. Two important variables must be defined, however, before undertaking the computer modeling, the cleaning parameter, a_c and the K_2 value.

2.2.3 Fraction of Filter Surface Cleaned (a_c)

In the case of filter cleaning by bag collapse and reverse flow, the amount of dust removed (expressed as fraction of the filter surface cleaned) was related to the fabric dust loading immediately before cleaning (W_p) by the empirical equation:

$$a_c = 1.51 \times 10^{-8} \ W_p^{2.52} \qquad (4)$$

in which W_p is expressed in grams/m^2. The term W_p has the special significance of identifying the fabric loading associated with the fabric pressure loss just before initiating the cleaning action.

In the original modeling study,[1] it was postulated that the gravity field or artificially generated acceleration of the dust loading on the fabric surface produced tensile or shearing forces that constituted the principal mechanism for dust dislodgement. When the magnitude of these forces exceeded the local adhesion forces, it was expected that the cake would detach at the dust/fabric interface. The net force in a gravity field is defined by Wg whereas in a mechanically shaken system the force becomes $W\bar{a}$. In the latter case, $\bar{a}$ is the acceleration of the dust and fabric produced by an essentially horizontal motion of the driving shaker arms that can be calculated as:

$$\bar{a} = 29.6f^2 \ A \ (\text{cm/sec}^2) \qquad (5)$$

In Equation (5), f refers to the shaking frequency (sec^{-1}) and A to the shaker arm amplitude (half stroke) in centimeters.

During the present study, further investigation was made of the factors involved in estimating how much cleaning is achieved.

2.2.4 Specific Resi[illegible] Coefficient (K_2)

The parameter K_2 has been shown to increase with the velocity of dust deposition, presumably due to increased dust layer compaction and hence lower cake porosity.[1,8,9] For fly ash/glass fabric systems considered in the original modeling study, K_2 was adequately defined by the Equation:

$$K_2 = 1.8V^{\frac{1}{2}} \ (\text{N-min/g-m}) \qquad (6)$$

with V expressed in m/min. For broader applications, the general functional form is applicable when it is desired to compute K_2 for a different face velocity and gas temperature (gas viscosity); i.e.,

$$K_2 = \left(\frac{V \text{ actual}}{V \text{ measured}}\right)^{\frac{1}{2}} \left(\frac{\mu \text{ actual}}{\mu \text{ measured}}\right) \qquad (7)$$

These relationships appeared satisfactory over the velocity range 0.3 to 1.5 m/min. The effect of velocity on K_2 was also given further treatment in the present study, along with a reappraisal of the possible merit of various theoretical procedures for calculating K_2 from fundamental measurements.

2.3 DUST PENETRATION WITH WOVEN GLASS FABRICS

Laboratory and field measurements coupled with an analysis of the filtration process with twill-weave glass fabrics indicate that fly ash emissions are due mainly to excessive gas flow through the low resistance paths presented by unblocked pores, pinholes or damaged filter areas.

Furthermore, because few particles are removed from the gas fraction passing through the pores (nearly 100 percent penetration for diameters $< 15\ \mu m$), the size distributions are nearly the same for upstream and downstream aerosols provided that size properties are measured in the immediate vicinity of the dirty and cleaned filter faces.

The above findings suggest that mass emissions from glass fabrics should depend upon both inlet concentration, C_i and the unblocked pore area. The latter variable, which is governed by the amount of dust deposited on the filter following resumption of filtration, may cease to be important once a substantial dust layer has reaccumulated. In the absence of visible defects, the relationships between outlet concentration, C_o, and fabric dust loading and velocity appear as shown in Figure 2. The latter effect suggests strongly that seeking to reduce collector size by increasing the face velocity (air-to-cloth ratio) may lead to unacceptably high emission levels.

Another contributor to outlet loading is the low level, steady state, slough-off agglomerated dust from the downstream region of the dust deposit as the result of reentrainment augmented by mechanical vibrations. A safe estimate of this residual concentration (C_R) places it as not greater than a 0.5 mg/m^3 contributor to the outlet concentration.

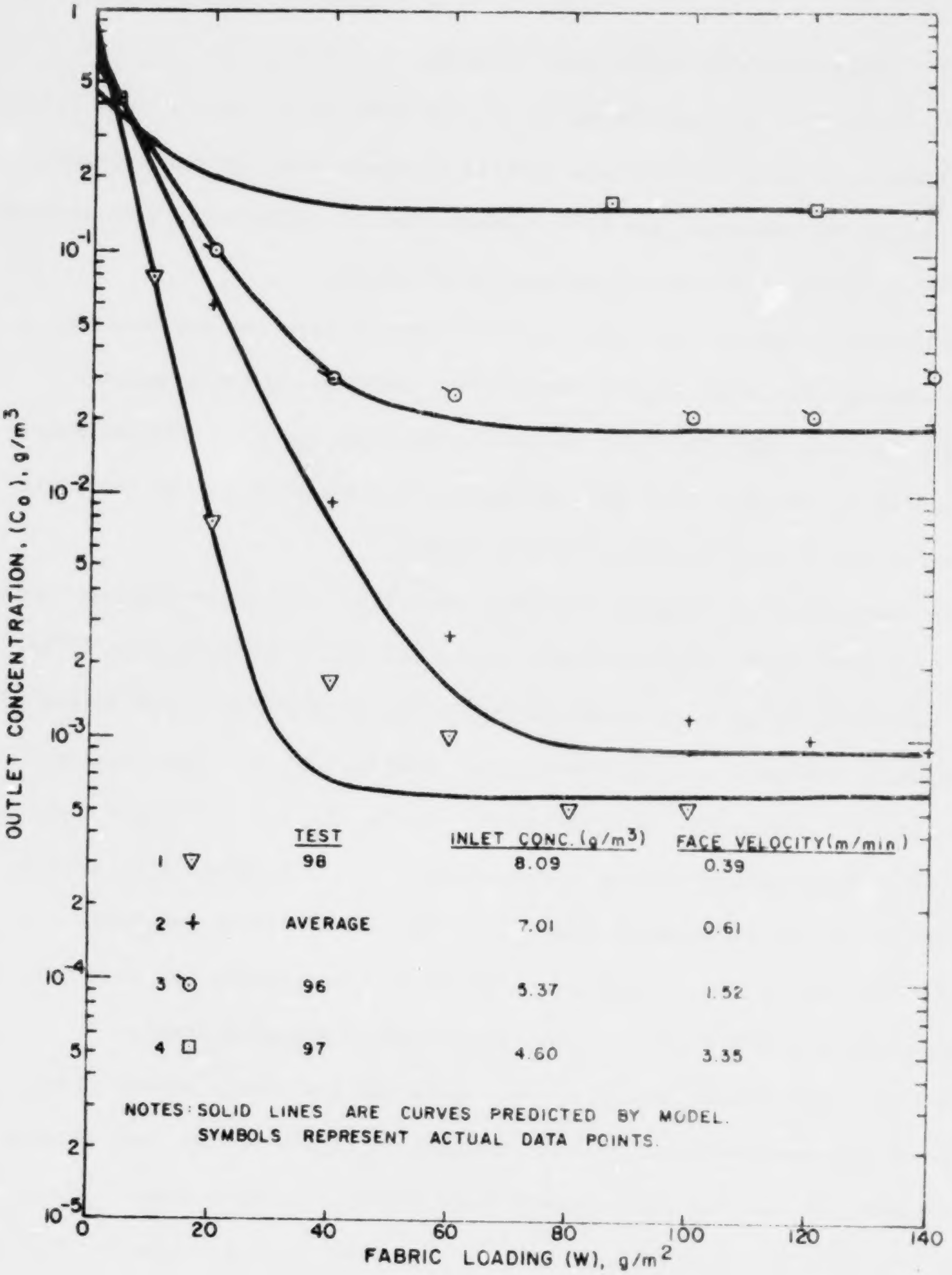

	TEST	INLET CONC. (g/m^3)	FACE VELOCITY (m/min)
1 ▽	98	8.09	0.39
2 +	AVERAGE	7.01	0.61
3 ⊙	96	5.37	1.52
4 □	97	4.60	3.35

NOTES: SOLID LINES ARE CURVES PREDICTED BY MODEL.
SYMBOLS REPRESENT ACTUAL DATA POINTS.

Figure 2. Predicted and observed outlet concentrations for bench scale tests. GCA fly ash and Sunbury fabric.[1]

The curves shown in Figure 2 represent the best mathematical fits to the experimental data. The outlet concentration, C_o, is defined by the local penetration level (Pn), the inlet dust concentration (C_i), and the previously cited residual concentration, $C_R = 0.5\ mg/m^3$:

$$C_o = Pn\ C_i + C_R \qquad (8)$$

The actual equations and their applications in the filtration model are given in Appendix A. For present purposes, it suffices to indicate that substitution of the necessary relationships into the general expression:

$$Pn \text{ or } C_o = f\ (\phi,\ C_i\ W,\ V,\ C_R) \qquad (9)$$

determines penetration or effluent concentration as a function of ϕ, a parameter characterizing the dust/fabric combination of interest; constant inlet and residual concentrations, C_i and C_R, respectively; and the time and position dependent variables; i.e., local face velocity, V, and local fabric dust loading, W. It is again emphasized that because direct leakage is responsible for nearly all of the particulate emissions, the size properties of typical coal fly ashes* do not enter directly into the estimation of dust penetration.

The total (and average) filter system penetration, Pn, at some time, t, for a system consisting of I compartments and J areal subdivisions per bag is determined by successive iterations in accordance with the general summation:

$$Pn_t = V_t\ I\ J \sum_{i=i}^{I} \sum_{j=1}^{J} Pn_{ij_t}\ V_{ij_t} \qquad (10)$$

---

*Coal fly ash MMD = 5 to 20 μm, σg = 2.5 to 3.5 depending upon the firing method.

2.4 MODEL APPLICATIONS

The basic operations performed within the filtration model are indicated schematically in Figure 3. The approaching aerosol is distributed among I separate compartments and J separate filtration regions on each bag. It is assumed for simplification that the performance of each compartment is represented by any single bag within the compartment and that there are no concentration gradients for C_i and W in the system. The model describes the overall effect of many parallel flow paths through fabric surface elements bearing different dust loadings. The local performance of each element is defined by the working equations presented earlier in this paper.

The data inputs required to model the Nucla filtration process have been given in Table 1. The actual numerical values for the filter system[6] have been listed in the "Description" column to show the approximate magnitude for these variables in field applications.

Items 1 through 3 are based upon system design or operating data provided by the manufacturer. The 2-minute minimal time interval, Item 4, was chosen by the model user so that successive, stepwise iterations would always indicate maximum, minimum, and average system resistance while any one compartment was off-line for cleaning.

Average face and average reverse flow velocities, Items 5 and 6, respectively, are operating parameters usually chosen by the filter manufacturer.

Inlet dust concentration and average filtration temperature, Items 6 and 7, are determined mainly by the combustion process and the type of fuel. The estimates of S_O, K_2 and W_R, Items 9 through 11, respectively, are best determined by direct measurement if not already defined.

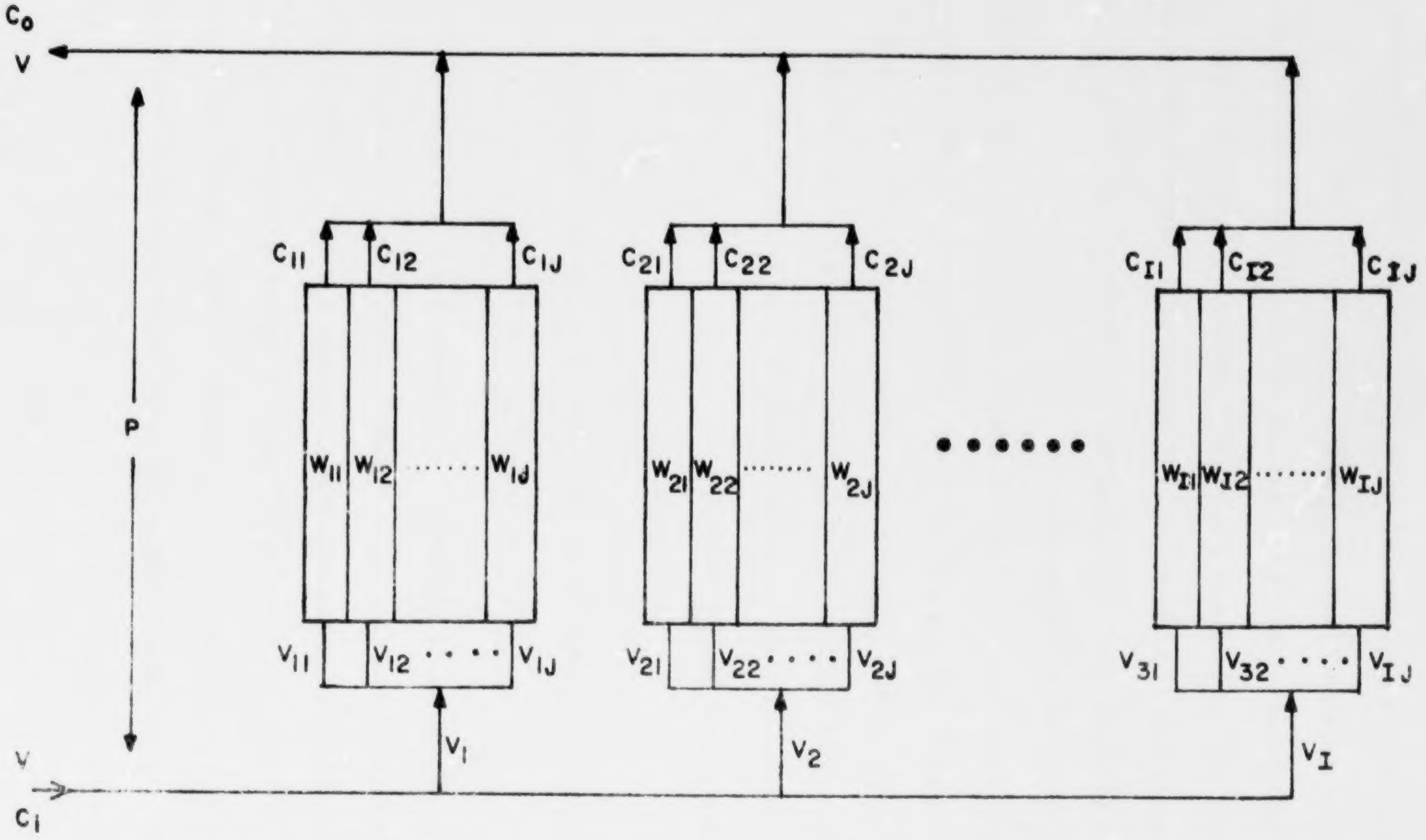
C_o
V
P
C_{11}
C_{12}
C_{1J}
W_{11}
W_{12}
W_{1J}
V_{11}
V_{12}
V_{1J}
V_1
C_{21}
C_{22}
C_{2J}
W_{21}
W_{22}
W_{2J}
V_{21}
V_{22}
V_{2J}
V_2
C_{I1}
C_{I2}
C_{IJ}
W_{I1}
W_{I2}
W_{IJ}
V_{31}
V_{32}
V_{IJ}
V_I
V
C_i

Figure 3. System breakdown for I bags and J areas per bag.

From the perspective of the model user, the only data inputs involving decision-making (or supplementary calculations) are Items 4 and 13.

Item 4 is easily satisfied; i.e., data points for maximum, minimum and average resistance and penetration for on-line compartments during fabric cleaning, if the minimum time increment for output data points is half that specified as the cleaning time per compartment. However, Item 4 will be estimated by the program in the new model.

In the case of Item 13, the original model required an outside calculation although it is planned that the revised model will incorporate the computation of a_c within the model. The original process required that the uniformly distributed fabric dust holding, W_p, corresponding to the assigned pressure threshold at which cleaning is to be initiated (Column 12) be computed from Items 5, 9, 10 and 12 as indicated below:

$$W_p = (P_L/V - S_E)K_2 \qquad (11)$$

Then by means of Equation (2-8) the value of a_c can be determined:

$$a_c = 1.51 \times 10^{-8} W_p^{2.52} \qquad (12)$$

In the case of the Nucla operation, the availability of performance data allowed a preliminary evaluation of the model's capability. The superposition of predicted and observed system resistance curves, Figure 4, shows fairly good agreement although the model does predict a somewhat larger interval, 164 versus 126 minutes, between cleaning cycles. Table 2 shows that average emissions during the cleaning cycles were about eight times those observed when all Nucla compartments were on-line.

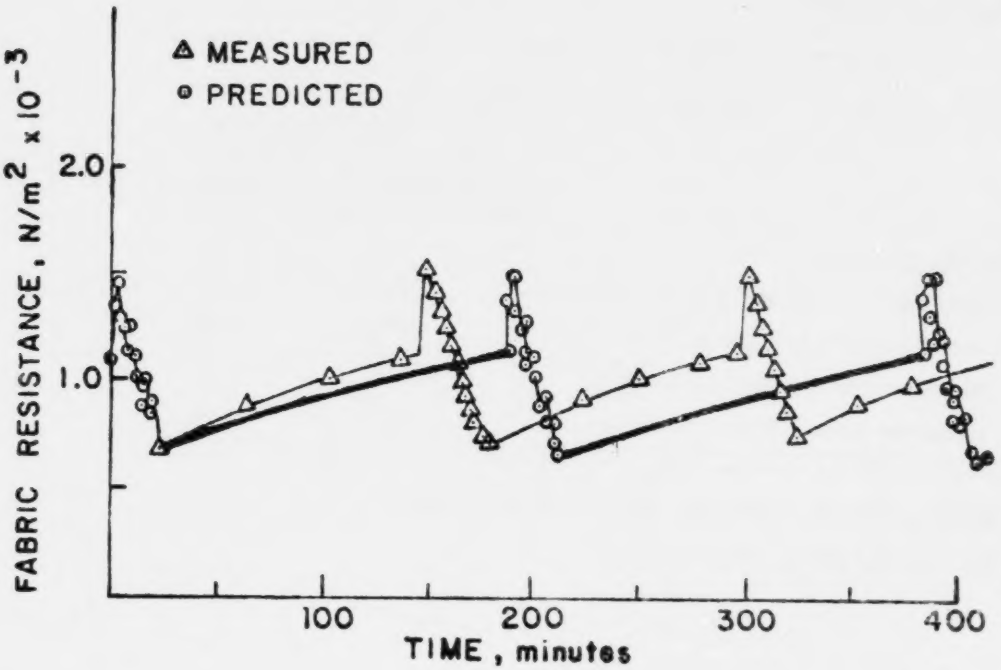

Figure 4. Nucla baghouse simulation, resistance versus time.

TABLE 2. **MEASURED AND PREDICTED PERFORMANCE FOR WOVEN GLASS BAGS WITH COAL FLY ASH**

	Percent penetration	
	Measured*	Predicted*
Nucla, Colorado[6]	0.21	0.19 (1.52)†

	Resistance--N/m^2	
	Measured	Predicted
Nucla, Colorado[6]		
Average, cleaning and filtering	1030	972
During cleaning only	1700	1520
Maximum just before cleaning	1160	1160
Minimum just after cleaning	850	760

*Averaged over cleaning and filtering cycles.

†During cleaning cycle only.

2.5 SUMMATION

The preceding discussions have provided the relevant background on the basic structure of the original filtration model and its intended application. In the program results discussed in this report, a primary objective was to establish an approximate ordering of what are considered to be the principal variables in the filtration modeling process. The most important variables are those for which a fixed error in estimation produces the greatest deviation in the estimate of key output parameters such as dust penetration and filter resistance.

A second objective was to ascertain whether the physical processes originally presumed to describe filtration and fabric cleaning phenomena are consistent with experimental findings and if not, how to better define the filtration process.

A third objective was to reexamine certain parameters to determine which might be evaluated from fundamental measurements, for example K_2, and what degree of accuracy (or error) might result if these parameters were calculated rather than measured directly.

Table 3 provides a tentative listing without regard to priority of those variables to be studied in the sensitivity analyses along with an indication of their expected impact areas. Although not stated explicitly in Table 3, it is presumed that those variables that influence the cleaning frequency may also affect the intensity of cleaning where the latter item appears as an option; e.g., mechanical shaking with shaking frequency and amplitude as the intensity factors.

It was planned that the description, method of calculation and/or method of measurement of the varibles entering into the sensitivity analyses would

TABLE 3. VARIABLES SCHEDULED FOR SENSITIVITY ANALYSIS

Variable	Expected impact areas
1. Filtration Velocity	Emission levels Cleaning frequency
2. Cleaning intensity and frequency	Emission levels Resistance
3. Adhesion, dust cake	Cleaned area fraction, a_c Emission level Resistance
4. Specific Resistance coefficient (K_2)	Cleaning frequency Emission level
5. Number of compartments	Emission level Resistance range
6. Length of filtration cycle	Emission level Resistance
7. Linear versus non-linear model	Emission level Resistance
8. Rear face slough off	Emission level
9. Inlet concentration	Emission level Cleaning frequency
10. To be identified (if appropriate)	

be examined on an individual basis prior to assessing their roles in the fabric filtration model. This step was intended to provide a rough estimate of the trial ranges for system variables when tested in the model. The first section of this report deals specifically with variables that are either difficult to measure or perhaps are only partial descriptors of the true physical processes taking place during filtration or fabric cleaning.

3.0 CRITIQUE OF MAJOR SYSTEM VARIABLES, THEORY AND PRACTICE

3.1 DUST DISLODGEMENT AND ADHESION

3.1.1 Concepts Used in the Original Model

No practical forecast of filter system performance can be made until the relationship between the method of fabric cleaning (which includes type, frequency, and intensity) and the amount and location of dust removal has been established. It was clearly demonstrated in recent studies[1,10] that the dust dislodgement process for woven glass fabrics cleaned either by mechanical shaking or bag collapse with reverse air flow consisted of the detachment of dust slabs or flakes with the separation occurring at the dust/fabric interface. Furthermore, the cleaned fabric regions immediately below the dislodged layers were shown to display nearly constant residual dust holdings and resistance properties for many dust/fabric combinations.

Since the fabric loading and resistance properties are readily determinable for both cleaned and uncleaned regions of a fabric, it is only required that the fraction of cleaned area be known in order to compute the overall filter performance. The above approach has been discussed in detail in prior reports and in the open literature.[1,2] At present, no reliable theoretical approaches are available to determine how much cleaned fabric area, a_c, is exposed for various cleaning conditions with any dust/fabric combination. Limited, semi-empirical solutions to this problem have been described which have proven effective for various fly ashes and woven glass fabrics.[*] The empirical formulas:

$$a_c = 1.51 \times 10^{-8} W^{2.52} \tag{13}$$

and

$$a_c = 2.33 \times 10^{-8} (f^2 AW)^{2.52} \tag{14}$$

deriving from Figure 5 appeared to provide reasonable estimates of a_c in terms of the average fabric loading, W, just before cleaning for a collapse and reverse flow system, Equation (13), and a mechanically shaken system, Equation (14). In the latter instance, the terms f and A, respectively, refer to the frequency and amplitude (half stroke) of the shaking action.

Although dust separation from a fabric surface can be explained rationally by several comparatively simple physical processes, more experimentation is required to develop highly accurate cleaning descriptors. In prior reports, it was indicated that a dust layer should detach from the fabric surface when the tensile force exerted at the dust cake fabric interface exceeds the adhesive force bonding the dust layer to the fabric. Because there are fewer contacts between particles and fibers at the dust cake fabric interface than there are particle-to-particle contacts within the cake per se, the interface region with the weaker bonding constitutes the boundary for dust layer separation. A graphic image of this separation phenomenon is shown in Figure 6, where an interior light source within a real filter bag reveals the sharp line of demarcation between the cleaned and uncleaned zones.

---

[*] 3/1 twill weave, 9.2 oz/yd^2, Teflon coating - Menardi Southern
3/1 twill weave, 10.5 oz/yd^2, graphite-silicone coating - W. W. Criswell.

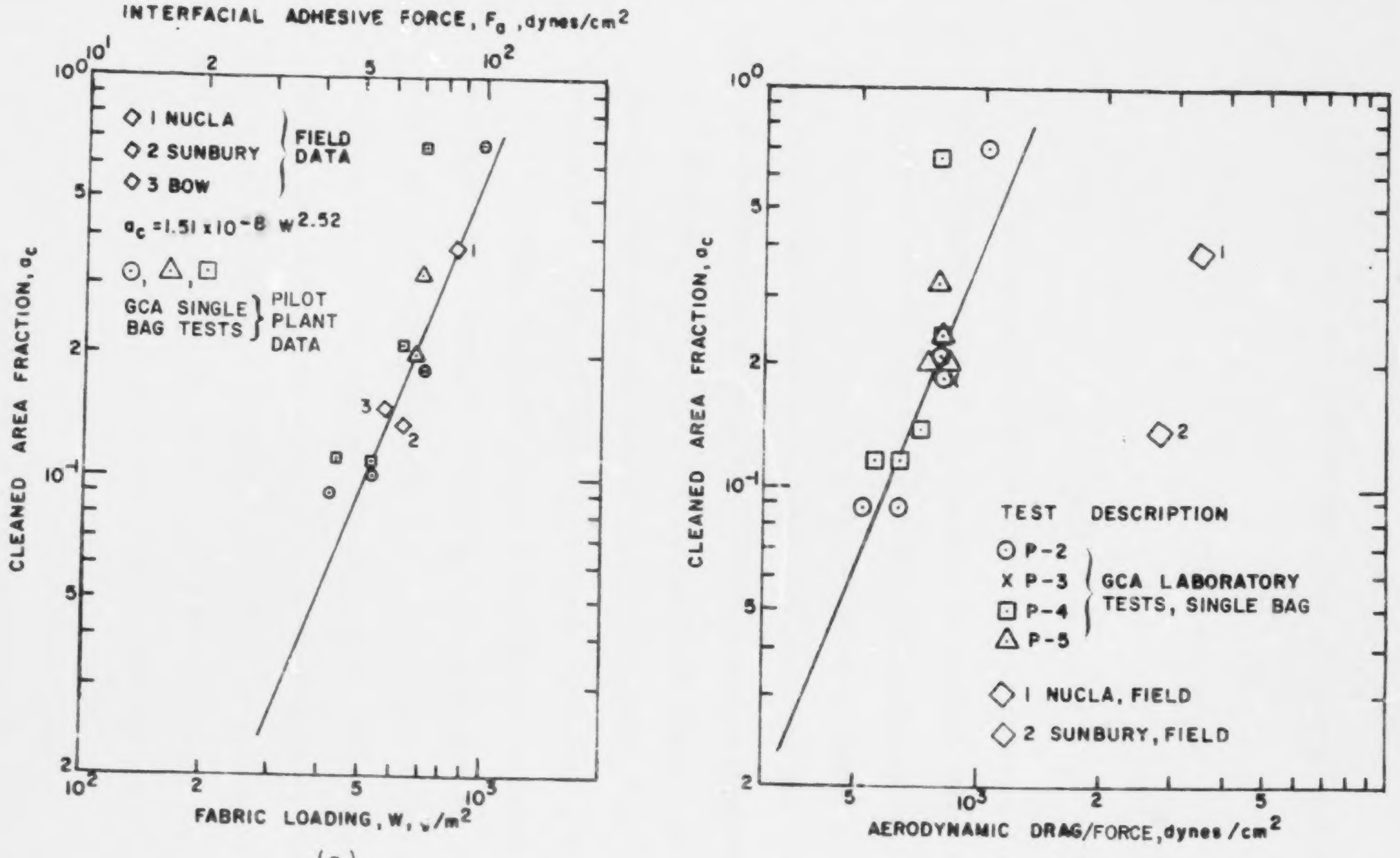

(a)

(b)

Figure 5. Estimated cleaned area fraction, a_c, based upon dust removal by (a) gravity and/or shaking acceleration forces or (b) aerodynamic drag forces caused by reverse air flow. Coal fly ash and twill weaves glass fabrics.

Reproduced from
best available copy.

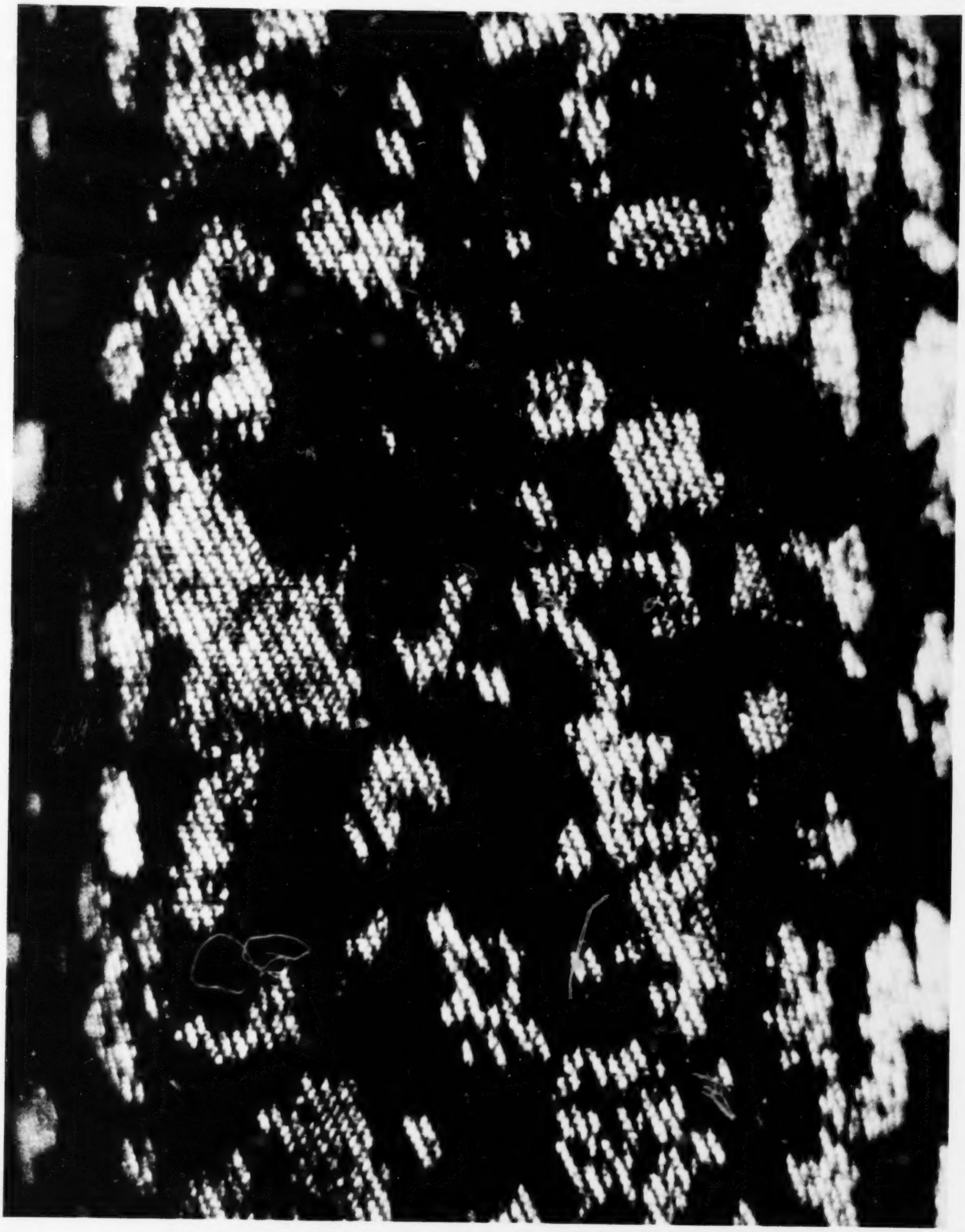

Figure 6. Cleaned bag surface with inside illumination by fluorescent tube.

Preliminary estimates of the intracake cohesive forces were determined from the relationship:

$$F_a = 10^2 d_p \text{ (dynes)} \qquad (15)$$

where d_p is the particle diameter in centimeters. For a monodisperse system of 10 μm particles, use of Equation (15) predicts a cohesive or tensile strength of 10^5 dynes/cm^2. If one assumes a typical polydisperse fly ash size distribution; e.g., MMD = 6.4 μm and $\sigma g = 3.3$, the number of particle-to particle contacts increase significantly such that the computed cake strength increases to about 10^6 dynes/cm^2.

At the present time, only very rough estimates can be made of the adhesive forces at the dust/fabric interface. In the case of collapse-reverse flow systems, where tensile and shearing forces generated in a gravity field were considered to be the major separating force, interfacial adhesive forces were estimated to range from 50 to 100 dynes/cm^2. The actual separating or tensile force exerted by a 0.1 cm thick dust cake suspended from a horizontally aligned fabric surface, for example, is roughly 100 dynes/cm^2. If the interfacial tensile stress is produced by mechanical shaking, the force field is now defined by the local cake acceleration, usually in the range of 4 to 5 g's, and calculable from the amplitude and frequency of the shaker arm. Since the shaker and gravity acceleration vectors usually act perpendicularly to each other, the absolute value for the resultant vector may be defined by the shaker acceleration alone when a is > 4 g.

The preceding discussion reflects the status of the dust removal aspects of the modeling program at the beginning of the present study. Despite the point scatter, Figure 5a indicated a significant correlation between cleaned area fraction, a_c, and the fabric loading, W, at the inception of cleaning. The same level of correlation was also observed with respect to the cleaning force, F_c, associated with the fabric loading and its resultant acceleration.

The fact that Point 3, which derives from tests on a mechanically shaken system, falls on the curve appears to justify the concept that acceleration forces, either artificially or gravity generated, are at least major factors in causing dust dislodgement by some combination of tension and/or shearing forces. It was assumed in the above analyses that tensile and shear forces of equal magnitude would exert the same cleaning effect.

It is also pointed out in prior studies that the apparent adhesive force levels suggested by Figure 5a reflect the interfacial bond strength after the fabric has undergone several flexings (repeated cleanings). Therefore, although the net bonding strength is difficult to predict, it appears reasonable to assume that it might be appreciably lower than that exhibited prior to initial flexure (at least 40 percent according to previous studies).[1]

It was also recognized that the rapidity of bag collapse (and hence rate of flexure) and the ultimate radius of curvature of bag surface elements might also be instrumental in the cake loosening process. The reverse air velocity alone was not considered a major factor in cake dislodgement insofar as aerodynamic drag was considered. For example, the reverse air velocities of 0.15, 0.33, and 0.43 actual m/min, respectively for GCA, Nucla, and Sunbury tests, had no apparent effect on the amount of cleaning. The basis for the above statement was the fact that data points from the above sources fell on the regression line without any velocity adjustments.

More recently, however, a significant improvement in reverse air cleaning has been reported when the reverse flow rate was increased by a factor of 2.5.[11] Therefore, the potential effects of both cleaning velocity and pressure gradient across the fabric were reexamined to determine whether the original relationships proposed for estimating the degree of fabric cleaning (a_c); i.e., Equations (13) and (14), require modification.

3.1.2 Dust Dislodgement Factors - Reappraisal

As stated previously, gravity and/or artificially generated acceleration forces were considered to be the main dust dislodging forces wherein tensile or shear stresses exerted at the dust/fabric interface were assumed to overcome the adhesive bonds. Without attempting to quantify the following factors, it was also indicated that the rate and degree of fabric (and dust cake) flexing or bending represented additional mechanisms that could lead to severance of adhesive bonds. Electric charge and humidity were also presumed to influence the strength of the dust cake itself via their effects on cohesive bonds and the capability of the dust cake to detach itself from the fabric surface. Although reverse flow velocity was expected to influence dust separation, limited measurements appeared to place it as a secondary factor with respect to the original data sources. In the foregoing discussion, the role of reverse flow velocity has been reexamined for those filtration systems evaluated in the design and development of the original filtration model.

3.1.3 Aerodynamic Drag

During the period of reverse air flow, the resulting aerodynamic drag produces a tensile force that must be matched at the dust-fabric interface if the dust layer is to be retained. Ordinarily, no provisions are made to measure the actual pressure drop across a filter during the reverse flow interval. Its initial magnitude can be estimated, however, from the observed pressure drop through the fabric as a function of the system face velocity and the fabric dust loading immediately before cleaning. In terms of the system drag parameter, the drag during reverse flow, $\overline{S}_r$, is computed as:

$$\overline{S}_r = S_{E_f} (V_r/V_f) + K_{2_f} (V_r/V_f)^{\frac{1}{2}} W_f \qquad (16)$$

where the subscripts r and f refer to the reverse flow and normal filtration velocities, respectively. The resultant aerodynamic drag force per unit area (or simply pressure drop) then becomes:

$$F_d = \overline{S}_r V_r \qquad (17)$$

presuming that the reverse flow and filtration air temperature are the same. Graphing of the data appearing in Table 4 gives a curve form very similar to that reported earlier for the fractional cleaning, a_c, versus fabric loading relationship, W (and the corresponding gravity separating force per unit area W.g) Figure 5b. This is to be expected because with a constant reverse flow velocity any calculated aerodynamic drag force must vary linearly with fabric dust loading (or cake thickness). However, if the drag force is considered to be the predominant dust separating mechanism, one should also assume that any dust not dislodged from the filter is retained by an adhesive force at least as strong as the opposing drag force. Additionally, it would appear that dust losses via the avenues of gravity or mechanical shaking forces would be relatively unimportant compared to the drag effects since the former forces are calculated to be about 10 times smaller.

The above concepts, however, appear to be contradicted by the mechanical shaking process. Although shaking systems are not accompanied by reverse

TABLE 4. ESTIMATES OF MAXIMUM AERODYNAMIC DRAG FORCES DURING REVERSE FLOW CLEANING[*]

Run No.[†]	Fabric loading at beginning of run (g/m^2)	Fabric loading before cleaning (g/m^2)	Fabric loading after cleaning (g/m^2)	Cleaned area fraction (a_c)	Aerodynamic drag[‡] ($dynes/cm^2$)
P-2-1	113	937	345	0.67	1,040
P-2-2	327	422	387	0.09	530
P-2-3	387	545	498	0.09	640
P-2-4	498	723	598	0.19	820
P-3[§]	–	735	–	0.19	830
P-4-1[†]	85.9	696	274	0.65	790
P-4-2	274	429	382	0.12	550
P-4-3	382	536	476	0.12	630
P-4-4	476	631	549	0.14	720
P-4-5	549	704	550	0.23	800
P-5-1	550	705	501	0.32	800
P-5-2	501	656	537	0.20	750
P-5-3	537	692	554	0.21	790
P-5-4	554	709	553	0.24	810
P-5-5	553	708	559	0.23	810
P-5-6	559	714	579	0.20	815

[*] Pilot scale tests on a 10 ft × 4 in. woven glass bag (Menardi-Southern).

[†] Run numbers appearing in Reference 1 (EPA-600/7-77-084).

[‡] Based on reverse flow velocity of 0.15 m/min.

[§] Average of 19 successive filtration cycles.

flow, significant dust dislodgement is attainable even when the acceleration forces are 10 times lower than the estimated aerodynamic drag forces. For example, the removal of coal fly ash from sateen weave cotton bags indicated a_c values in the 50 percent range for an estimated acceleration force of only 250 dynes/cm^2. It should be noted that a bag undergoes many shakes, 50 to 250, to accomplish the observed cleaning levels. However, after a finite number of shakes (or repeated bag collapses in the case of reverse cleaning systems), the dust removal appears to approach a limiting value based on the acceleration imparted to the fabric and its dust holding.

A second inconsistency is noted when filter systems using different reverse flow velocities are compared on the basis of dust separation by aerodynamic drag.[1,11] If one assumes that the reverse flow velocities reported for Nucla and Sunbury tests were correct, the prior relationships between laboratory pilot tests and real measurements, Figure 5a, appear to break down. In the following discussion, possible reasons for the lack of correlation are explored.

3.1.4 Instantaneous and Average Aerodynamic Drag

On the assumption that dust cake adhesive forces over the fabric surface will follow some statistical distribution, the application of the aerodynamic drag force calculated for the undisturbed dust cake is expected to dislodge any surface element of dust for which the local adhesive force is exceeded. In actual practice, the process of bag collapse itself invariably leads to appreciable spalling off of dust as well as producing many cracks and defects in the cake. At the same time, it must be presumed that a large fraction of the underlying adhesive bonds are severed.

Once a cleaned fabric area has been exposed, the flow now redistributes itself such that a much larger fraction passes through the lower resistance path. The result is an immediate reduction in overall air flow resistance with a corresponding decrease in the drag force. How this phenomena affects any subsequent cleaning action is summarized in Table 5. In the case of Run No. P-2-1, the dust was uniformly distributed over the fabric prior to cleaning with no flexing of the dust laden surface until the first bag collapse. Upon resumption of filtration, Run No. P-2-2, most of the dust deposited on the "just cleaned region" because of its low resistance to air flow. Therefore, the filter drag, S, only increases about 7 percent for the original uncleaned region, (695 to 740 N min/m^3) wheras it is nearly doubled for the just cleaned area (49.3 to 167 N min/m^3). The key factor in this analysis is that once a small fraction of dust has dislodged, the aerodynamic drag forces appear to diminish to the general level of the tensile and shear forces attributed to gravity and mechanical shake cleaning.

It is important to note that the estimated drag forces before cleaning, Column 5, Table 5, were calculated on the assumption that the cake had not been disturbed by the collapsing motion of the bag following compartment isolation and preceding the initiation of reverse flow. Therefore, a high estimate is suspected in Column 5, because no adjustment has been made for the pressure reduction due to the increased permeability of the damaged cake. One conclusion drawn from the above analysis is that the severance of adhesive bonds by the flexing and related geometric perturbations of the cake induce cake dislodgement due to gravity effects alone without the need for supporting aerodynamic drag forces. In effect, any moderate "push" exerted by a fairly

TABLE 5. **INSTANTANEOUS AND FINAL AERODYNAMIC DRAG DURING REVERSE FLOW CLEANING, FLY ASH FILTRATION WITH WOVEN GLASS BAGS**

Run No.	**Previous fabric cleanings**[*]	**Fabric** loading before cleaning (g/m^2)	Area fraction cleaned	Aerodynamic drag force ($dynes/cm^2$)	
				Before dust loss[†]	After dust loss[‡]
P-2-1	0	937	0.61	1,040	106
P-2-2	1	422	0.09	530	240
P-2-3	2	545	0.10	640	325

[*] **Each flexing** reduces adhesive bonding of any residual dust.

[†] **Dust cake assumed** to be completely intact.

[‡] **Cleaned area** lowers overall filter resistance. Drag based upon new distribution of fabric loading for Run Nos. P-2-2 and P-2-3.

wide velocity range may result in essentially the same dust removal. As noted in the next section, however, there are other velocity effects that may play secondary roles in dust dislodgement.

3.1.5 Effect of Hoop Stresses on Cake Structure

In view of the several factors that may alter the contours of a collapsed bag before and during the reverse flow phase; e.g., bag tension, fabric stiffness, assymetry due to seam effects, anticollapse rings and pressure gradient, it appears extremely difficult to make any rigid quantitative estimates of their combined impact on dust cake loosening.

When a bag without support rings (and under 50 to 70 lbs tension) reaches the collapsed state, its external contour at some cross section as seen from an axial perspective might appear as indicated schematically in Figure 7. Tensioning of the bag can prevent total flattening under the influence of the pressure gradient, $P_c - P_d$, from outside (clean) to inside (dirty) produced by the reverse flow. As with a pressure vessel, the hoop stress, s_t, acting over the wall cross section $t \times 1$ where t is the dust cake thickness and 1 the bag length is computed as follows:

$$s_t = Pd_b'/2t \qquad (16)$$

where P is the pressure gradient and d_b' is the diameter that characterizes the local radius of curvature of the bag. To fit the convoluted depressed surfaces shown in Figure 7, it would appear that the local "diameter" should be roughly one-half that for the fully inflated bag; i.e., roughly $d_b'/2$. Since the pressure is a linear function of both cake thickness and reverse flow velocity, the hoop stress also can be expressed in the form:

$$s_t = \beta\, V_r d_b'/2 \qquad (17)$$

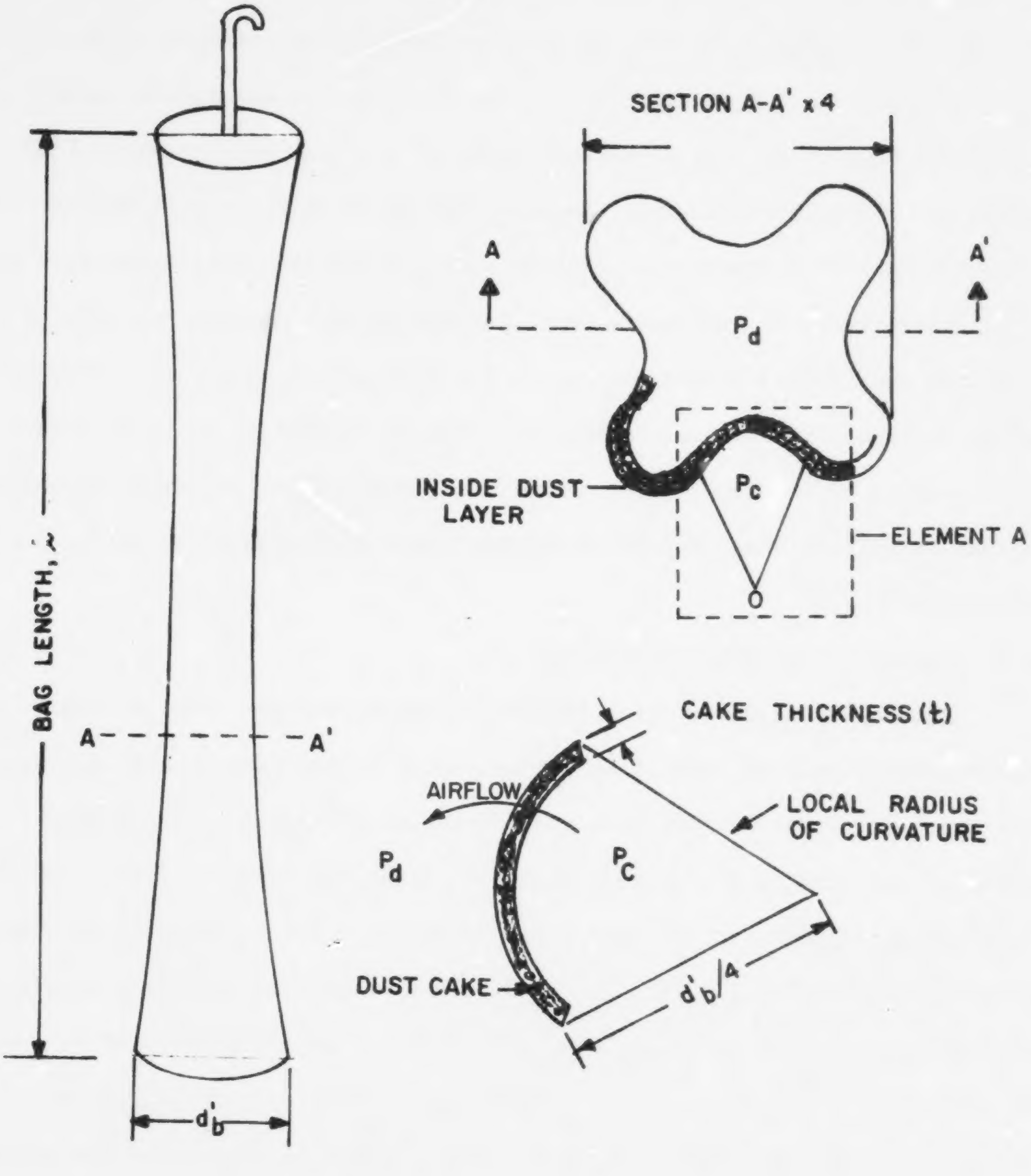
BAG LENGTH, ℓ
A
A'
d'b
SECTION A-A' x 4
A
A'
Pd
Pc
INSIDE DUST LAYER
ELEMENT A
O
CAKE THICKNESS (t)
AIRFLOW
LOCAL RADIUS OF CURVATURE
Pd
Pc
DUST CAKE
d'b/4

Figure 7. Schematic, hoop stressing during reverse flow for depressed region, collapsed bag with clean side (external) pressure exceeding dirty side (internal) pressure, $P_c > P_d$.

which simply states that s_t depends only upon the reverse flow velocity, V_r, the local radius of curvature, $d_b'/2$ and a constant, β, that is uniquely related to the dust cake physical properties. For the fly ash used in the tests summarized in Table 4, the numerical value for β is approximately 1.4×10^4. Thus, for a reverse flow velocity of 0.15 m/min and an assumed "diameter" of curvature of 5 cm for the depressed region of the bag, the estimated hoop stress would be 5.25×10^3 dynes/cm^2. Because the latter value is considerably lower than the estimated adhesive or tensile strength for the undisturbed dust cake ($\tilde{}10^6$ dynes/cm^2), it does not appear that significant surface cracking or checking should have arisen during the P-2 test series as a result of hoop stress. Thus, the flexing of the cake prior to initiation of reverse flow is suspected to be the major cause of surface "checking" or cracking, in which either tensile or shear forces resulting from compression could be the failure mechanism.

3.2 SPECIFIC RESISTANCE COEFFICIENT

It was emphasized in prior modeling studies that the specific resistance coefficient, K_2, should be determined by direct measurement, at least until more dependable prediction methods become available. At the same time, it was pointed out that if reliable sizing data were available for the field aerosols (such as the mass median diameter and the geometric standard deviation) in conjunction with good estimates of discrete particle density, ρ_p, and dust cake porosity, ε, good ($\pm$50 percent) approximations of K_2 should be attainable. Although the above level of accuracy is not sufficient to determine operating parameters for a filter system, it does alert the designer to the probable degree of difficulty to be expected in filtering a given dust. It is emphasized that a $\pm$50 percent precision level is attainable only when one computes the specific surface parameter, S_o, for the distribution of sizes making up the dust cake. Then K_2 for various fly ashes may be estimated from the Carman-Kozeny relationship:

$$K_2 = k'\mu\, S_o{}^2 \left(\frac{1-\varepsilon}{\varepsilon^3}\right) = \frac{\mu S_o{}^2 R}{2} \qquad (18)$$

where k' is a modified Carmen-Kozeny constant with a value of 1.6, μ the gas viscosity, and ε the cake porosity. The porosity is also definable as:

$$\varepsilon = 1 - \left(\frac{\bar{\rho}}{\rho_p}\right) \qquad (19)$$

where $\bar{\rho}$ is the bulk density of the cake and ρ_p the density of the discrete particles.

In a recent paper by Rudnick and First,[12] the authors indicated that use of the Happel "free surface" flow field model provides a better estimate of dust cake K_2 values than the Kozeny-Carman equation when cake porosities exceed 0.7. A graphical presentation of their calculations, Figure 8, shows that K_2 values are actually much larger than those predicted by the Carmen-Kozeny method when porosity values are greater than 0.8. Therefore, earlier data showing measured and predicted K_2 values were updated with respect to the Happel concept[13] as shown in Table 6. For those fly ash porosity values within the 0.42 to 0.59 range, both predictive methods agree within 5 to 7 percent. In the case of granite dust with an estimated porosity of 0.68, the Happel relationship predicts only a moderate, ~20 percent, increase in K_2. However, a nearly 1.8 times increase in predicted K_2 values results when the porosity increases to 0.84. Although the Happel model has the broader application, its predictive capabilities are still strongly dependent upon the accuracy with which the porosity, bulk density and discrete particle density

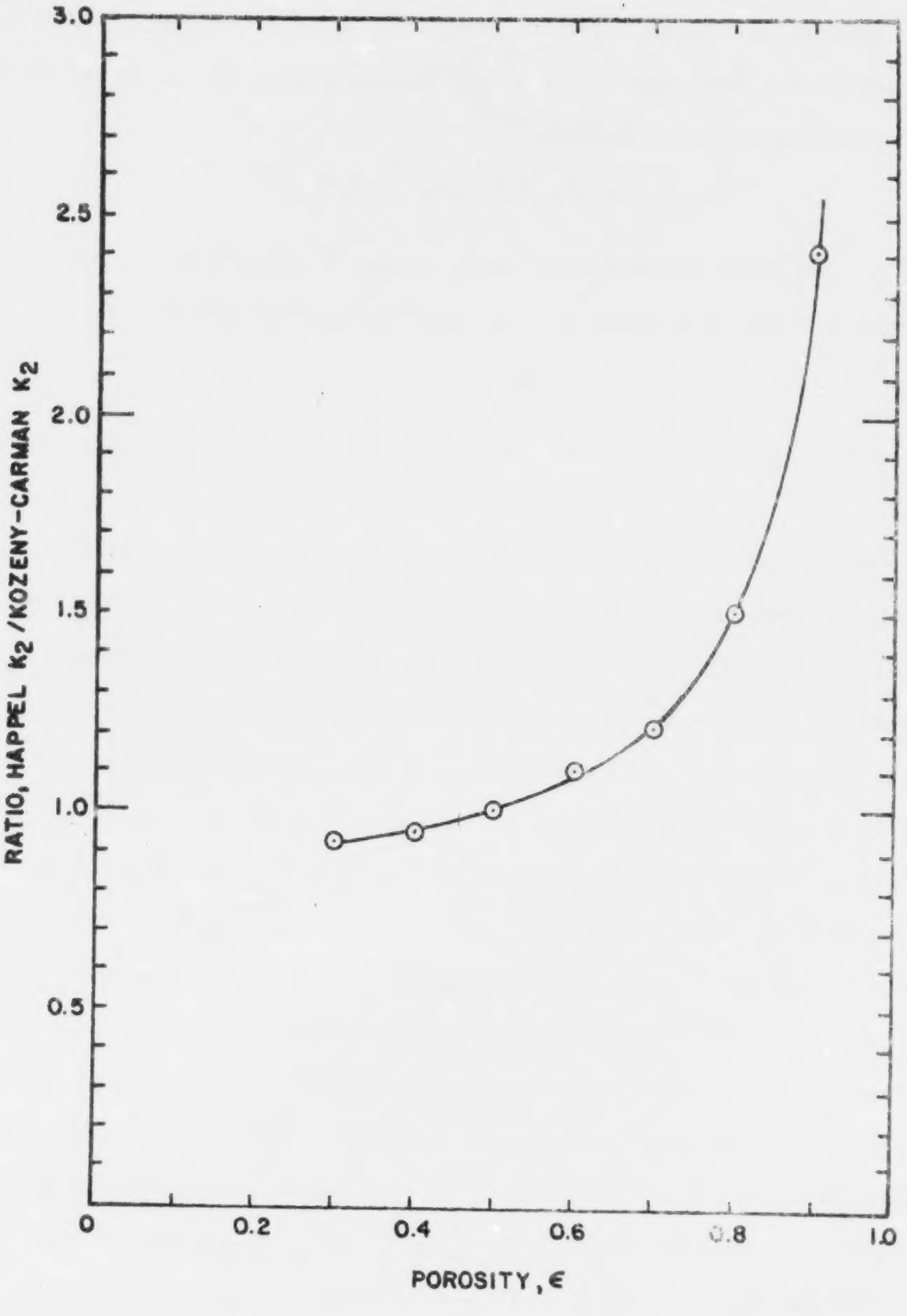

Figure 8. Ratio of K_2 values predicted by Happel and Kozeny-Carman equations versus dust cake porosity.

TABLE 6. PREDICTED AND MEASURED K_2 VALUES FOR VARIOUS DUST/FABRIC COMBINATIONS, SIZE PROPERTIES AND OPERATING PARAMETERS

Test dust	Dust parameters					Filtration parameters		Filter fabric	Measured K_2 ambient conditions $21^{o}C$ (0.605 m/min)	Predicted K_2 @ $21^{o}C$		K_2 ratio predicted (H)
	MMD[*] (μm)	σg	Particle density (g/cm^3)	S_o^2 (cm^{-2})	Cake porosity (ε)	Velocity (m/min)	Temp (^{o}C)			K/C[‡]	H[†]	(measured)
Coal fly ash Public Service Co., NH (GCA)	4.17(I)	2.44	2.0	4.73×10^8	0.59	0.915	21	Glass, 3/1 twill	1.85	5.72	6.12	3.31
	5.0 (M)	2.13	2.0	2.58×10^8	0.59	0.915	21	Napped cotton sateen weave	1.85	3.74	4.00	2.14
	6.38(I)	3.28	2.0	3.55×10^8	0.59	0.605	21	Glass, 3/1 twill	1.40	5.14	5.50	3.93
Coal fly ash Public Service Co., NH	3.8 (I)	3.28	2.0	9.94×10^8	0.59	0.823	138	Glass, 3/1 twill	4.45	14.4	15.9	3.46
Coal fly ash Detroit Edison (EPA)	3.2 (M)	1.8	2.0	4.78×10^8	0.59	0.915	21	Napped cotton, sateen weave	1.00	6.19	6.63	6.63
Coal fly ash Public Service Co., NH (GCA)	2.42(M)	1.77	2.0	8.49×10^8	0.59	0.915	21	Napped cotton, sateen weave	1.77	11.0	11.8	6.66
Coal fly ash Nucla, CO	11.3(I)	3.55	2.0	1.28×10^8	0.59	0.851	124	Glass, 3/1 twill	0.75	1.84	1.97	2.63
Lignite fly ash Texas Power and Light	8.85(I)	2.5	2.4	1.06×10^8	0.46	0.605	21	Glass, 3/1 twill	1.34	3.67	3.60	2.69
	8.85(I)	2.5	2.4	1.06×10^8	0.42	0.605	21	Glass, 3/1 twill	1.34[‡]	5.16	4.90[‡]	3.66
	8.85(I)	2.78	2.4	1.30×10^8	0.46	0.605	21	Glass, 3/1 twill	1.34	4.49	4.40	3.28

(continued)

TABLE 6 (continued)

Test dust	Dust parameters					Filtration parameters		Filter fabric	Measured K_2 ambient conditions 21°C (0.605 m/min)	Predicted K_2 @ 21°C		K_2 ratio predicted (H)
	MMD* (μm)	σg	Particle density (g/cm³)	S_o^2 (cm^{-2})	Cake porosity (ε)	Velocity (m/min)	Temp (°C)			K/C†	H†	(measured)
Granite dust	9.21(I)	4.83	2.2	5.05×10^8	0.68	0.605	21	Glass, 3/1 twill	1.38	2.64	3.11	2.26
	9.21(I)	4.55	2.2	4.13×10^8	0.68	0.605	21	Glass, 3/1 twill	1.38	2.15	2.54	1.84
	9.21(I)	4.05	2.2	2.88×10^8	0.68	0.605	21	Glass, 3/1 twill	1.38	1.50	1.77	1.28
	8.1 (I)	3.88	2.2	3.24×10^8	0.68	0.605	21	Glass, 3/1 twill	1.38	1.70	2.01	1.46
	9.84(I)	4.32	2.2	3.44×10^8	C.68	0.605	21	Glass, 3/1 twill	1.38	1.69	2.00	1.45
	9.21(I)	4.83	2.2	5.05×10^8	0.60	0.605	21	Glass, 3/1 twill	1.38‡	5.28	6.23‡	4.45
	1.23(I)	2.38	2.2	5.10×10^9	0.68	0.605	21	Glass, 3/1 twill	12.3	26.7	31.5	2.54
Talc	2.77(I)	2.9	2.2	1.51×10^9	0.84	0.915	21	Napped cotton, sateen weave	4.71‡	2.35	4.00‡	0.85
	2.77 I)	2.9	2.2	1.51×10^9	0.82	0.915	21	Napped cotton, sateen weave	4.71‡	2.72	4.35‡	0.92
	2.77(I)	2.9	2.2	1.51×10^9	0.73	0.915	21	Napped cotton, sateen weave	4.71‡	5.78	7.40‡	1.57

*(I) refers to cascade impactor sizing; (M) refers to microscope sizing (light field, oil immersion).

†K/C = Kozeny-Carman equation; H = Happel equation.

‡Not used for regression line statistics.

Note: Based on original data from Reference .

can be measured. In the following discussion, their accuracy levels are examined with respect to their impact upon the final estimation of K_2.

Given the situation where porosity is determined by an independent estimate of void volume (in which no measurement of discrete particle density is required), numerical values for the porosity function $(1 - \varepsilon)/\varepsilon^3$ vary with porosity ε as shown in Figure 9. As indicated in a prior report,[1] a 10 percent error in the estimation of ε can lead to a 50 percent error in the porosity factor and therefore a 50 percent error in the determination of K_2 by the Kozeny-Carman equation.

When the porosity is calculated from bulk density, $\bar{\rho}$, and discrete particle density, ρ_p, measurements, it is again shown that relatively small errors in estimating either term may lead to large errors in K_2 via the impact of the porosity function, Figure 10. For example, if the true bulk density were 1.1 rather than 1.0 g/cc, the error in K_2 estimation would be 50 percent for a discrete particle density of 2.0 g/cc. A similar K_2 error results when a 10 percent error is made in the estimation of discrete particle density. Since K_2 also varies inversely with the square of the particle diameter, d_{sp}, characterizing specific surface; i.e., $\frac{1}{{d_{sp}}^2} = f\ (S_o)^2$, it is also apparent that any error in size measurement will have a significant effect on K_2 estimation. Although the discussion so far has dealt with the Kozeny-Carman equation, use of the Happel theory as discussed by Rudnick and First[12] will lead to essentially the same error ranges for K_2. In the generalized notation for calculating K_2:

$$K_2 = \frac{18\ \mu\ R}{\rho_p\ {d_{sp}}^2 C_s} = \frac{R}{\tau\ C_s} \qquad (20)$$

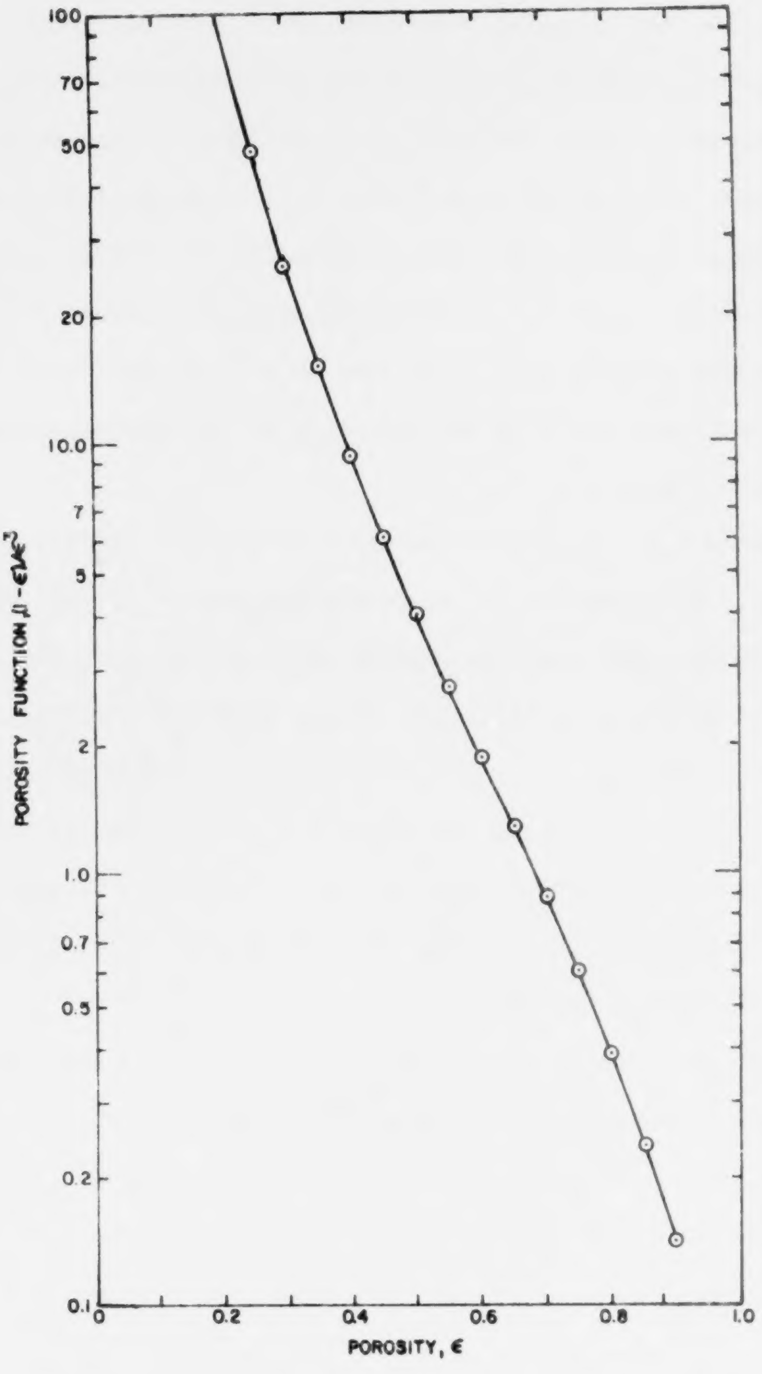

Figure 9. Variations in porosity functions with porosity.

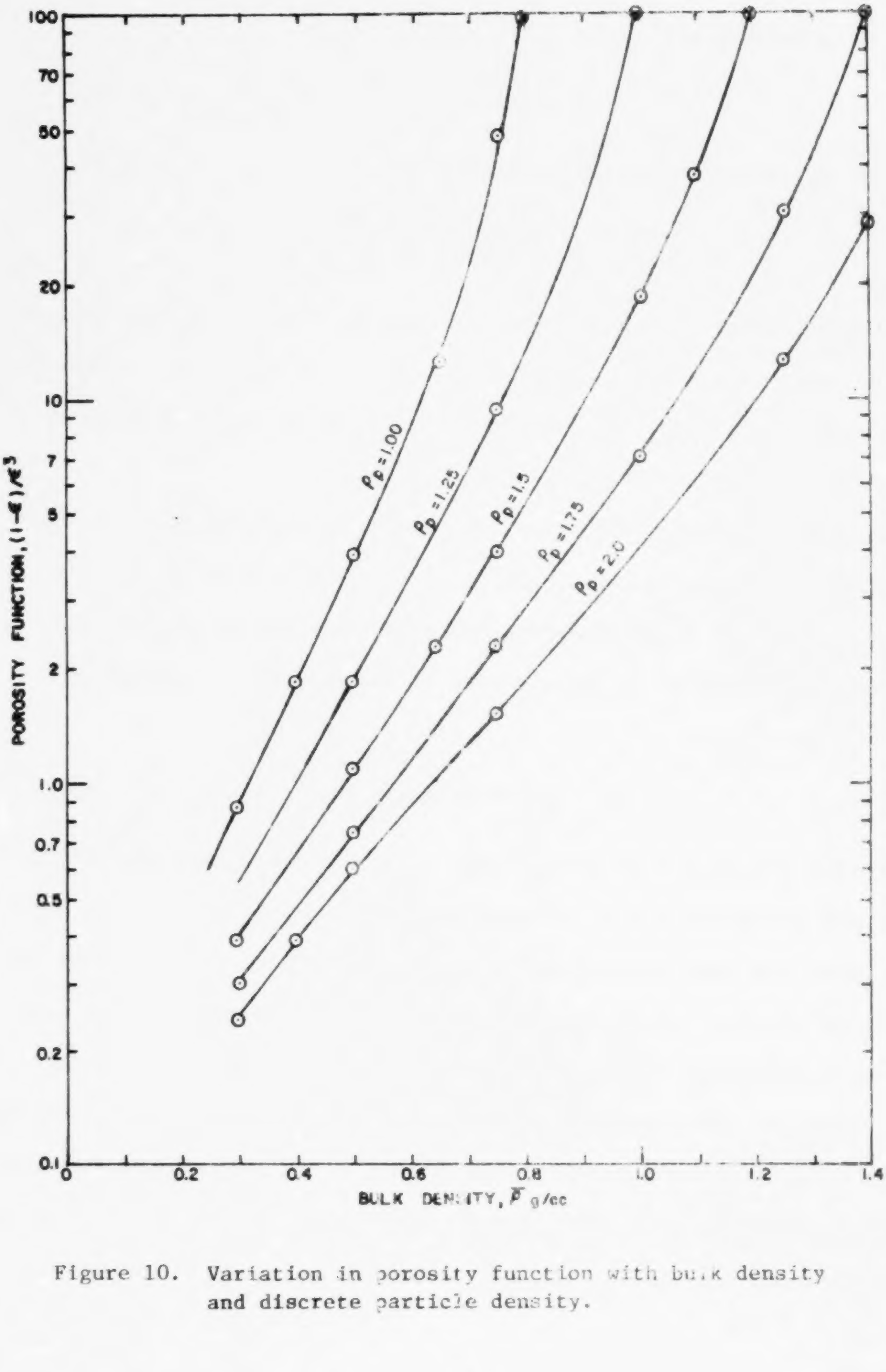

Figure 10. Variation in porosity function with bulk density and discrete particle density.

the term R is defined as:

$$R = 2\ k\ (1-\varepsilon)/\varepsilon^3 \tag{21}$$

for use in the Kozeny-Carman equation and:

$$R = \frac{3 + 2\ (1-\varepsilon)^{5/3}}{3 - 4.5\ (1-\varepsilon)^{1/3} + 4.5\ (1-\varepsilon)^{5/3} - 3\ (1-\varepsilon)^2} \tag{22}$$

when the Happel model is selected. Both equations reflect the fact that K_2 becomes a complex exponential function of porosity in which a highly precise determination of ε is required to provide good working estimates for K_2.

3.3 EFFECT OF FILTRATION VELOCITY ON K_2

In a previous report, laboratory filtration of coal fly ash aerosols showed that K_2 was also dependent upon face velocity as well as upon the variables called out in the Kozeny-Carman equation. For certain coal fly ash/glass fabric systems[1] K_2 was observed to increase as the square root of the velocity; i.e.:

$$K_2 = 1.8\ V^{0.5}\ \ \text{N-min/g-m} \tag{23}$$

over the velocity range 0.39 to 1.53 m/min. It was postulated that the increased particle momentum associated with higher velocities increased the dust cake solidity and hence reduces its porosity. The former effect should not be confused with porosity changes caused by the gradual compression of a dust cake and/or underlying fabric substrate as the pressure drop across the system increases. The change in cake porosity associated with gas stream and particle velocity is readily identified since a linear relationship between pressure loss and gas velocity will ensue when dust free air is passed through the dust cakes formed at different face velocities. On the other hand, very loose dust deposits and heavily napped fabrics may display a curvilinear relationship (concave up) between pressure loss (ordinate) and velocity(abscissa) as the velocity of dust free air is increased, Figure 11.

In a recent communication,[12] Rudnick has indicated that K_2 values for Arizona road dust in the submicrometer size range showed only a weak dependency on filtration velocity; i.e., $K_2 = f\ (V)^{0.19}$ Although confirming measurements are lacking, it is postulated that two factors may contribute to the stability of cake structure in the above instance. First, Rudnick's tests were performed with a dust having a narrower size range than found for most coal fly ashes. Hence, one expects the more uniformly sized particles to deposit in a denser packing because the probability of random void space formation is reduced. In the absence of significant voids, which may lead to an unstable cake structure, any increase in face velocity would have little effect on porosity because the initial deposit already has reached its maximum density.

A second explanation for the relatively constant K_2 values may lie with the fact that the smaller the particle diameters the greater the adhesive and cohesive bonds in the system. Therefore, unless the gas stream lines change radically with flow rate, there is a strong tendency for each approaching particle to remain where it first contacts the fabric or a previously deposited particle. Conversely, larger particles may undergo a gradual migration and assume a stabler and denser packing as the gas flow increases.

If the above concepts are correct, at least from the qualitative viewpoint, it appears that considerable research is required in the cake structure area before any generalized procedure can be established to related K_2 to face velocity. In addition, there are still no quantitative relationships to describe the effects of electrical change, humidity, and particle shape on the

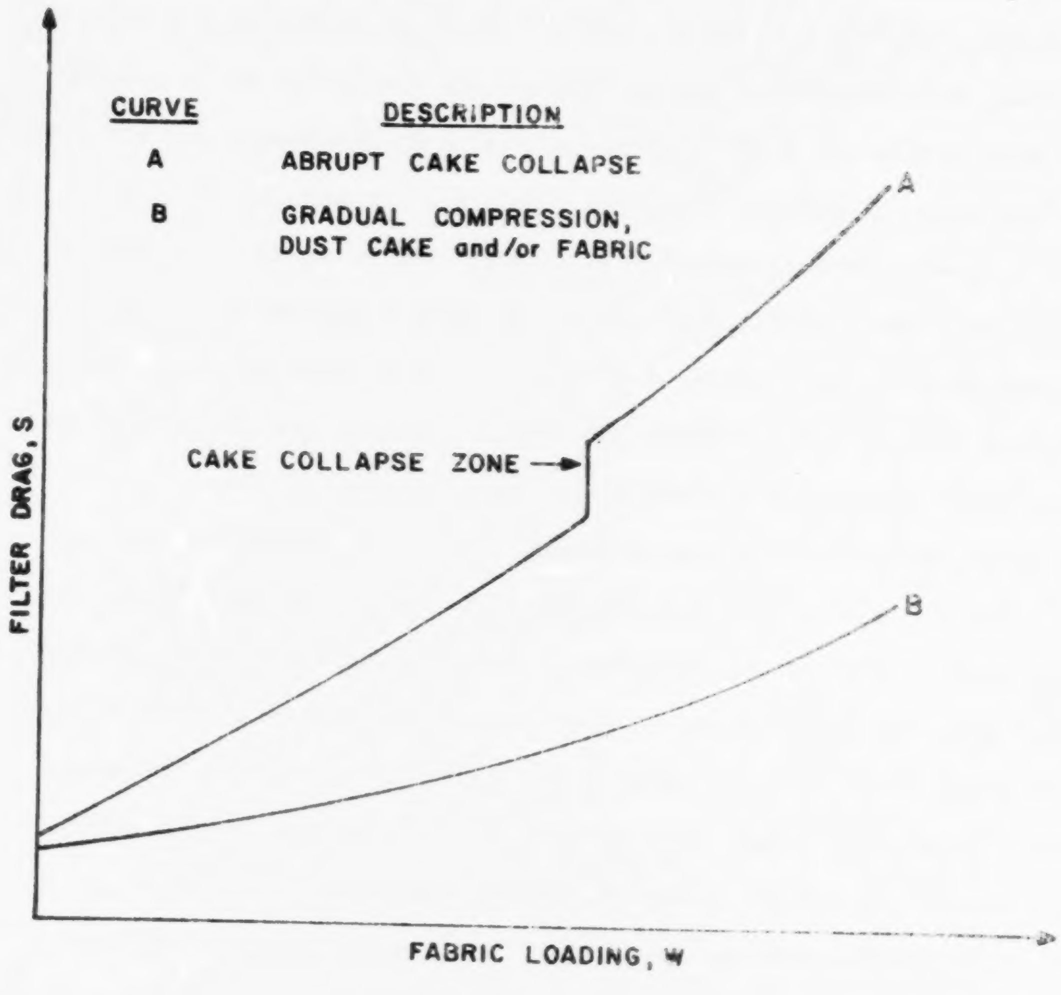

Figure 11. Drag versus fabric loading curves typifying abrupt cake collapse and gradual cake and/or fabric compression.

porosity of a deposited dust layer. For the above reasons, it is strongly advised that direct measurements be made on the dust/fabric system of interest.

Earlier studies by Spaite and Walsh[14] were reexamined to determine how particle shape and velocity changes affected K_2 values. A ground mica described as nominal 5 to 10 μm flakes with 0.5 μm thickness appeared to behave very much like fly ash when filtered through twill weave glass fabrics. Because of uncertainties in interpreting the testing procedures, a regression line was established for all data points regardless of fabric type, Figure 12. Despite the differences in shape factor between fly ash and mica (roughly spherical and platelets, respectively), both dusts appear to react the same to velocity changes; i.e., $K_2 \sim f\ (V)^{0.5}$. With respect to the mica particles, it is easy to imagine a gradual collapsing of a card-like structure as the pressure gradient increases across the dust layer. Thus, the apparent nonlinearity of the data point array suggests that both momentum effects and compression may be taking place. Reexamination of drag/loading curves reported by Borgwardt et al. for the field filtration of fly ash suggests that the velocity exponent might well be nearer to 0.75 than the reported 1.5 value.[15] The current interpretation is based upon analyses of recent tests[1] coupled with the fact that the extrapolation of long term, average measurements to define short-term changes in any filtration system is a risky process. Despite the fact that the proposed K_2/velocity relationship for fly ash; i.e., $K_2 = f\ (V)^{0.5}$ appears reasonable, it is recommended that the precise relationship be determined by experiment whenever practicable.

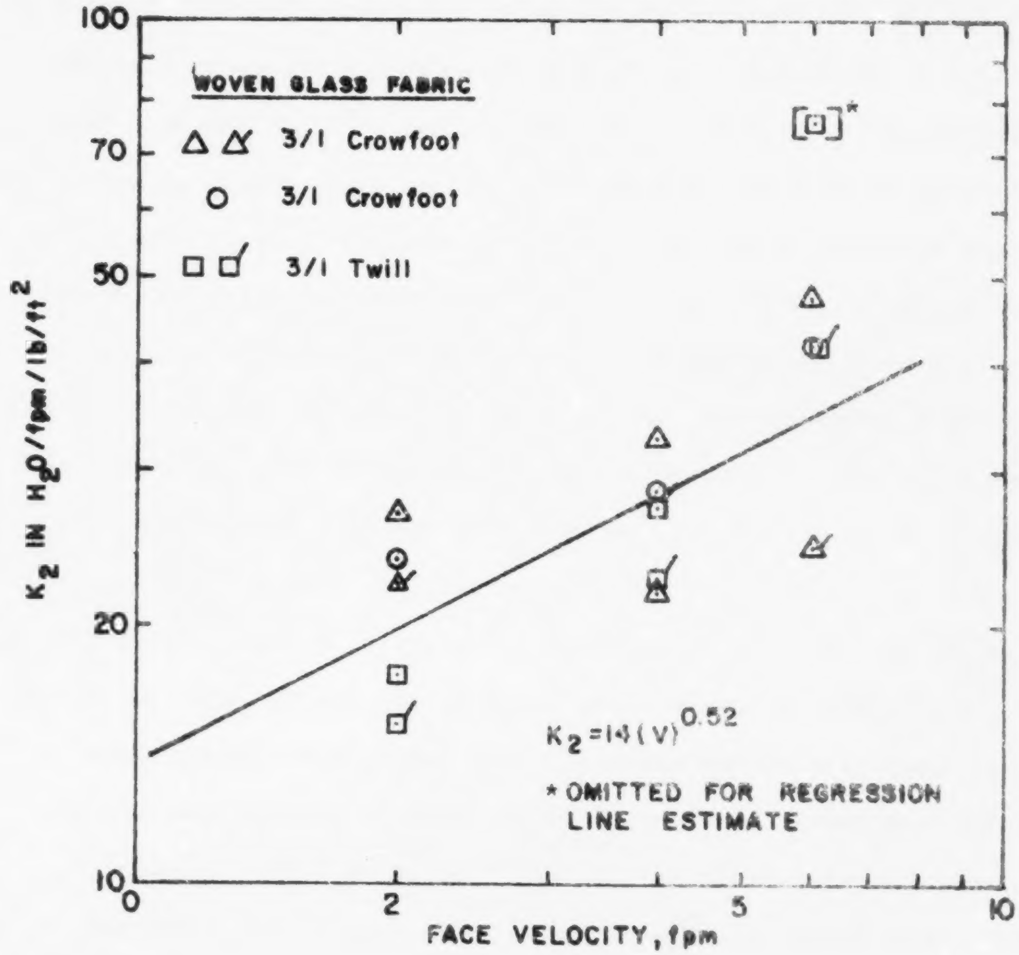

Figure 12. K_2 versus velocity for wet ground mica. From Spaite and Walsh.

4.0 SENSITIVITY ANALYSES

4.1 PRELIMINARY SCREENING TESTS

4.1.1 Objectives

In order to reduce the number of tests necessary for the sensitivity analysis, several screening tests were performed to determine which input parameters had the greatest effect on system performance. At present, the model requires 10 input parameters as well as the fabric and dust properties to completely describe a system. If each input parameter were assigned three possible values and all test combinations were investigated, over 1,000 tests would be required. By varying a single input parameter over a typical range of values with all other parameters held constant, the impact of that parameter on system performance and the importance of the parameter relative to other parameters can be determined for an "average" set of circumstances. A system similar to that for the Nucla Station operation was chosen as a "baseline" test to which subsequent tests could be compared. The operating parameters for the baseline conditions are presented in Table 7. Although the system described by the parameters in Table 7 is a pressure controlled cleaning system, it may, in some instances, be forced into a continuous cleaning mode.

4.1.2 Variables Studied During Screening Tests

Each of the parameters shown in Table 7, with the exception of cleaning cycle time, gas temperature and the fabric and dust properties, were varied over typical field ranges and the results analyzed. A summary of the results

TABLE 7. INPUT PARAMETERS SELECTED FOR BASELINE TESTS

Parameter	Value
Number of compartments	10
Cleaning cycle time	30 min
Compartment cleaning time (off-line time)	3 min
Reverse flow velocity	0 m/min
Limiting pressure drop	1000 N/m^2 (4.0 in. w.c.)
System velocity	0.61 m/min (2 ft/min)
Gas temperature	150°C (300°F)
Inlet particulate concentration	6.87 g/m^3 (3 grains/ft^3)
Specific cake resistance, K_2*	1.0 N-min/g-m (6.0 in.w.c.-min-ft/lb)
Effective drag, S_E†	400 N-min/m^3 (0.49 in.w.c.-min/ft)
Residual fabric loading, W_R	50 g/m^2 (0.0102 lb/ft^2)
Residual drag, S_R‡	0
Initial slope, K_R‡	0
Time increment (for iterations)	1.0 min
Fractional area cleaned, a_c	0.40

*Measured at a face velocity of 0.61 m/min and a temperature of 25°C. At 150°C K_2 has a value of 1.322.

†Measured at a temperature of 25°C. At 150°C S_E has a value of 528.

‡Zero values indicate no measurements available and automatic selection of linear drag model.

is presented in Table 8. Values shown under input parameter variations in Table 8 indicate the value of the parameter in the baseline test and the value used in the corresponding test. The reported maxima and minima are those occuring at any time during a complete operating cycle.

4.1.3 Performance Parameters, Maximum and Minimum Values

Continuously cleaned systems exhibit a maximum resistance and a minimum penetration just be initiation of cleaning of any compartment. Conversely, the resistance is at a minimum and the penetration at a maximum immediately following the cleaning process because of the reintroduction of freshly cleaned fabric surface. The above effects are repeated cyclically as cleaning continues such that pressure loss and penetration always oscillate between the same fixed limits.

Pressure and time controlled systems also display maxima and minima except that the values are not repetitive from compartment to compartment. In the latter systems, the minimum penetration occurs prior to cleaning the first compartment and the maximum pressure drop occurs just before the first compartment is returned to service. Minimum pressure drop occurs after the last compartment cleaned is put back on line.

The point at which penetration is at a maximum is less easily defined since two opposing effects act concurrently during a cleaning cycle. As cleaning progresses, the velocity gradients diminish thus favoring decreased penetration while fabric loadings simultaneously decrease leading to increased penetration. Maximum penetration appears to take place about halfway through the cleaning cycle immediately after a cleaned compartment has been returned to service.

TABLE 8. EFFECT OF VARIATIONS IN INPUT PARAMETERS ON SYSTEM PERFORMANCE

Input parameter variations*	Penetration (percent)			Time between cleanings† (min)	Pressure drop (N/m^2)		
	Minimum	Maximum	Average		Minimum	Maximum	Average
Baseline test	0.015	1.1	0.13	81	650	1,165	860
V, 0.61 → 0.3	0.0078	2.0	0.037	672	360	1,165	725
0.61 → 1.22	0.35	1.1	0.57	0	1,510	1,745	1,690
0.61 → 1.53	0.81	1.6	1.06	0	2,200	2,700	2,600
P_L, 1000 → 500	0.089	0.73	0.36	0	500	565	560
1000 → 1500	0.015	1.5	0.09	160	750	1,755	1,160
C_I, 6.87 → 2.29	0.029	1.1	~0.13	~270	580	1,160	810
6.87 → 22.9	0.013	1.1	0.17	10	850	1,210	1,050
a_c, 0.4 → 0.1	0.028	0.34	0.13	8	965	1,170	1,130
0.4 → 1.0	0.013	2.5	0.15	171	425	1,170	715
No. compartments, 10 → 5	0.015	1.9	0.14	82	645	1,385	880
10 → 20	0.015	0.66	0.12	81	645	1,080	840
Time increment, 1 → 3	0.015	1.1	0.17	81	660	1,180	885
1 → 0.6	0.015	1.1	0.12	81	650	1,165	860
1 → 0.3	0.015	1.1	0.12	81	645	1,160	850
Δt = 0.3, V = 1.53	0.86	1.5	1.02	0	2,170	2,645	2,550
Δt = 1.0, v = 1.53	0.81	1.6	1.06	0	2,200	2,700	2,600
Compartment cleaning time, 3 2	0.015	1.0	0.13	81	650	1,170	855
3 1	0.015	1.0	0.12	82	645	1,165	845
3 0.1	-	-	0.12	82	-	-	830
Reverse flow velocity 0 0.61	0.015	1.1	0.13	81	650	1,325	895
S_E, 400 200	0.015	1.6	0.12	104	495	1,176	776

*Indicated values are (1) the base line levels of Table 4-1 or (2) modifications in base line levels. For example, V, 0.61 → 0.3 means system velocity of Table 4-1 decreased from 0.61 to 0.3 m/min with all other base line values unchanged.

†Refers to time interval between the end of the cleaning cycle and the start of the next.

Reproduced from
best available copy.

The performance characteristics of the system used to determine the importance of various input parameters are average penetration, average pressure drop and the actual length of time between successive cleaning cycles. Penetration will determine whether or not a particular system can meet a given emission requirement. Pressure loss estimates will indicate whether the existing fan capacity and the structural soundness of the baghouse are adequate. Pressure loss and frequency of cleaning will also have a significant bearing on system power requirements and fabric service life.

4.1.4 Identification of Key Variables

According to the results of preliminary screening tests, the following parameters appear to exert the greatest impacts on system performance.

- System face velocity (air-to-cloth ratio), V
- Limiting or maximum permissible pressure drop, P_L
- Inlet particulate concentration, C_i
- Specific resistance coefficient, K_2
- Fractional area cleaned, a_c

4.1.4.1 Face Velocity (Air-to-Cloth Ratio)--

Variations in system face velocity greatly affected average penetration and pressure drop as well as the time between successive cleaning cycles. The largest impact of velocity was on the average penetration, wherein a twofold velocity increase produced approximately a fourfold increase in penetration. This result is not altogether surprising since laboratory tests on filter panels[1] yielded results which indicated that at fabric loadings of 100 g/m^2 and greater, penetration varied as velocity raised to the 2.2 power.

The effects of velocity on average pressure drop and the time between cleanings are interrelated. First, K_2 will increase as the velocity to the

0.5 power as stated earlier. As a result, the dust cake drag will increase in similar fashion. However, since the pressure drop is a linear function of both drag and velocity, the pressure drop across a uniformly loaded filter should increase as the velocity to the 1.5 power. Finally, velocity also exerts a linear impact on the loading rate (mass of material deposited on the filter per unit area per unit time. Thus for a single bag or compartment system, the overall pressure drop would be expected to increase as the 2.5 power of velocity. When the number of bags is increased, however, and sequential cleaning is initiated the velocity effects are less dramatic. An increase in velocity from 0.3 to 0.61 m/min increased the average pressure drop by only 19 percent, as opposed to 400 or 500 percent which would have been predicted based on the preceding analysis. The effect of velocity may have been de-emphasized for the multicompartment systems either because of the number of compartments or the frequency of cleaning. It should be noted, however, that the time between cleaning cycles has been reduced from 672 to 81 minutes which means that the bags are being cleaned five times as much (a matter of concern with respect to service life.)

A further increase in velocity from 0.61 to 1.22 m/min forces the system to clean continuously; i.e., the time between cleaning cycles reduces to zero minutes. This situation arises because the cleaning process cannot keep up with the fly ash deposition rate and still maintain a pressure drop of less than 1000 N/m^2, the preset limit. The increase in velocity from 0.61 to 1.22 m/min also produced a twofold change in the average pressure drop. A third increase in velocity from 1.22 to 1.53 m/min caused an increase in average pressure drop of about 50 percent, roughly equivalent to a velocity exponent of 1.8. It appears that as the time between cleaning cycles decreases the effect of velocity becomes more important in regulating system performance. Under the above conditions, the average performance is dictated mainly by filter system behavior during the cleaning cycle.

4.1.4.2 Limiting Pressure Drop--

Variations in the limiting pressure drop (P_L) at which cleaning is initiated produced foreseeable results in the average pressure drop. An increase in limiting pressure drop causes an increase in the average pressure drop. Average penetration varies inversely with pressure changes. System penetration is generally higher during the cleaning cycle than during the filtration period between cycles. During cleaning, the flow from one compartment is diverted to the remaining on-line compartments thereby increasing the average velocity. Also, a cleaned compartment returned to service presents much less resistance to air flow than an uncleaned compartment and the velocity through the cleaned portions of the compartment is much higher than through the rest of the baghouse. High velocity and low fabric loadings both serve to increase penetration. During the period between cleaning cycles, the velocities in each compartment tend to equalize as fabric loadings increase. Therefore, penetration will decrease as time increases during the extended filtration period. Referring to Table 8, as the limiting pressure drop increases, the time between cleaning cycles also increases. As this time increases, the high penetration levels produced during cleaning become, in effect, diluted by the much lower levels associated with extended filtration periods.

4.1.4.3 Inlet Dust Concentration--

The greatest impact of variations in inlet particulate concentration is on the time between cleaning cycles, due mainly to fabric loading rate changes. The time between cleanings affects the importance of cleaning cycle penetration relative to the penetration during the extended filtration period and, consequently, affects average penetration. An increase in inlet concentration, C_i, from 2.29 to 22.9 g/m^3 also produced a small increase, ~ 30 percent, in the average pressure drop.

4.1.4.4 Fabric Cleaning Parameter--

Variations in the cleaning parameter, a_c, (the fractional area cleaned) produced significant changes in the time between cleanings and, to a lesser extent, changes in the average pressure drop. The time between cleaning cycles would be expected to decrease as the amount of dust removed from the bags is decreased, (i.e., smaller a_c) since less dust must be added to the bags to reestablish the previous loading conditions. With less dust removal the system would operate at a larger average fabric loading and therefore, a larger average pressure drop. Average penetration was not greatly affected by changes in a_c. Although higher local velicities through the cleaned area are expected when a_c is reduced (and thus higher local penetrations) the fact that the fraction of air passing through the cleaned region is reduced minimizes dust contributions from these areas. Hence, the impact on overall emission rate is relatively small.

4.1.4.5 Number of Compartments--

The number of compartments was varied between 5 and 20 with little effect on performance. The maximum pressure drop and maximum penetration increased as the number of compartments decreased. However, this effect is often diminished when the extended filtration period and the cleaning cycle are incorporated into an average value. The effect of changes in the number of compartments should be more pronounced in continuously cleaned systems.

4.1.4.6 Time Increment for Iterations--

Due to the iterative nature of the model calculations, a time increment must be determined before any calculations can be performed. The results of the calculations performed at any time (t) in the cycle are also used as input to the calculations for a time ($t + \Delta t$), the next iteration period. Furthermore, computed values for system parameters such as local drag and velocity are held constant for the ($t + \Delta t$) interval. Therefore, in situations where local velocity, drag or deposition rates undergo rapid changes, too large a value for the time increment may reduce the accuracy of predictions. The results of the tests performed to investigate the sensitivity of predicted performance to time increment duration are presented in Table 8. In only one case was penetration severely affected by changes in the time increment; i.e., Δt of 3 minutes. Little effect was observed with regard to pressure drop or time between cleanings. For the compartment cleaning time of 3 minutes cited in the "baseline" test data of Table 7, an iteration time of 3 minutes means that all system variables are held constant from the time a cleaned compartment is returned to service until the next compartment to be cleaned is returned to service.

Since local face velocity and drag are likely to change more rapidly during a cleaning cycle than during the extended filtration period, extended averaging periods may conceal important transient changes in system performance. Therefore, additional tests were performed for time increments of 0.3 and 1.0 minutes at a face velocity of 1.53 m/min. The above iteration times had little effect on average penetration or pressure drop for the latter tests with respect to a constant face velocity.

4.1.4.7 Compartment Cleaning Time and Reverse Flow Velocity--

Compartment cleaning time (off-line time) and reverse flow velocity had little or no effect on system performance. The main effect of increasing reverse flow velocity from 0 to 0.61 m/min was to increase the maximum pressure drop from 1165 to 1325 m/m^2. However, the average pressure drop increased by only 4 percent. The effect of reverse flow velocity is expected to be more evident in a continuously cleaned system. This follows from the fact that dust penetration, which is highly velocity sensitive, is greatest during the cleaning intervals. With no dimunition of overall penetration by extended noncleaning intervals, the maximum velocity impact is shown in the emissions.

Based on the results of the preliminary tests, a series of tests was performed in which the four key parameters were varied independently with the remaining parameters held constant. The results of these tests are discussed in the next section.

4.2 MULTIVARIABLE SENSITIVITY TESTS

4.2.1 Introduction

The special tests described in this section serve two purposes. First, they indicate how accurately various input parameters should be measured to estimate filter system performance within acceptable error boundaries. Second, they show how various combinations of variable changes interact in determining overall filter system performance.

Each of those parameters that were found to have a significant effect on the predicted system performance were varied over the ranges listed in Table 9. Different combinations of the values for the parameters listed in the table were used as inputs to the model with all remaining parameters (see Table 7) held constant.

TABLE 9. VALUES OF KEY PARAMETERS USED IN SENSITIVITY ANALYSES*

Velocity (V) (m/min)	Limiting pressure drop (P_L) (N/m^2)	Inlet concentration (C_i) (g/m^3)	Fractional area cleaned (a_c)
0.3	500	2.29	0.1
0.61	1,000	6.87	0.4
(0.91)†	1,500	22.9	1.0
1.22	2,000	-	-
1.53	(2,500)†	-	-
(1.75)†	-	-	-

*Not all combinations of all variables were tested.

†Only used when results of other tests warranted further investigation.

Certain variable combinations were excluded from the sensitivity testing because they appeared to be well beyond the range of any practical field conditions. For example, with a continuously cleaned system involving the following input parameters; $V = 1.75$ m/min, $C_i = 22.9$ g/m^3, and $a_c = 1.0$, pressure drop and penetration values would have been unacceptable in any real situations. In other cases, extrapolation from a partial test array was sufficient to depict the entire range of variable combinations of interest.

The results of all tests are presented in Appendix B in tabular form and in Figures 13 through 34. Average pressure drop and penetration (for an entire cycle) have been plotted as functions of system velocity for various pressure-drop-controlled and continously cleaned systems in Figures 13 through 26. The time between cleaning cycles is presented as a function of the same variables in Figures 27 through 33. Each of the Figures 13 through 33 represents a system of constant inlet concentration, C_i, and cleaning intensity, a_c. From these figures, the variations in system performance due to changes in operating conditions can be determined, estimates of the performance characteristics for a given system can be made, or values for system operating parameters to achieve a specific emission or pressure limitation can be determined. Interpolation is necessary for any system not operating at the inlet dust concentrations or cleaning levels for which the curves were developed. To simplify the interpolation procedure and, also, to present a broader description of the relationships between operating and performance parameters, the results of the sensitivity tests have been replotted in several alternate formats. The resultant curves are presented in Appendix C. The data have been plotted for selected combinations of C_i, V and P_L and

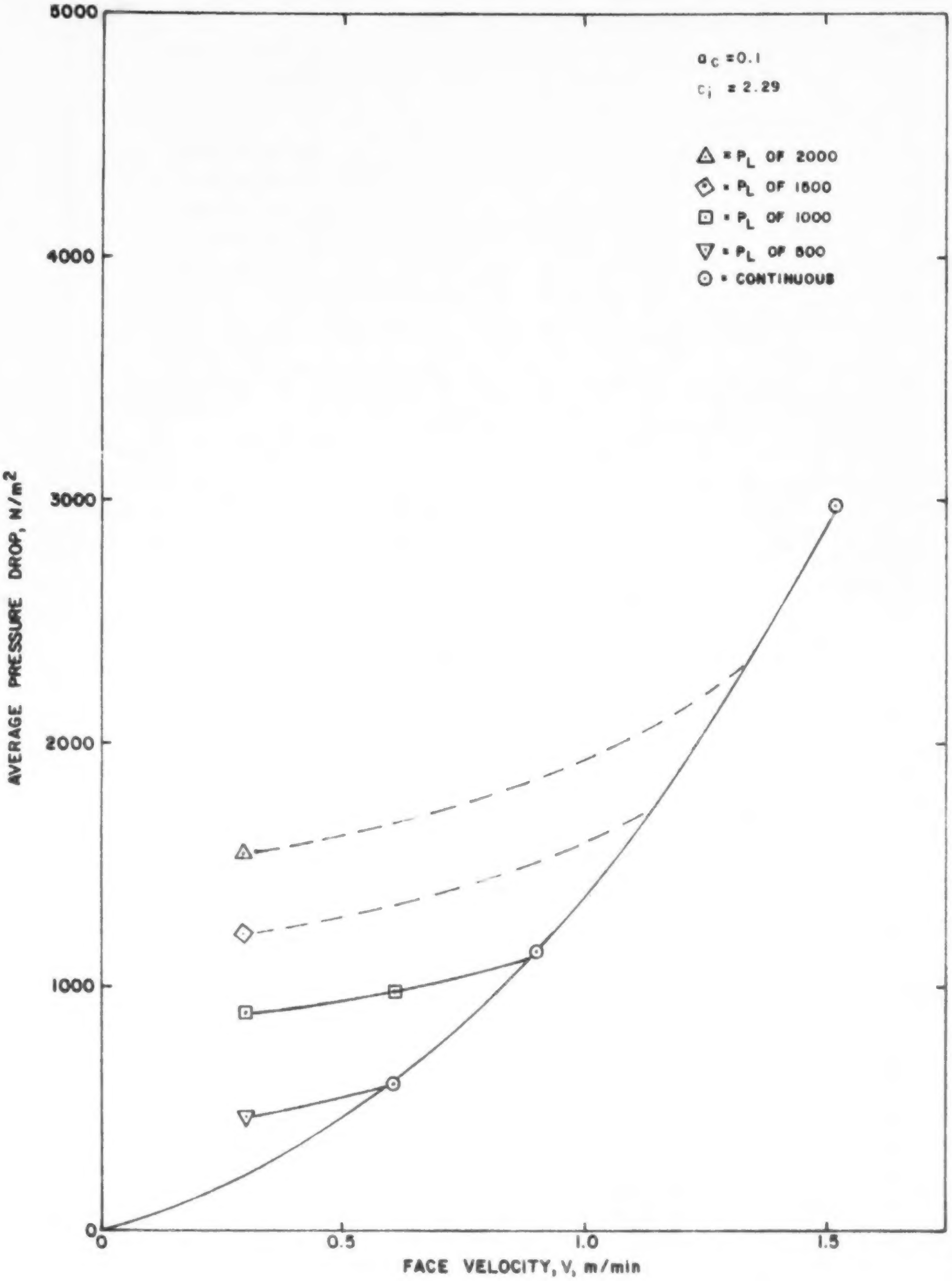

Figure 13. Effect of face velocity and limiting pressure drop on average pressure loss.

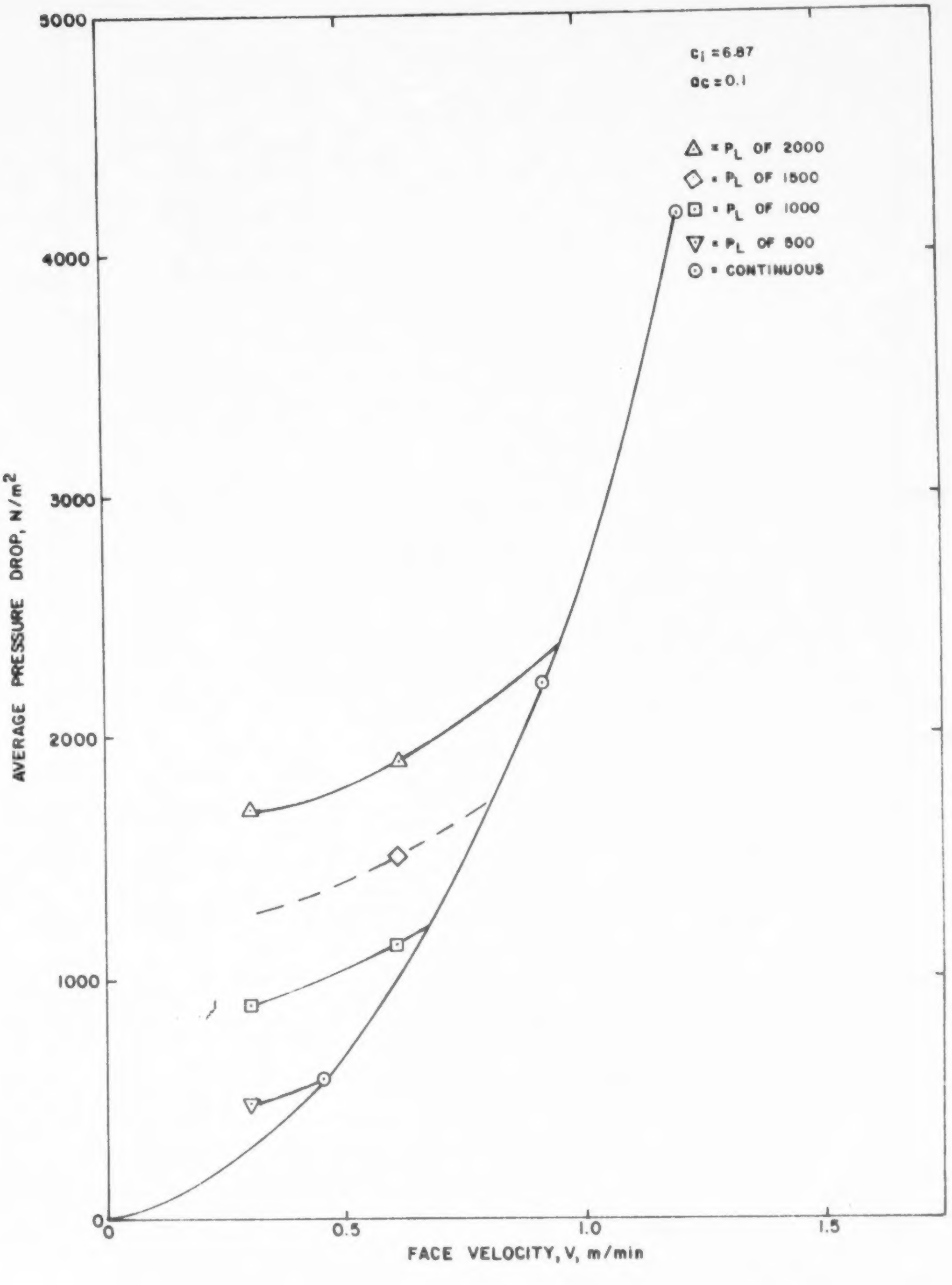

Figure 14. Effect of face velocity and limiting pressure drop on average pressure loss.

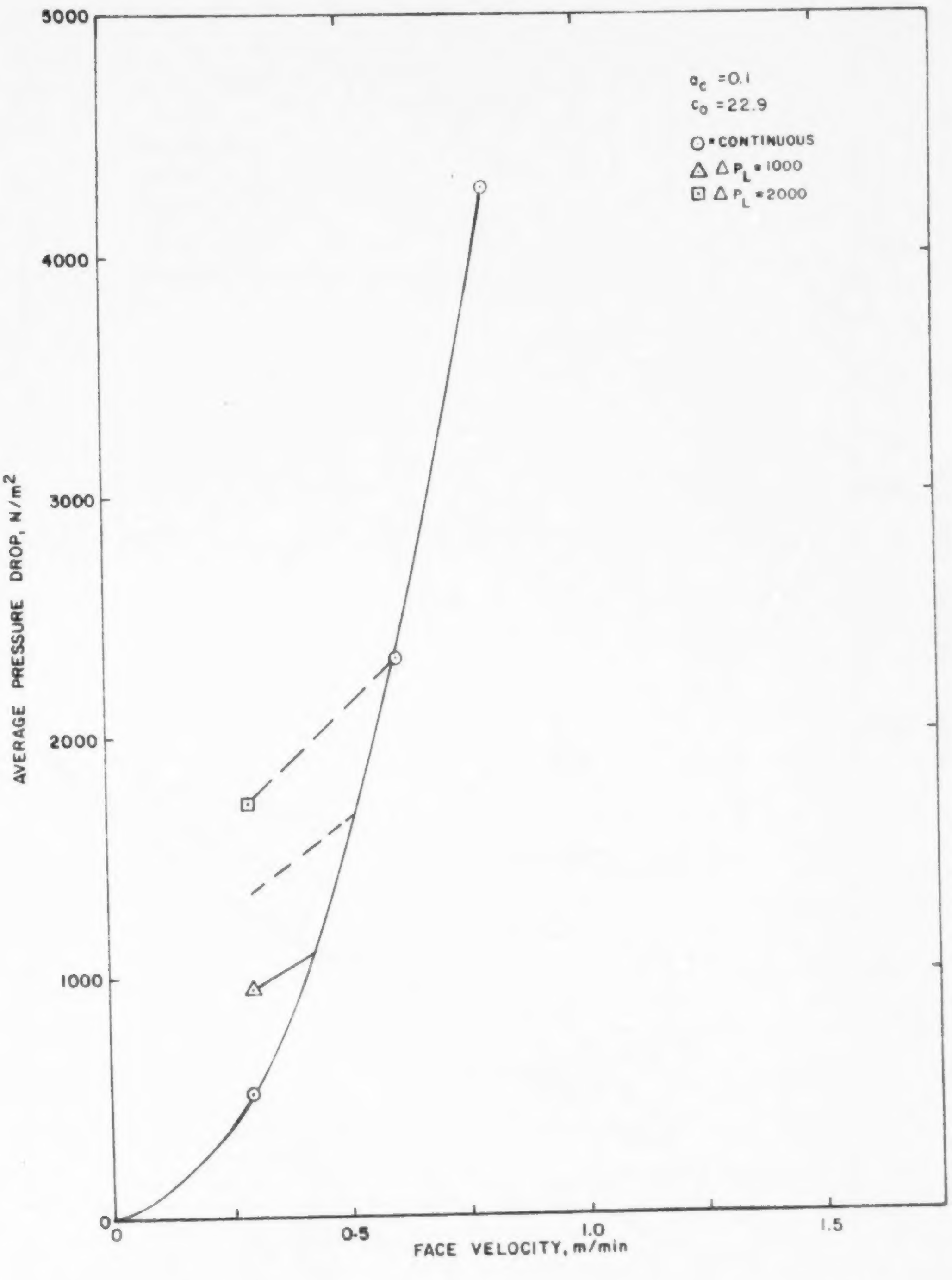

Figure 15. Effect of face velocity and limiting pressure drop on average pressure loss.

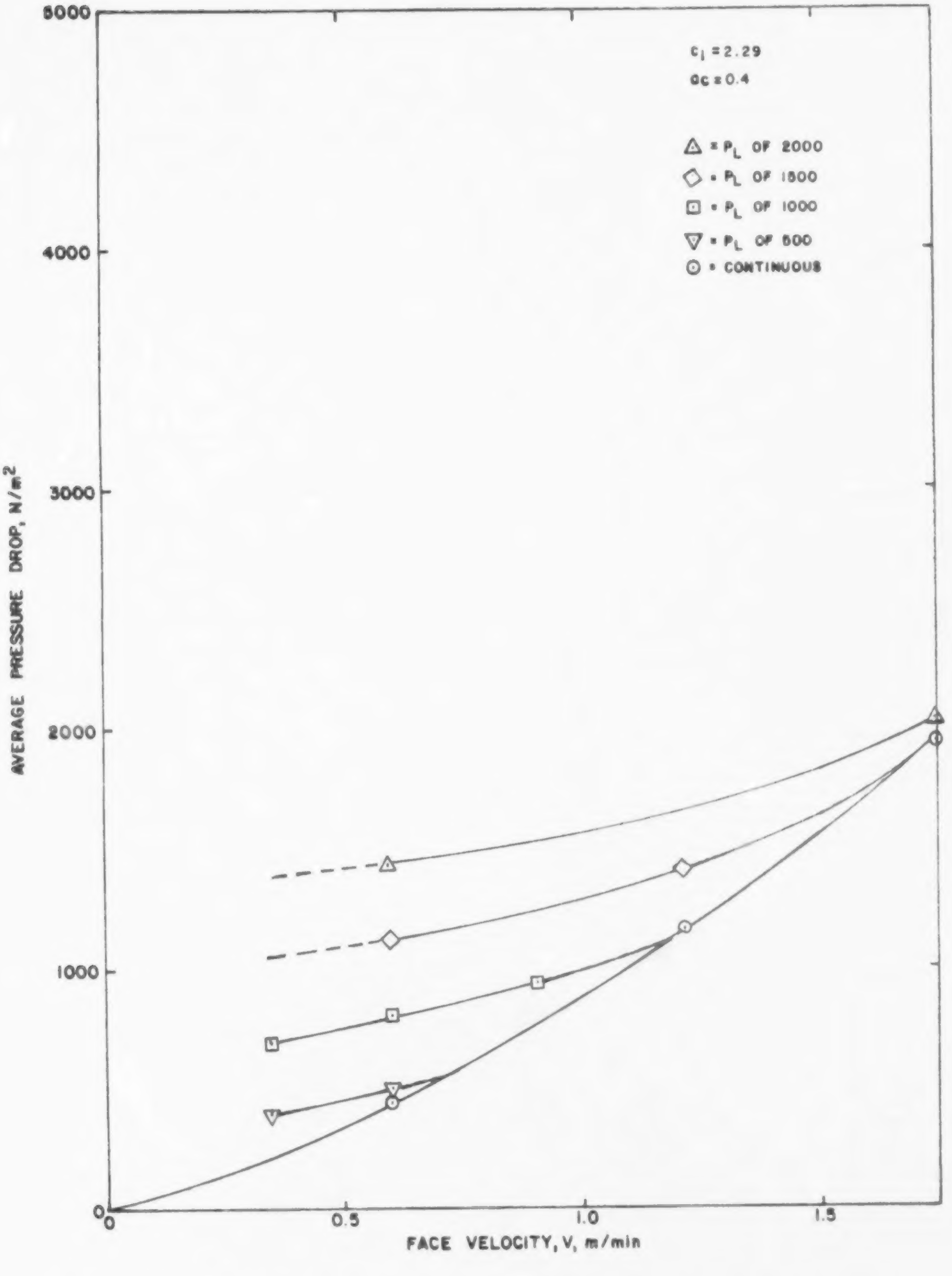

Figure 16. Effect of face velocity and limiting pressure drop on average pressure loss.

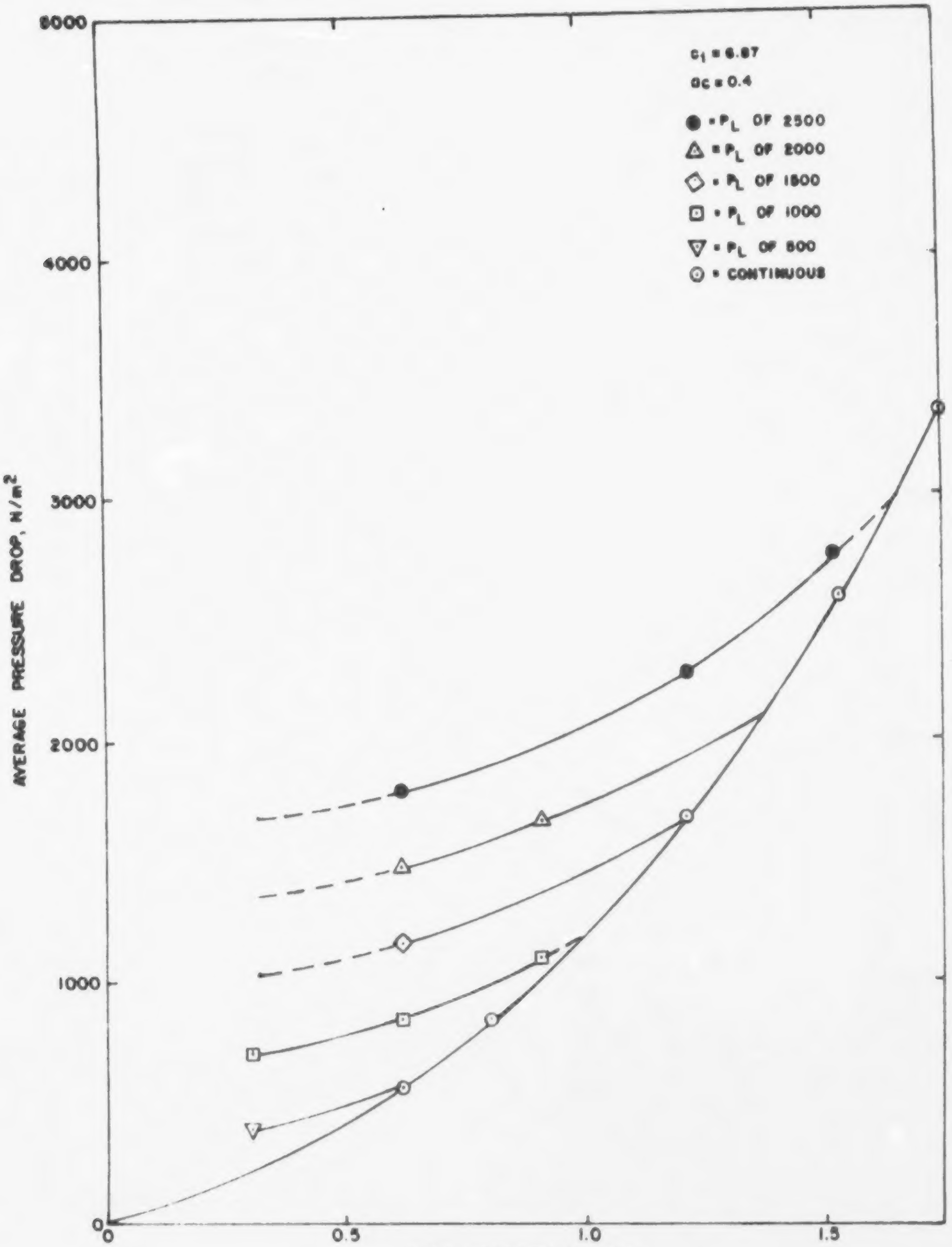

Figure 17. Effect of face velocity and limiting pressure drop on average pressure loss.

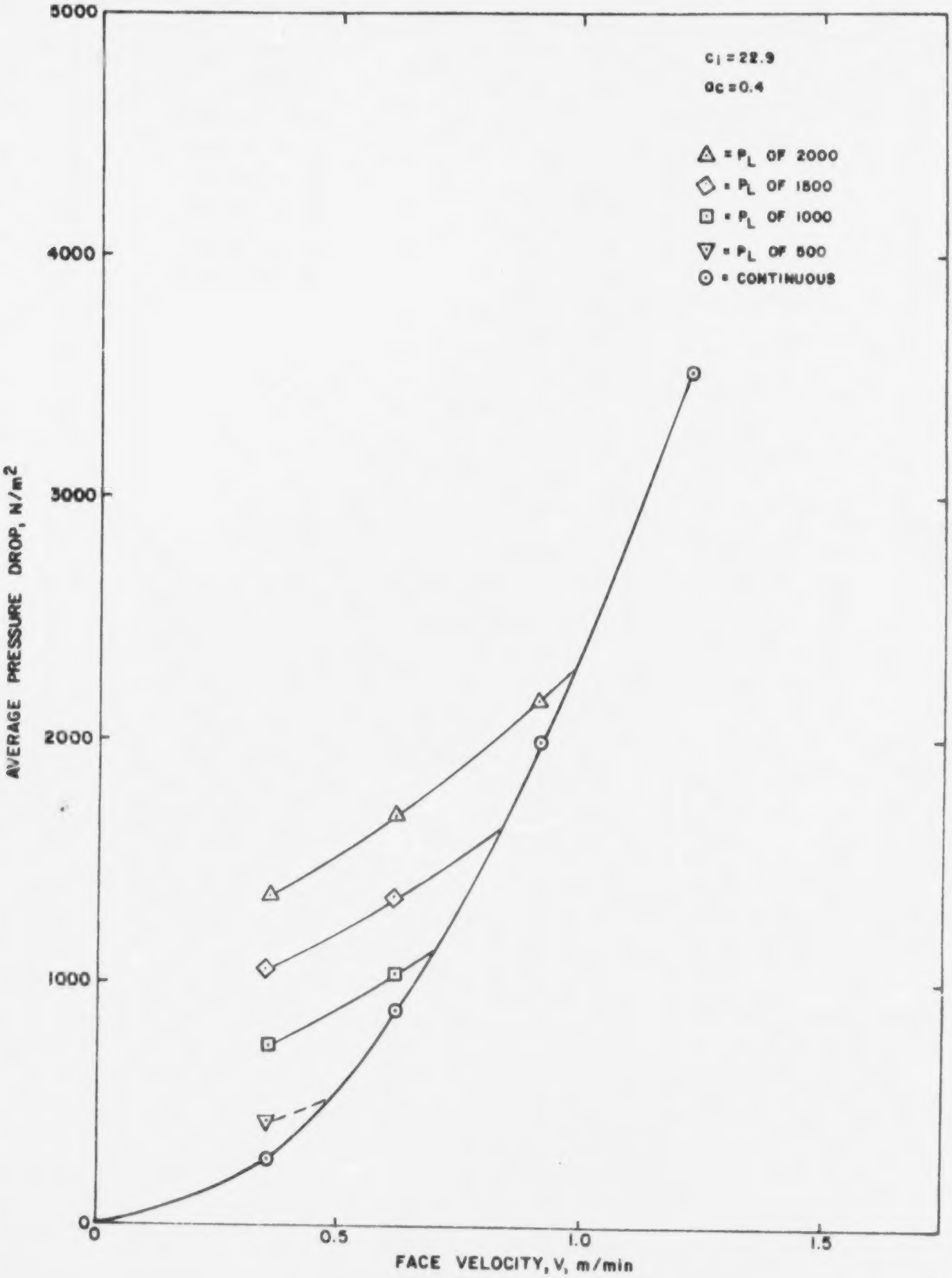

Figure 18. Effect of face velocity and limiting pressure drop on average pressure loss.

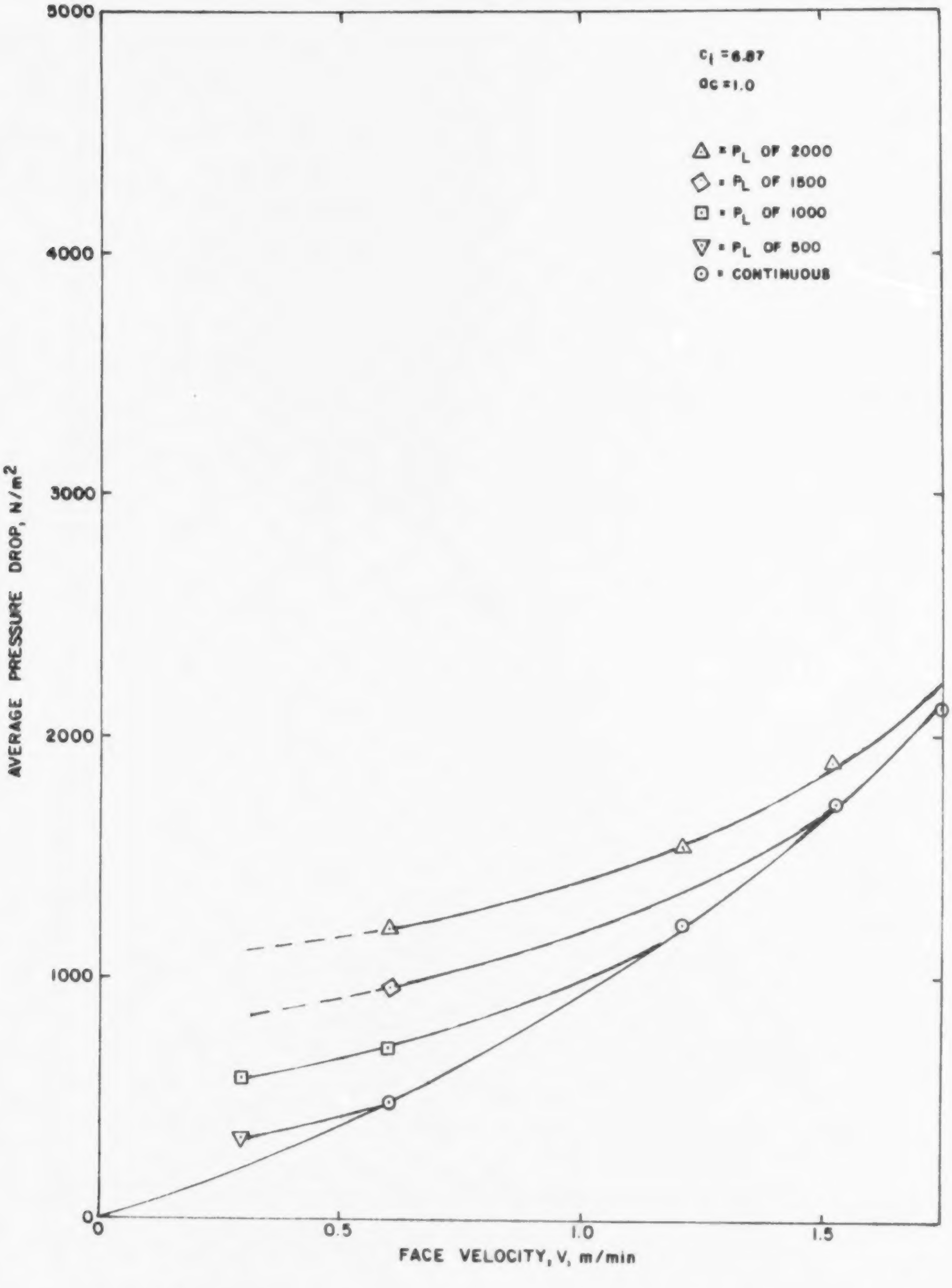

Figure 19. Effect of face velocity and limiting pressure drop on average pressure loss.

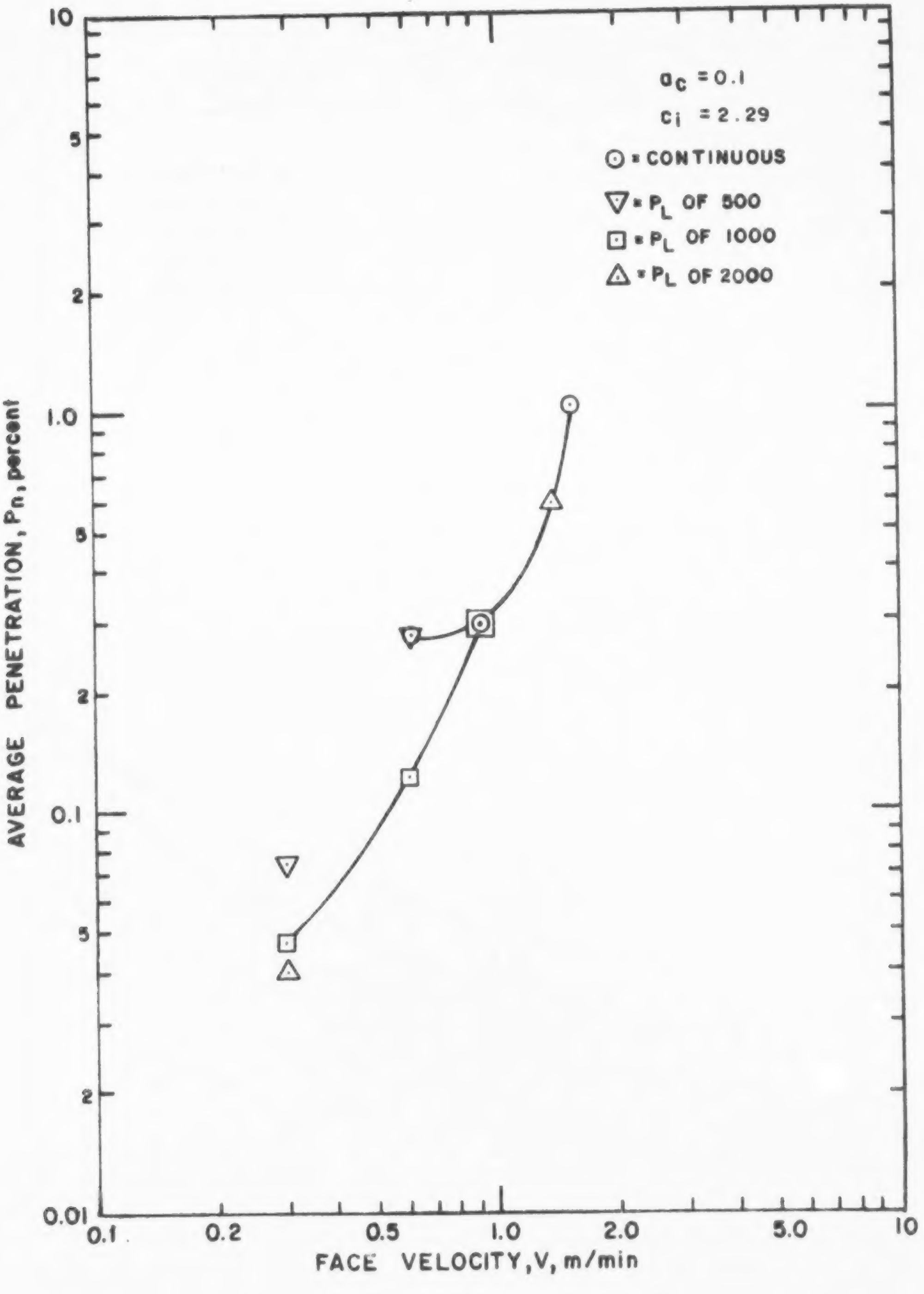

Figure 20. Effect of face velocity and limiting pressure drop on average penetration.

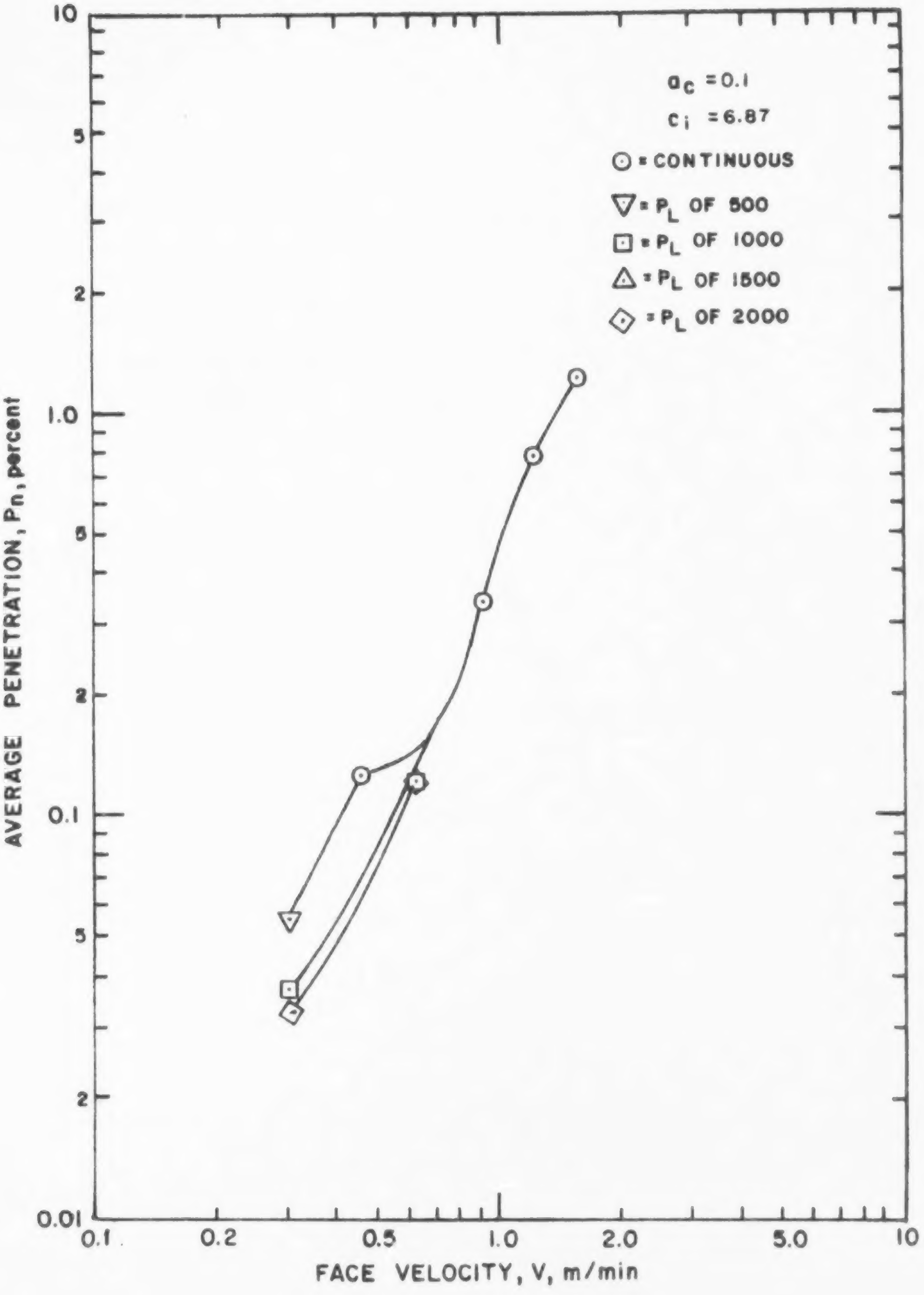

Figure 21. Effect of face velocity and limiting pressure drop on average penetration.

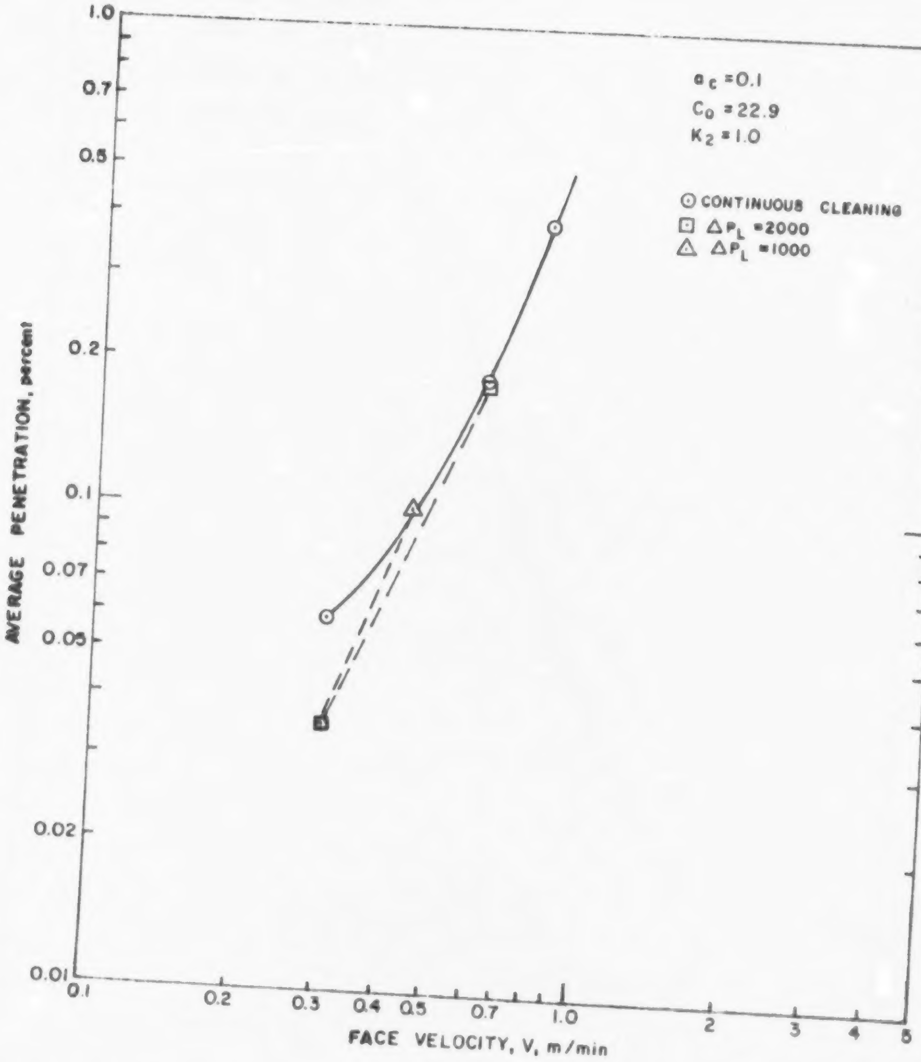

Figure 22. Effect of face velocity and average pressure drop on average penetration.

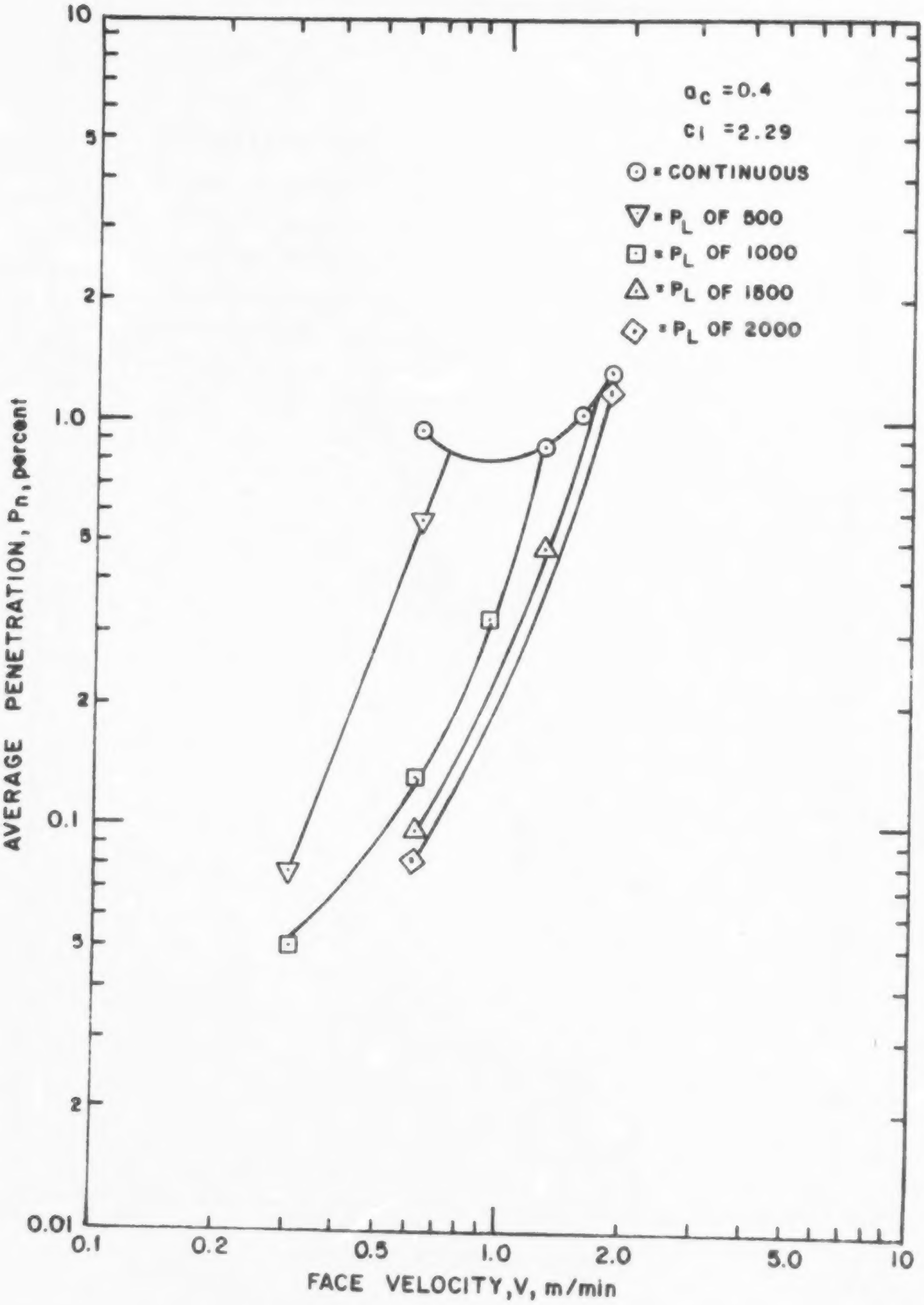

Figure 23. Effect of face velocity and limiting pressure drop on average penetration.

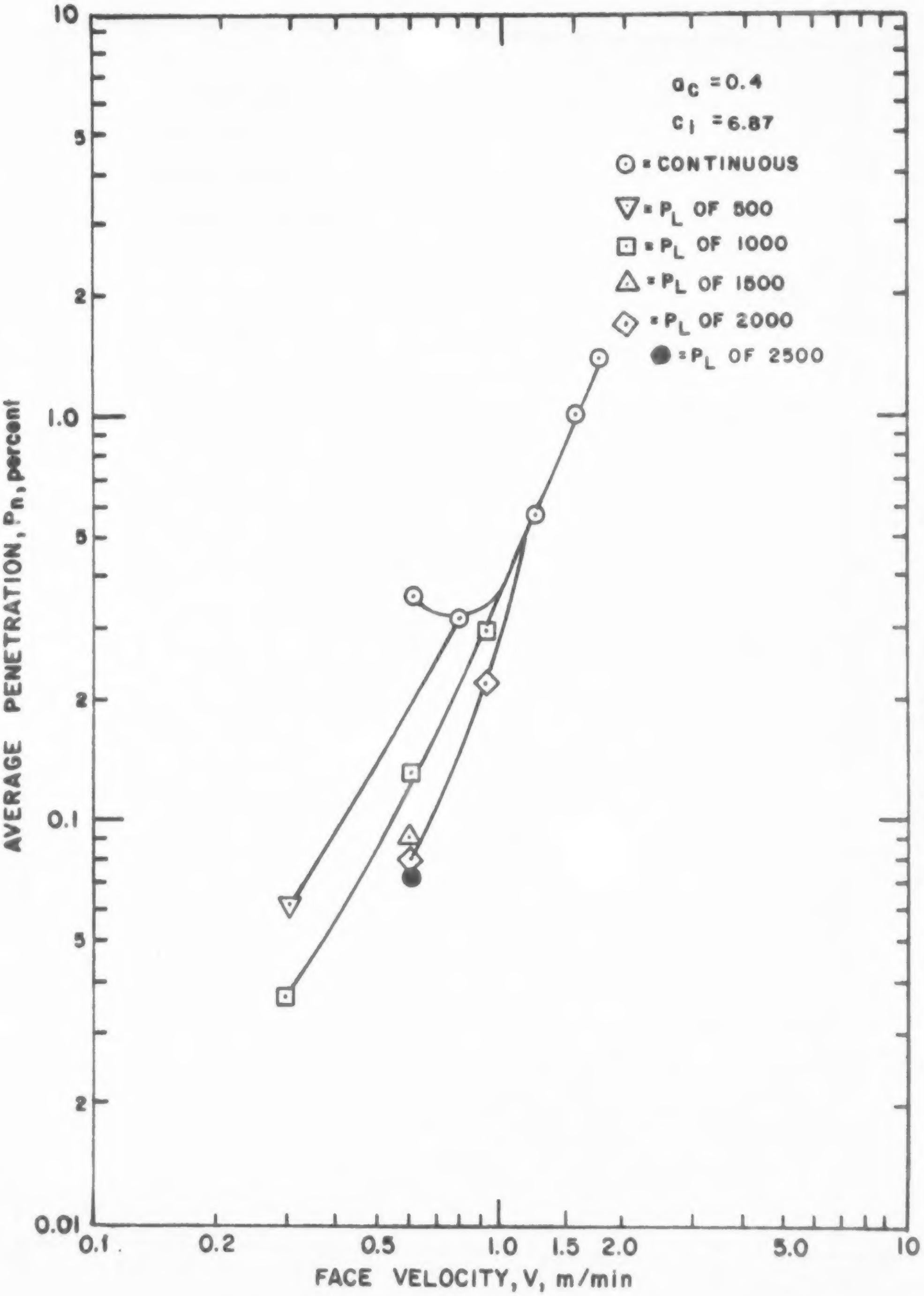

Figure 24. Effect of face velocity and limiting pressure drop on average penetration.

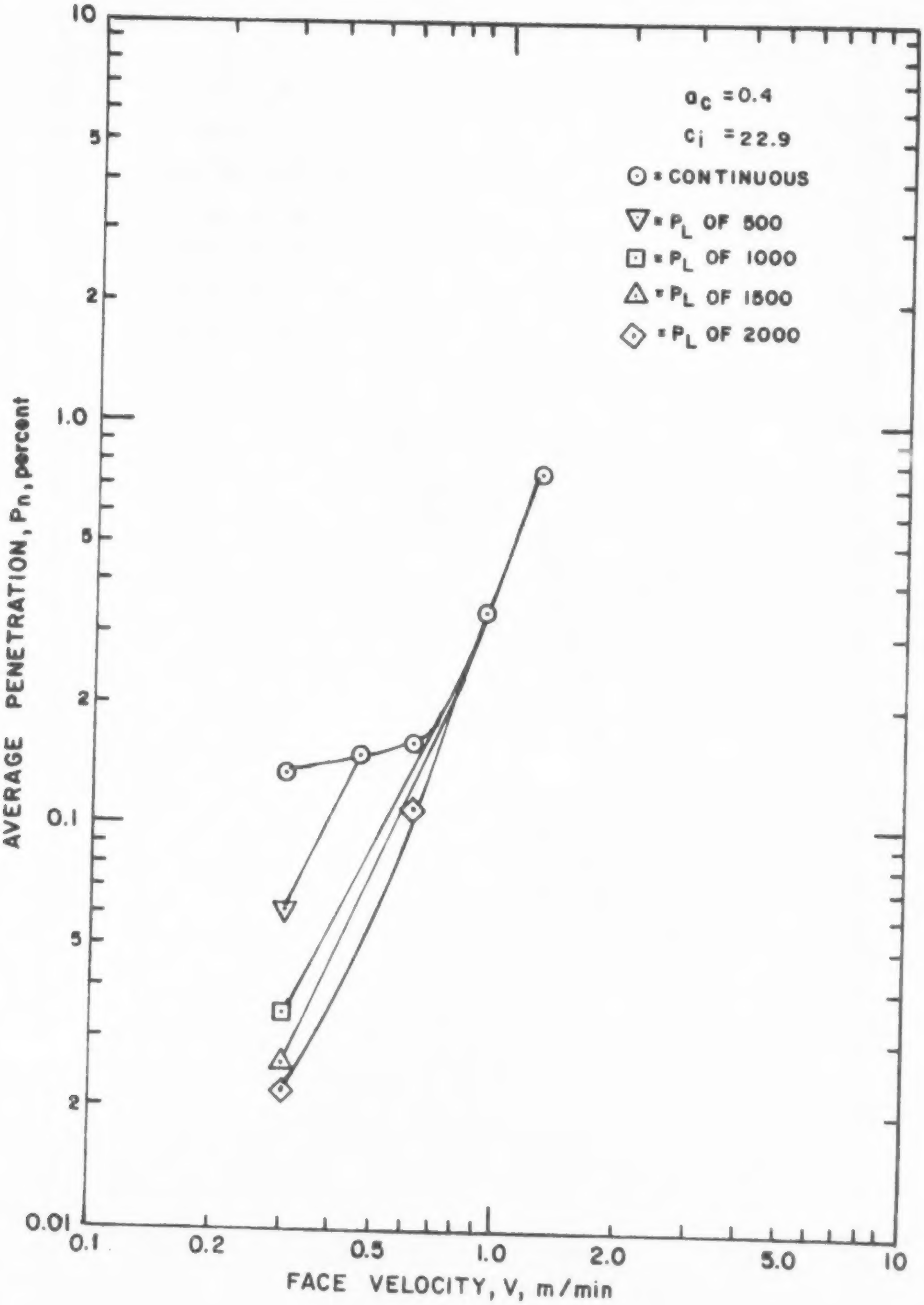

Figure 25. Effect of face velocity and limiting pressure drop on average penetration.

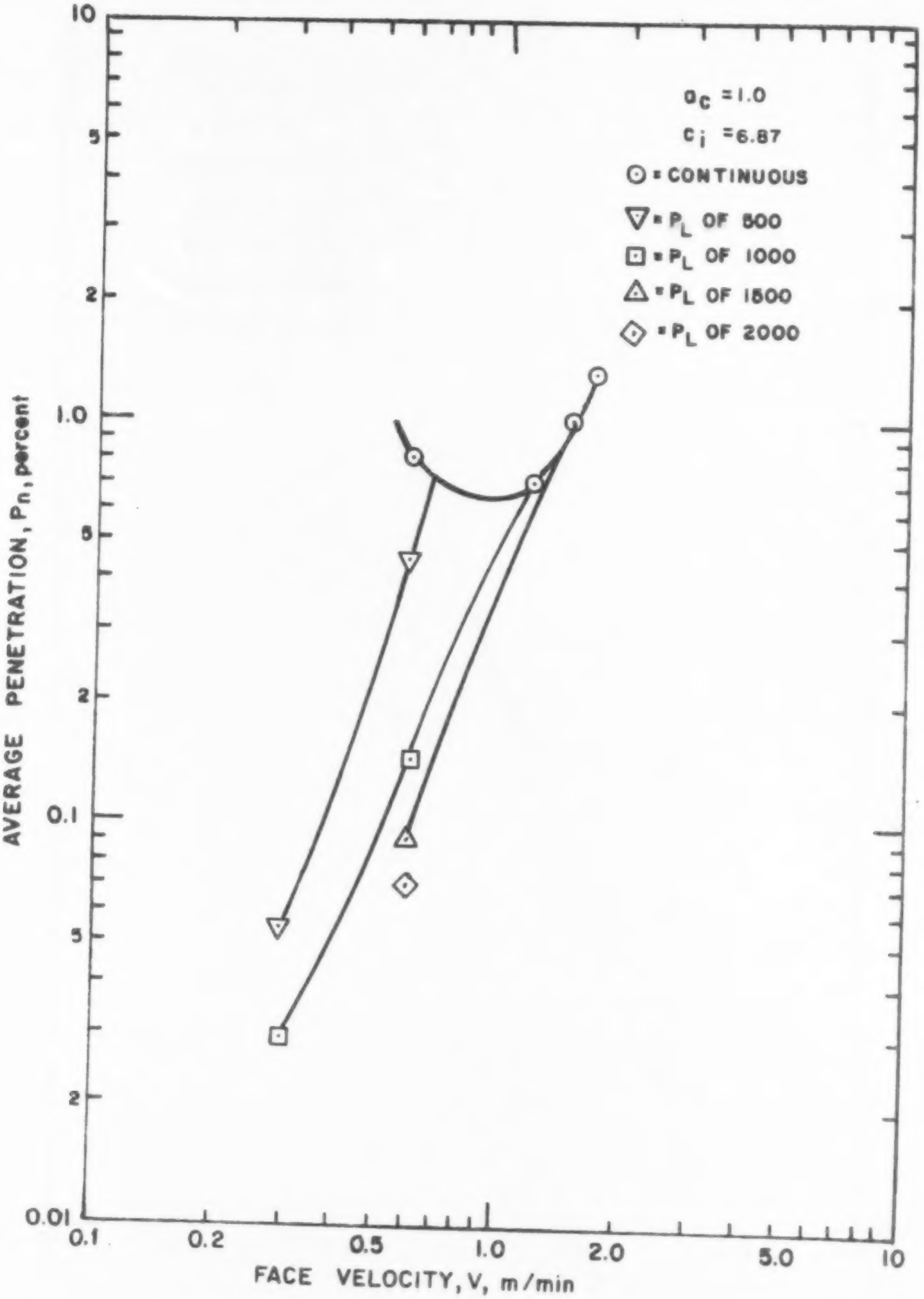

Figure 26. Effect of face velocity and limiting pressure drop on average penetration.

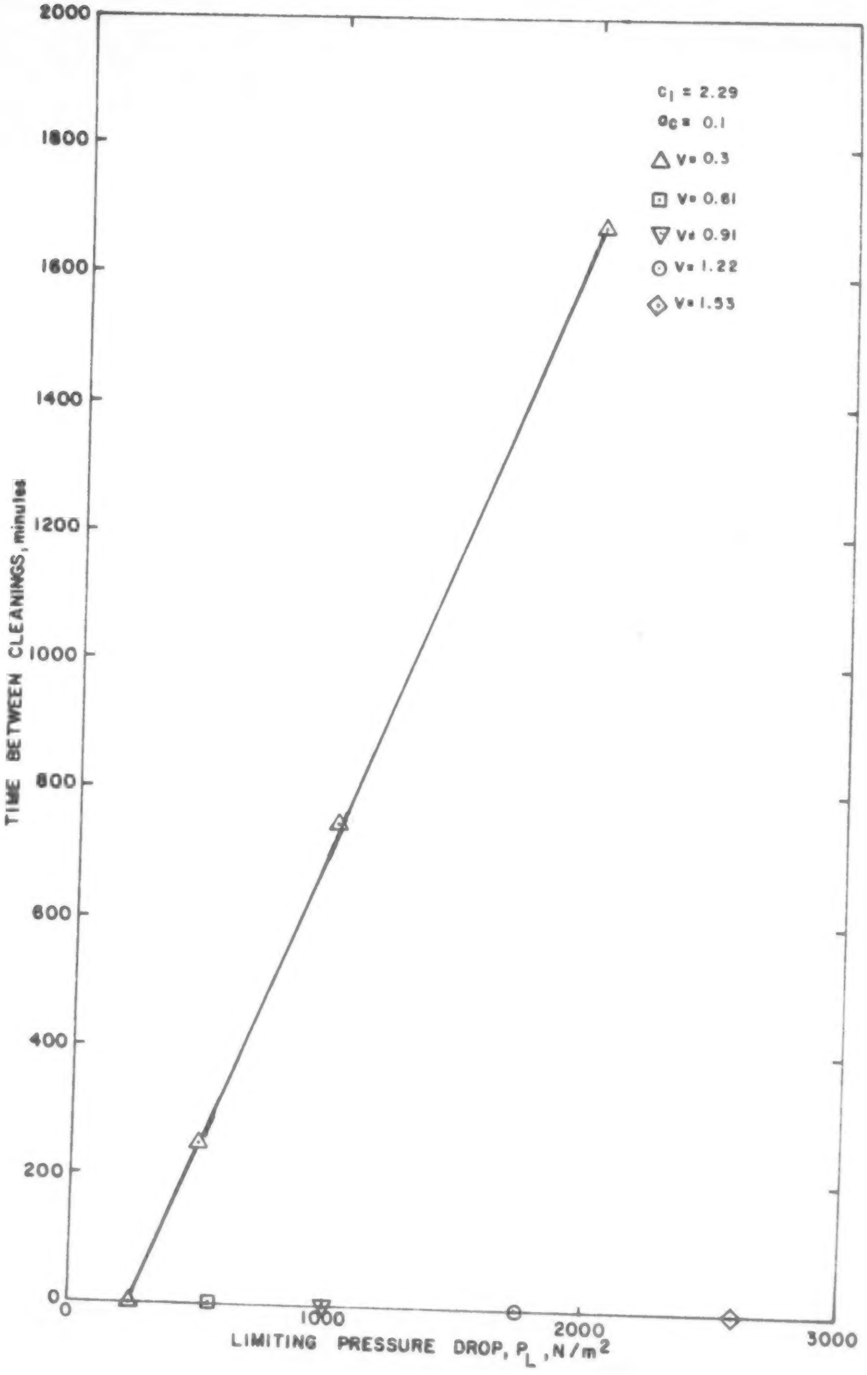

Figure 27. Relationship between time between cleaning cycles, limiting pressure loss and face velocity.

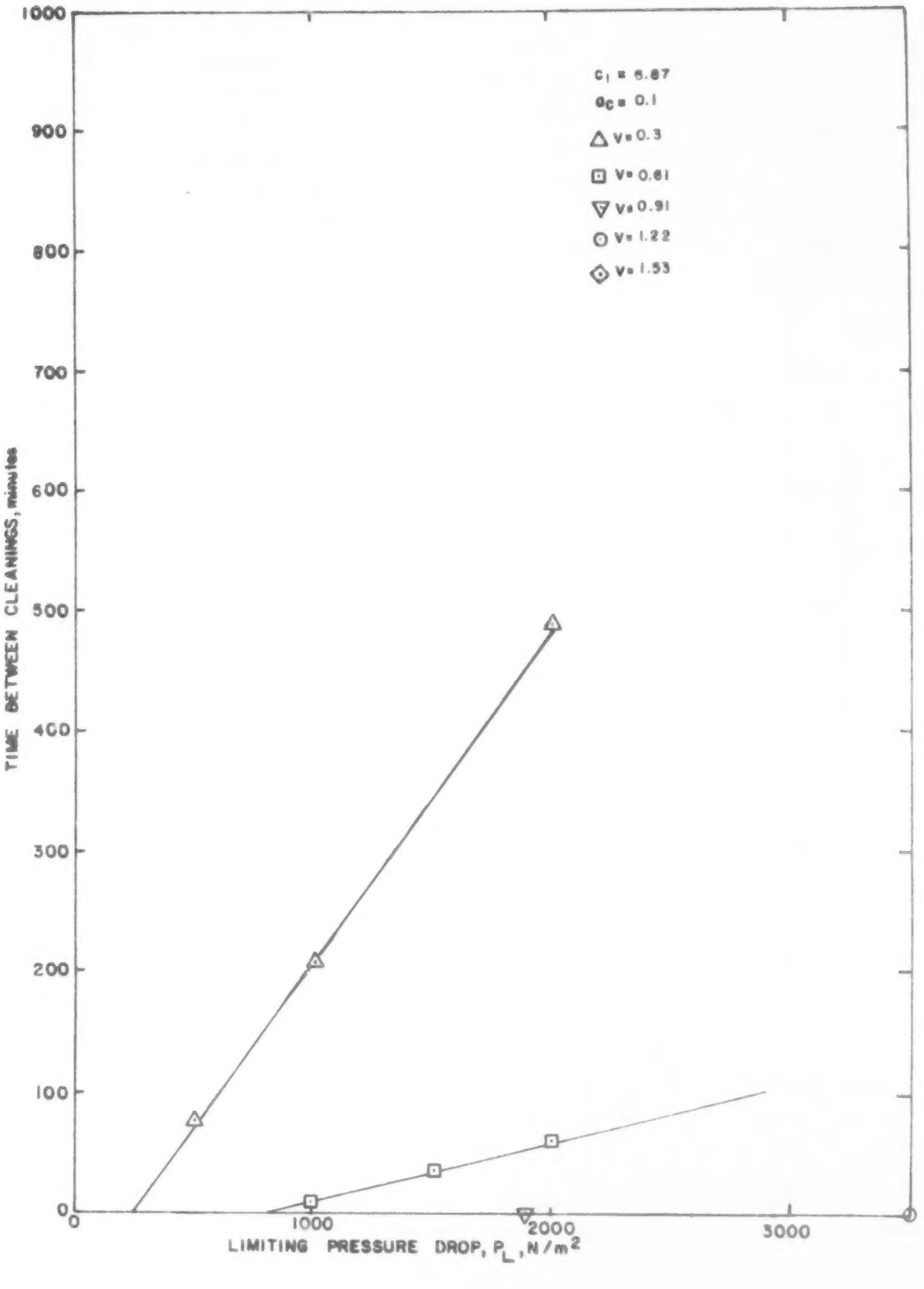

Figure 28. Relationship between time between cleaning cycles, limiting pressure loss and face velocity.

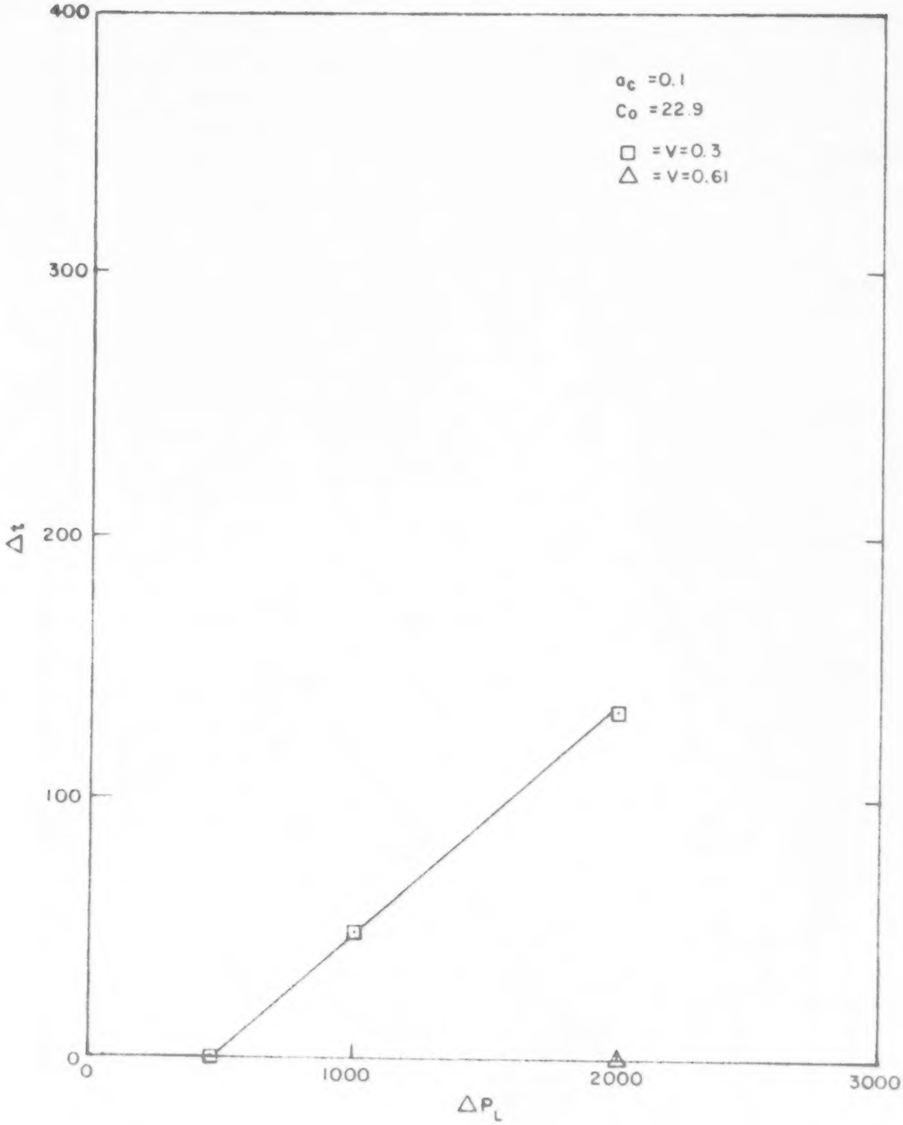

Figure 29. Relationship between time between cleaning cycles, limiting pressure loss and face velocity.

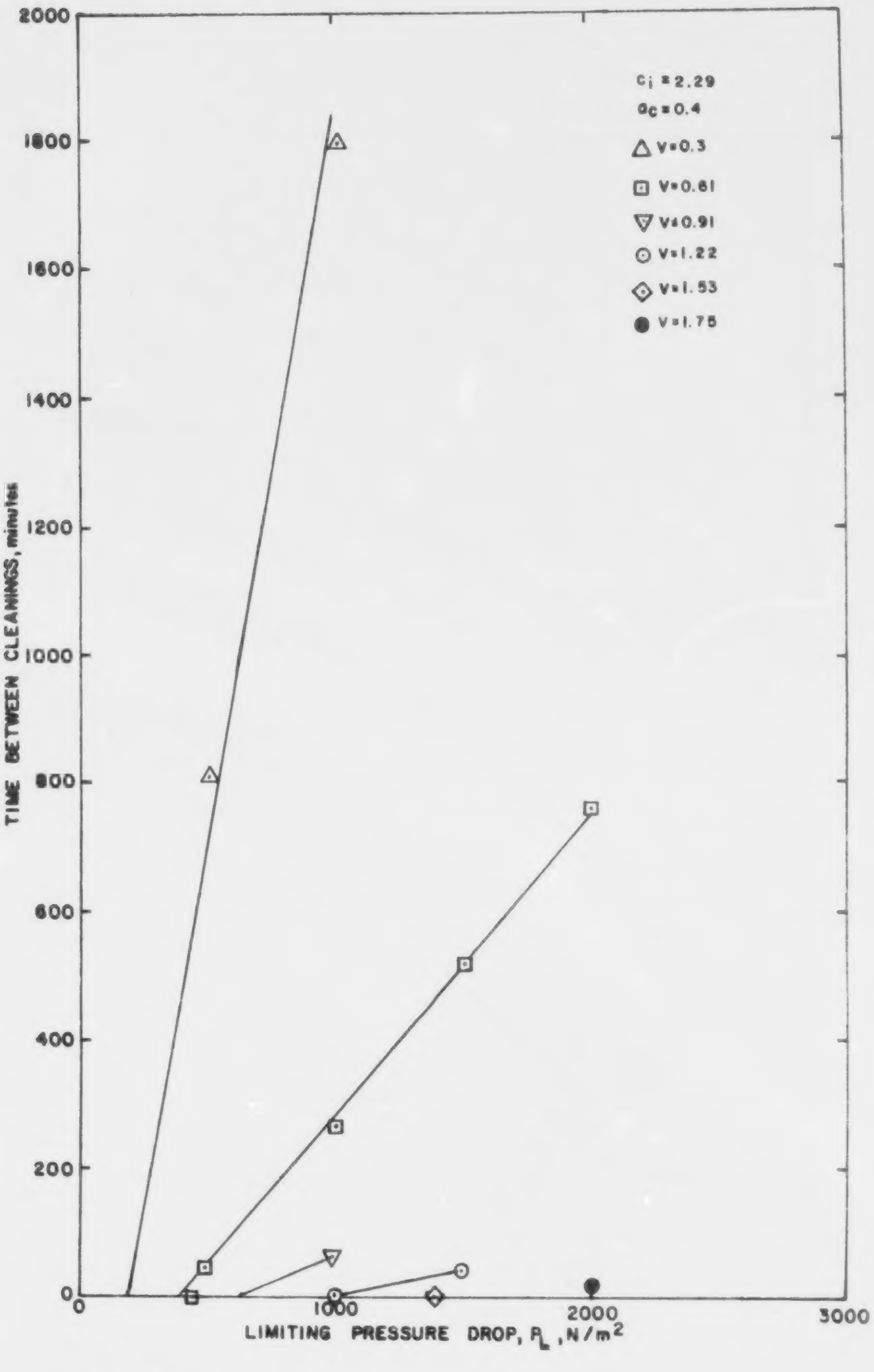

Figure 30. Relationship between time between cleaning cycles, limiting pressure loss and face velocity.

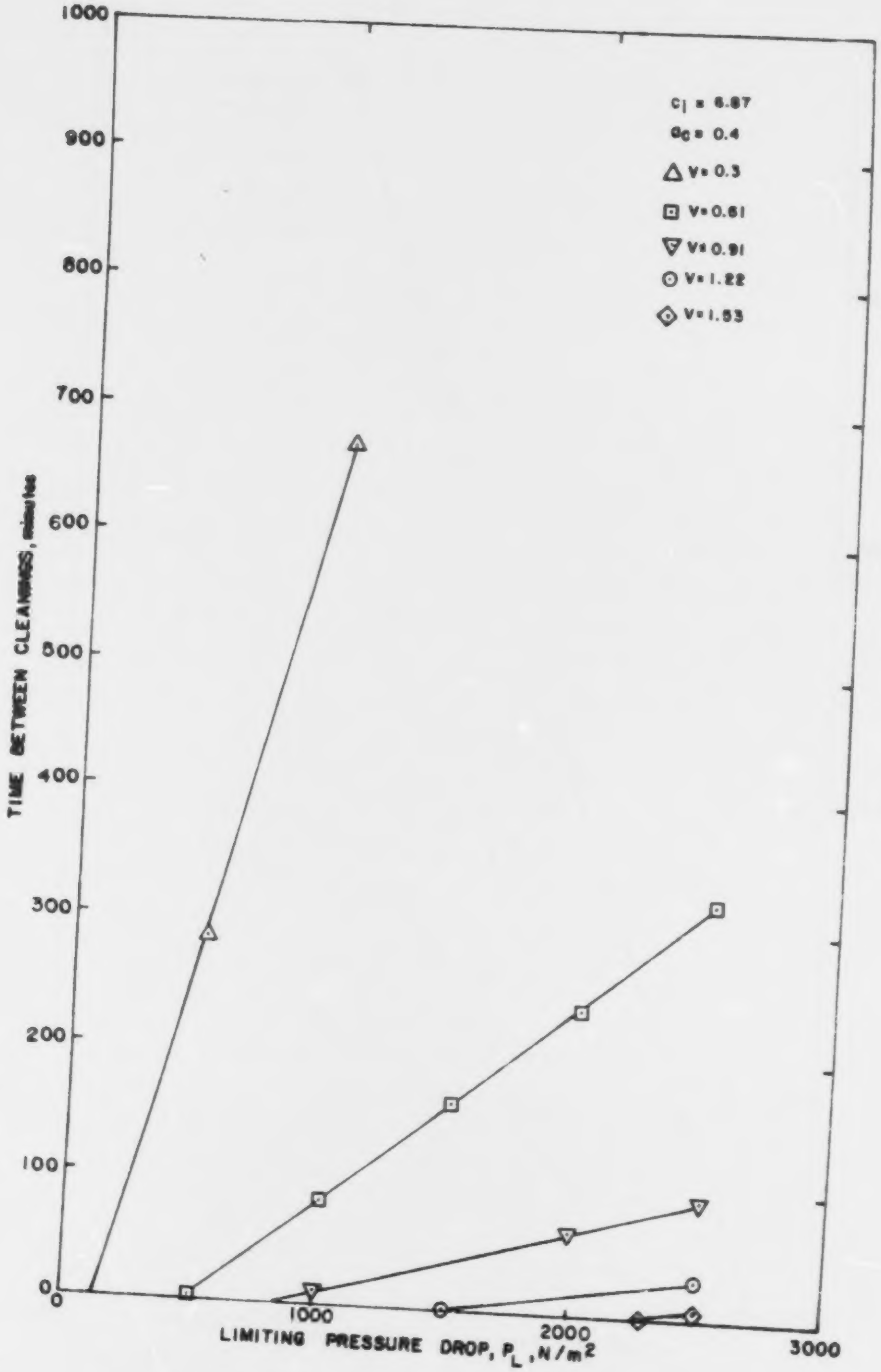

Figure 31. Relationship between time between cleaning cycles, limiting pressure loss and face velocity.

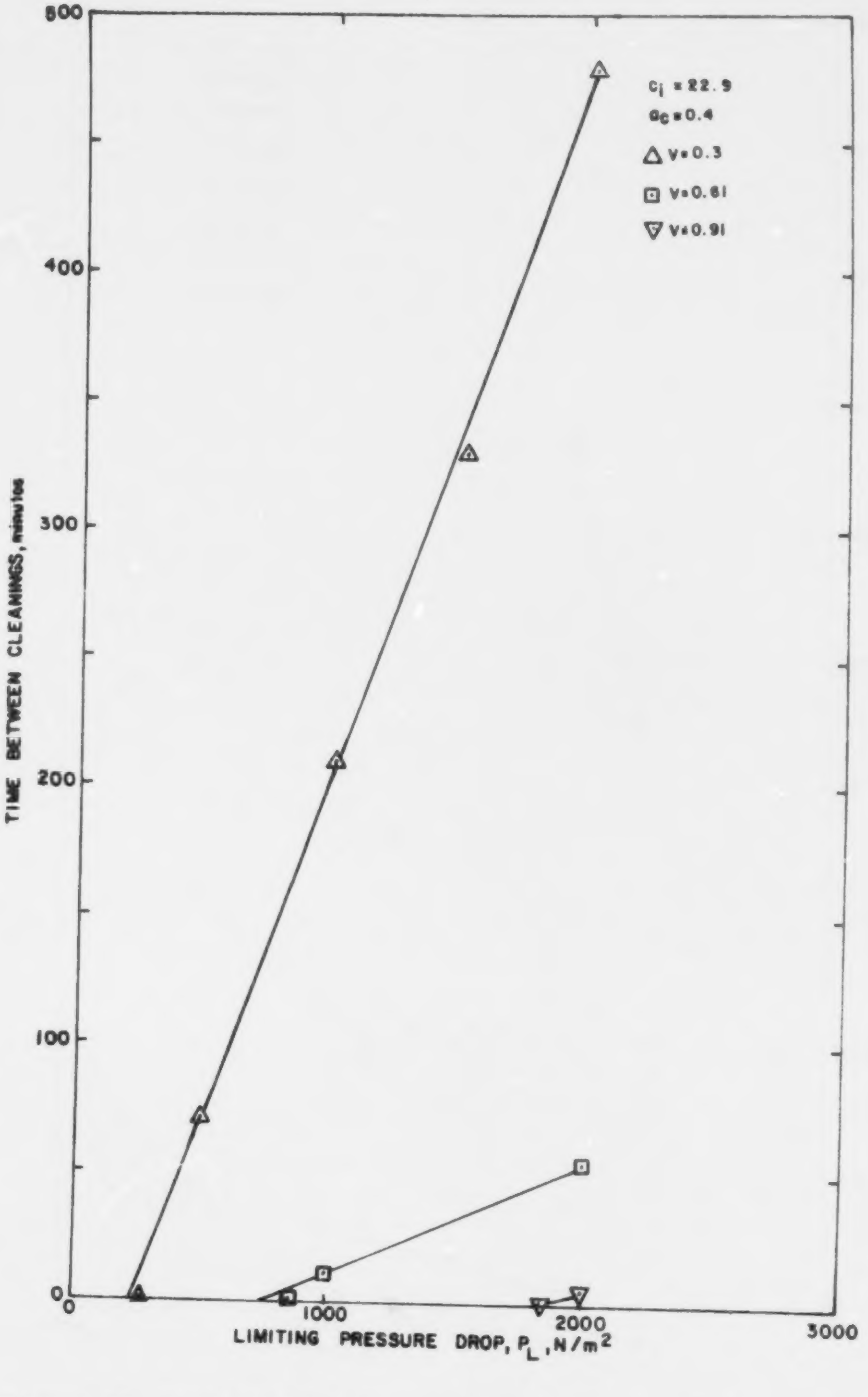

Figure 32. Relationship between time between cleaning cycles, limiting pressure loss and face velocity.

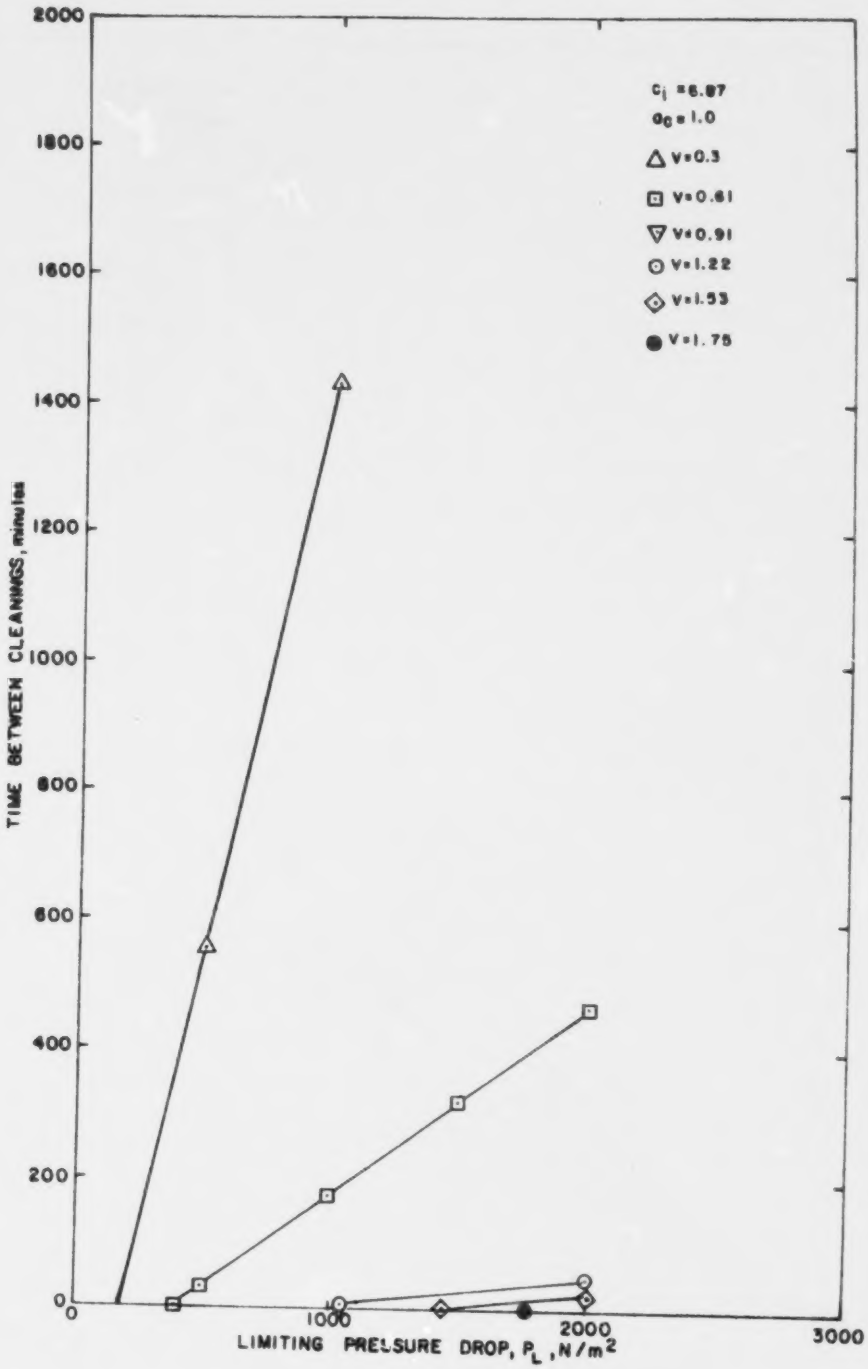

Figure 33. Relationship between time between cleaning cycles, limiting pressure loss and face velocity.

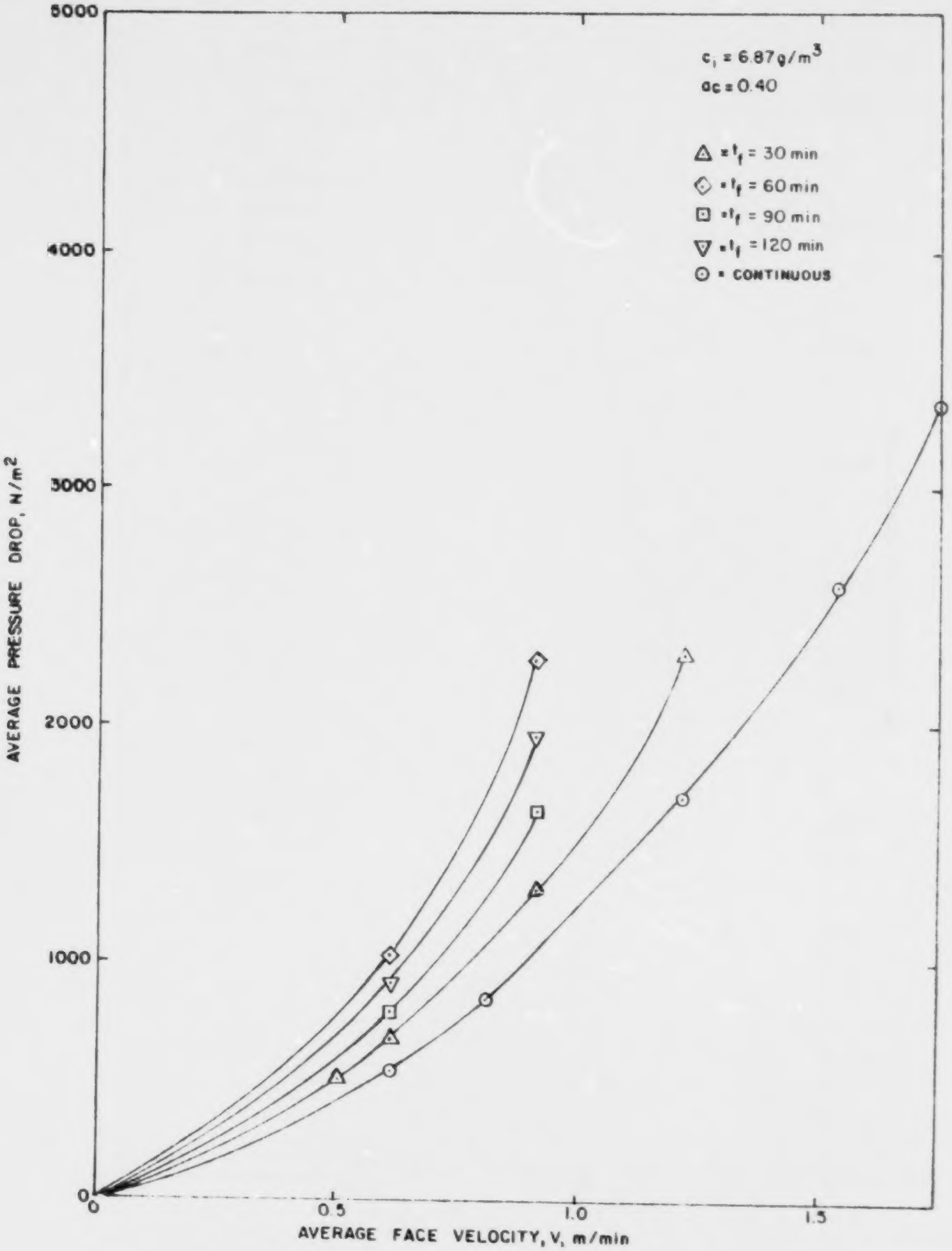

Figure 34. Effect of velocity on average pressure loss for timed cleaning cycle systems.

a_c, V and P_L. The use of figures shown in Appendix C and those presented here will be discussed later in this section. Before discussing graph applications, however, their development and interpretation will be reviewed in the following paragraphs.

4.2.2 Description of Graphs Developed from Sensitivity Analyses

4.2.2.1 Average Pressure Drop--

As stated previously, Figures 13 through 19 are graphs of average system pressure drop versus velocity. The figures represent fabric filter systems with fixed inlet concentrations (C_i) and cleaning parameters (a_c). In each figure, average system pressure drops for various combinations of velocity and limiting pressure drop are presented. The value of other parameters, such as number of compartments and cleaning cycle times, which are the same for all the tests, have been listed in Table 7.

The systems described in Figure 17 operate at an inlet concentration of 6.87 g/m^3 (3 grain/ft^3) and with a cleaning intensity such that 40 percent of the dust is removed during cleaning (a_c = 0.4). The lowermost curve in Figure 17 shows the relationship between average pressure drop and system face velocity for a continuously cleaned system. The remaining curves depict systems whose cleaning cycles are initiated at selected pressure drop levels. A given limiting pressure drop curve intersects the continuous cleaning curve when the minimum pressure drop (after the entire baghouse has been cleaned) equals the limiting pressure drop. If the face velocity of a given system is increased beyond this intersection point, the system must clean continuously to keep up with the increased deposition rate and pressure drop. Although data points are not shown at some intersections, the former can be determined by plotting the minimum pressure drop after the cleaning cycle is complete versus velocity for a given system. Velocities below 0.3 m/min were not used in the sensitivity analysis since the empirical relationship between penetration, velocity and fabric loading was developed from field and laboratory tests which were conducted at velocities greater than 0.3 m/min.

4.2.2.2 Average Penetration--

In Figure 24, the average penetration curves that correspond to the systems described in Figure 17 are presented. Figure 24 also shows a continuous cleaning curve with which the curves for pressure drop limited systems ultimately intersect. Note that the continuous cleaning curve appears to have a minimum at a velocity of about 0.8 m/min. This minimum is attributed to the fact that velocity changes produce opposing effects on dust penetration and dust deposition. Whereas penetration increases with velocity, it also decreases with the quantity of dust deposited on the filter, the latter factor being directly related to face velocity. Hence, the velocity/cake depth interaction suggests that the concept of a minimum effluent for the continuous cleaning system of Figure 24 is tenable. As the limiting pressure loss and/or the face velocity is allowed to increase, however, the face velocity alone dominates the penetration.

The graph of the time between cleaning cycles which corresponds to the data inputs of Figures 17 and 24 is presented in Figure 31. Time has been plotted versus limiting pressure drop for various face velocities to facilitate use of the curves. Note that the intersections of the curves with the abcissa indicate continuous cleaning systems (i.e., time between cleanings of zero).

4.2.3 Effect of Parameter Covariance on Predicted Performance

4.2.3.1 Simplified Single Equation Definition--

Due to the complex interrelationships among the operating parameters, it is difficult to describe accurately the impact of these parameters on system performance on the basis of a single variable change or a simple algebraic expression. However, by means of some simplifying assumptions, relationships between average pressure loss and key operating parameters were developed (See Appendix D). Although not intended to be accurate predictors of filter system performance, these equations may be used to forecast general trends in system pressure loss or to identify controlling variables among a specific set of input parameters.

The average pressure loss estimator for a *limiting pressure* or *timed cycle* system is:

$$\overline{P} = \tfrac{1}{2}\left[1 + \frac{1}{(n-1)(1 + t_f/t_c)}\right]\left[(2-a_c)P_L + a_c S_E V_i + (1-a_c)C_i K_2 V_i^2 t_c/2\right] \quad (24)$$

and for a continuous system is:

$$\overline{P} = \frac{2n-1}{2n-2}\, C_i K_2 V_i^2 t_c \Big/ \ln\left[1 + \frac{C_i K_2 V_i t_c}{S_E + C_i K_2 V_i t_c (1-a_c)/a_c}\right] \quad (25)$$

The time between cleaning cycles or the limiting pressure drop can be estimated from the following expression:

$$t_f = (a_c-1)t_c/2 + a_c(P_L-S_E V_i)/(C_i K_2 V_i^2) \quad (26)$$

By rearrangement of Equation (4-3), P_L is readily determined when t_f is a known quantity; i.e.,

$$P_L = \frac{K_2 C_i V_i^2}{a_c}\,(t_f + (1-a_c)t_c/2) + S_E V_i \quad (27)$$

System face velocity and limiting pressure drop were found to exert the greatest impact on system performance. The quantitative effects of these parameters on average pressure drop, average penetration and the time between cleanings are shown in Figures 13 to 19, 20 to 26, and 27 to 33, respectively.

4.2.3.2 Average Pressure Relationships--

By comparing the continuous cleaning curves, or the lines of constant limiting pressure, for selected values of inlet concentration and level of cleaning, it can be seen that the effect of any one operating parameter on performance is often a function of the magnitude of the other operating parameters. With reference to Figures 13 and 14, changes in velocity at an inlet concentration of 6.87 g/m^3 produce greater changes in average system pressure drop than at a concentration of 2.29 g/m^3. This same effect can be seen in Figures 16 and 13, where the fractional area cleaned, a_c, decreases from 0.4 to 0.1 (40 to 10 percent). Average pressure drop increases with increasing velocity more rapidly at low levels of cleaning and high inlet concentrations.

Although limiting pressure drop has a significant effect on average pressure drop, the magnitude of the effect is not as dependent on other operating parameters as is the effect of velocity. Changes in limiting pressure drop produce roughly equivalent changes in average pressure drop, regardless of inlet concentrations or level of cleaning (see Figures 13 and 14, and 13 and 16).

4.2.3.3 Average Penetration Relationships--

The effects of velocity and limiting pressure drop on average penetration are not as obvious as those on average pressure drop (see Figures 23, 24 and 25). The minimum average penetration on the continuous cleaning curve occurs at lower velocities as the inlet concentration increases. This is consistent with the previous explanation for the appearance of a minimum. It was postulated that at low fabric loadings the effect of reduced loadings counteracts the effects of reduced velocity. At higher inlet concentrations the minimum should then occur at a lower velocity.

The effect of limiting pressure drop on penetration also appears to be a complex function of several operating parameters. At a velocity of 0.61 m/min limiting pressure drop has greater influence on penetration at a low concentration (Figure 23) than at a high concentration (Figure 25). Changes in average penetration due to limiting pressure drop are also influenced by face velocity. As velocity increases, such that the system is forced into continuous operation, the effect of limiting pressure drop disappears since the system must now operate on a continuous cleaning basis. For example, with reference to Figure 24, at velocities greater than about 1.1 m/min, changing a limiting pressure drop from 1000 to 500 N/m^2 has no effect since if either of these is chosen, the system is forced into continuous operation.

4.2.3.4 Time Between Cleaning Relationships--

The effect of the time between cleaning cycles, t_f, on performance is described in Figures 34 and 35. These curves were developed by cross-plotting data excerpted from Figures 17, 24 and 31. Time between cleaning variations and limiting pressure variations exert similar effects on average pressure loss; i.e., with fixed values assigned to velocity, concentration and cleaning level, the change in average pressure loss will be roughly proportional to the change in either t_f or P_L.

Since P_L and t_f are linearly related (See Figures 27 to 33), the proportionality should be expected. The effect of t_f on average pressure loss is also dependent on the face velocity, as shown in Figure 34. A change of 30 minutes in t_f has a greater effect on average pressure loss when the face velocity is increased from 0.6 m/min than at 0.9 m/min. Since both pressure loss and dust deposition rate are linearly related to velocity and since there exists no upper limit for pressure drop, average pressure loss would be expected to experience larger deviations at higher velocities. There is, of course, a practical upper limit to pressure drop that is governed by draft fan capacity.

The effect of the time between cleaning cycles, t_f, on average penetration is generally similar to that for limiting pressure drop, P_L. The effect is also more pronounced at low t_f values than at high values (See Figure 35). This same effect on penetration can be seen in Figure 24 with regard to limiting pressure loss. Large excursions in average penetration result when P_L is varied from the indeterminate continuous cleaning level to 1000 N/m^2 (at a velocity of 0.91 m/min). The penetration changes are considerably less for higher P_L values.

4.2.3.5 Fractional Area Cleaned and Inlet Concentration--

The effects of the fractional area cleaned, a_c, and inlet concentration, C_i, on system performance can be best demonstrated by inspection of Figures 36 through 39, the latter excerpted from the cross plots presented in Appendix C. The two curves shown on each of the figures were chosen to represent those conditions under which a_c and C_i exert minor or major impacts on system performance.

Varying the cleaning parameter, a_c, can produce significant changes in average pressure loss when the system face velocity is high (See Figure 36). At low a_c levels, variations or errors in a_c estimation produce much greater effects than at high a_c levels.

The pressure loss response due to changes in inlet concentration show a similar dependence on average face velocity. In the latter case, however, the effect is not as pronounced.

The effects of C_i and a_c on average penetration are also influenced by several operating parameters. As illustrated in Figure 38, a ten fold change

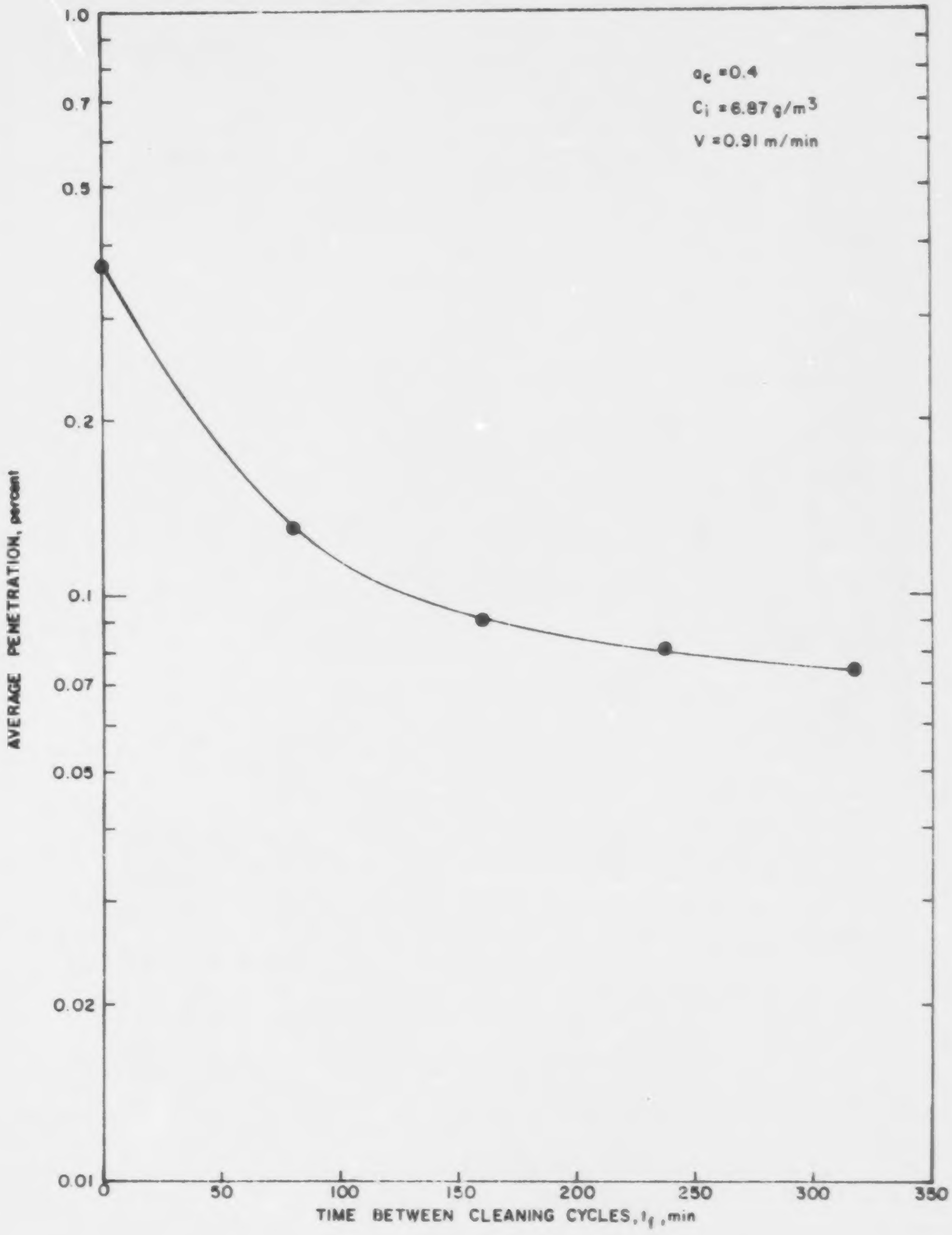

Figure 35. Effect of time between cleaning cycles, t_f, on average penetration.

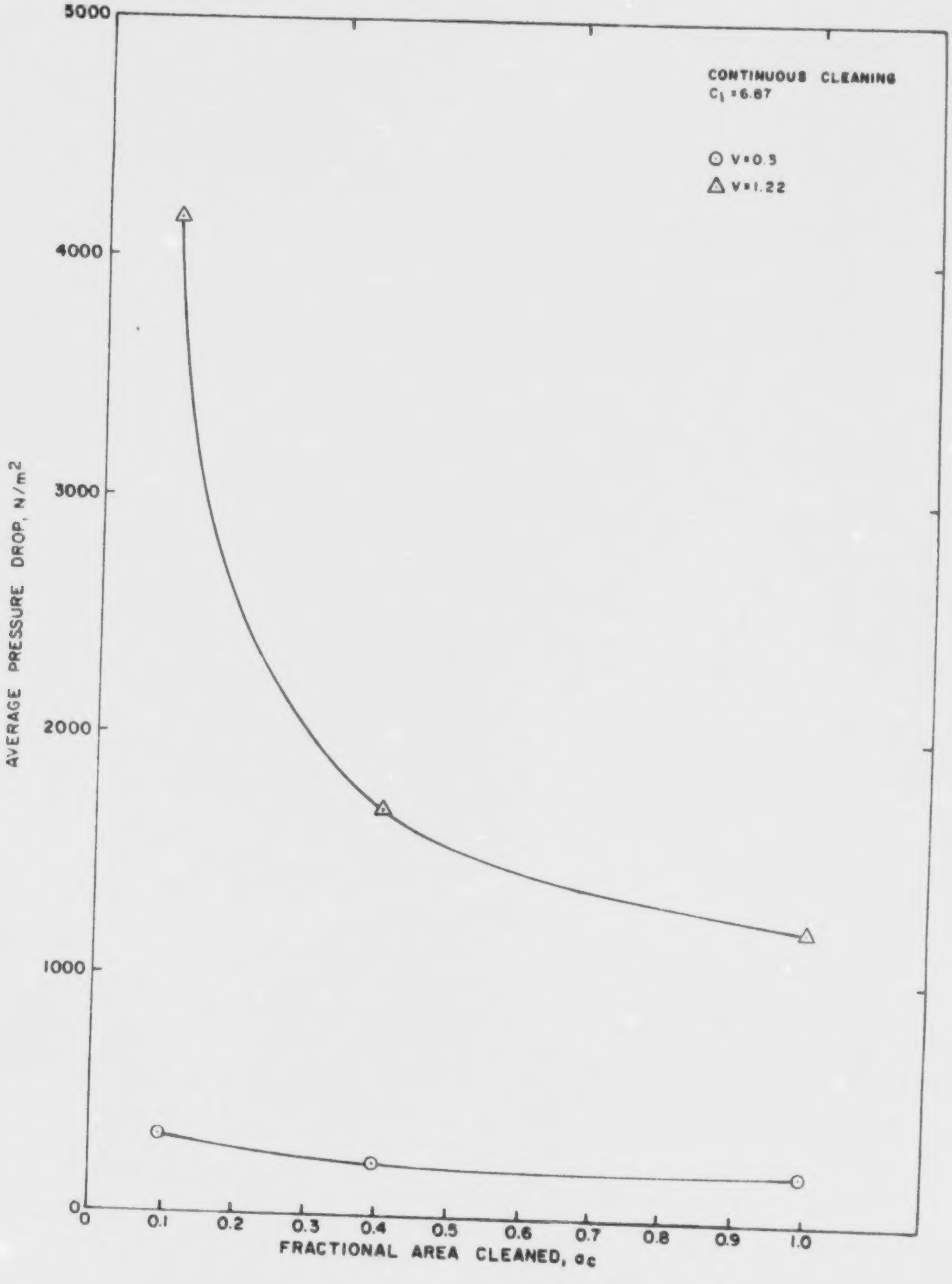

Figure 36. Effect of variations in cleaning intensity on average pressure drop.

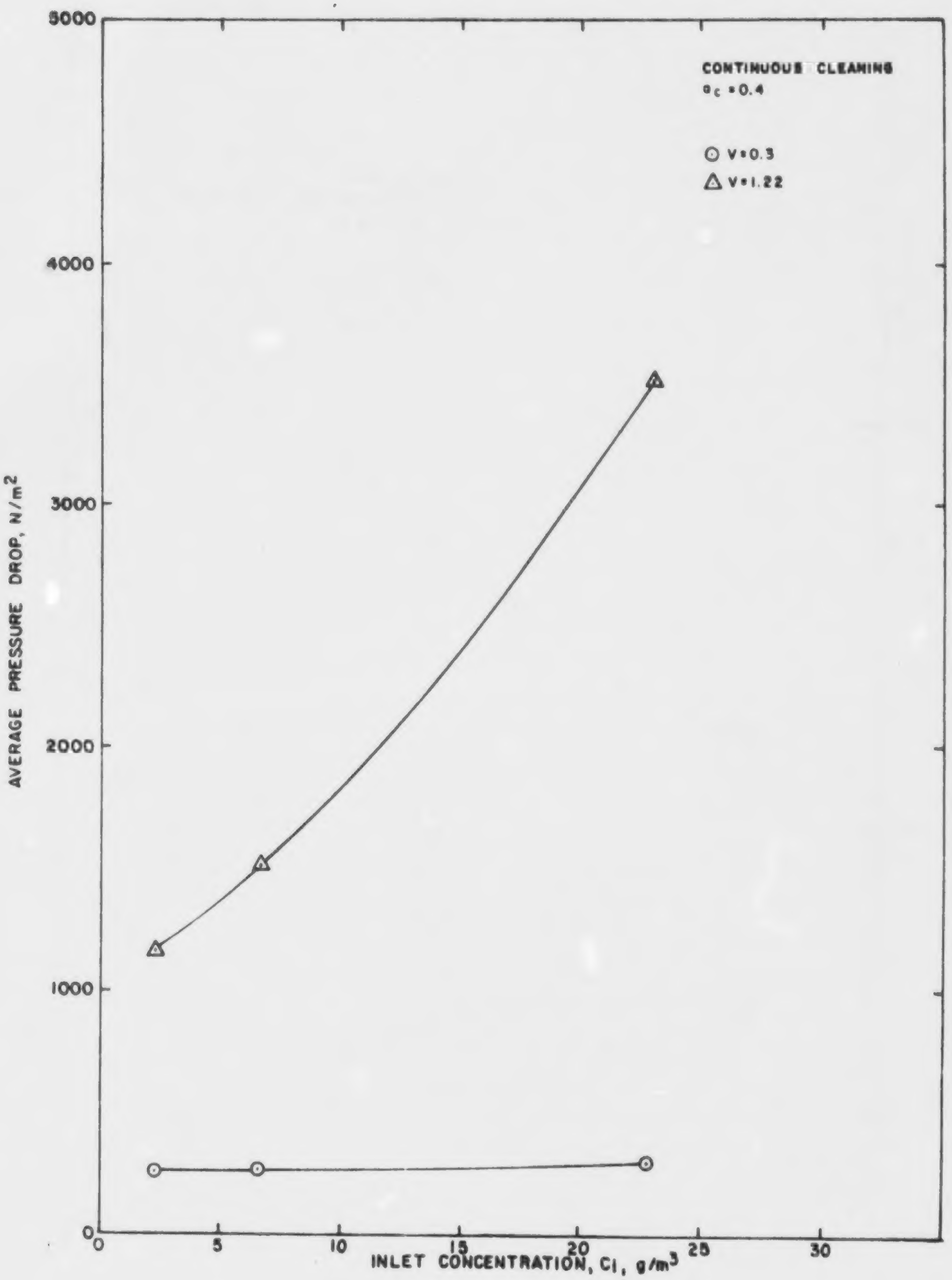

Figure 37. Effect of variations on inlet concentration on average pressure drop.

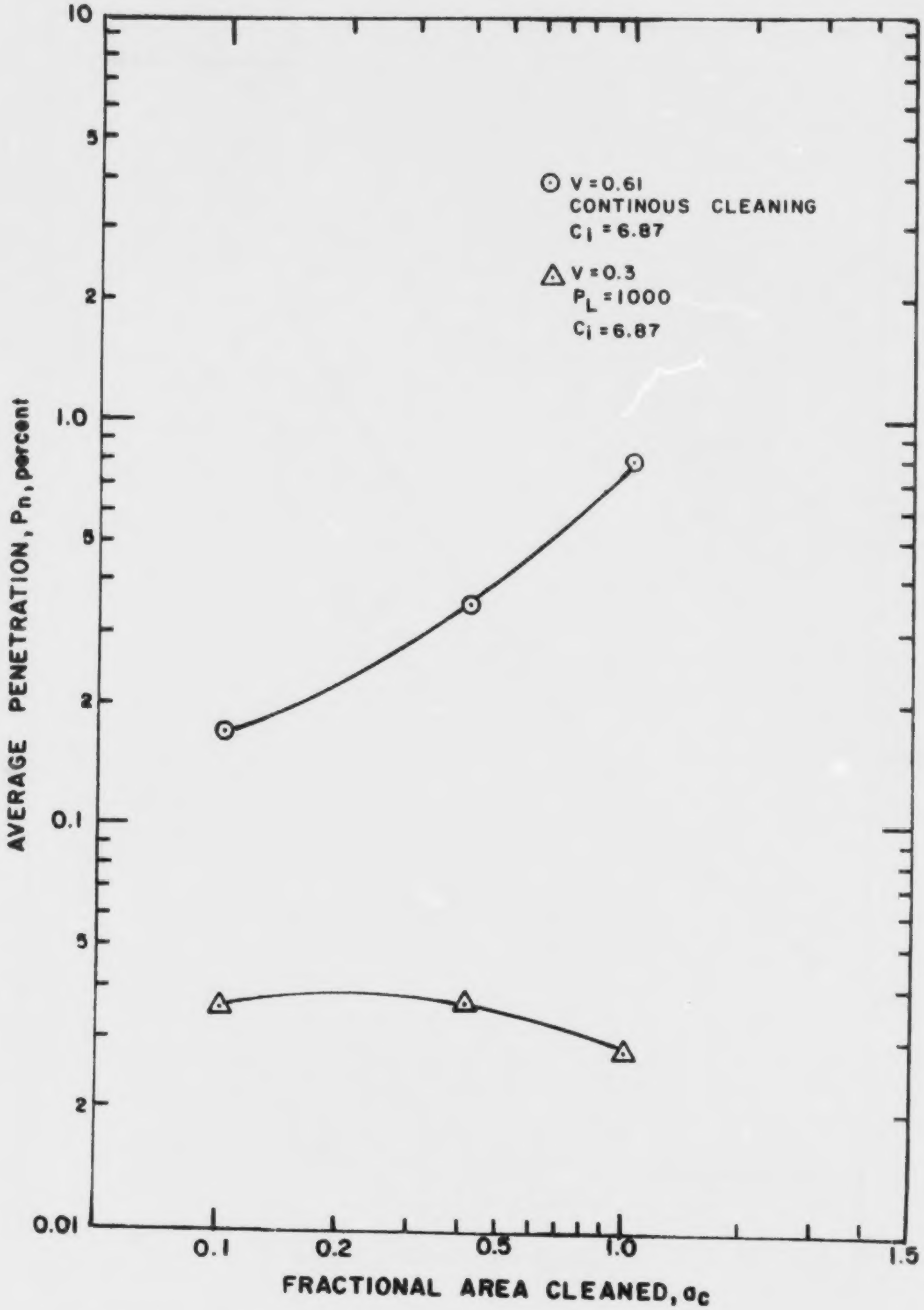

Figure 38. Effect of cleaning intensity on average penetration.

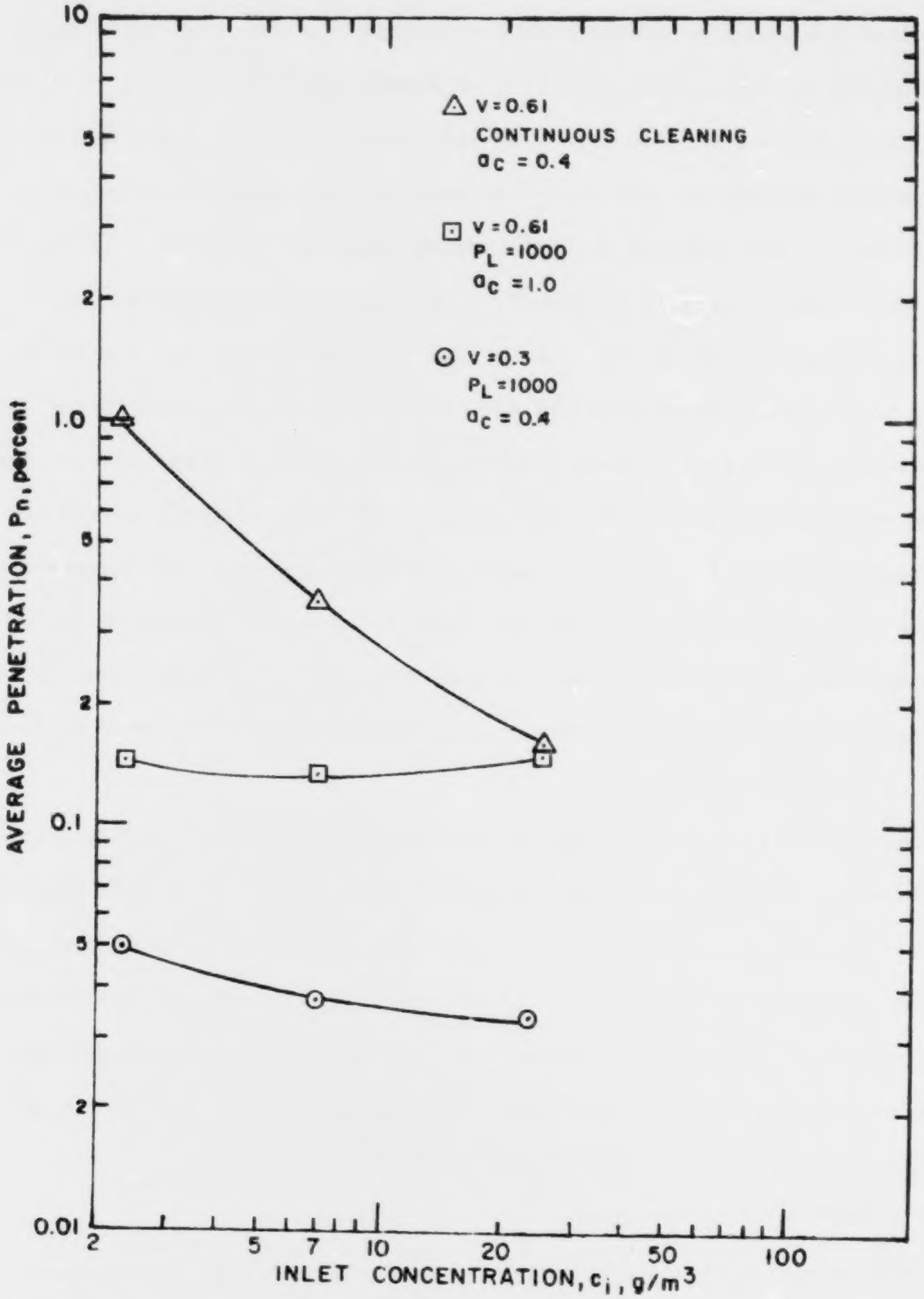

Figure 39. Effect of inlet concentration on average penetration.

in the fractional area cleaned produces only a 20 percent change in penetration for a limiting pressure system at low velocity. On the other hand, for a continuously cleaned system operating at a moderate face velocity (0.61 m/min), the same a_c variation produces a four fold change in average penetration. Two opposing effects are the likely reasons for the minimal penetration variations for the limiting pressure system shown in Figure 38. As the fractional area cleaned is increased, more areas of low resistance and low loading are generated. However, more time is required for the system to return to its limiting pressure of 1000 N/m^2. During this intervening period the system will operate at much lower penetration levels than those encountered during the cleaning cycle. The net result is that penetration levels are only weakly dependent on a_c for limiting pressure systems. In the continuously cleaned system (top curve, Figure 38) there is no way to compensate for the increased penetration during the cleaning cycle; i.e., extended periods of filtration without cleaning. Thus, penetration continues to increase as the level of cleaning increases.

The relationship between average penetration and inlet concentration is presented for various operating conditions in Figure 39. The effect of inlet concentration on penetration is also dependent on other system operating parameters. Penetration changes for limiting pressure systems are less responsive to changes in C_i than their counterparts in continuously cleaned systems. Differences in velocity and the level of cleaning can also modify the effect of concentration (lower curves on Figure 39).

4.2.3.6 Effect of K_2 Variations--

Variations in the specific resistance coefficient, K_2, can produce significant changes in performance. The relationship between performance and

K_2 is presented in Figures 40 to 42. Performance variables have also been plotted versus several parameters on the same graphs so that relationships could be developed between K_2 and other operating parameters whose effects have been previously established. Average pressure loss has been plotted versus K_2 (the filled symbols) for a continuous and limiting pressure system in Figure 40. As might be expected, an increase in K_2 produces an increase in average pressure loss and the effect is more pronounced for continuously cleaned systems as indicated by the steeper slope.

4.2.3.7 K_2 and Inlet Concentration--

Average pressure loss has also been plotted against the relative or dimensionless inlet concentration (C_i/C_{Ref}). The data were graphed in this manner so that coordinates at $K_2=1$ and $C_i=6.87$ could be superimposed. By using this approach it is demonstrated that the effect of K_2 on average pressure loss is approximately the same as that for inlet concentration. For example, using the point $K_2 = 1$ (or $C_i = 6.87$) as a reference point, increasing K_2 by a factor of 3 at a constant inlet concentration of 6.87 g/m^3 produces roughly the same change in average pressure loss as increasing C_i by a factor of 3 at a constant K_2 of 1. This means that average pressure loss can be described equally well by the product $K_2 \times C_i$ as may be deduced from the classical expression for pressure loss,

$$\Delta P = K_2 VW = K_2 V C_i V \Delta t$$

Precise adherence to the above relationship should not be expected because in real filter systems the average pressure loss is defined by a nonuniform rather than uniform fabric loading. For continuously cleaned systems, a change in K_2 is expected to have little effect on penetration since the latter is related mainly to fabric loading and face velocity. This follows from the fact that for a continuously cleaned system, the fabric loadings will be

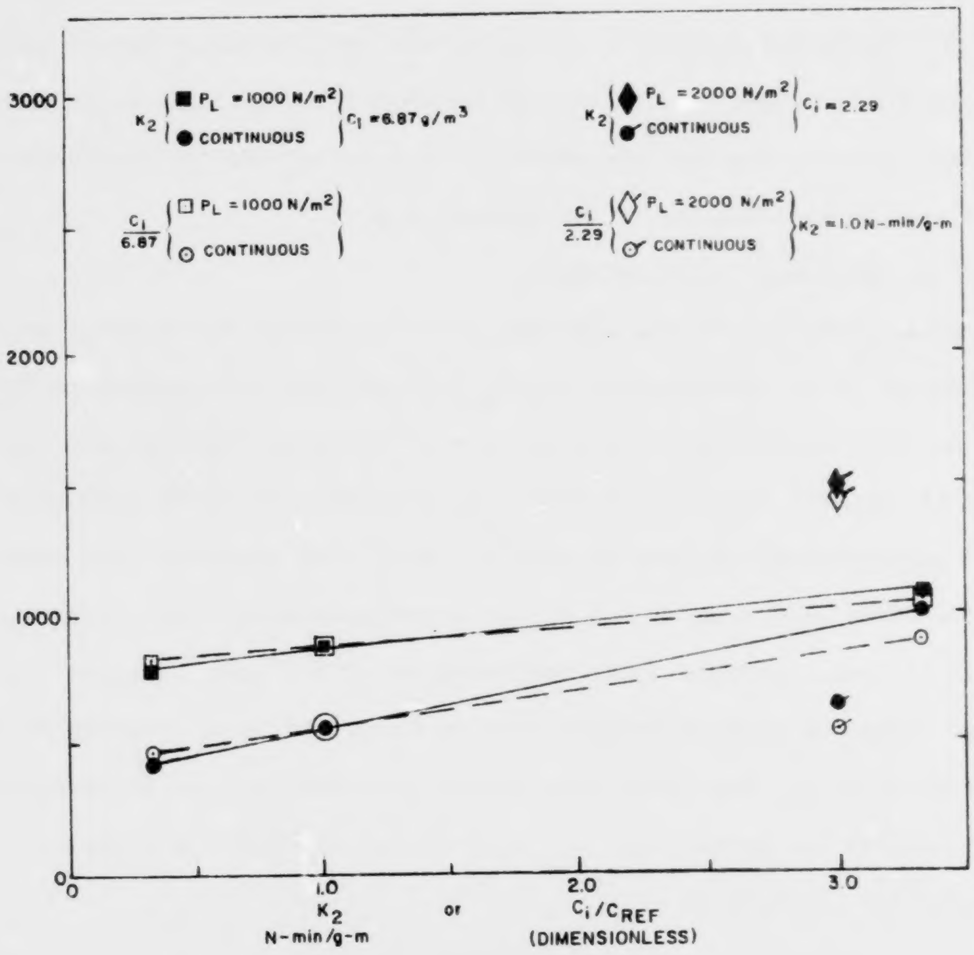

Figure 40. Effect of K_2 and C_i on average pressure loss.

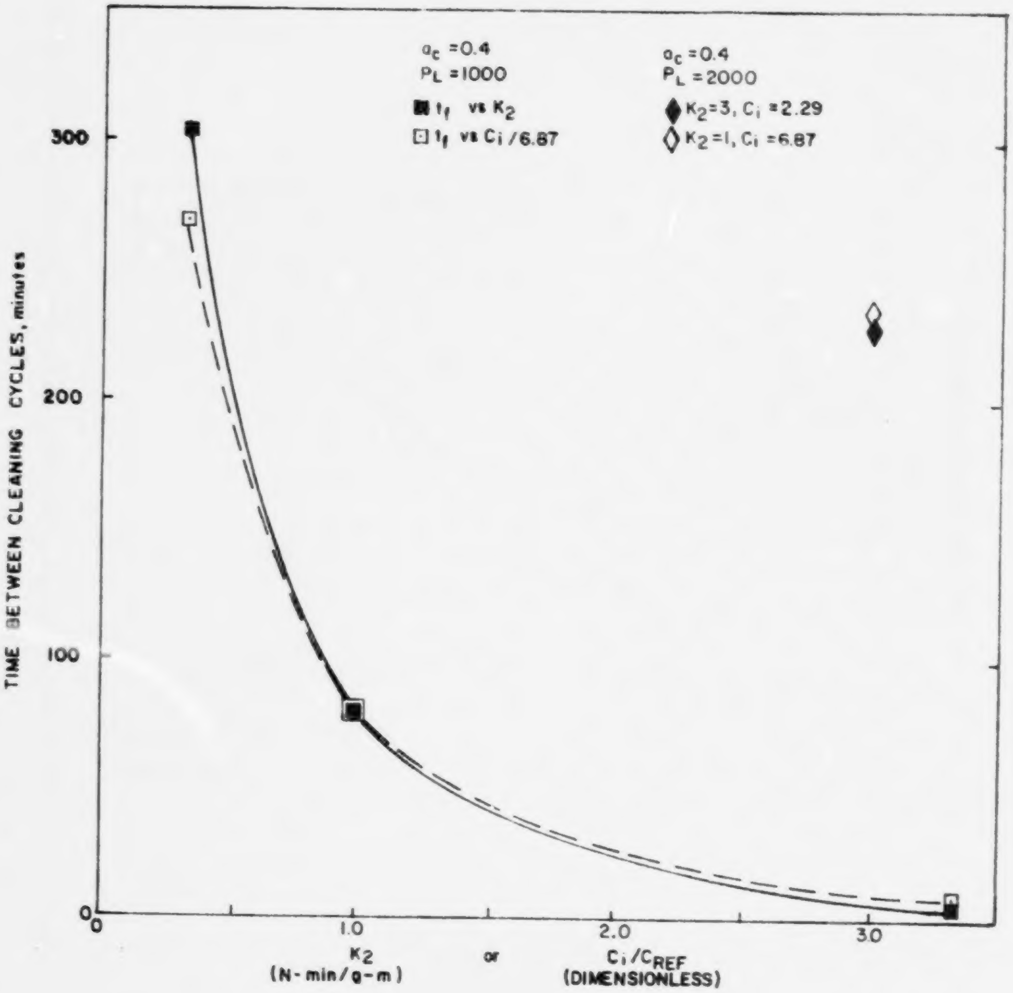

Figure 41. Effect of K_2 and C_i on time between cleaning cycles.

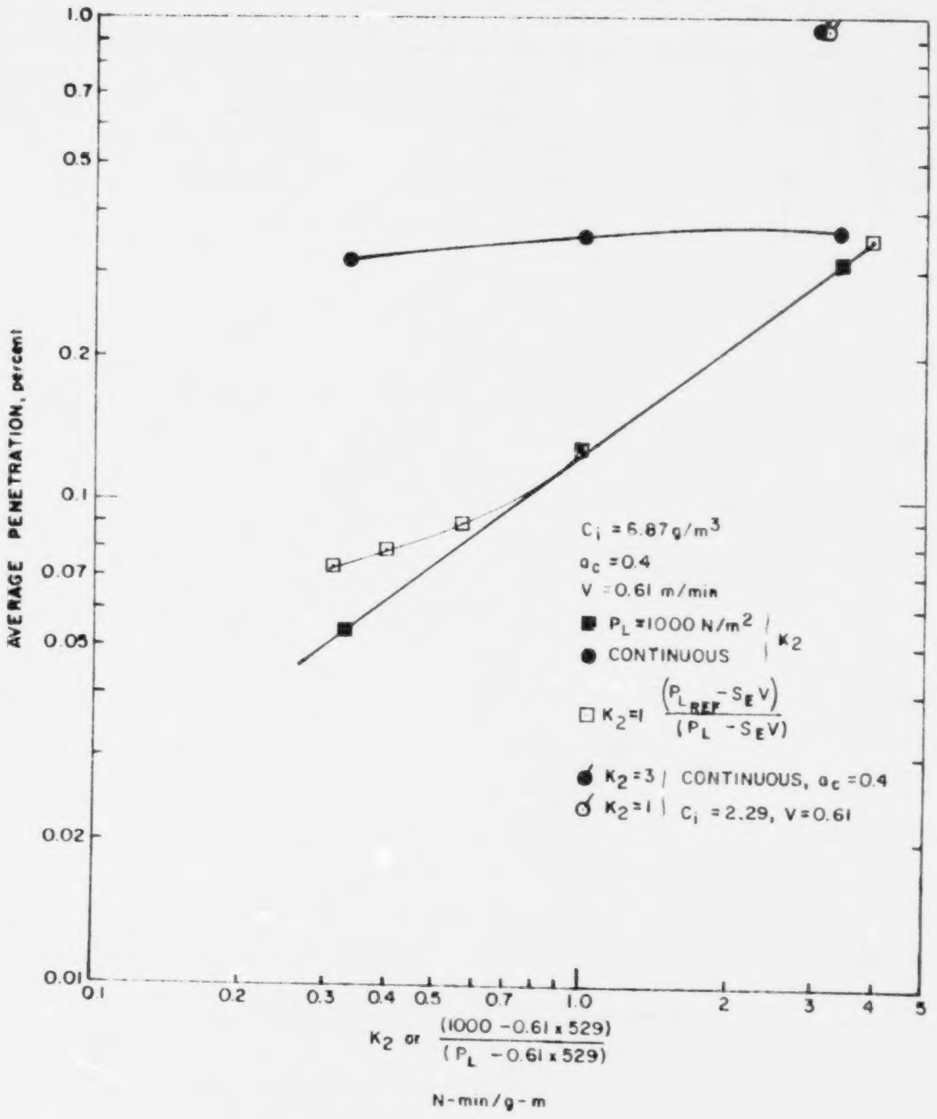

Figure 42. Effect of K_2 and C_i on average penetration.

controlled mainly by the data inputs a_c, V_i, C_i and t_c, none of which are affected by K_2.

Minor variations may be observed, again for the reason that velocity and drag usually differ from one location to another on fabric surfaces in real filter systems. A typical case is illustrated by the upper curve of Figure 42 in which minimal penetration changes are indicated for K_2 variations in a continuously cleaned system. Actually, a tenfold increase in K_2 led to only a 16 percent increase in average penetration.

Limiting pressure controlled systems, on the other hand, exhibit a strong dependence on K_2 as shown in the lower curve of Figure 42. As K_2 increases, the average fabric loading must be less at any instant because of the limiting pressure constraint. Hence, with a reduced dust cover, an increase in penetration is expected.

4.2.3.8 K_2 and Limiting Pressure--

The rationale for the projected interrelationship of $\underline{K_2 \text{ and } C_i}$ with respect to pressure drop can also be extended to limiting pressure, P_L, and K_2 with respect to penetration. The same "$K_2 \times C_i$" relationship, however, does not apply to penetration, because K_2 and C_i have no direct influence on penetration. A similar correlation describing the combined impact of P_L and K_2 on average penetration can be developed, however, by examining their (P_L, K_2) effects on those parameters that relate directly to penetration, such as fabric loading and velocity. If K_2 and P_L are allowed to increase simultaneously by two independent paths but with the constraint that the final fabric loadings be identical, then the resultant penetrations should be approximately the same, regardless of the path. The following discussion presents the development of this concept.

First, for the two independent systems cited previously, the identical fabric loadings prior to cleaning, W_1 and W_2, respectively, may be expressed by the relationship in

$$W_1 = W_2 = \left[\frac{P_L - S_E\ V_i}{K_2\ V_i}\right]_1 = \left[\frac{P_L - S_E\ V_i}{K_2\ V_i}\right]_2 \qquad (28)$$

Now if the K_2 value is fixed for the first system and the value of P_L is fixed for the second system (while V_i is maintained at the same level in both systems to eliminate any velocity effects on penetration) a relationship can be derived between P_L and K_2 for the respective systems. Additionally, a rearrangement of Equations (28), makes it possible to treat the effect of P_L variations on penetration for the first system as if they depicted the effect of K_2 variations in the second system. In other words, penetration may be conveniently graphed as a function of P_L as well as K_2.

The curve passing through the open squares in Figure 42 is a graph of average penetration versus the P_L function,

$$(P_{L_{REF}} - S_E\ V_i)/(P_L - S_E\ V_i) \times K_{2_{REF}} \qquad (29)$$

for a fixed K_2 value of 1.0 N-min/g-m. Reference values of 1.0 N-min/gm and 1,000 N/m^2 were chosen for K_2 and P_L, respectively, which by forcing curve superposition at an abscissa value of 1.0, permits ready comparison of the relative impacts of K_2 and/or P_L on penetration.

Had the two curves coincided completely, a relationship between K_2 and P_L could have been established over the entire abscissa scale such that the effects of K_2 variation could be described equally well by P_L variations. In fact, this situation is reflected in Figure 42 for all abscissa values greater than 0.6. Over the K_2 range of 0.3 to 0.6 N-min/g-m, which is equivalent to a P_L range of 2,500 to 1,500 N/m^2) curve superposition is no longer indicated. A possible explanation for the deviation is that the velocity distributions over the fabric surfaces are different for the two systems.

For any specified abscissa value, the points on the two curves relate to two systems for which all operating parameters except K_2 and P_L are the same. For example, an abscissa value of 0.57 on the lower K_2 curve (solid square) depicts a system where P_L is 1,000 N/m^2 and K_2 0.57 N-min/g-m. The upper $f(P_L)$ curve (open square) relates to a system in which P_L = 1,500 N/m^2 and K_2 = 1.0 N-min/g-m. These two systems, in accordance with the definition of the P_L function (Equation 28) operate at about the same average fabric dust loadings. In addition, average face velocities, inlet concentrations and cleaning parameters are the same for the two systems.

The time intervals between cleaning cycles are also approximately the same for the two systems. Therefore, at any specified time during an operating cycle, these two systems should be almost identical with respect to the fabric loading and its distribution. It then follows that with the same average face velocity, the penetrations should be similar for both systems. It should by noted, however, that the velocity distributions are dependent upon local drag values which are, in turn, are related to K_2. Since the values of K_2 are different for the two systems, the velocity distribution may differ despite the same average velocity. Hence, some difference in penetration might be expected.

4.2.3.9 Summary of K_2 Relationships--

Although some differences exist between the K_2 and $f(P_L)$ curves, Figure 42, it appeared that the investigation of the effects of K_2 variations on penetration was but pursued indirectly by investigating the effect of P_L on concentrations. The reason for this approach was that some 21 figures and 50 related cross plots had already been developed to describe the relationship between key operating parameters and system performance. To add another degree of freedom; i.e. K_2, would require approximately 42 additional figures.

Since the computer filtration model should be used in any final analysis of system performance, and since the figures presented here are intended to be used for preliminary assessments only the following procedure should be used when investigating filter systems for which the K_2 value of the dust is other than 1.0 N-min/g-m. For continuously cleaned systems K_2 variations exert only minor effects on penetration. There the sensitivity analysis curves (Figures 13 to 33 and those in Appendix C) can be used without modification. In the case of limiting pressure systems the present penetration curves (Figures 20 and 62 to 82) can be used by generating a revised P_L value from the actual limiting pressure; i.e.,

$$(P_L)_{revised} = \frac{1.322}{K} \Big((P_L)_{actual} - S_E V_i\Big) + 529 V_i \qquad (30)$$

where

$(P_L)_{actual}$ = the limiting pressure of the system under investigation, N/m^2.

$(P_L)_{revised}$ = the limiting pressure to be used in conjunction with the sensitivity analysis curve, N/m^2.

K_2 = the value of the specific resistance coefficient of the dust in question, reported at a velocity of 0.61 m/min and the actual gas temperature, N-min/g-m.

V_i = the average system face velocity, m/min.

S_E = effective residual drag for the fabric/dust combination in question at the actual gas temperature.

If an average pressure loss or the interval between cleaning cycles is sought for either continuous or pressure controlled systems, then the inlet concentration (rather than the limiting pressure) should be corrected to:

$$(C_i)_{revised} = (C_i)_{actual} \times K_2/1.322 \tag{31}$$

where $(C_i)_{actual}$ = the inlet dust concentration of the system under investigation, g/m^3.

$(C_i)_{revised}$ = the inlet concentration to be used in conjunction with the sensitivity analysis curves, g/m^3.

4.3 USE OF THE SENSITIVITY TEST DATA

4.3.1 Key Variables and Fixed Terms

There are three ways in which the results of the sensitivity tests described in this report may be used to aid the solution of filtration problems.

- The probable impact of uncertainties or errors in the key input parameters upon predicted filter system performance can be estimated.
- Preliminary estimates of filter system performance can be made based upon specified input parameters.
- Preliminary design parameters can be established for new filter systems.

It is emphasized that the role of the sensitivity analyses is to aid, but in no way substitute for, the formal computer modeling process. Of necessity, several parameters were held constant during the sensitivity trials to keep the graphical material and computer utilization within the program constraints. Those parameters held constant were as follows: the number of compartments (10), cleaning cycle time (30 min.), compartment cleaning time (3 min.), reverse flow velocity (0 m/min), gas temperature (150°C) and effective drag, S_E, (400 $N\text{-}min/m^3$). Thus, the use of the data for determining the performance of a system whose operating parameters differ appreciably from those used in developing the curves and tables will present some error.

Use of the sensitivity analyses to investigate the effects of errors in the operating parameters or to predict the performance of an existing fabric filter system is a straightforward process. Provided that the approximate value(s) for the principal input parameters are known in the above cases, the performance of a filter system can be estimated directly from the appropriate graphs with allowance for K_2 variations taken into account. Since a measured value for the cleaning parameter may not be readily available, an estimate of a_c must be made.

4.3.2 Estimation of a_c

Three relationships between a_c and various operating parameters were presented in Section 3 of this report for limiting pressure systems:

$$W_p' = \frac{P_L - S_E V_i}{K_2 V_i} + \frac{C_i V_i t_c}{2} \qquad (32)$$

$$\text{Collapse/Reverse Flow, } a_c, = 1.51 \times 10^{-8} (W_p')^{2.52} \qquad (33)$$

$$\text{Mechanical Shaking, } a_c = 2.33 \times 10^{-12} (f^2 A W_p')^{2.52} \qquad (34)$$

Two equations have been given for continuously cleaned or time cycle cleaning:

$$\text{Collapse/Reverse Flow, } a_c = 0.006 \left[C_i V_i (t_f + t_c)\right]^{0.716} \qquad (35)$$

$$\text{Mechanical Shaking, } a_c = 4.90 \times 10^{-4} \left[f^2 A C_i V_i (t_f + t_c)\right]^{0.716} \qquad (36)$$

The definitions of the terms and the appropriate units for their entry into Equations (32) through (36) are given in Table 10 in the order of their appearance.

Although the equation structure may appear inconvenient to manipulate, it should be noted that only one equation, Equation (35) or (36), need be used for continuous or time cycle cleaning. If a limiting pressure system applies, Equation (32) in conjunction with either Equation (33) or Equation (34)

TABLE 10. DATA INPUTS REQUIRED FOR ESTIMATION OF THE CLEANING PARAMETER, a_c

---

where

a_c = fractional area cleaned, dimensionless

W'_p = average dust loading on the fabric during cleaning, g/m^2.

P_L = limiting pressure loss, N/m^2.

S_E = effective drag at the actual gas temperature, $N\text{-}min/m^3$

V = actual system face velocity, m/min, average value

C_i = inlet dust concentration at actual conditions, g/m^3.

t_c = cleaning cycle time, min.

K'_2 = specific resistance coefficient corrected to actual gas temperature and face velocity, see Equation (7), N-min/g-m.

f = shaker arm frequency, cycles/sec.

A = shaker arm half-stroke amplitude, cm.

t_f = filtration time between cleaning cycles for timed cycle cleaning systems, min. Enter as zero for continuously cleaned system.

must be used. Had a_c been treated as a variable within the computer runs used to generate the graphs, an unnecessarily large number of graphs and computer simulations would have resulted.

Again, it is emphasized that aside from using the sensitivity analyses as preprogramming guidelines, they can also provide rapid estimates (< 1 hour) of filter system performance when delayed programming activities or lack of computer access might readily entail a 24-hour delay.

The data inputs for the a_c computations are those related to the actual filter operating conditions. In the case of K_2, a correction is required to convert K_2 by means of Equation (2-7) to the temperature and velocity conditions of the filtration process. Having computed the a_c value, the performance of the fabric filter system of interest can be estimated from the appropriate graphs with the aid of interpolation.

4.3.3 Guideline Table [illegible] ensitivity Test Use

Table 4-4 has been prepared as a convenient guide to identify and locate the various graphs used for preliminary estimates of fabric filter performance. The information is presented in three groups for which the three indices of filter system performance, average pressure loss, average penetration and time between cleaning cycles are treated as the dependent variables (ordinates) while inlet concentration, fractional area cleaned, and face velocity are plotted as the independent variables (abscissas). Each group in turn is represented by matrices (partially or nearly completed) in which the invariant terms of each graph (a_c, V_i) (C_i, V_i) and (C_i, a_c), respectively, are represented by families of curves. Thus by providing an interpolation capability, more input parameters can be treated as system variables. Although not specified within the matrix structure itself, the limiting pressure, P_L, is also treated as a variable on several graphs by the construction of 4 to 5 constant P_L curves that embrace its expected range of field values.

If two of the three field values for a_c, C_i and V_i conform approximately to those shown for the variable combinations on Table 11, it is then possible to estimate the predicted field performance of the system in terms of average pressure loss, $\overline{P}$, average penetration, $\overline{Pn}$, and time (interval) between cleaning cycles. Variations in limiting pressure drop, P_L, are evaluated by interpolation between the constant P_L lines shown on the appropriate graphs.

It is again pointed out that certain parameters listed in Table 7 were held fixed in constructing the families of sensitivity curves; e.g., the number of compartments, the compartment cleaning time, reverse flow velocity, effective drag, residual fabric loading and the time increment for iteration. According to the results of preliminary sensitivity testing summarized in Table 8, except for the highly unusual situation, deviations from the base line values shown in Table 8 should not cause any serious estimating errors.

A simple example of the use of Table 11 is given for an assumed set of input parameters, $C_i = 6.87\ g/m^3$, $a_c = 0.3$, $V = 0.9$ m/min and $P_L = 1200\ N/m^2$ that apply to a proposed filter system. If it is desired to estimate the average pressure loss, $\overline{P}$, reference is made to Figure 49, which describes precisely the $\overline{P}$ versus a_c relationship for the indicated concentration and velocity inputs. Interpolation between the lines of constant P_L (1,000 and 1,500 N/m, respectively) then enables the location of the resultant $\overline{P}$ value, roughly 1,450 N/m^2. A similar procedure is used to estimate average penetration by now referring to Figure 68 and carrying out a similar P_L interpolation.

TABLE 11. FIGURE KEY FOR ESTIMATING MAJOR FILTER PERFORMANCE PARAMETERS - AVERAGE PRESSURE LOSS ($\overline{P}_L$), AVERAGE PENETRATION ($\overline{P}n$), TIME BETWEEN CLEANINGS (t_f)

Ordinate	V_i a_c	0.3	0.61	0.91	1.22
$\overline{P}$	0.1	C-11*	C-12	C-13	C-14
$\overline{P}_n$		C-32	C-33	C-34	C-35
t_f		C-48	C-49	-	-
$\overline{P}$	0.4	C-15	C-16	C-17	C-18
$\overline{P}_n$		C-36	C-37	C-38	C-39
t_f		C-50	C-51	C-52	C-53
$\overline{P}$	1.0	-	C-19	-	-
$\overline{P}_n$		-	C-40	-	-
t_f		-	C-54	-	-

Note: Figure numbers for graphs of $\overline{P}$, $\overline{P}_n$, t_f versus inlet concentration, C_i, at selected values of a_c, V and P_L (P_L also indicated as variable on several graphs.)*

(continued)

TABLE 11 (continued)

Ordinate	V_i C_i	0.3	0.61	0.91	1.28
$\overline{P}$	2.29	C-1	C-2	C-3	C-4
$\overline{P}_n$		C-20	C-21	C-22	C-23
t_f		C-41	C-42	-	-
$\overline{P}$	6.87	C-5	C-6	C-7	C-8
$\overline{P}_n$		C-24	C-25	C-26	C-27
t_f		C-43	C-44	-	C-45
$\overline{P}$	22.9	C-9	C-10	-	-
$\overline{P}_n$		C-28	C-29	C-30	C-31
t_f		C-46	C-47	-	-

Note: Figure numbers for graphs of $\overline{P}$, $\overline{P}_n$, t_f versus fractional area cleaned, a_c at selected values of C_i, V_i and P_L.

Ordinate	a_c C_i	0.1	0.4	1.0
$\overline{P}$	2.79	4-1	4-4	-
$\overline{P}_n$		4-8	4-11	-
t_f		4-15	4-18	-
$\overline{P}$	6.87	4-2	4-5	4-7
$\overline{P}_n$		4-9	4-12	4-14
t_f		4-16	4-19	4-21
$\overline{P}$	22.9	4-3	4-6	-
$\overline{P}_n$		4-10	4-13	-
t_f		4-17	4-20	-

Note: Figure numbers for graphs of $\overline{P}$, P_n, t_f versus velocity, V_i at selected values of C_i, a_c and P_L.

*C refers to Appendix C

4.3.4 Predicting Filter Performance with Graphical Aids

In the following discussion, we have provided a specific example of how the tabular and graphical descriptions of filter system performance generated under the sensitivity analyses program can be used to make preliminary estimates of filter system performance. There are three main reasons for conducting premodeling analyses before engaging in a formal modeling study.

- First, the tentative data inputs supplied by the filter user and/or manufacturer can be screened to determine whether the predicted system operation will fall within practical boundaries.
- Second, one can estimate what degree of accuracy (or margin of error) can be accepted for any one data input without seriously impairing the model's predictive capability.
- Third, in the event that computer availability will cause lengthy delays in data retrieval (~ few days), the need for an immediate assessment of a proposed filter system's capability can be made in less than an hour with the aid of the graphical and tabular material presented.

We wish to point out that the working ranges of some sensitivity curves are limited because the primary role of the sensitivity analyses was to suggest optimum procedures for improving the original fabric filter model.[1] Hence, certain computer runs were cancelled when a satisfactory guideline had been established. Since the use of the curves for premodeling estimating purposes was only a secondary objective and not intended to be more than a screening process, it was not deemed advisable to extend the sensitivity testing beyond the present range. In those cases where extrapolation beyond measured data points has been required, dotted lines have been constructed on the appropriate graphs.

4.3.5 Sample Field Problem

A Pollution Control Agency would like to determine whether or not Plant A's proposed baghouse will achieve the level of performance necessary to meet a specified emission level as well as operating at pressure losses within the capacity range of the draft fans. The following operating data are available for a baghouse utilizing woven glass bags and cleaned by collapse and reverse flow air.

TABLE 12. OPERATING DATA FOR SAMPLE FIELD PROBLEM

Number of compartments	(n)	15
Cleaning cycle time	(t_c)	22 min
Limiting pressure loss	(P_L)	1,250 N/m
Inlet dust concentration	(C_i)	4.0 g/m
Average face velocity at operating temperature	(V_i)	0.9 m/min
Filtration temperature	(T)	121°C
Effective residual drag at 25°C	(S_{E_m})	433 N-min/m^3
K_2 at 25°C and 1.1 m/min	(K_{2_m})	0.83 to 1.44 N-min/g-m

With respect to the available values cited for K_2 (K_{2m}), it is uncertain as to where in the 0.83 to 1.44 range the correct value for K_2 should fall. Therefore, before performing final computer simulations, the Agency would like to determine the potential impact of the above K_2 variations on performance. The graphs and tables developed provide the means for this preliminary assessment.

The first step in investigating the effect of K_2 variations is to correct the measured values of K_2 and S_E to the gas viscosity corresponding to the filtration temperature.

$$K_{2f} = K_{2m}\left(\frac{\mu\ 121^{\circ}C}{\mu\ \ 25^{\circ}C}\right) = K_{2m}\left(\frac{0.022\ cp}{0.018\ cp}\right)$$

$$S_{E_f} = S_{E_m}\left(\frac{\mu\ 121^{\circ}C}{\mu\ \ 25^{\circ}C}\right) = S_{E_m}\left(\frac{0.022\ cp}{0.018\ cp}\right)$$

With the above corrections, the K_{2_f} range becomes 1.01 to 1.76 N-min/g-m and S_{E_f} is increased to 529 N-min/m^3.

For use with the graphs listed in Table 4-4, K_{2m} must also be corrected to the reference velocity, 0.61 m/min, that was used in the generation of the graphs.

$$K_{2_{f,r}} = K_{2f}\sqrt{\frac{V_r}{V_m}} = K_{2f}\sqrt{\frac{0.61 \text{ m/min}}{1.1 \text{ m/min}}}$$

Hence, when using the graphs listed in Table 11, the $K_{2_{f,r}}$ of 0.75 to 1.31 N-min/g-m is the proper data input for the K_2 parameter.

A value for a_c is also required prior to using the sensitivity graphs. Since the filter system operation is to be governed by a limiting pressure, P_L, it is necessary to calculate a_c by means of Equations (32) and (33).

$$W'_p = \frac{P_L - S_E V_i}{K_{2_{f,r}} V_i} + \frac{C_i V_i t_c}{2} \qquad (32)$$

$$a_c = 1.51 \times 10^{-8} W'^{2.51}_p \qquad (33)$$

noting that $K_{2_{f,v}}$ is the proper value to use in Equation (32). Here, the subscript v indicates that the K_2 value has also been corrected from its original measurement velocity of 1.1 m/min to the actual velocity at which filtration takes place, 0.9 m/min.

$$K_{2_{f,v}} = K_{2f}\sqrt{\frac{V_f}{V_m}} = K_{2f}\sqrt{\frac{0.09 \text{ m/min}}{1.1 \text{ m/min}}}$$

The resulting $K_{2_{f,v}}$ range, 0.91 to 1.59 N-min/g-m, when used in conjunction with Equations (32) and (33) leads to an a_c input range of 0.89 to 0.22, respectively.

As a final step, additional adjustments must be applied to C_i and P_L because the graphs were generated on the basis of a constant K_2 value of 1.0. This requires that P_L and C_i be revised in accordance with Equations (30) and (31), respectively,

$$(P_L)_{adj.} = \frac{1.322}{K_{2_{f,r}}} \quad P_L - S_{E_f} \; (V_f) \quad + 529 \quad V_f \tag{30}$$

and

$$(C_i)_{adj.} = C_i \; K_{2_{f,r}}/1.322 \tag{31}$$

The values of $K_{2f,r}$ to be used above are those calculated previously as 0.75 to 1.31 N-min/g-m. The corresponding range for revised P_L values becomes 1,820 to 1,260 N/m^2 while the revised concentrations increase from 2.3 to 3.96 g/m^3.

The actual numerical value for V_i, a_c, C_i and P_L used with the sensitivity curves to predict the differences in filter systems performance when K_2 (as measured) ranges from 0.83 to 1.44 N-min/g-m are listed in Table 13.

TABLE 13. CORRECTED INPUT PARAMETERS FOR ESTIMATING EFFECT OF K_2 VARIABILITY ON FILTER SYSTEM PERFORMANCE

	Lower limit K_2 = 0.83 N-min/g-m	Upper limit K_2 = 1.44 N-min/g-m
V_i (m/min)	0.9	0.9
a_c (fraction)	0.84	0.22
C_i (g/m^3)	4.0* or 2.3†	4.0* or 3.96†
P_L (N/m^2)	1,820* or 1,250†	1,260* or 1,250†

*Used for estimation of penetration

†Used for estimation of pressure loss

Note that two choices for P_L and C_i are shown for each K_2 value. When penetration is to be estimated for the lower limit, the *actual* inlet concentration, 4.0 g/m^3, and the *revised* limiting pressure, 1,820 N/m^2, are used. Conversely, if average pressure loss and time between cleanings are sought, the *revised* concentration, 2.3 g/m^3 and the *actual* limiting pressure, 1,250 N/m^2 are to be used.

In conjunction with the input parameters listed in Table 13, the proper working graphs for estimating pressure loss and penetration characteristics can be selected from Table 11.

TABLE 14. SENSITIVITY CURVE SELECTIONS FOR ESTIMATING EFFECT OF K_2 VARIABILITY ON FILTER SYSTEM PERFORMANCE.

	Lower limit K_2 = 0.83 N-min/g-m	Upper limit K_2 = 1.44 N-min/g-m
$\overline{P}$, N/m^2	C-3	C-3, C-7
$\overline{Pn}$, percent	C-22, C-26	C-22, C-26

Based upon interpolation and/or extrapolation as needed, the following estimates can be made for average pressure loss, $\overline{P}$, and average penetration, $\overline{Pn}$:

	Lower Limit K_2 = 0.83 N-min/g-m	Upper limit K_2 = 1.44 N-min/g-m
$\overline{P}$ N/m^2	~1,000	(1,250 to 1,625)1400
$\overline{Pn}$ percent	(~0.15 to 0.18)0.16	(~0.27 to 0.29)0.28

The resulting analysis suggests that one should expect a pressure loss increase of 400 N/m^2 (1.6 in. w.c.) when K_2 ranges from 0.83 to 1.44 N-min/g-m. The corresponding range for penetration is 0.16 to 0.28 percent. The increase in dust penetration is caused by the fact that less operating time is required to reach the preset limiting pressure. Thus, at a constant inlet loading less dust is deposited on the fabric surface.

When Equations (24) and (26) were used to investigate the effect of K_2 changes on pressure loss, the predicted range was 860 to 1,200 N/m^2 which is in fair agreement with the value deduced from the sensitivity curves. It is again emphasized that the above applications of the sensitivity analyses are intended to establish whether rational performance levels will be attainable with the given input parameters or whether any one input parameter is suspect.

REFERENCES

1. Dennis, R., et al. Filtration Model for Coal Fly Ash With Glass Fabrics. Report No. EPA-600/7-77-084. August 1977. 455 p.

2. Dennis, R., R. W. Cass, and R. R. Hall. Dust Dislodgement From Woven Fabrics Versus Filter Performance. J Air Pollut Control Assoc. 48 No. 1. 47:32, 1978.

3. Dennis, R. and H. A. Klemm. Modeling Coal Fly Ash Filtration With Glass Fabrics. Third Symposium on Fabric Filters for Particulate Collection. Report No. EPA-600/7-78-087. June 1978. p. 13-40.

4. Dennis, R. and H. A. Klemm. A Model for Coal Fly Ash Filtration. (Presented at the 71st Annual Meeting of the Air Pollution Control Association. Houston, Texas. June 22-30, 1978.)

5. Dennis, R. and H. A. Klemm. Verification of Projected Filter System Design and Operation. (Presented at the Symposium on the Transfer and Utilization of Particulate Control Technology Sponsored by the U.S. Environmental Protection Agency. Denver, Colorado, July 24 to 28, 1978.

6. Bradway, R. M. and R. W. Cass. Fractional Efficiency of a Utility Boiler Baghouse - Nucla Generating Plant. Report No. EPA-600/2-75-013a. (NTIS No. PB240-641/AS.) August 1975. 148 p.

7. Dennis, R. and H. A. Klemm. Fabric Filter Model Format Change. Vol. I Detailed Technical Report, Vol. II User's Guide. U.S. Environmental Protection Agency, Industrial Environmental Research Laboratory, Research Triangle Park, North Carolina. EPA-600/7-79-043a, EPA-600/7-79-043b. February 1979.

8. Billings, C. E. and J. E. Wilder. Handbook of Fabric Filter Technology. Volume I, Fabric Filter Systems Study. Environmental Protection Agency. Publication Number APTD-0690 (NTIS No. PB-200-648). December 1970. 649 p.

9. Ensor, D. S., R. C. Hooper, and R. W. Scheck. Determination of the Fractional Efficiency, Opacity Characteristics, and Engineering Aspects of a Fabric Filter Operating on a Utility Boiler," Final Report. EPRI-FP-297. November 1976.

10. Dennis, R. and J. E. Wilder, Fabric Filter Cleaning Studies. U.S. Environmental Protection Agency, Control Systems Laboratory, Research Triangle Park, North Carolina. EPA-650/2-75-009 (NTIS No. PB-240-372/3G1). January 1975.

11. Snyder, J. W. Mobile Fabric Filter Unit at Southwestern Public Service Company, Harrington Station, Amarillo, Texas. Industrial Environmental Research Laboratory, U.S. Environmental Protection Agency. EPA Contract No. 68-02-1816, Technical Operations Report No. 5, November 1977.

12. Rudnick, S. N. and M. W. First. Specific Resistance (K_2) of Filter Dust Cakes: Comparison of Theory and Experiments. Third Symposium on Fabric Filters for Particulate Collection. Report No. EPA-600/7-78-087. June 1978. p. 251-288.

13. Happel, J. Viscous Flow in Multiparticle Systems: Slow Motion of Fluids Relative to Beds of Spherical Particles. AIChE J. 4:197-201, 1958.

14. Spaite, P. W., G. W. Walsh. Effect of Fabric Structure on Filter Performance. Amer Ind Hyg Assoc J. 24:357-365. 1963.

15. Borgwardt, R. H. and J. F. Durham. Factors Affecting the Performance of Fabric Filters. (Presented at 60th Annual Meeting of the American Institute of Chemical Engineers. New York. 1967).

APPENDIX A

EQUATIONS FOR ESTIMATING DUST PENETRATION

The general form selected for the mathematical function defining penetration is:

$$Pn = Pn_s + (Pn_o - Pn_s) \exp(-aW) \qquad (37)$$

where Pn = penetration

Pn_s = penetration at steady state

Pn_o = initial penetration at $W = W_R$

W = increase in fabric loading above the residual value, W_R

a = concentration decay function

Equation (37) reflects both the rapid exponential decay observed for outlet loadings as well as their ultimate leveling off at a fixed emission rate as filtration progresses.

The constants Pn_s, Pn_o and a were evaluated for velocities of 0.39 to 3.35 m/min. A Pn_o value of 0.1 was used for the initial penetration.

$$Pn_s = 1.5 \times 10^{-7} \exp \left\{ 12.7 \left| 1-\exp(-1.03V) \right| \right\} \qquad (38)$$

$$a = \frac{3.6 \times 10^{-3}}{V^4} + 0.094 \qquad (39)$$

where V is the local face velocity, m/min.

Equations (37) through (39) provide the means for predicting penetration as a function of face velocity and fabric loading. The outlet concentration, C_o, is found by multiplying the inlet concentration, C_i, by the actual penetration followed by the addition of the residual outlet concentration, C_R; i.e.,

$$C_o = Pn\, C_i + C_R$$

APPENDIX B

RESULTS OF SENSITIVITY TESTS

A complete summary of all sensitivity tests is presented in Tables 15 through 23. Because of the similarities in data content for Tables 16 through 22, a brief guideline table (Table 15) was prepared to facilitate their use.

Insofar as predicted filter performance is concerned, maximum, minimum and average values are indicated for system pressure drop and dust penetration. A single value is given for the time between cleaning which provides an indirect measure of potential fabric wear and an indication as to how well higher dust loadings and/or higher air-to-cloth ratios might be tolerated without any significant increase in system pressure drop. Many additional tests involving variable combinations not specified in prior tables are shown in Table 23. The data given in Tables 16 through 23 have been used to prepare the graphical presentation of filter system performance.

TABLE 15. SENSITIVITY DATA SUMMARY FOR TABLES 16 THROUGH 22

Table	Dependent variables*	Independent variables	Fixed inputs	
	$\overline{P}(N/m^2)$, t_f(min) and $\overline{Pn}$ (percent)	V_i(m/min), $P_L(N/m^2)$	a_c	$C_i(g/m^3)$
B-2	$\overline{P}$ t_f $\overline{Pn}$	V_i, P_L	0.1	2.29
B-3	$\overline{P}$ t_f $\overline{Pn}$	V_i, P_L	0.1	6.87
B-4	$\overline{P}$ t_f $\overline{Pn}$	V, P_L	0.1	22.9
B-5	$\overline{P}$ t_f $\overline{Pn}$	V, P_L	0.4	2.29
B-6	$\overline{P}$ t_f $\overline{Pn}$	V, P_L	0.4	6.87
B-7	$\overline{P}$ t_f $\overline{Pn}$	V, P_L	0.4	22.9
B-8	$\overline{P}$ t_f $\overline{Pn}$	V, P_L	1.0	6.87

*Maximum, average and minimum values given for $\overline{P}$ and $\overline{Pn}$, single value given for t_f.

TABLE 16. PREDICTED SYSTEM PERFORMANCE WITH a_c = 0.1 AND C_i = 2.29 g/m^3 AS FIXED INPUTS AND V_i (m/min) AND P_L (N/m^2) AS INDEPENDENT VARIABLES

	P_L \ V	0.3	0.61	0.91	1.22	1.53
Pressure drop, N/m^2						
Maximum	C*	-	607	1,164	-	3,045
	500	576	-	-	-	-
	1,000	1,162	1,155	-	-	-
	1,500	-	-	-	-	-
	2,000	2,053	-	-	-	-
Average	C	-	601	1,149	-	2,983
	500	466	-	-	-	-
	1,000	877	976	-	-	-
	1,500	-	-	-	-	-
	2,000	1,690	-	-	-	-
Minimum	C	-	532	1,010	-	2,596
	500	412	-	-	-	-
	1,000	660	860	-	-	-
	1,500	-	-	-	-	-
	2,000	978	-	-	-	-
Time between cleaning cycles, min.						
	C	-	0	0	-	0
	500	255	77	-	-	-
	1,000	747	-	-	-	-
	1,500	-	-	-	-	-
	2,000	1,654	-	-	-	-
Penetration, percent						
Maximum	C	-	0.375	0.415	-	1.21
	500	0.628	-	-	-	-
	1,000	0.812	0.48	-	-	-
	1,500	-	-	-	-	-
	2,000	1.22	-	-	-	-
Average	C	-	0.279	0.298	-	1.05
	500	0.074	-	-	-	-
	1,000	0.046	0.122	-	-	-
	1,500	0.040	-	-	-	-
	2,000	-	-	-	-	-
Minimum	C	-	0.197	0.211	-	0.864
	500	0.023	-	-	-	-
	1,000	0.023	0.035	-	-	-
	1,500	0.023	-	-	-	-
	2,000	-	-	-	-	-

* C refers to continuous cleaning.

TABLE 17. PREDICTED SYSTEM PERFORMANCE WITH $a_c = 0.1$ AND $C_i = 6.87\ g/m^3$ AS FIXED INPUTS AND V_i (m/min) AND P_L (N/m^2) AS INDEPENDENT VARIABLES

	P_L \ V	0.3	0.45	0.61	0.91	1.22	1.53
	Pressure drop, N/m^2						
Maximum	C[*]	-	575	-	2,246	4,224	7,015
	500	578	-	-	-	-	-
	1,000	1,164	-	1,170	-	-	-
	1,500	-	-	1,753	-	-	-
	2,000	2,336	-	2,338	-	-	-
Average	C	-	557	-	2,235	4,171	6,883
	500	485	-	-	-	-	-
	1,000	890	-	1,130	-	-	-
	1,500	-	-	1,500	-	-	-
	2,000	1,700	-	1,894	-	-	-
Minimum	C	-	498	-	1,892	3,503	5,739
	500	425	-	-	-	-	-
	1,000	696	-	963	-	-	-
	1,500	-	-	1,272	-	-	-
	2,000	1,079	-	1,555	-	-	-
	Time before cleaning cycles, min.						
	C	-	0	-	0	0	0
	500	77.4	-	-	-	-	-
	1,000	207	-	8	-	-	-
	1,500	-	-	33.6	-	-	-
	2,000	491	-	59.4	-	-	-
	Penetration, percent						
Maximum	C	-	0.033	-	0.586	1.06	1.55
	500	0.356	-	-	-	-	-
	1,000	0.566	-	0.34	-	-	-
	1,500	-	-	0.486	-	-	-
	2,000	1.04	-	0.646	-	-	-
Average	C	-	0.126	-	0.344	0.780	1.24
	500	0.056	-	-	-	-	-
	1,000	0.036	-	0.13	-	-	-
	1,500	-	-	0.117	-	-	-
	2,000	0.033	-	0.13	-	-	-
Minimum	C	-	-	-	0.246	0.631	1.01
	500	0.008	-	-	-	-	-
	1,000	0.0082	0.257	0.028	-	-	-
	1,500	-	-	0.027	-	-	-
	2,000	0.0081	-	0.026	-	-	-

[*] C refers to continuous cleaning.

TABLE 18. PREDICTED SYSTEM PERFORMANCE WITH $a_c = 0.1$ AND $C_i = 22.9$ g/m^3 AS FIXED INPUTS AND V_i (m/min) AND P_L (N/m^2) AS INDEPENDENT VARIABLES

	V P_L	0.3	0.61	0.8
Maximum	C*	531	2,421	4,520
	500	-	-	-
	1,000	1,172	-	-
	1,500	-	-	-
	2,000	2,343	-	-
Average	C	520	2,321	4,300
	500	-	-	-
	1,000	947	-	-
	1,500	-	-	-
	2,000	1,740	-	-
Minimum	C	454	1,987	3,646
	500	-	-	-
	1,000	783	-	-
	1,500	-	-	-
	2,000	1,252	-	-
Time between cleaning cycles, min.				
	C	0	0	0
	500	-	-	-
	1,000	49	-	-
	1,500	-	-	-
	2,000	134	-	-
Penetration, percent				
Maximum	C	0.29	0.618	0.913
	500	-	-	-
	1,000	0.57	-	-
	1,500	-	-	-
	2,000	1.0	-	-
Average	C	0.058	0.182	0.392
	500	-	-	-
	1,000	0.035	-	-
	1,500	-	-	-
	2,000	0.038	-	-
Minimum	C	0.004	0.081	0.234
	500	-	-	-
	1,000	0.0032	-	-
	1,500	-	-	-
	2,000	0.0032	-	-

*C refers to continuous cleaning.

TABLE 19. PREDICTED SYSTEM PERFORMANCE WITH $a_c = 0.4$ AND $C_i = 2.29$ g/m^3 AS FIXED INPUTS AND V_i (m/min) AND P_L (N/m^2) AS INDEPENDENT VARIABLES

	V P_L	0.3	0.61	0.91	1.22	1.53	1.75
			Pressure drop, N/m^2				
Maximum	C[*]	-	457	-	1,156	1,621	1,961
	500	577	570	-	-	-	-
	1,000	1,163	1,160	1,154	-	-	-
	1,500	-	1,742	-	1,739	-	-
	2,000	-	2,328	-	-	-	2,350
Average	C	-	457	-	1,159	1,618	1,834
	500	400	500	-	-	-	-
	1,000	714	810	941	-	-	-
	1,500	-	1,128	-	1,421	-	-
	2,000	-	1,445	-	-	-	2,038
Minimum	C	-	453	-	1,004	1,395	1,904
	500	281	445	-	-	-	-
	1,000	337	580	792	-	-	-
	1,500	-	663	-	1,176	-	-
	2,000	-	720	-	-	-	1,815
			Time between cleaning cycles, min.				
	C	0	0	-	0	0	0
	500	809	46.8	-	-	-	-
	1,000	1,798	270	59.4	-	-	-
	1,500	-	520	-	-	-	-
	2,000	-	759	-	43.2	-	10.8
			Penetration, percent				
Maximum	C	-	1.23	-	1.09	1.37	1.67
	500	1.96	0.997	-	-	-	-
	1,000	2.4	1.1	1.17	-	-	-
	1,500	-	1.76	-	1.28	-	-
	2,000	-	2.07	-	-	-	1.77
Average	C	-	0.975	-	0.777	1.05	1.36
	500	0.076	0.574	-	-	-	-
	1,000	0.0496	0.13	0.322	-	-	-
	1,500	-	0.096	-	0.489	-	-
	2,000	-	0.083	-	-	-	1.27
Minimum	C	-	0.749	-	0.462	0.760	1.16
	500	0.0224	0.0283	-	-	-	-
	1,000	0.0226	0.029	0.064	-	-	-
	1,500	-	0.029	-	-	-	-
	2,000	-	0.0295	-	0.191	-	0.767

[*] C refers to continuous cleaning.

TABLE 20. PREDICTED SYSTEM PERFORMANCE WITH $a_c = 0.4$ AND $C_i = 6.87$ g/m^3 AS FIXED INPUTS AND V_i (m/min) AND P_L (N/m^2) AS INDEPENDENT VARIABLES

	P_L \ V	0.3	0.61	0.8	0.91	1.22	1.53	1.75
	Pressure drop, N/m^2							
Maximum	C*	-	566	860	-	1,746	2,700	3,500
	500	578	-	-	-	-	-	-
	1,000	1,164	1,166	-	1,175	-	-	-
	1,500	-	1,756	-	-	-	-	-
	2,000	-	2,335	-	2,346	-	-	-
	2,500	-	2,922	-	-	2,969	3,030	-
Average	C	-	560	855	-	1,690	2,600	3,358
	500	403	-	-	-	-	-	-
	1,000	726	860	-	1,097	-	-	-
	1,500	-	1,160	-	-	-	-	-
	2,000	-	1,480	-	1,679	-	-	-
	2,500	-	1,793	-	-	2,291	2,750	-
Minimum	C	-	500	737	-	1,510	2,200	2,819
	500	283	-	-	-	-	-	-
	1,000	359	649	-	935	-	-	-
	1,500	-	750	-	-	-	-	-
	2,000	-	819	-	1,456	-	-	-
	2,500	-	873	-	-	1,762	2,282	-
	Time between cleaning cycles, min.							
	C	-	0	0	-	0	0	0
	500	286	-	-	-	-	-	-
	1,000	672	80	-	6.6	-	-	-
	1,500	-	160	-	-	-	-	-
	2,000	-	236	-	63	-	-	-
	2,500	-	318	-	-	28.2	4.8	-
	Penetration, percent							
Maximum	C	-	0.73	0.762	-	1.1	1.61	2.0
	500	1.22	-	-	-	-	-	-
	1,000	2.0	1.1	-	0.869	-	-	-
	1,500	-	1.5	-	-	-	-	-
	2,000	-	1.87	-	1.44	-	-	-
	2,500	-	2.19	-	-	1.57	1.69	
Average	C	-	0.36	0.323	-	0.57	1.03	1.42
	500	0.06	-	-	-	-	-	-
	1,000	0.037	0.13	-	0.302	-	-	-
	1,500	-	0.09	-	-	-	-	-
	2,000	-	0.08	-	0.229	-	-	-
	2,500	-	0.074	-	-	0.54	1.02	-
Minimum	C	-	0.089	0.077	-	0.35	0.83	1.18
	500	0.008	-	-	-	-	-	-
	1,000	0.0078	0.015	-	0.065	-	-	-
	1,500	-	0.015	-	-	-	-	-
	2,000	-	0.015	-	0.057	-	-	-
	2,500	-	0.015	-	-	0.207	0.62	-

*C refers to continuous cleaning.

TABLE 21. PREDICTED SYSTEM PERFORMANCE WITH $a_c = 0.4$ AND $C_i = 22.9\ g/m^3$ AS FIXED INPUTS AND V_i (m/min) AND P_L (N/m^2) AS INDEPENDENT VARIABLES

	P_L \ V	0.3	0.61	0.91	1.22
	Pressure drop, N/m^2				
Maximum	C[*]	280	915	2,111	3,752
	500	582	-	-	-
	1,000	1,169	1,210	-	-
	1,500	1,756	-	-	-
	2,000	2,342	2,373	2,389	-
Average	C	276	887	1,995	3,517
	500	428	-	-	-
	1,000	739	1,050	-	-
	1,500	1,053	-	-	-
	2,000	1,368	1,073	2,156	-
Minimum	C	272	862	1,850	3,328
	500	321	-	-	-
	1,000	406	850	-	-
	1,500	458	-	-	-
	2,000	494	1,604	1,741	-
	Time between cleaning cycles, min.				
	C	0	0	0	0
	500	71.4	-	-	-
	1,000	209	10	-	-
	1,500	330	-	-	-
	2,000	479	55.2	5.4	-
	Penetration, percent				
Maximum	C	0.622	0.91	1.33	1.8
	500	1.16	-	-	-
	1,000	1.99	1.1	-	-
	1,500	2,64	-	-	-
	2,000	3.16	1.89	1.46	-
Average	C	0.133	0.159	0.351	0.768
	500	0.062	-	-	-
	1,000	0.034	0.17	-	-
	1,500	0.025	-	-	-
	2,000	0.0219	0.114	0.352	-
Minimum	C	0.0053	0.024	0.155	0.534
	500	0.0027	-	-	-
	1,000	0.0027	0.013	-	-
	1,500	0.0027	-	-	-
	2,000	0.0027	0.0104	0.102	-

[*] C refers to continuous cleaning.

TABLE 22. PREDICTED SYSTEM PERFORMANCE WITH $a_c = 1.0$ AND $C_i = 6.87\ g/m^3$ AS FIXED INPUTS AND V_i (m/min) AND $\bar{P}_L$ (N/m^2) AS INDEPENDENT VARIABLES

		0.3	0.61	0.91	1.22	1.53	1.75
			Pressure drop, N/m^2				
Maximum	C*	-	475	-	1,244	1,780	2,227
	500	578	576	-	-	-	-
	1,000	1,164	1,163	-	-	-	-
	1,500	-	1,750	-	-	-	-
	2,000	-	2,336	-	2,375	2,414	-
Average	C	-	475	-	1,209	1,705	2,113
	500	314	492	-	-	-	-
	1,000	591	713	-	-	-	-
	1,500	-	957	-	-	-	-
	2,000	-	1,203	-	1,504	1,889	-
Minimum	C	-	413	-	1,038	1,452	1,789
	500	183	415	-	-	-	-
	1,000	184	421	-	-	-	-
	1,500	-	425	-	-	-	-
	2,000	-	427	-	1,062	1,494	
			Time between cleaning cycles, min.				
	C	-	0	-	0	0	0
	500	553	25.2	-	-	-	-
	1,000	1,431	170	-	-	-	-
	1,500	-	317.4	-	-	-	-
	2,000	-	464.4	-	43	15	-
			Penetration, percent				
Maximum	C	-	1.57	-	1.70	2.04	2.37
	500	2.62	1.69	-	-	-	-
	1,000	4.04	2.5	-	-	-	-
	1,500	-	3.24	-	-	-	-
	2,000	-	3.87	-	2.46	2.36	-
Average	C	-	0.805	-	0.702	1.0	1.34
	500	0.054	0.459	-	-	-	-
	1,000	0.029	0.143	-	-	-	-
	1,500	-	0.0908	-	-	-	-
	2,000	-	0.070	-	0.42	0.872	-
Minimum	C	-	0.268	-	0.309	0.664	1.04
	500	0.0077	0.013	-	-	-	-
	1,000	-	0.013	-	-	-	-
	1,500	-	0.013	-	-	-	-
	2,000	-	0.0128	-	0.14	0.393	-

*C refers to continuous cleaning.

TABLE 23. PREDICTED SYSTEM PERFORMANCE FOR FIXED AND VARIABLE DATA INPUT COMBINATIONS NOT SPECIFIED IN TABLES 16 THROUGH 22

P_L	V	a_c	C_i	Other parameters	Pressure drop			Time between cleanings	Penetration		
					min.	max.	avg.		min.	max.	avg.
1,000	0.61	1.0	2.29	-	383	1,156	692	548	0.0273	3.04	0.15
1,000	0.61	1.0	22.9	-	539	1,196	797	40	0.0079	2.52	0.15
1,000	0.61	0.2	6.87	-	815	1,166	974	87	0.018	0.593	0.115
1,000	0.61	0.2	2.29	-	735	1,155	896	160	0.031	0.843	0.124
1,000	0.61	0.2	22.9	-	1,332	1,436	1,400	0	0.041	0.707	0.138
1,000	0.61	0.2	22.9	-	944	1,211	1,127	4	0.021	0.878	0.136
continuous	0.61	0.4	2.29	$K_2 = 3$	580	670	650	0	0.40	1.3	0.98
2,000	0.61	0.4	2.29	$K_2 = 3$	930	2,340	1,520	230	0.029	1.4	0.17
continuous	0.91	1.0	6.87	nonlinear model	530	770	700	0	0.093	3.3	0.67
continuous	0.61	0.1	22.9	nonlinear model	-	-	2,310	0	-	-	0.26
2,000	0.61	0.4	2.29	nonlinear model $K_2 = 3$	625	2,330	1,440	240	0.029	4.5	0.19
continuous	0.91	0.4	6.87	nonlinear model	790	1,053	980	0	0.12	2.0	0.39
continuous	0.91	0.1	6.87	-	-	-	2,140	0	-	-	0.40
1,000	0.61	0.4	6.87	$K_2 = 0.333$	553	1,156	790	304	0.014	1.2	0.054
1,000	0.61	0.4	6.87	$K_2 = 3.333$	918	1,197	1,075	6	0.030	0.92	0.32
continuous	0.61	0.4	6.87	$K_2 = 0.333$	380	430	425	0	0.15	0.65	0.32
continuous	0.61	0.4	6.87	$K_2 = 3.333$	983	1,030	1,000	0	0.12	0.86	0.37

APPENDIX C

SENSITIVITY ANALYSIS GRAPHICAL PRESENTATIONS FOR MULTIVARIABLE SYSTEMS

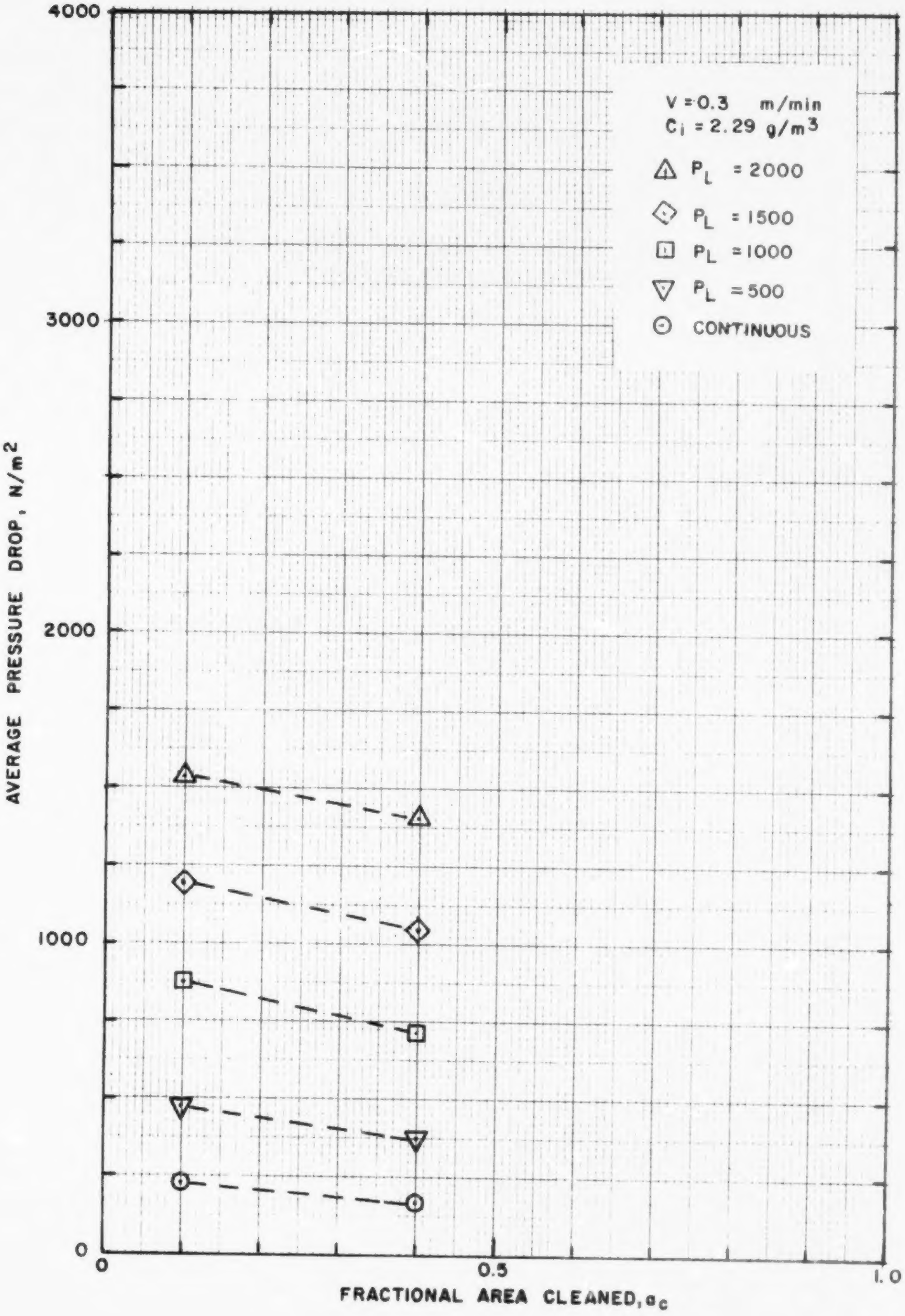

Figure 43. $\overline{P}$ versus a_c and P_L.

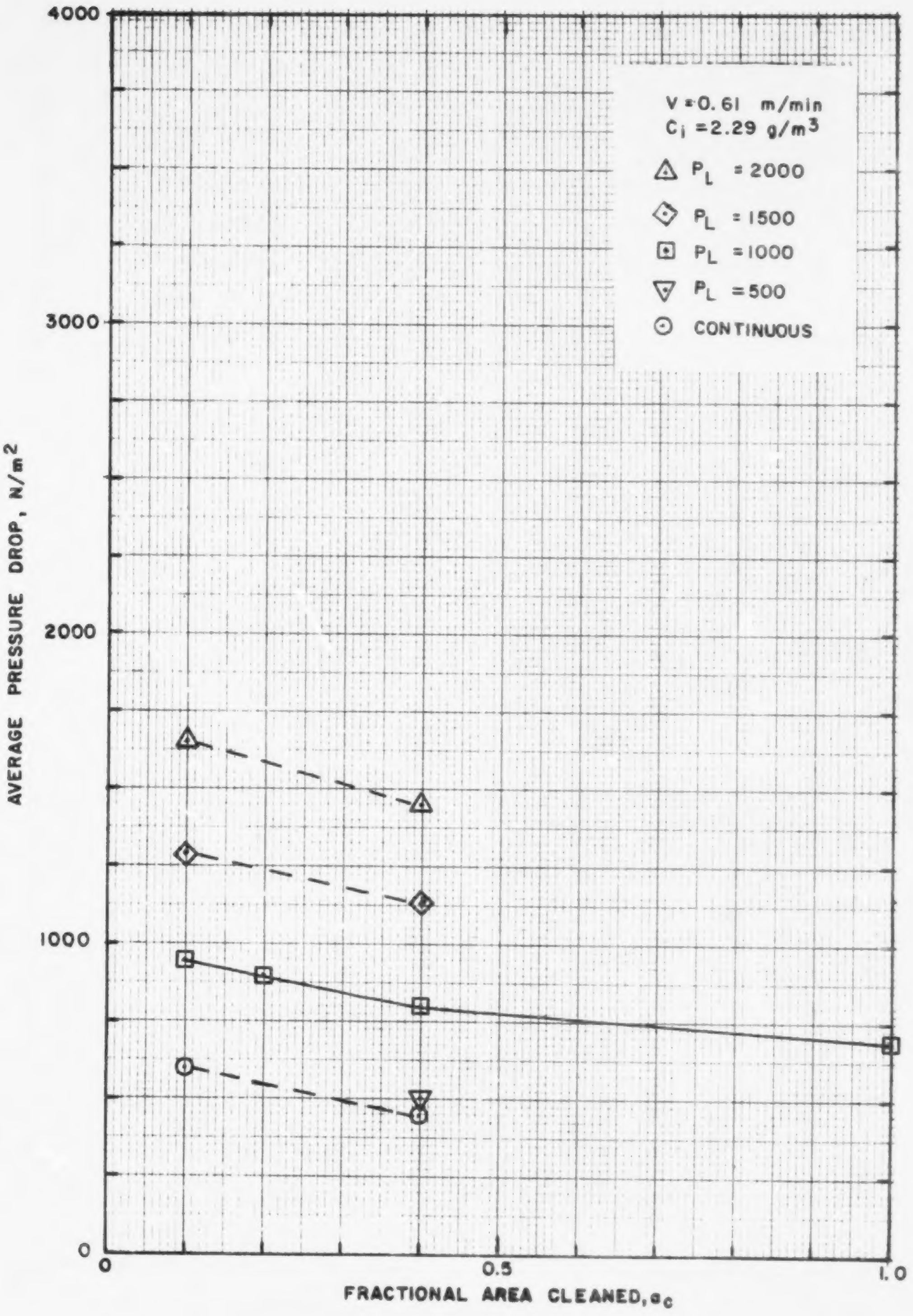

Figure 44. $\overline{P}$ versus a_c and P_L.

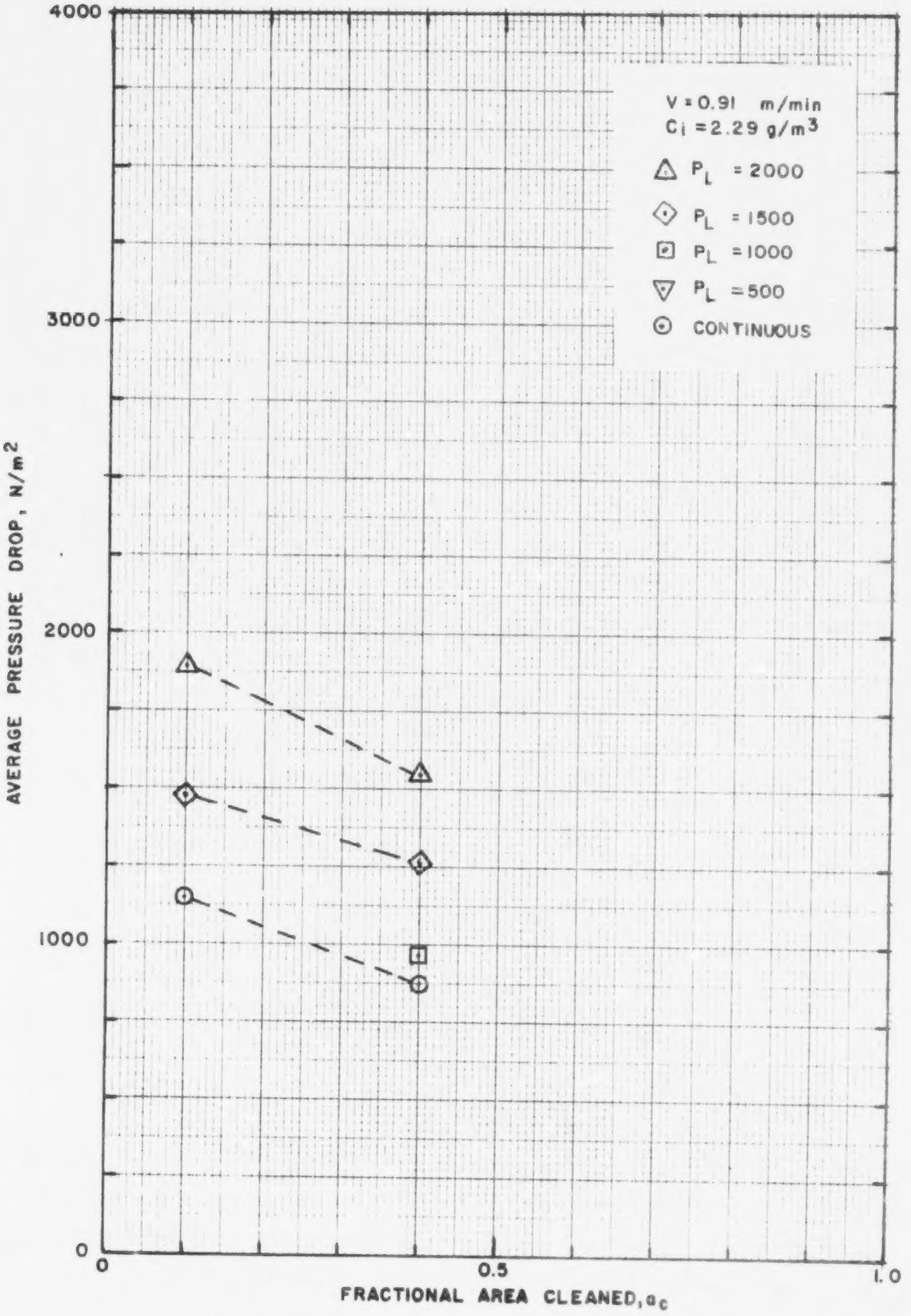

Figure 45. $\overline{P}$ versus a_c and P_L.

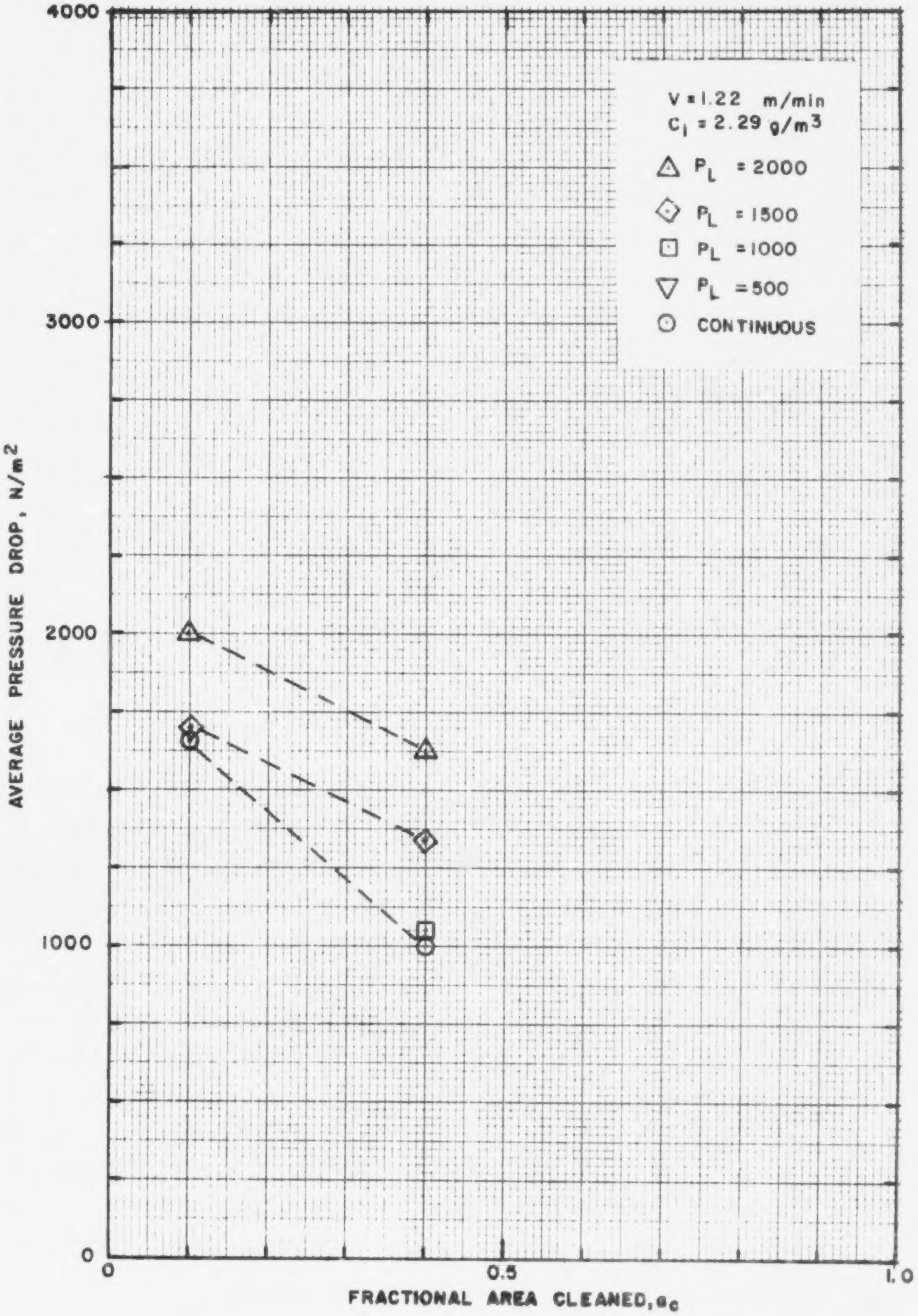

Figure 46. $\overline{P}$ versus a_c and P_L.

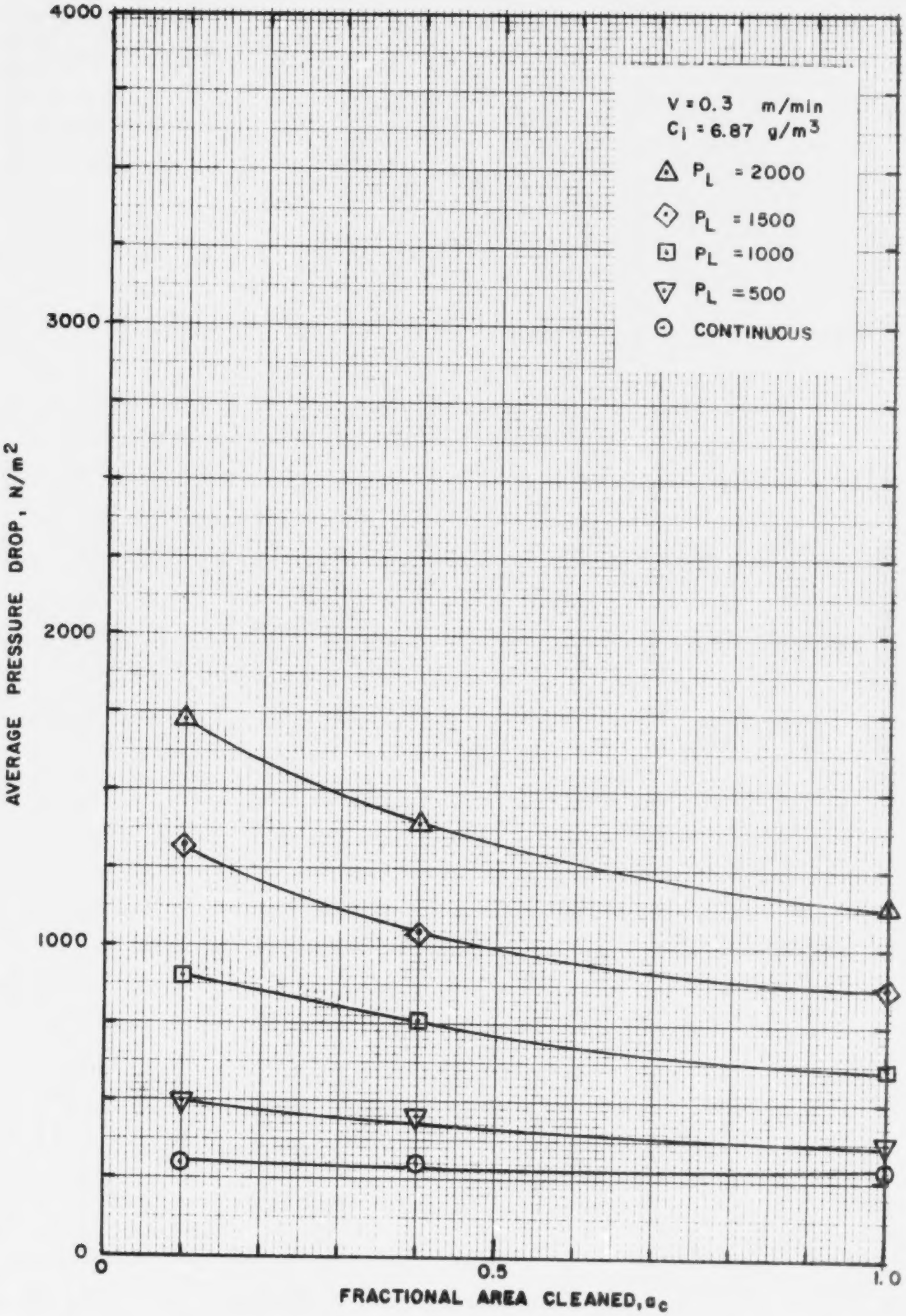

Figure 47. $\overline{P}$ versus a_c and P_L.

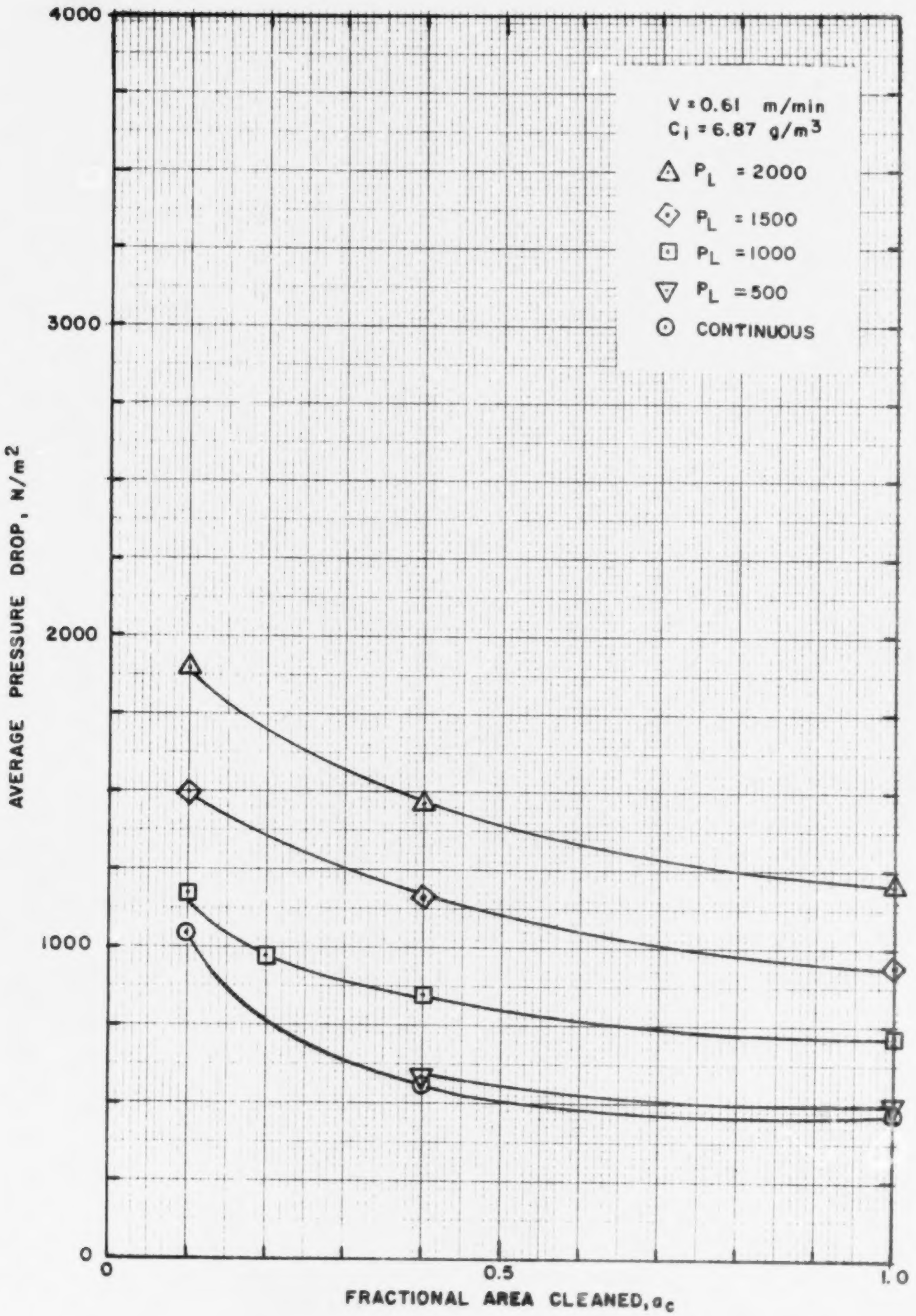

Figure 48. $\overline{P}$ versus a_c and P_L.

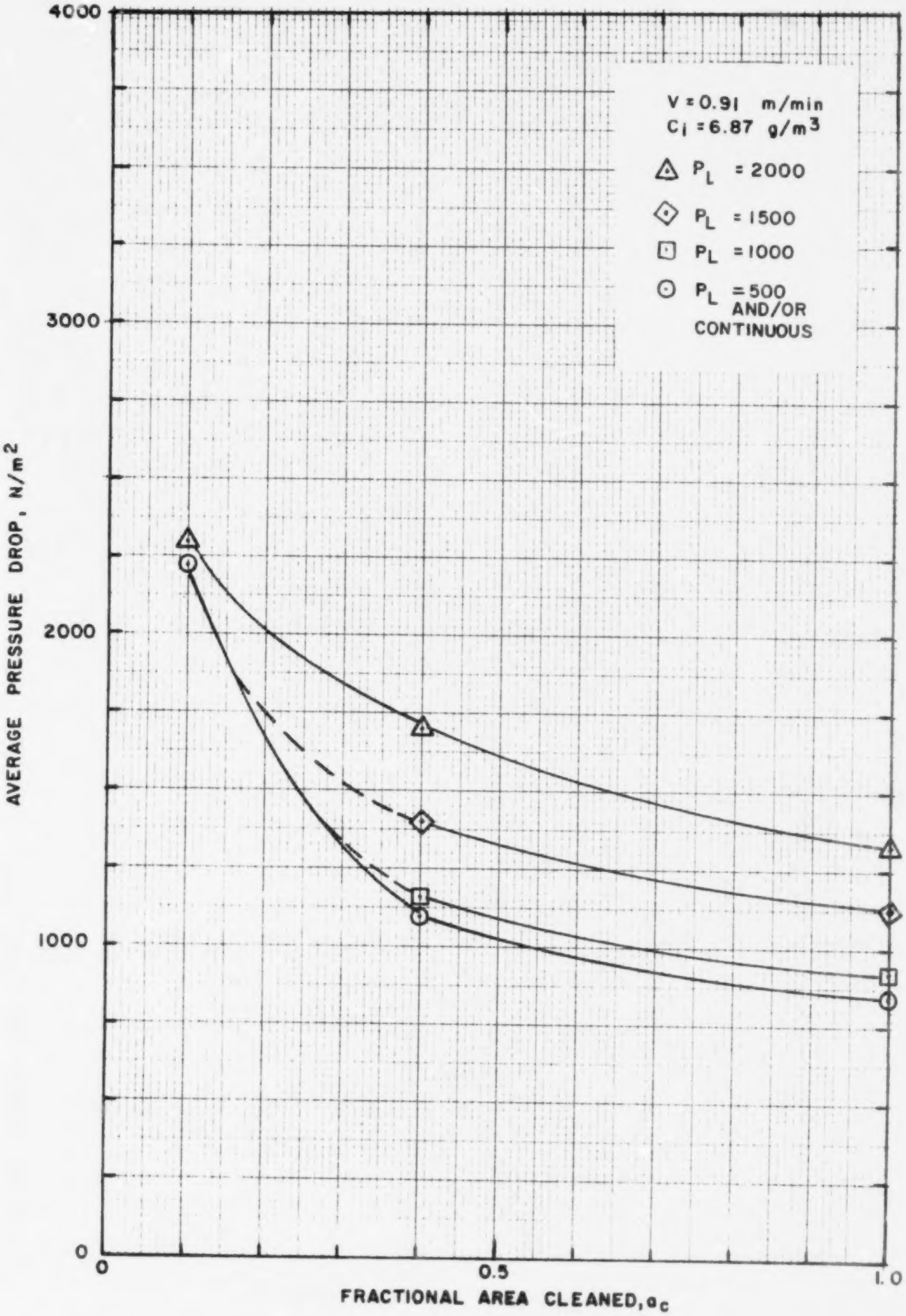

Figure 49. $\overline{P}$ versus a_c and P_L.

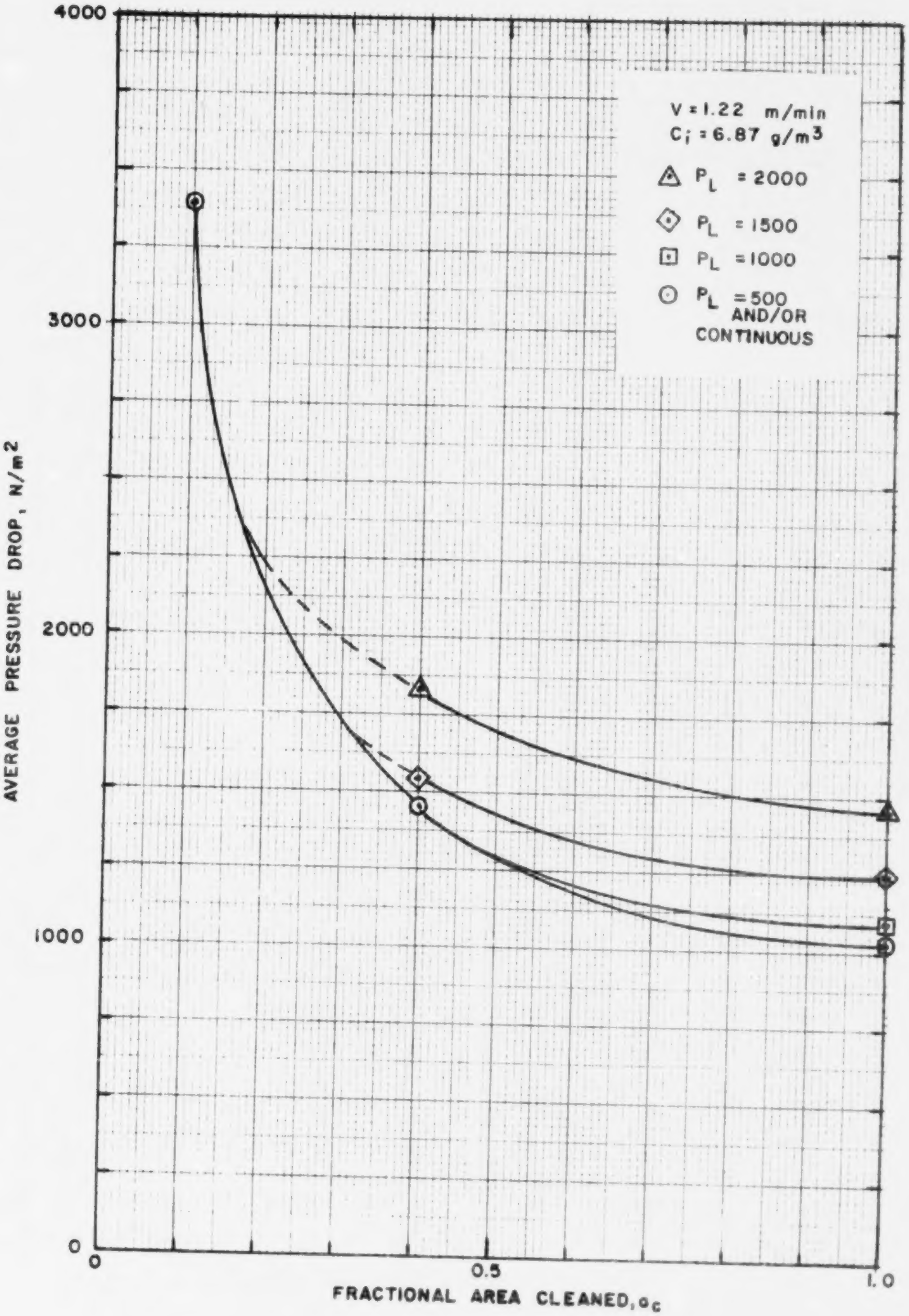

Figure 50. $\overline{P}$ versus a_c and P_L.

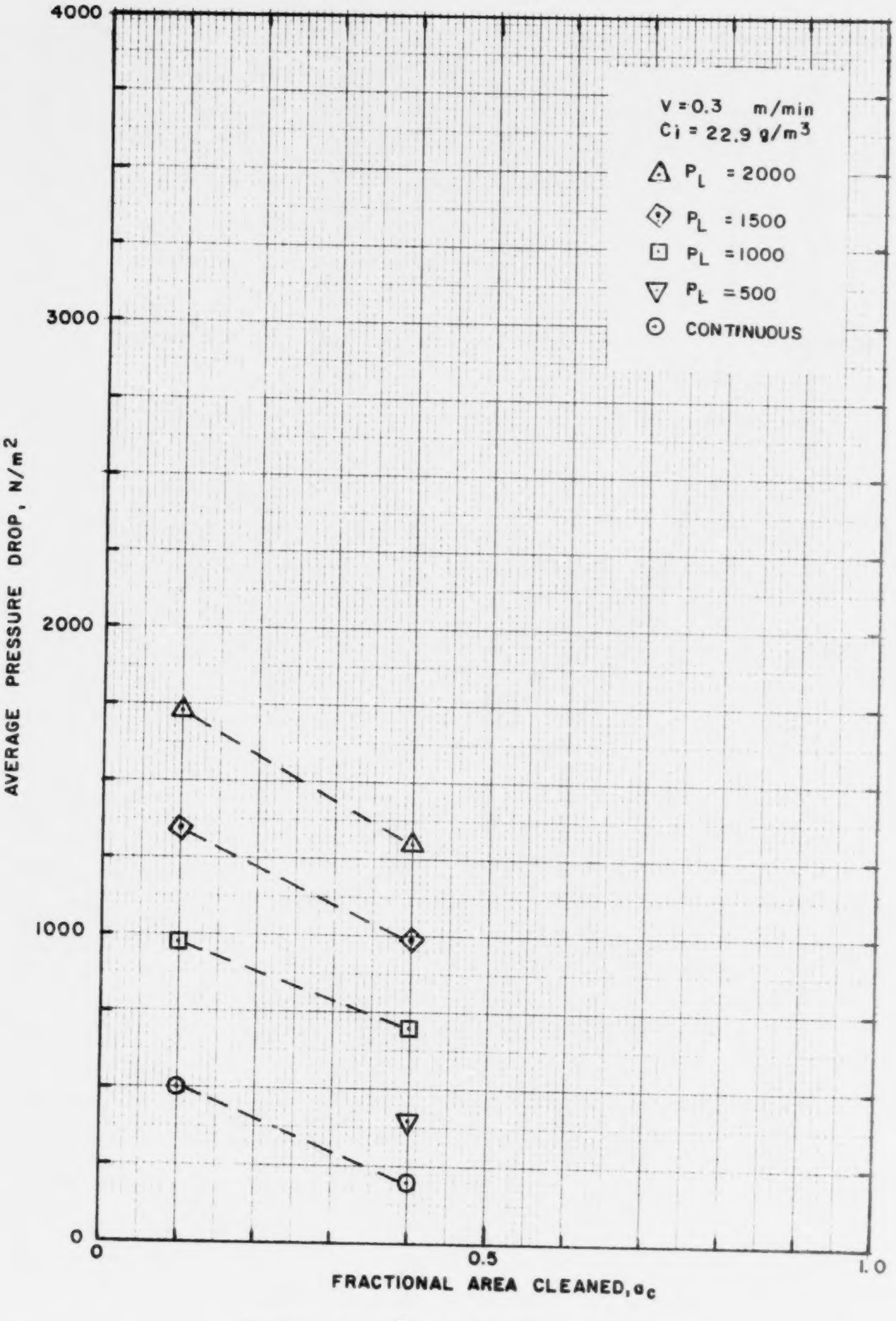

Figure 51. $\overline{P}$ versus a_c and P_L.

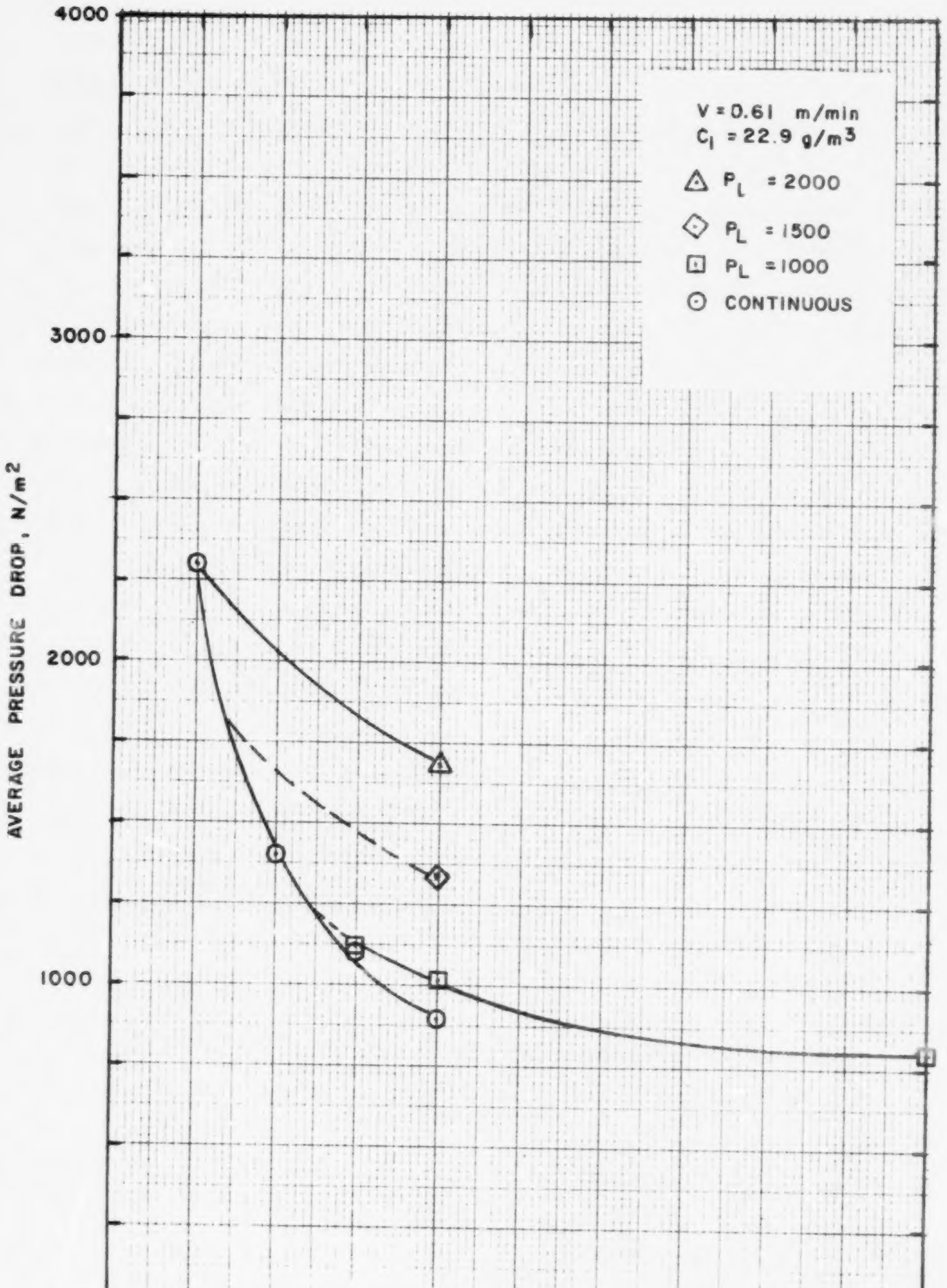

Figure 52. $\overline{P}$ versus a_c and P_L.

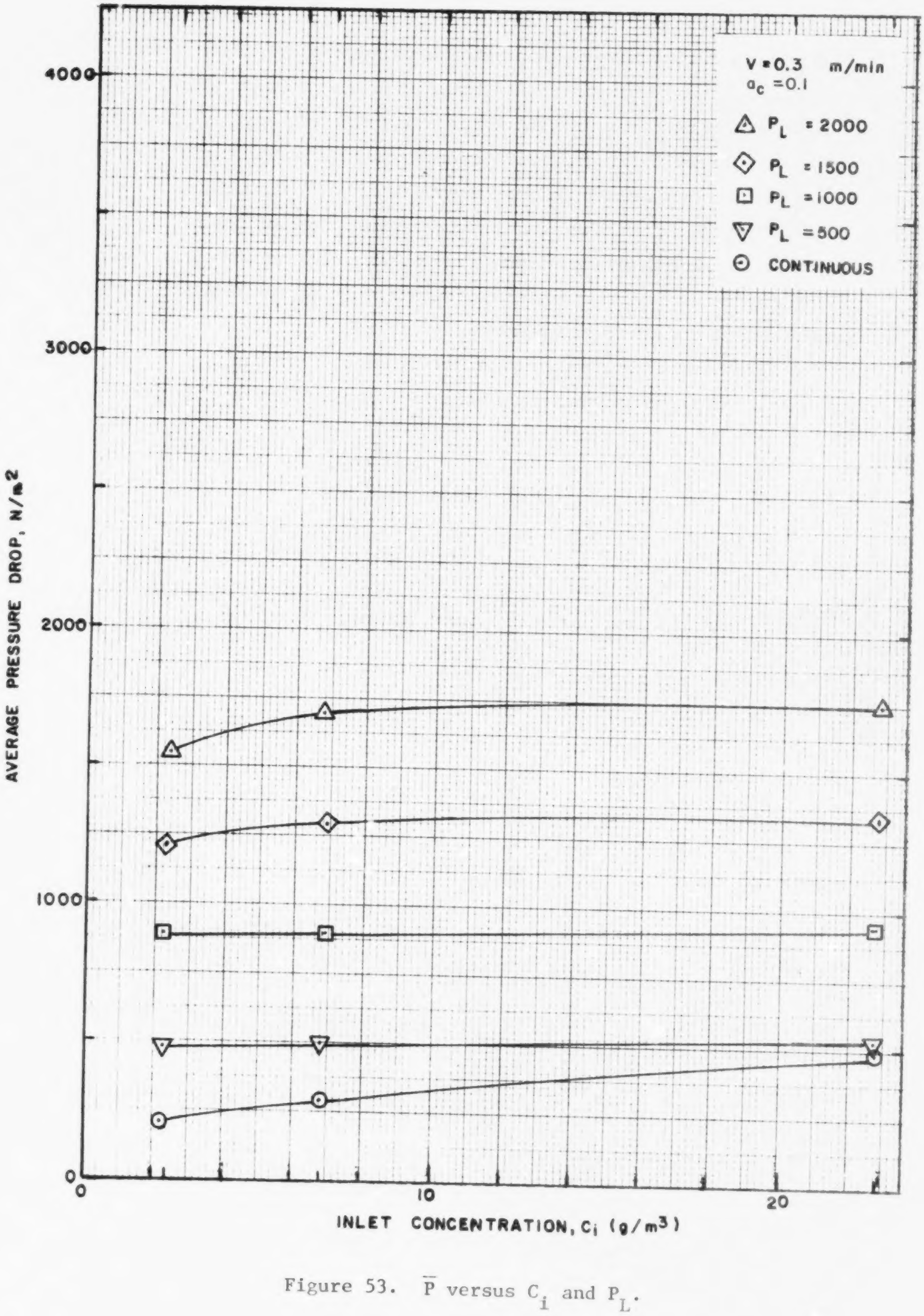

Figure 53. $\overline{P}$ versus C_i and P_L.

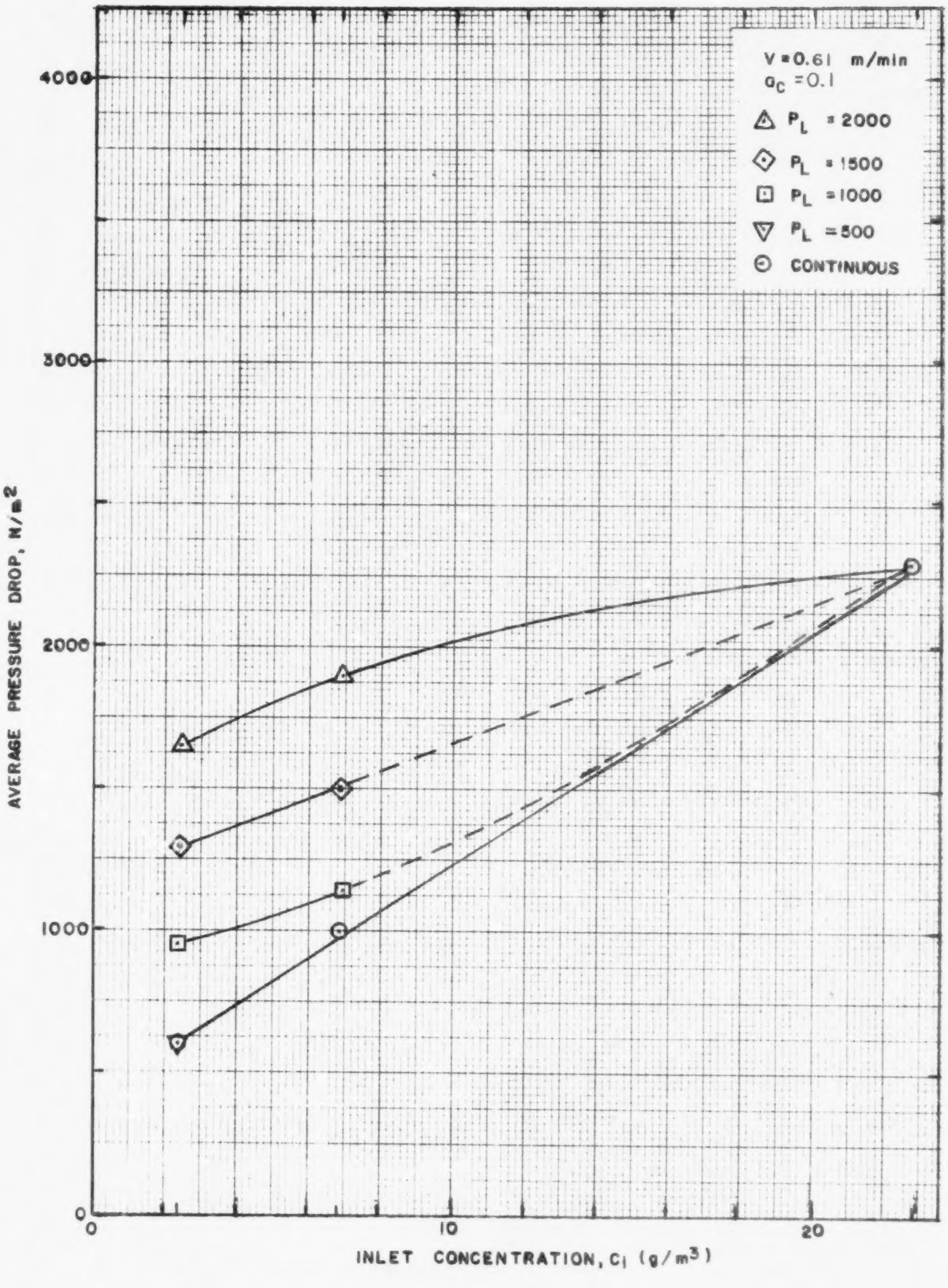

Figure 54. $\overline{P}$ versus C_i and P_L.

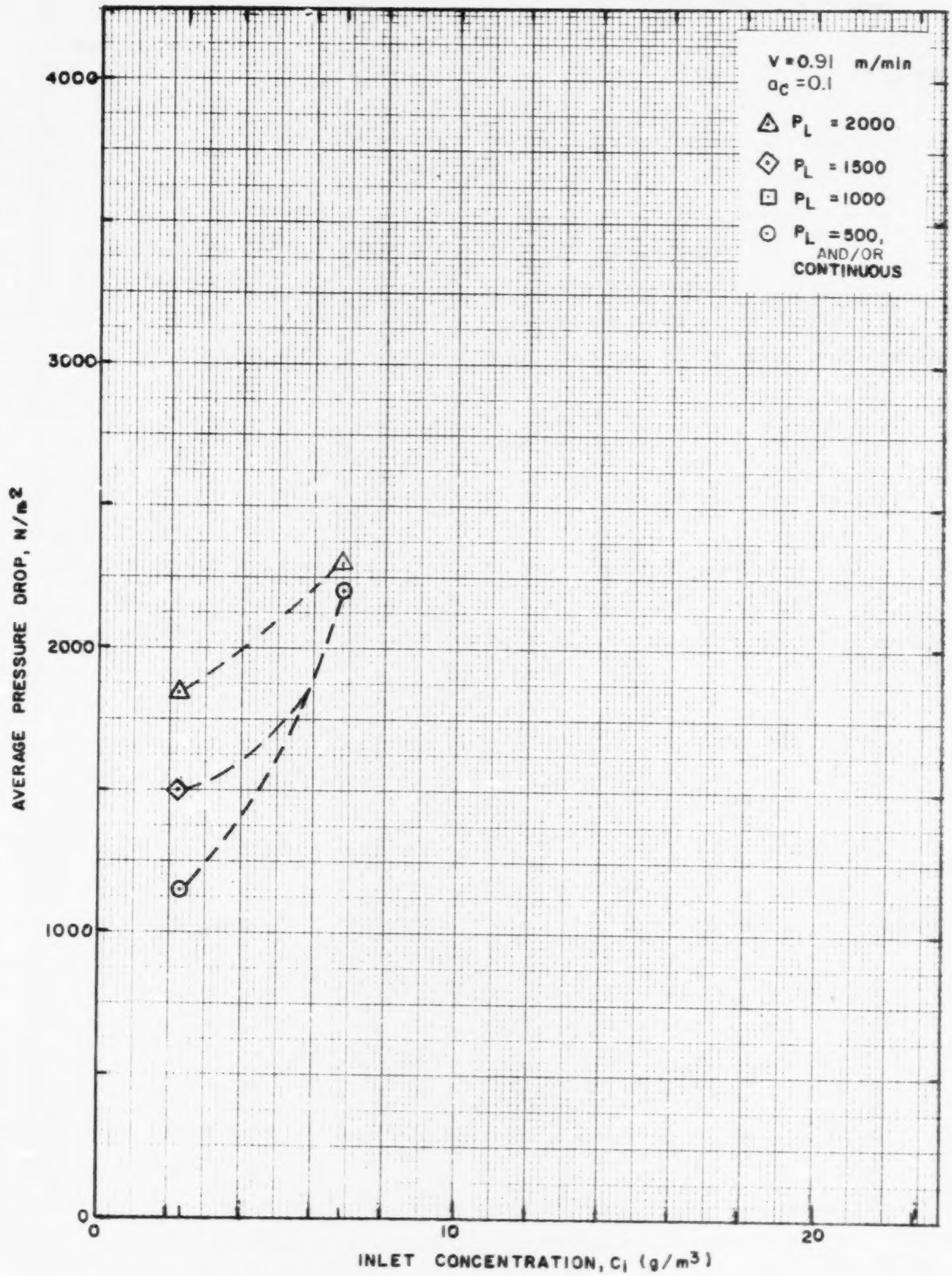

Figure 55. $\overline{P}$ versus C_i and P_L.

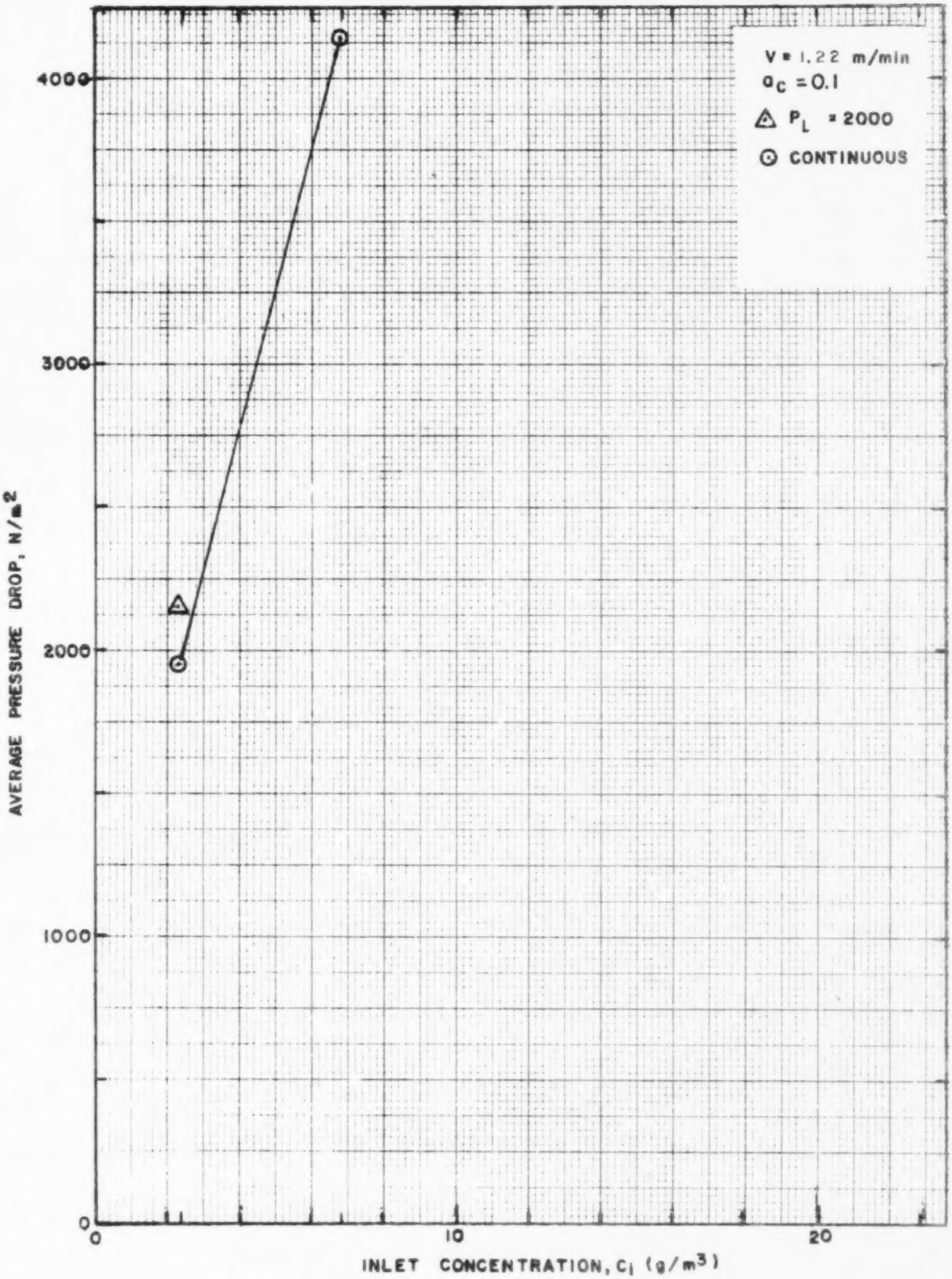

Figure 56. $\overline{P}$ versus C_i and P_L.

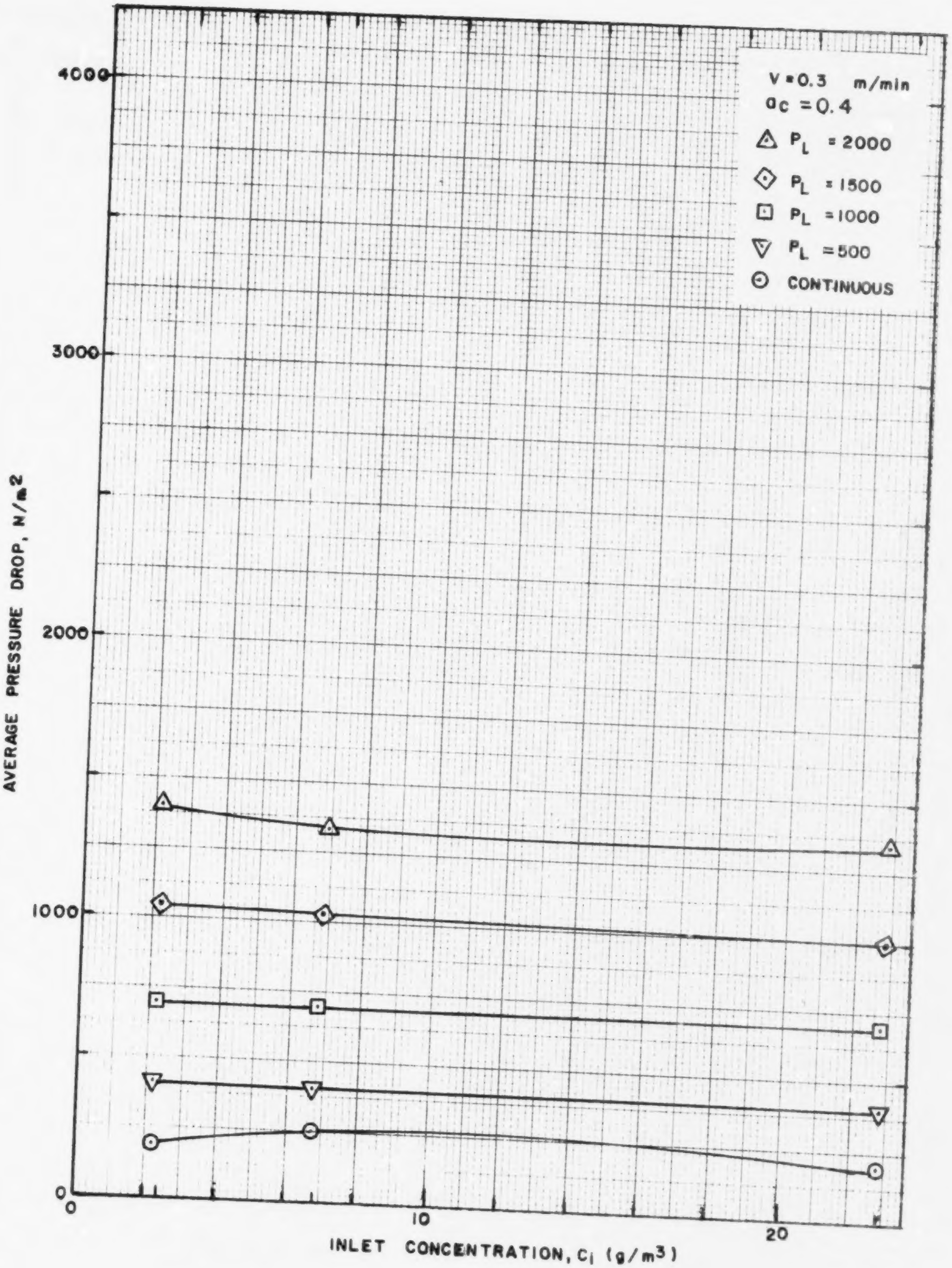

Figure 57. $\overline{P}$ versus C_i and P_L.

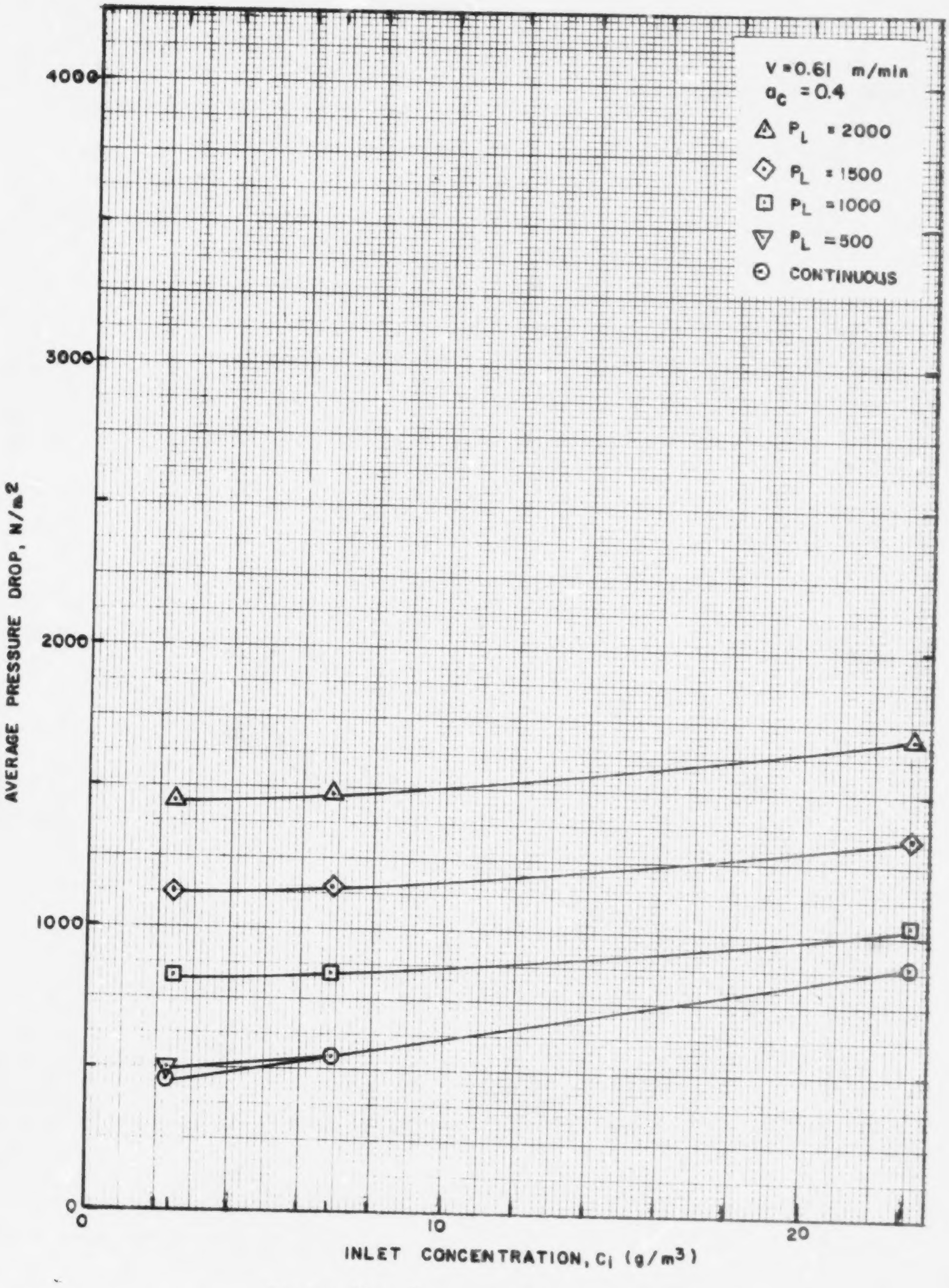

Figure 58. $\overline{P}$ versus C_i and P_L.

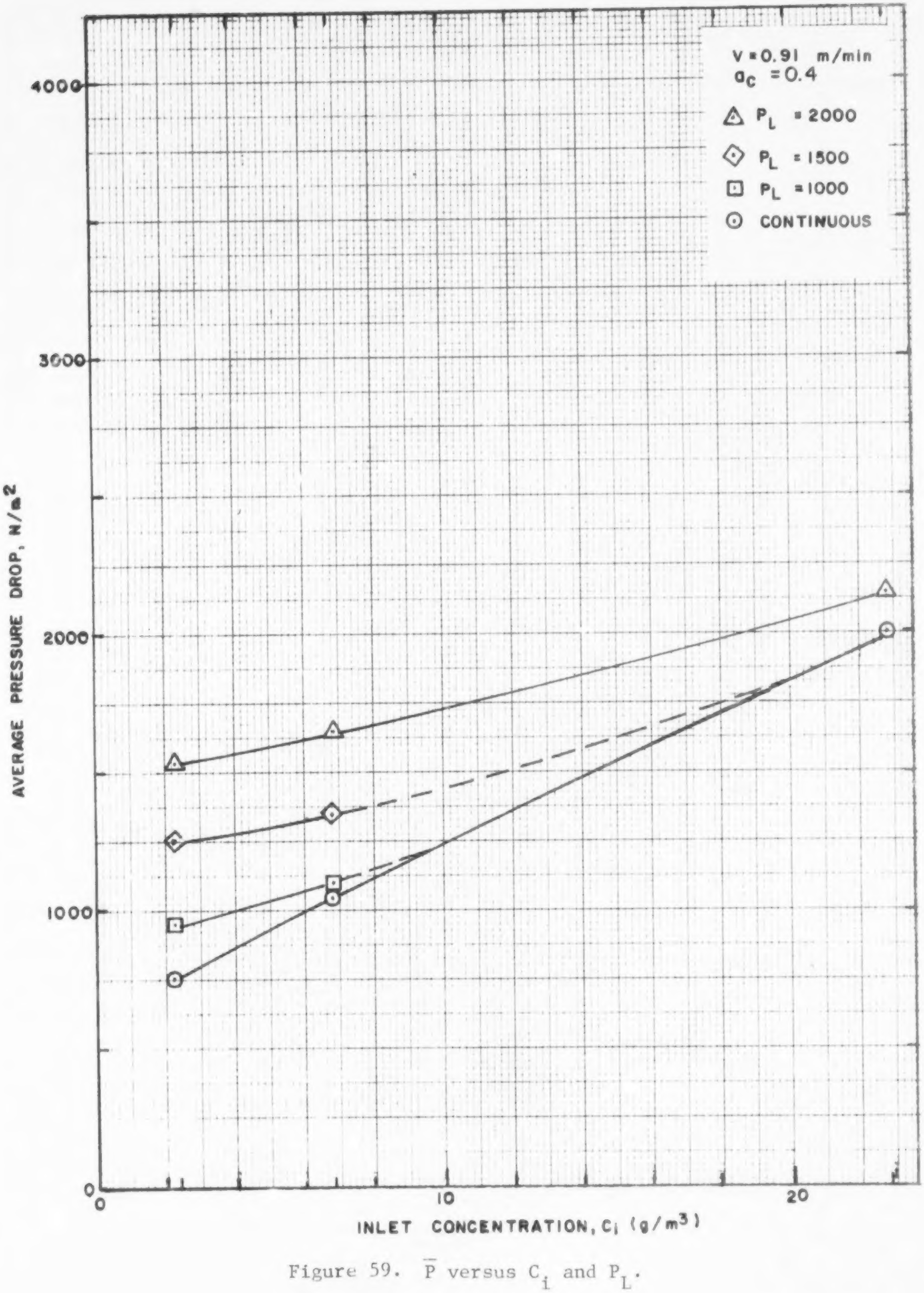

Figure 59. $\overline{P}$ versus C_i and P_L.

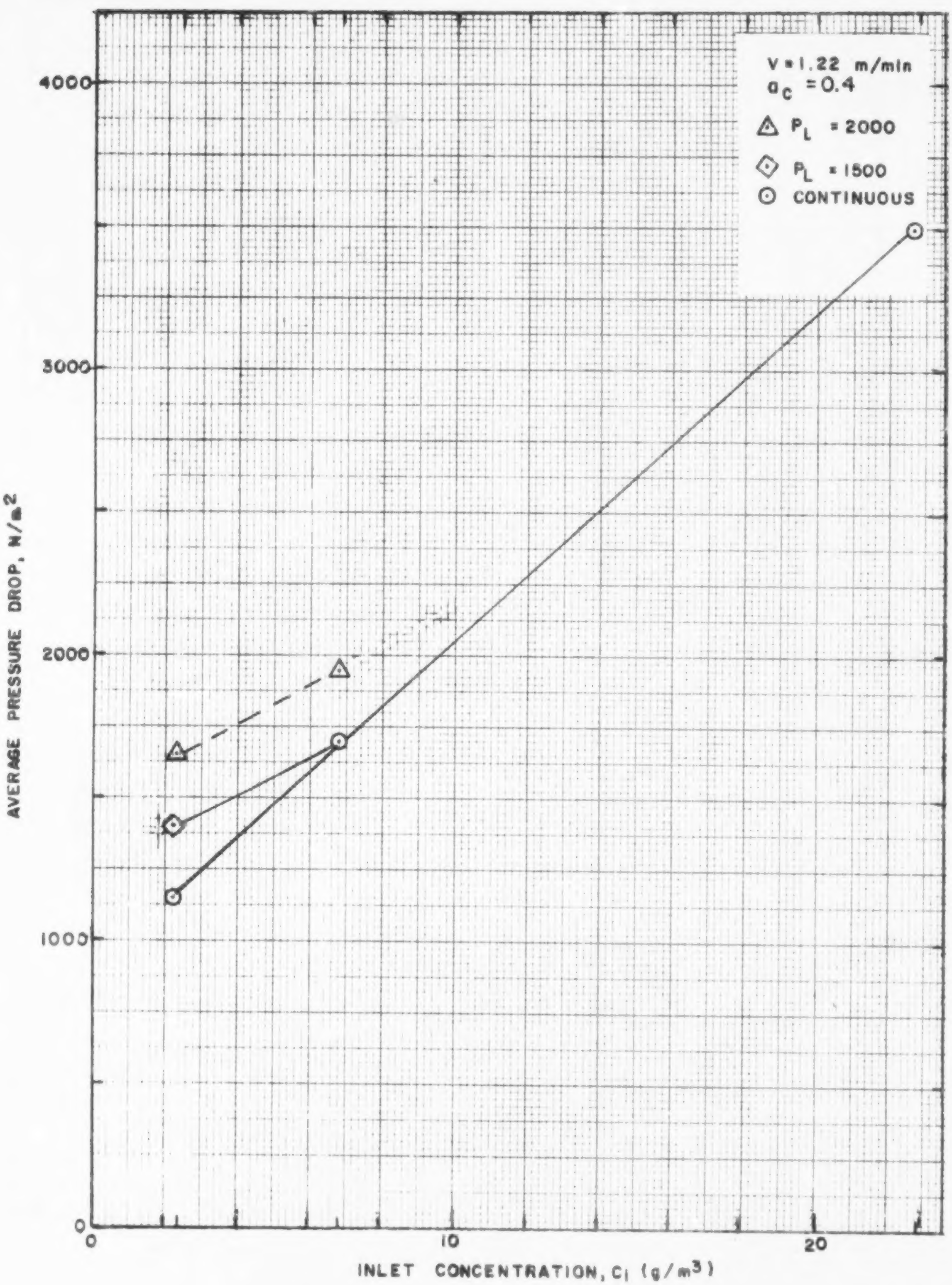

Figure 60. $\overline{P}$ versus C_i and P_L.

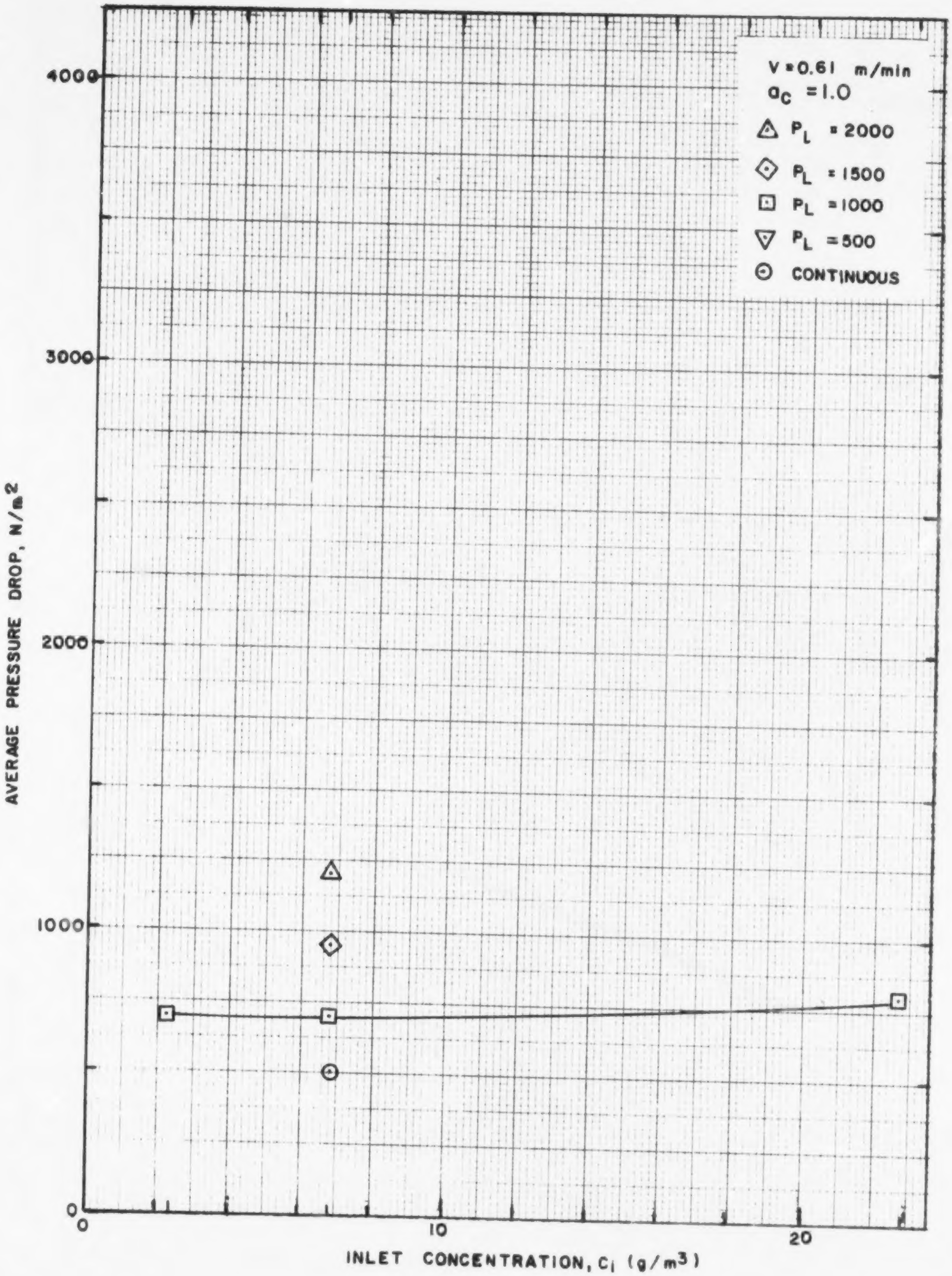

Figure 61. $\overline{P}$ versus C_i and P_L.

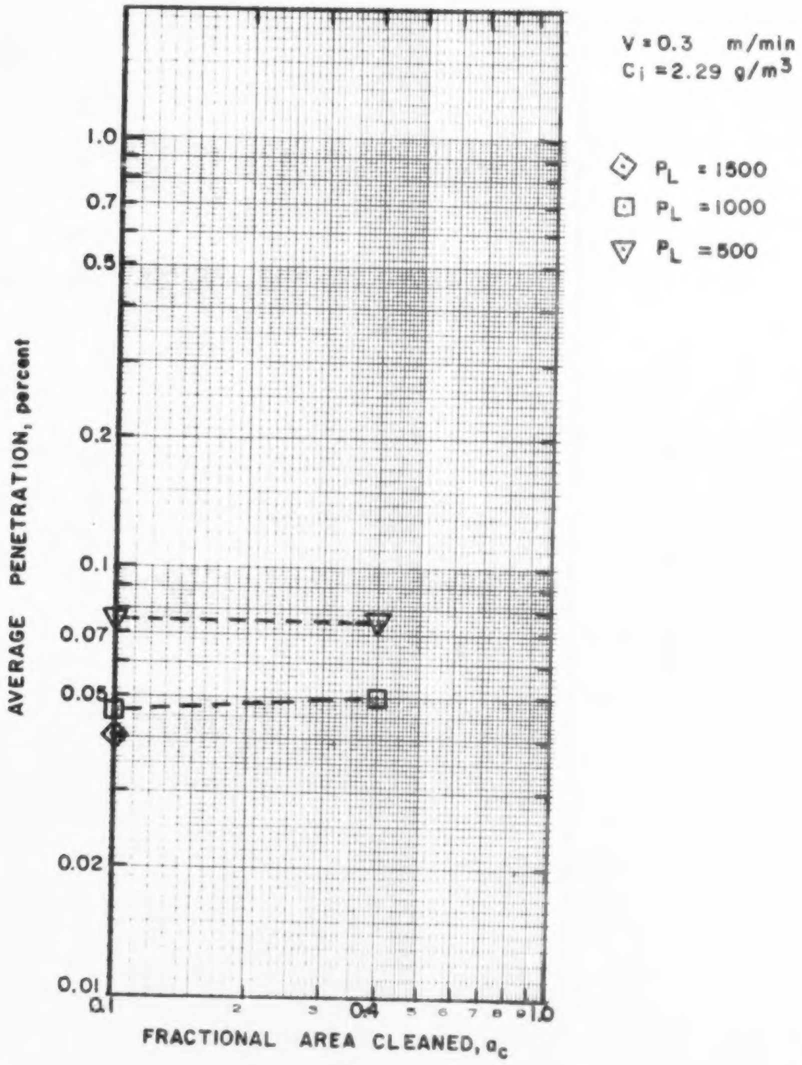

Figure 62. $\overline{P}n$ versus a_c and P_L.

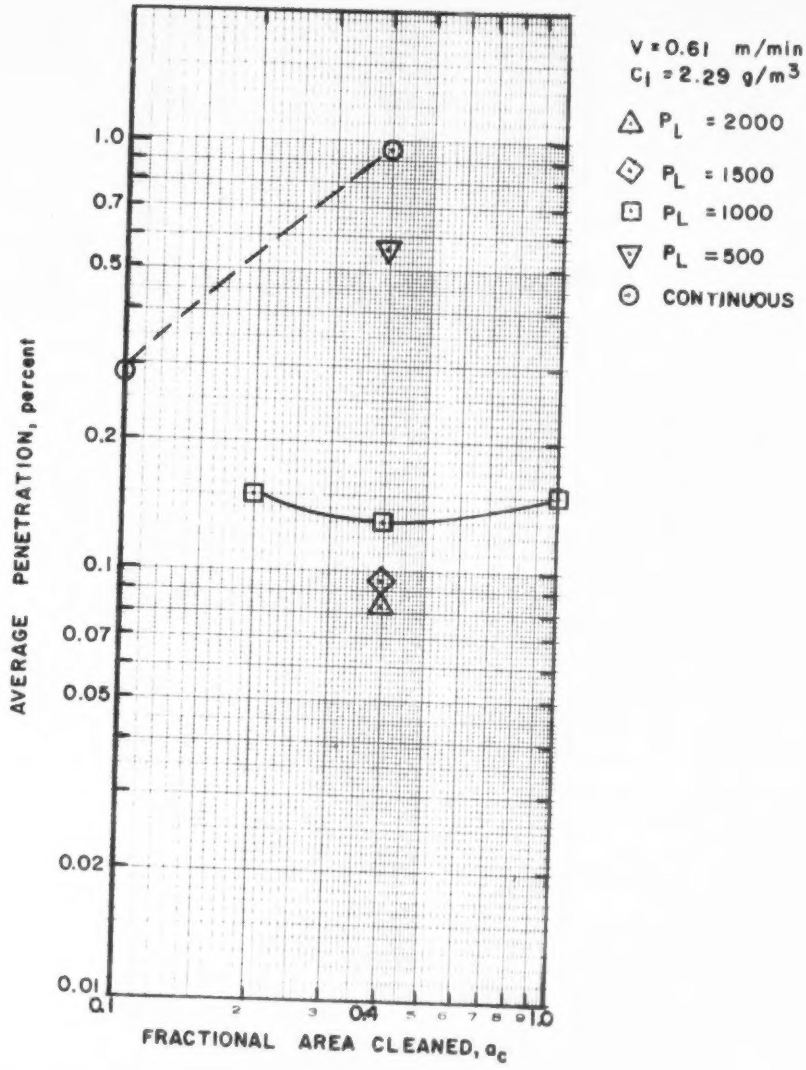

Figure 63. $\overline{Pn}$ versus a_c and P_L.

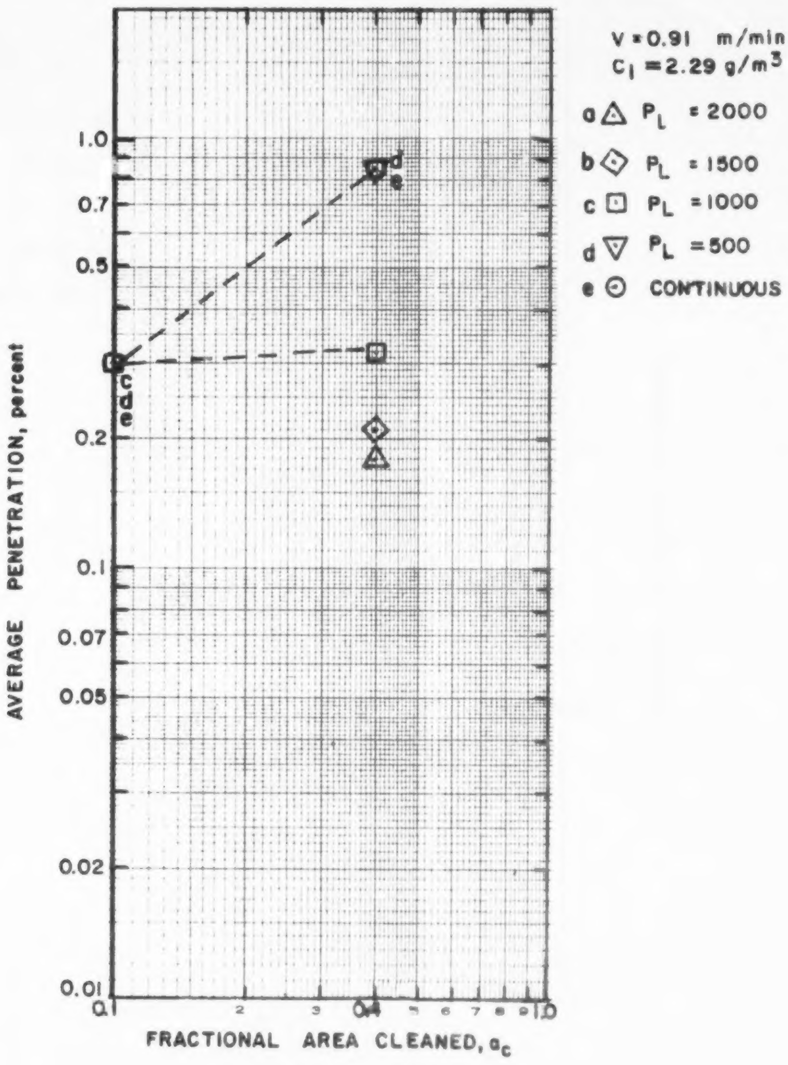

Figure 64. $\overline{Pn}$ versus a_c and P_L.

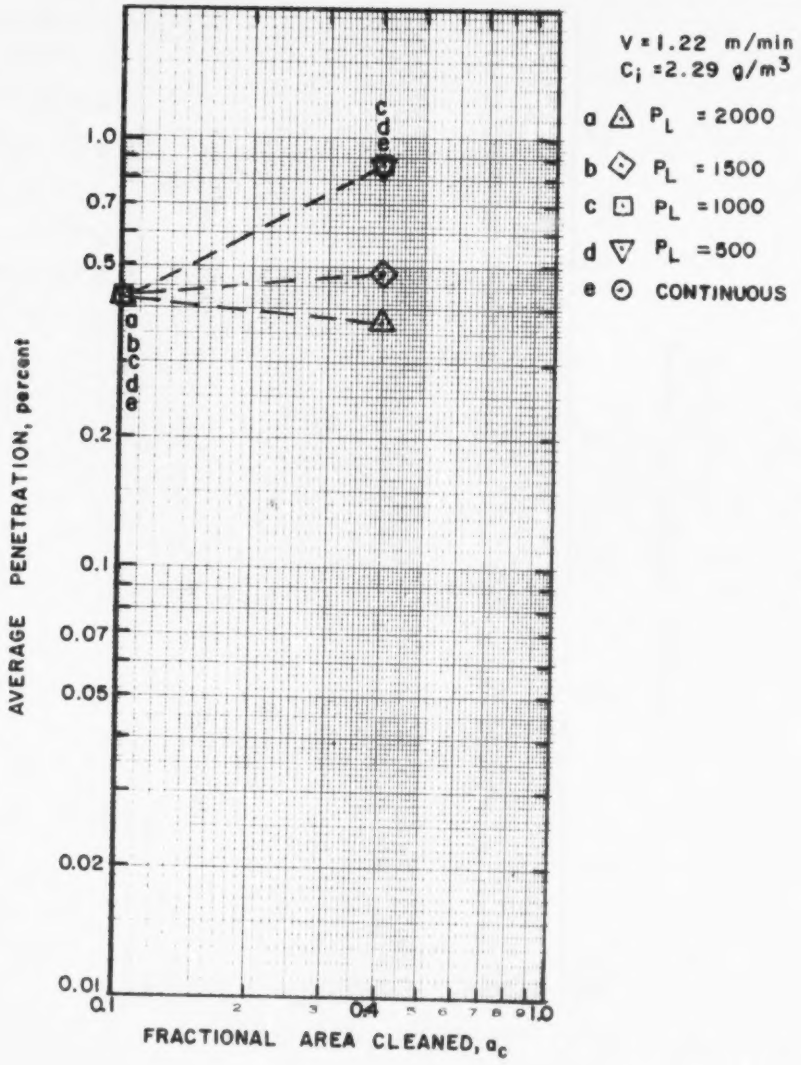

Figure 65. $\overline{Pn}$ versus a_c and P_L.

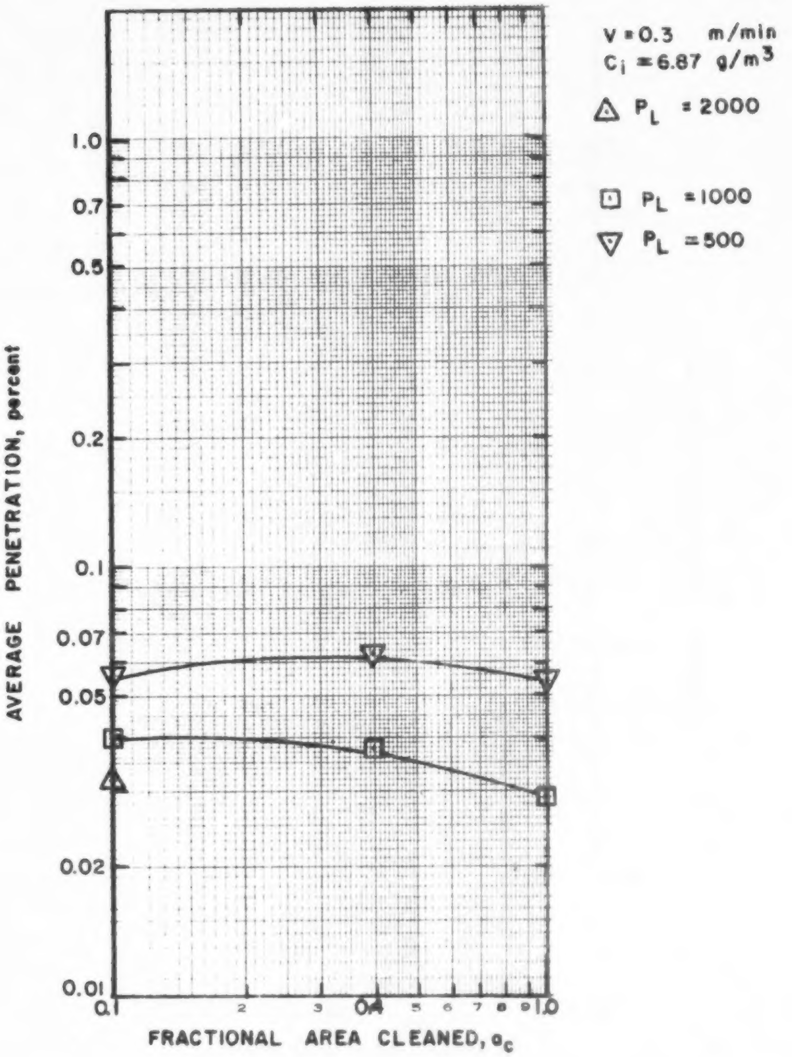

Figure 66. $\overline{Pn}$ versus a_c and P_L.

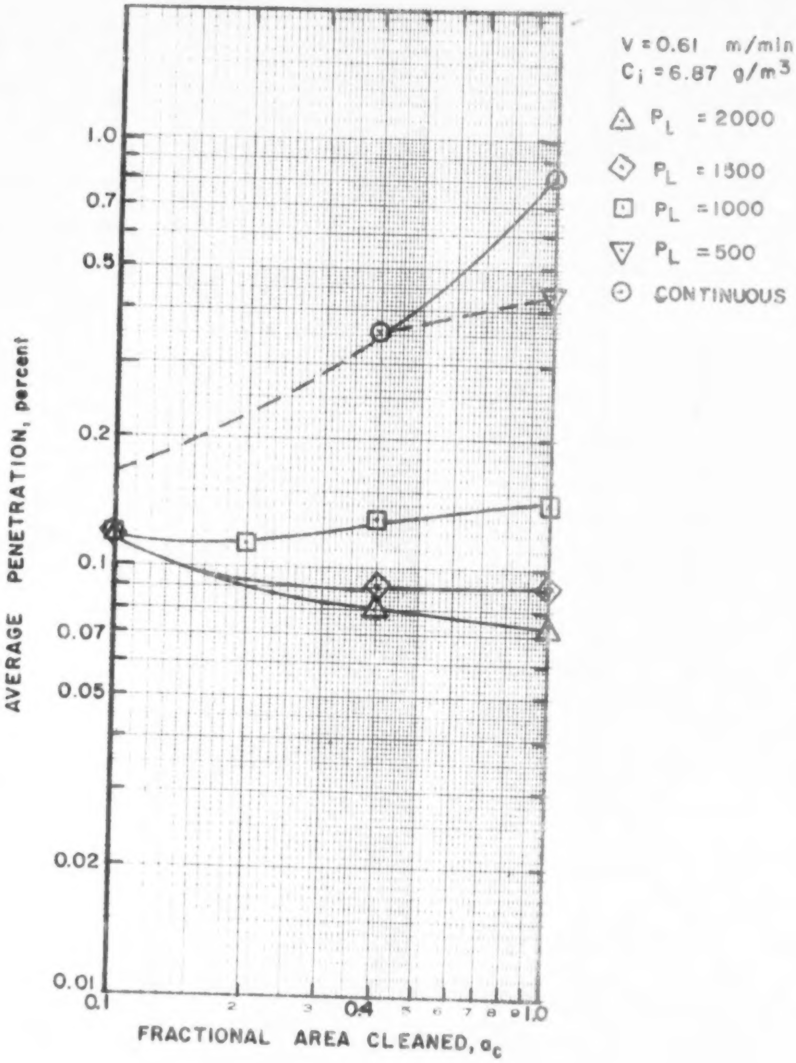

Figure 67. $\overline{Pn}$ versus a_c and P_L.

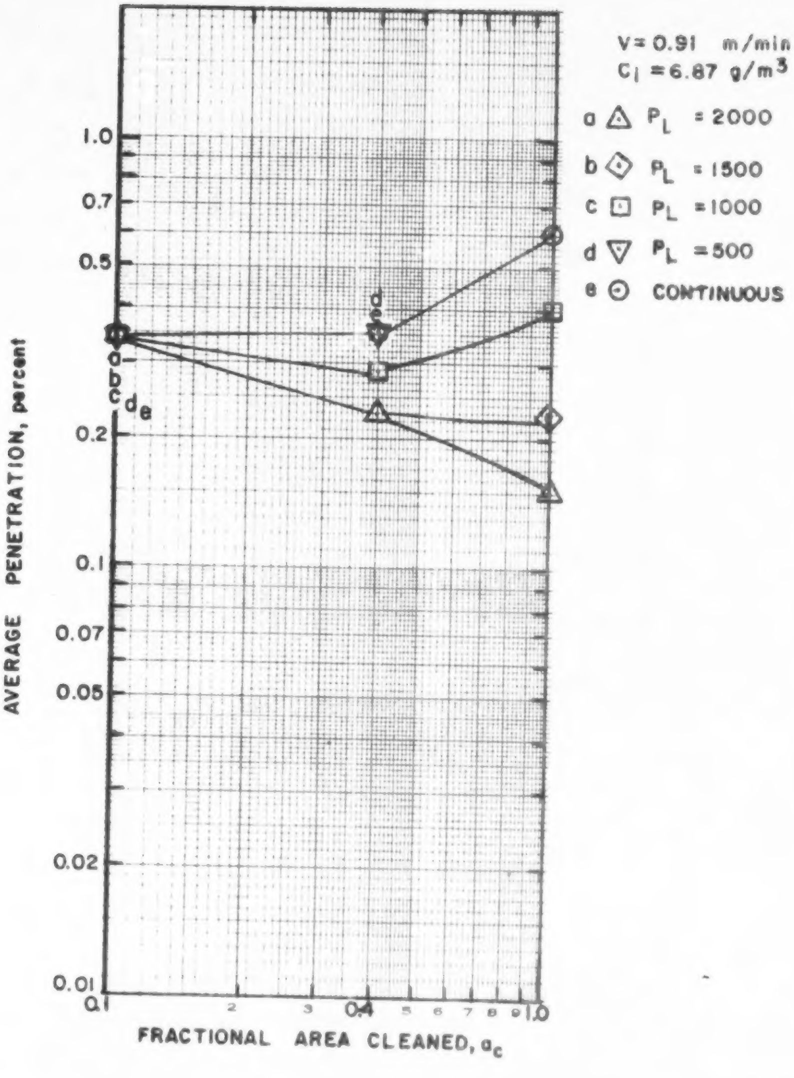

Figure 68. $\overline{Pn}$ versus a_c and P_L.

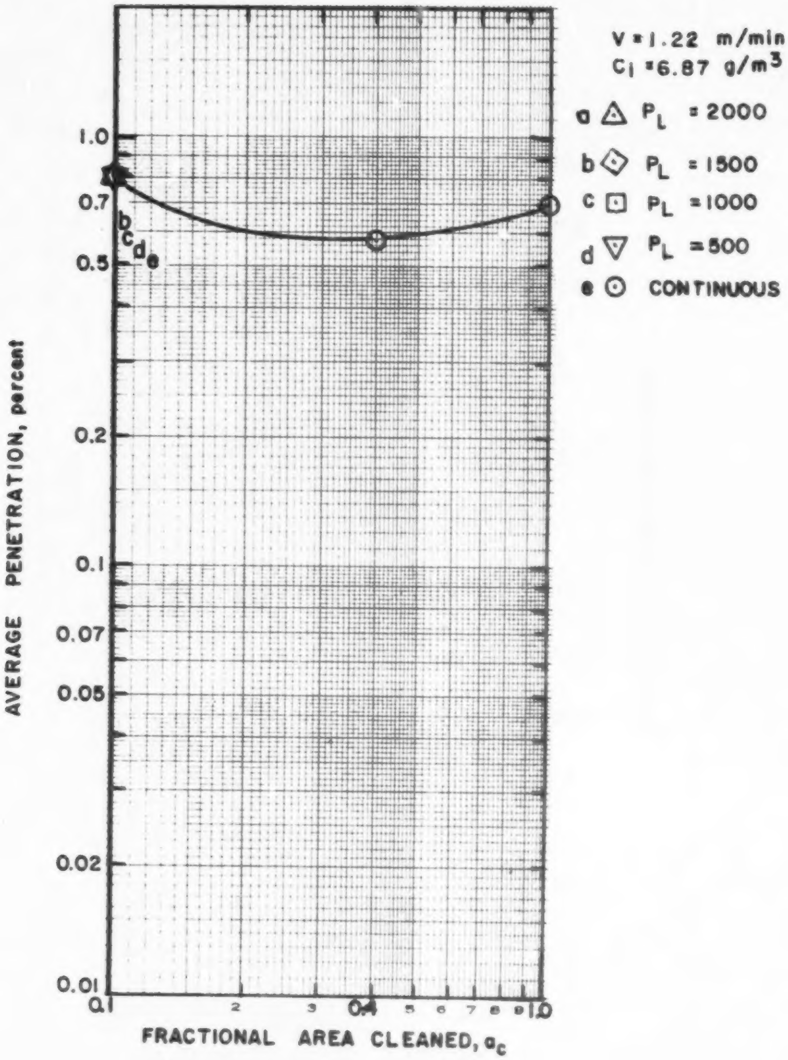

Figure 69. $\overline{Pn}$ versus a_c and P_L.

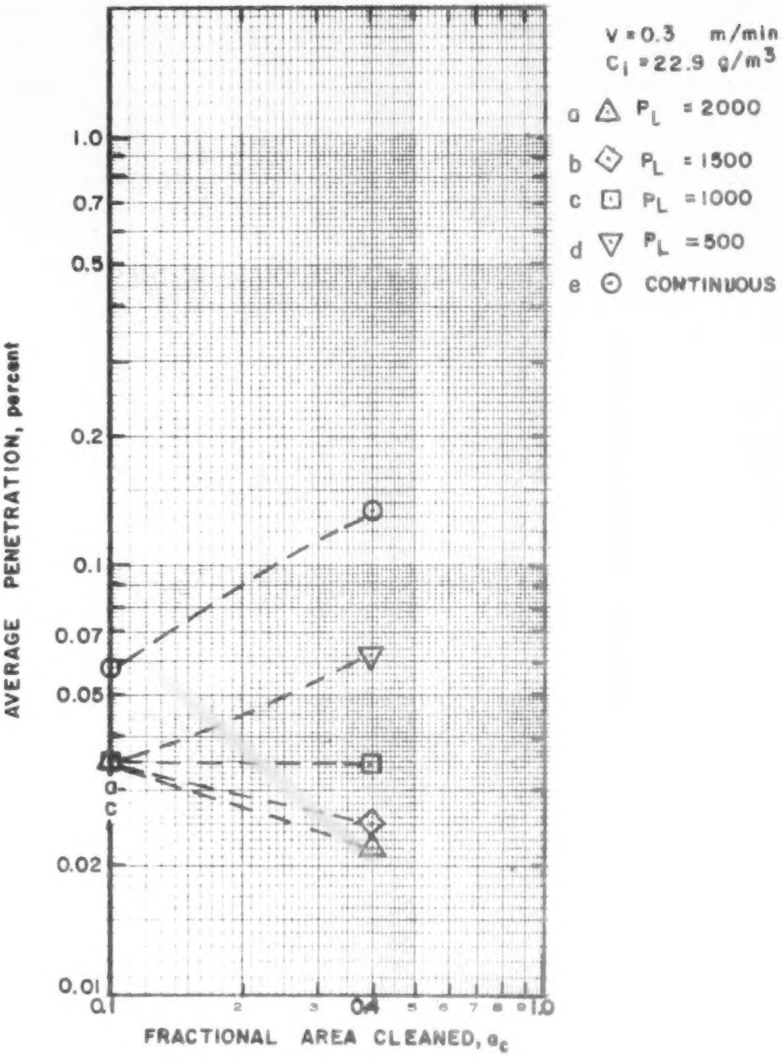

Figure 70. $\overline{P}n$ versus a_c and P_L.

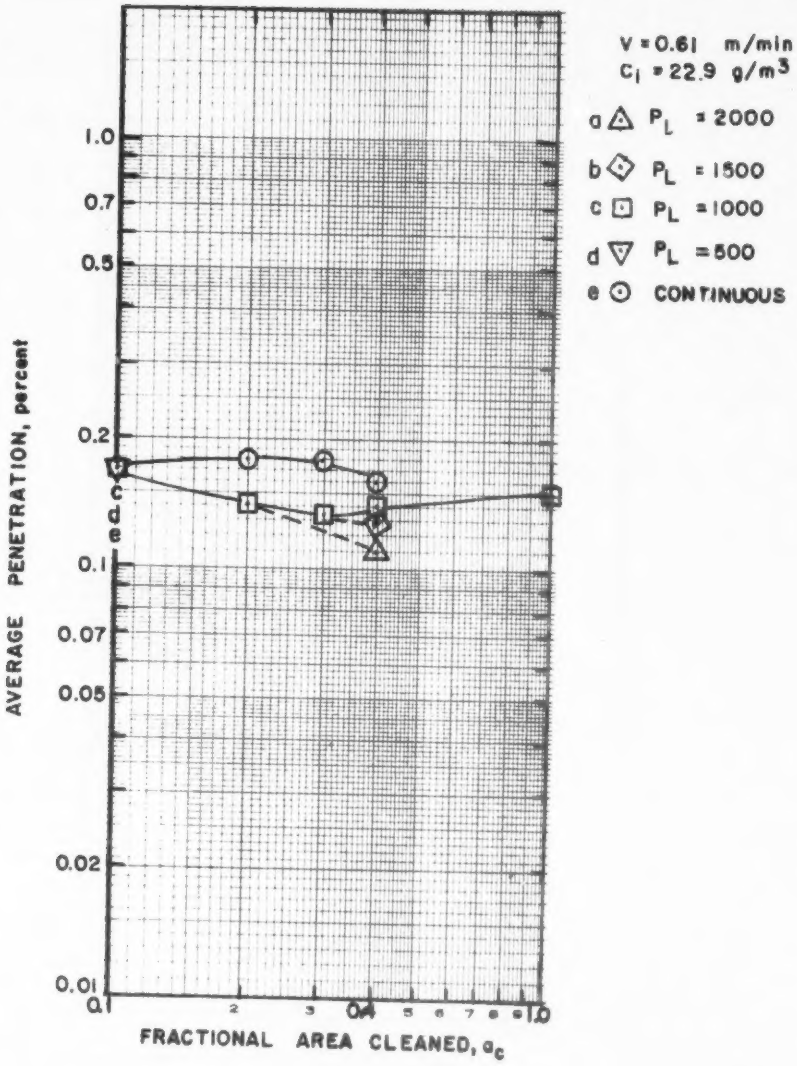

Figure 71. $\overline{Pn}$ versus a_c and P_L.

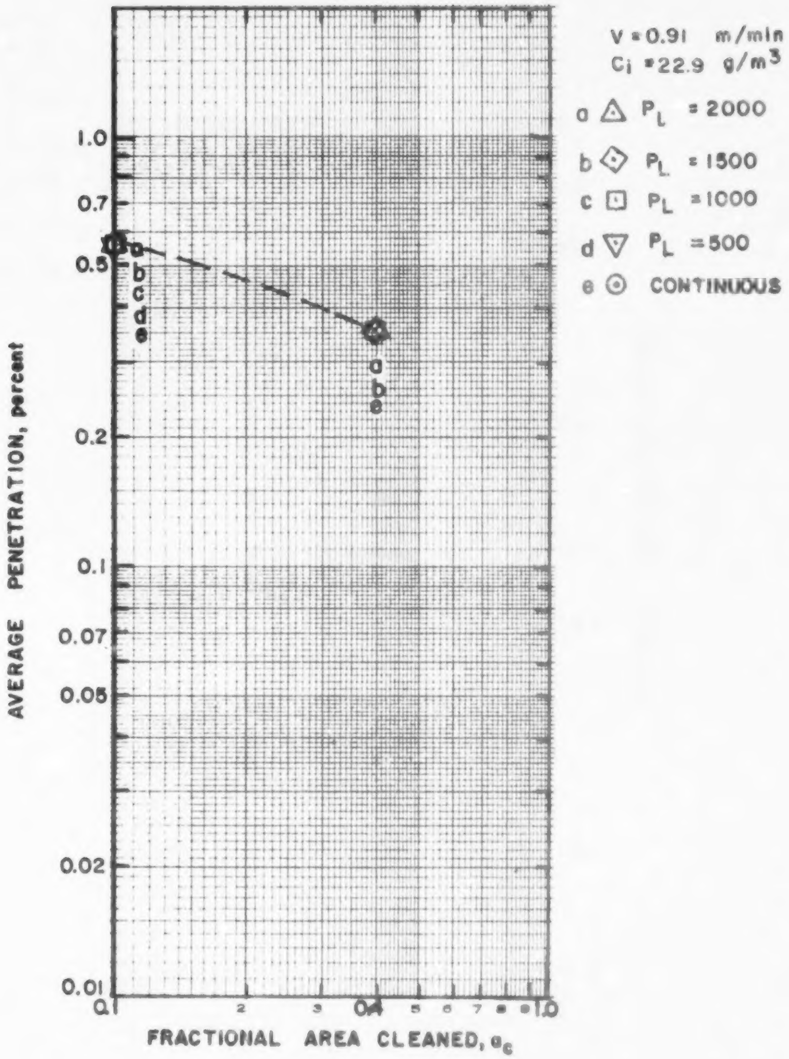

Figure 72. $\overline{Pn}$ versus a_c and P_L.

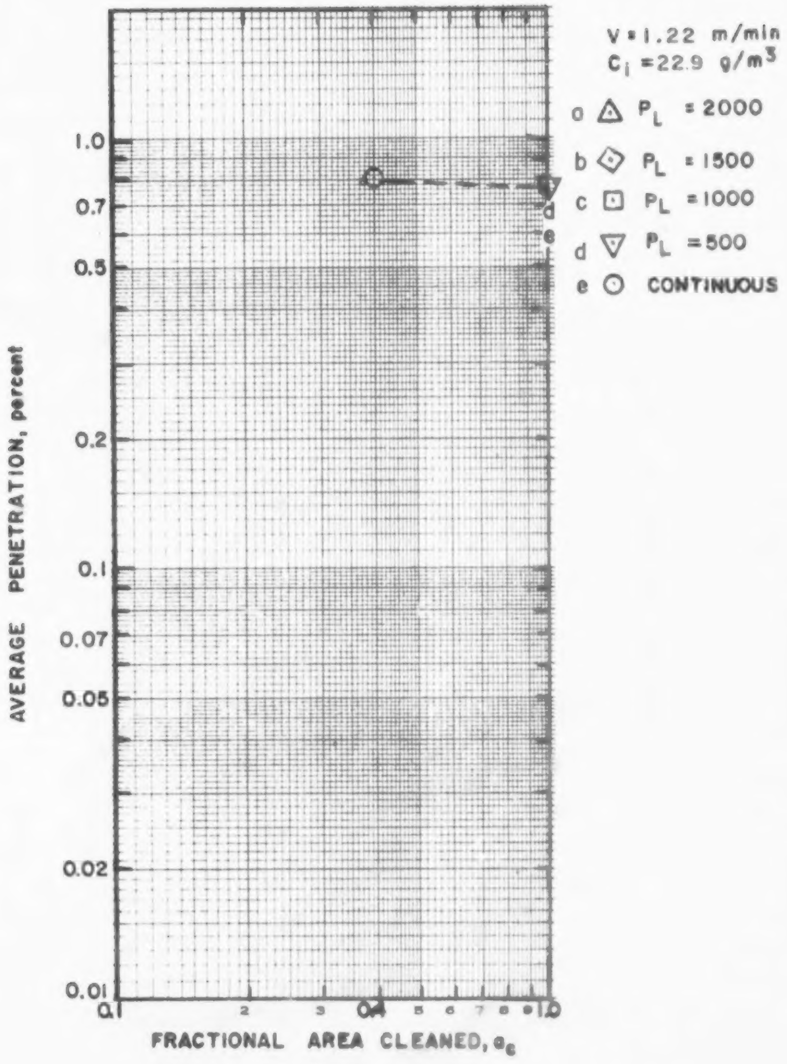

Figure 73. $\overline{Pn}$ versus a_c and P_L.

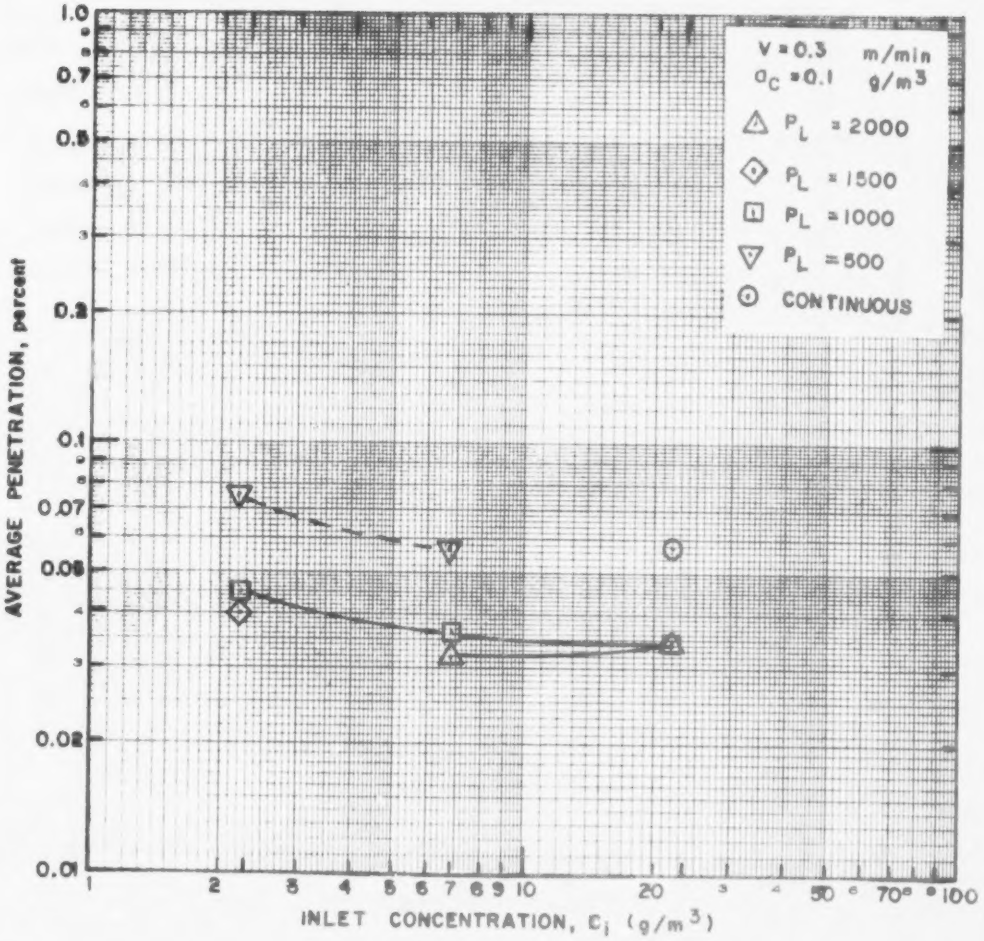

Figure 74. $\overline{Pn}$ versus C_i and P_L.

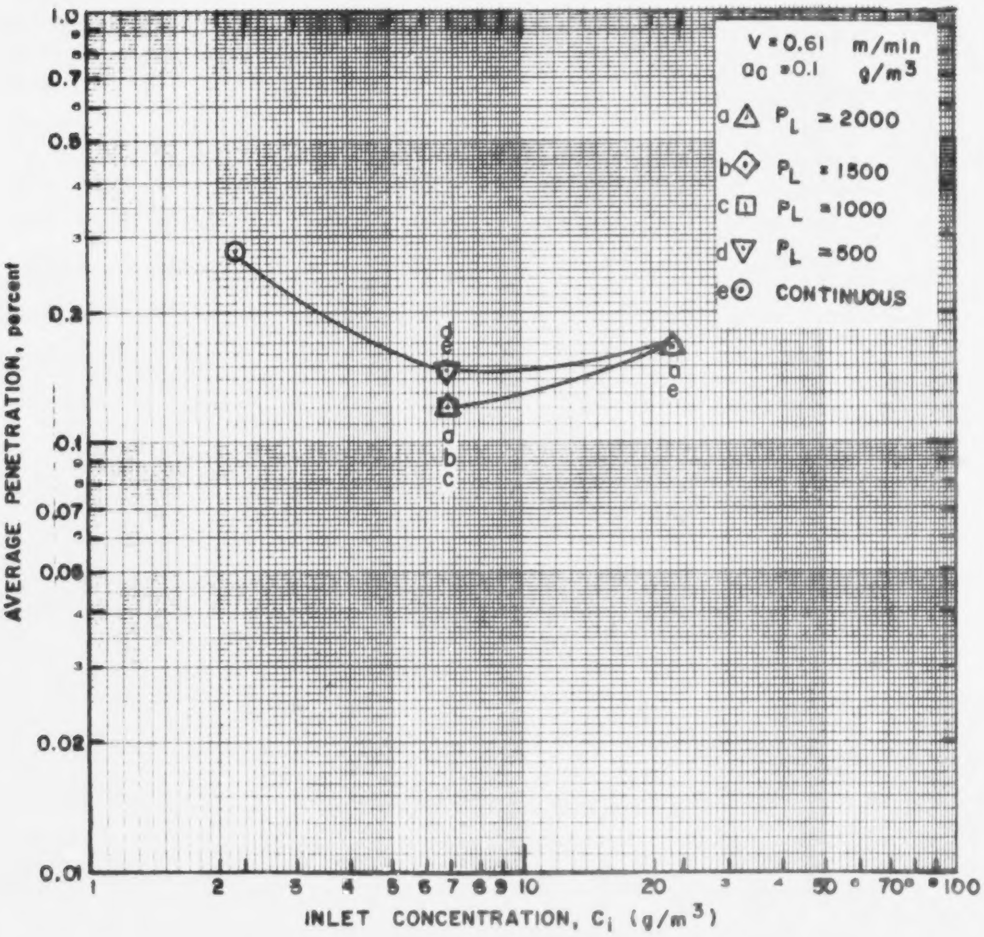

Figure 75. $\overline{Pn}$ versus C_i and P_L.

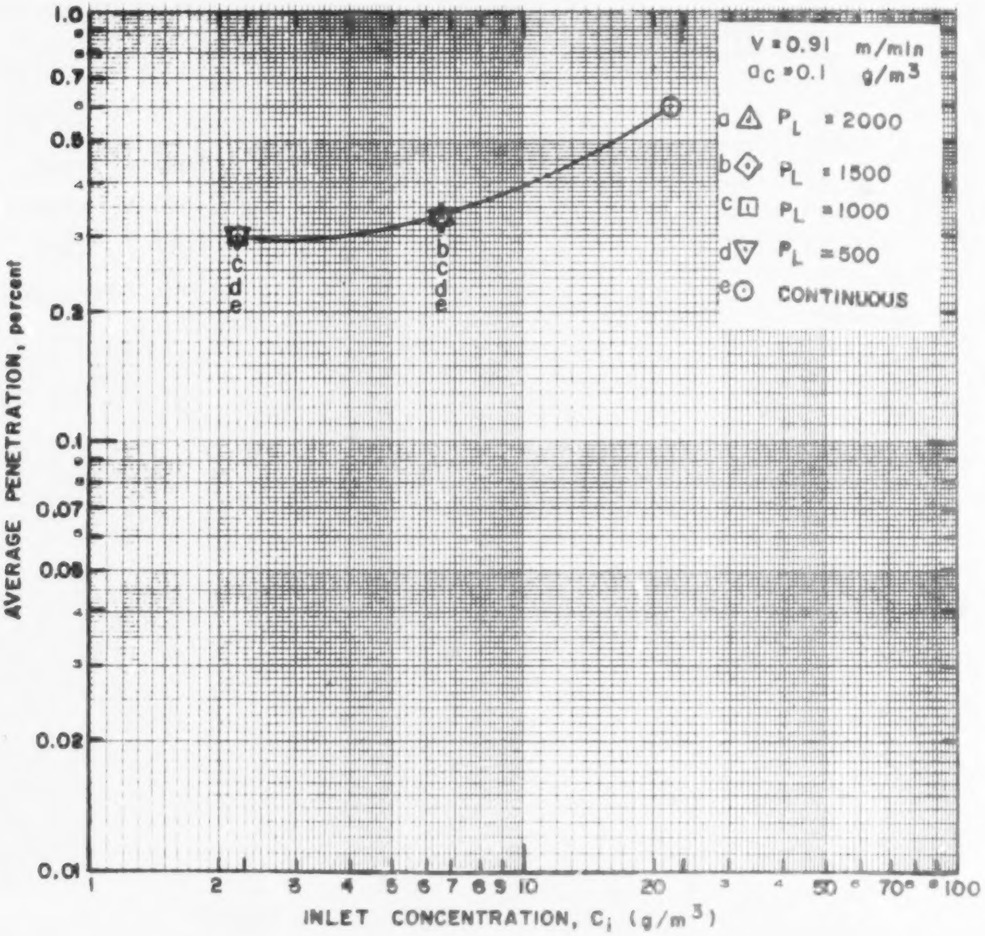

Figure 76. $\overline{P}n$ versus C_i and P_L.

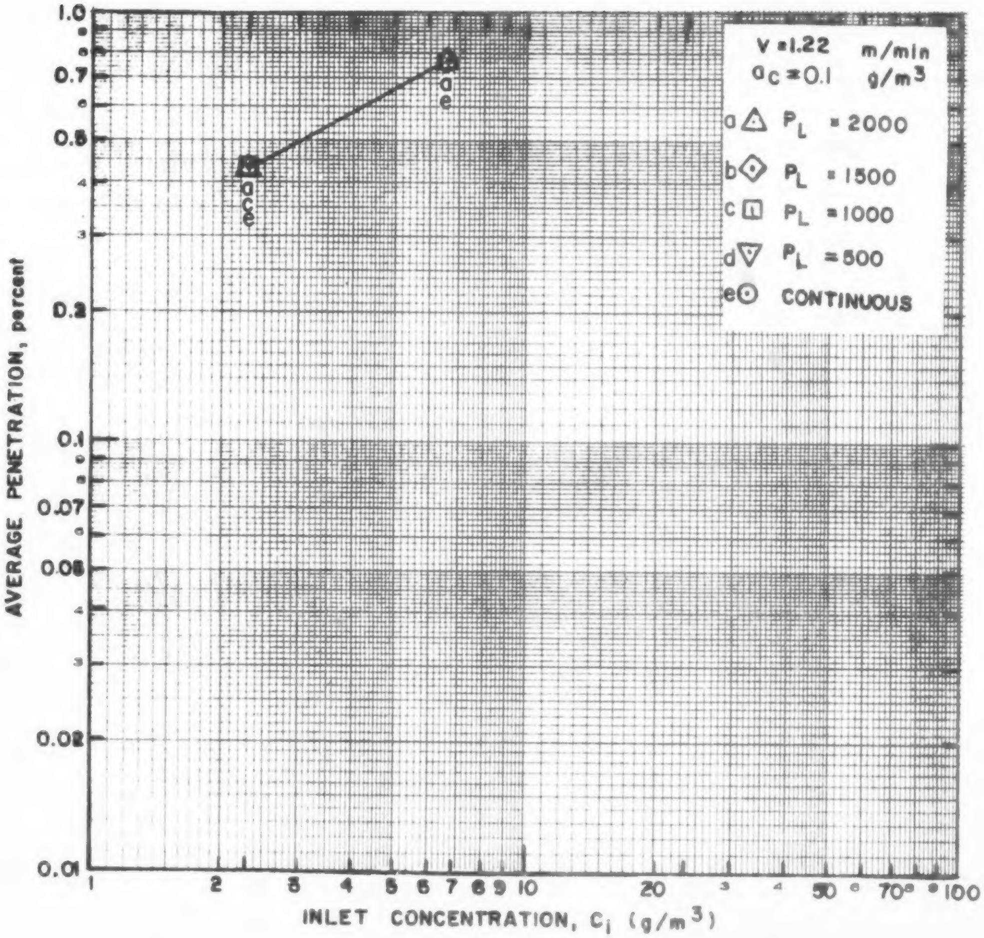

Figure 77. $\overline{Pn}$ versus C_i and P_L.

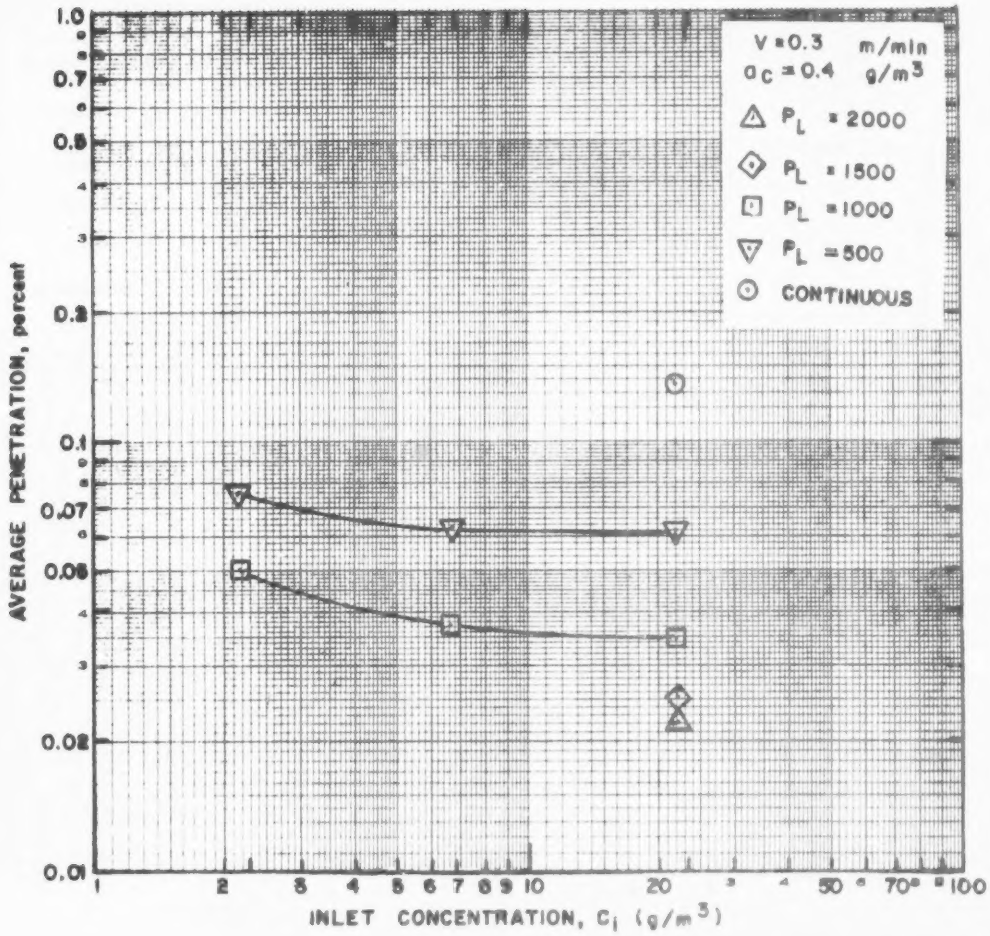

Figure 78. $\overline{Pn}$ versus C_i and P_L.

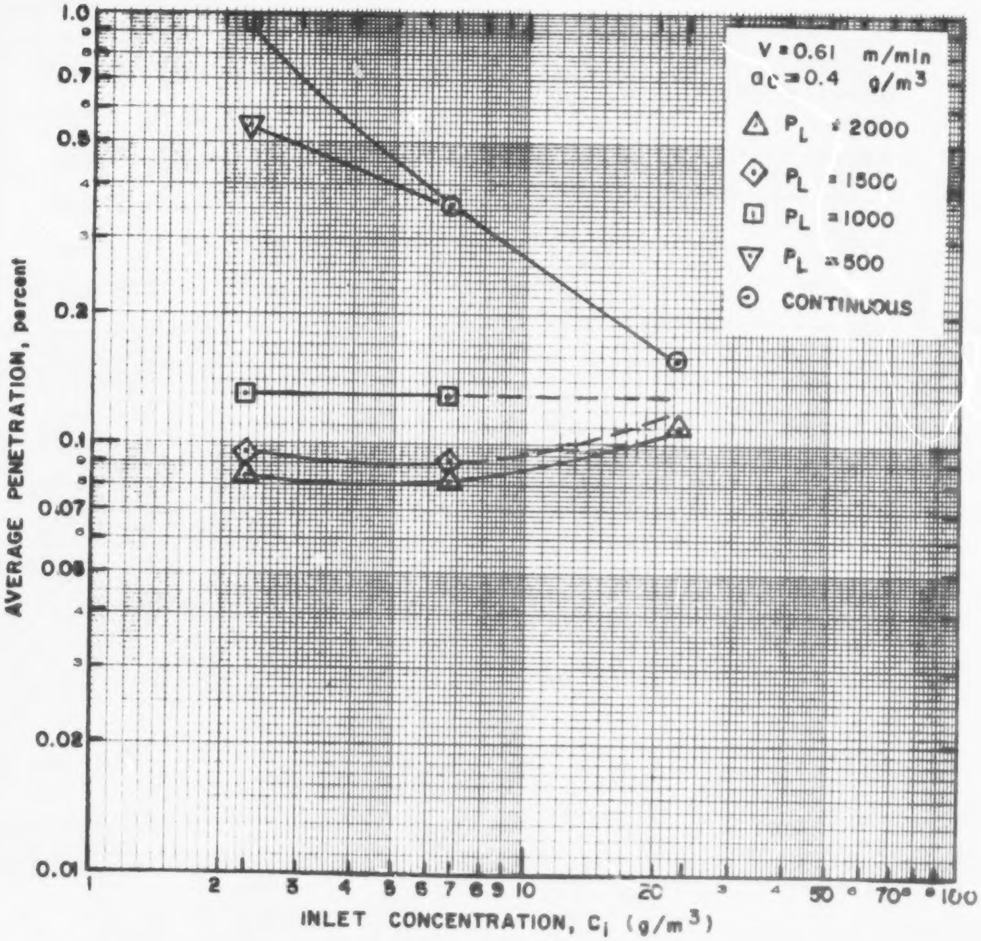

Figure 79. $\overline{Pn}$ versus C_i and P_L.

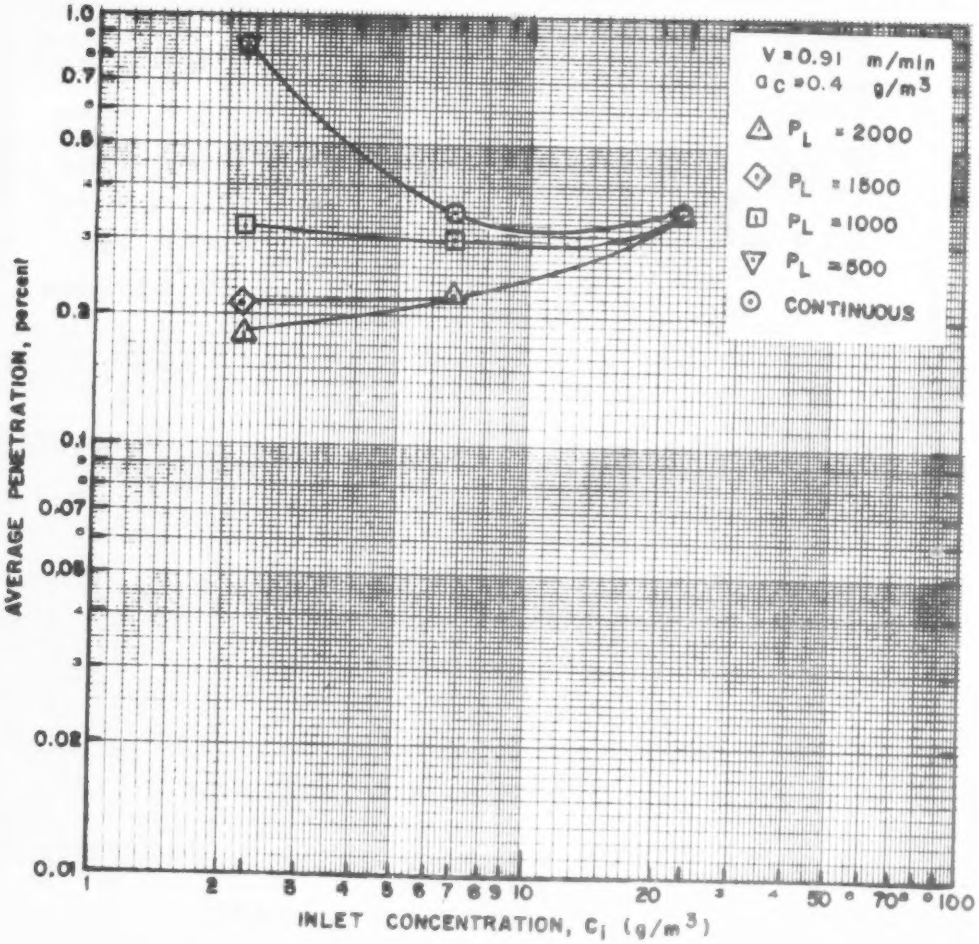

Figure 80. $\overline{Pn}$ versus C_i and P_L.

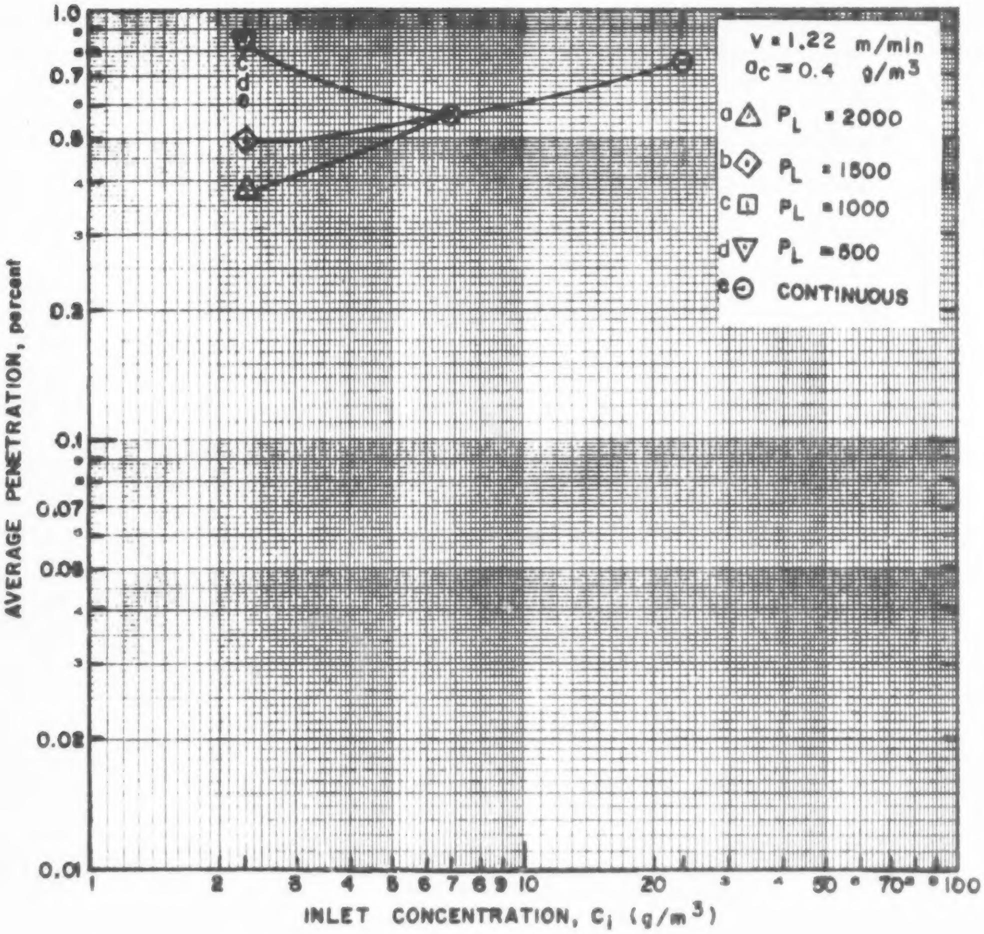

Figure 81. $\overline{P}n$ versus C_i and P_L.

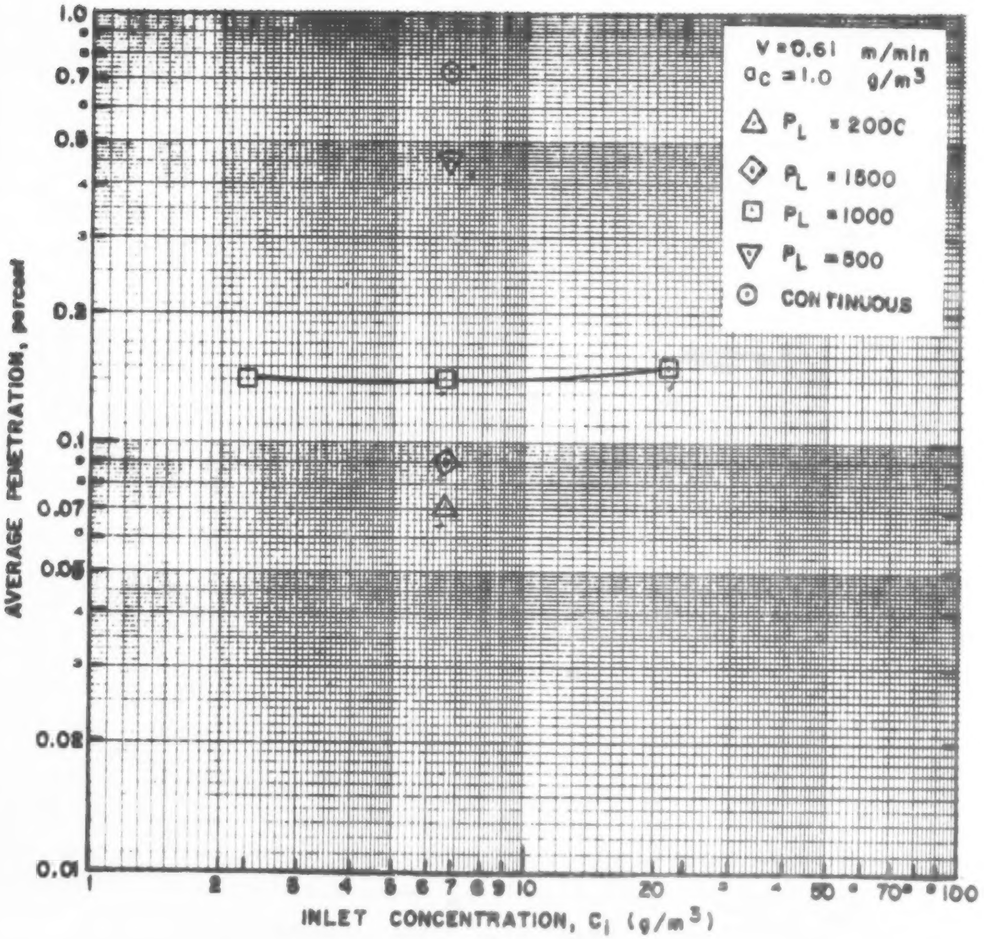

Figure 82. $\overline{Pn}$ versus C_i and P_L.

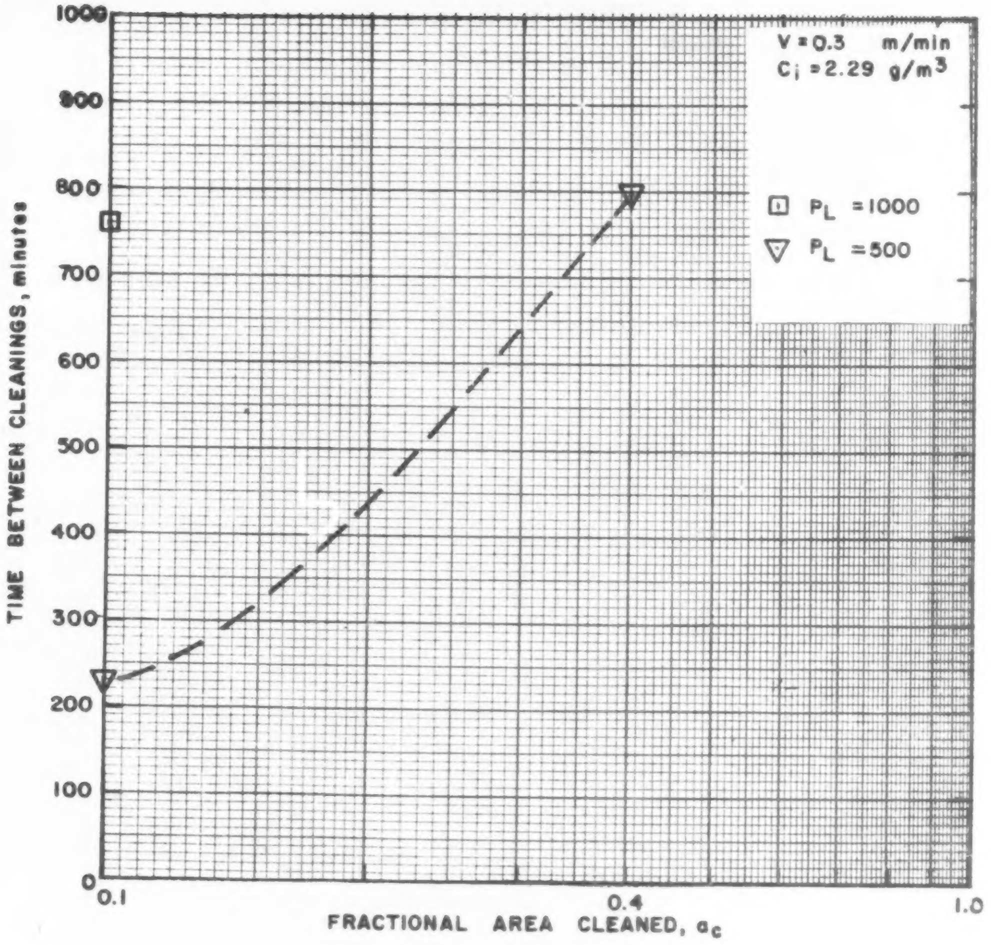

Figure 83. t_f versus a_c and P_L.

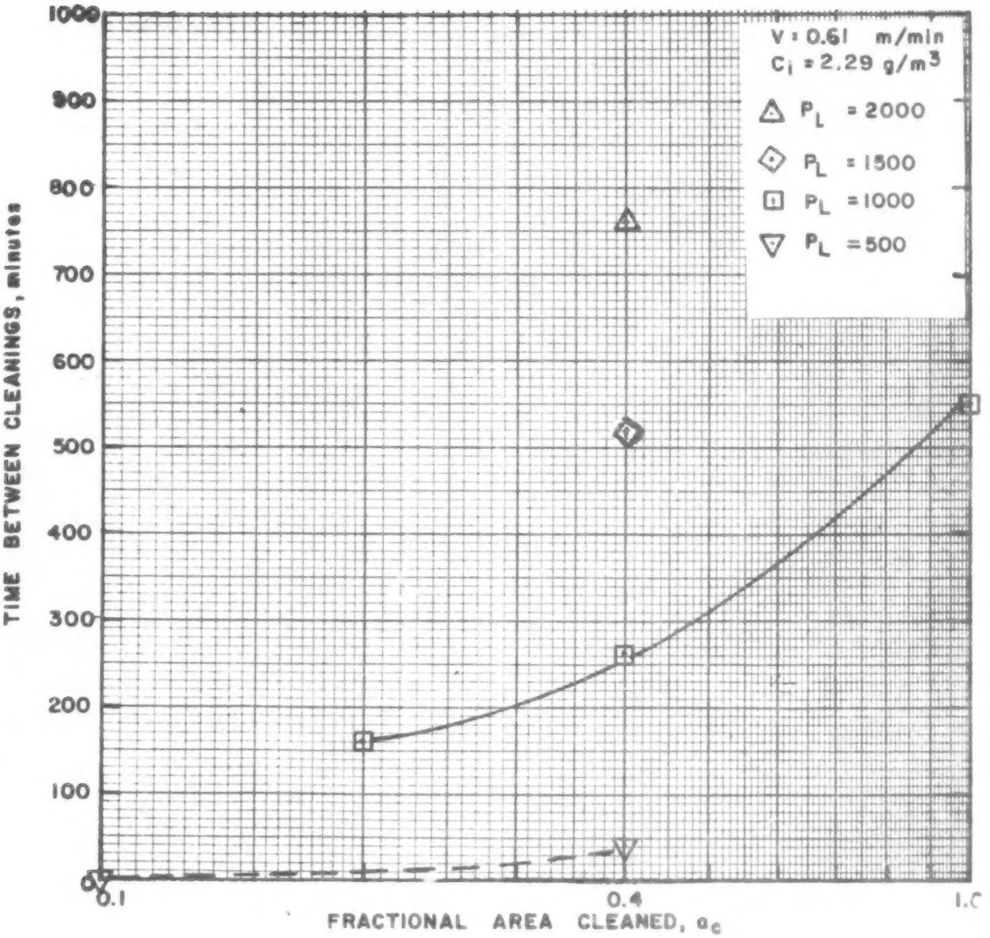

Figure 84. t_f versus a_c and P_L.

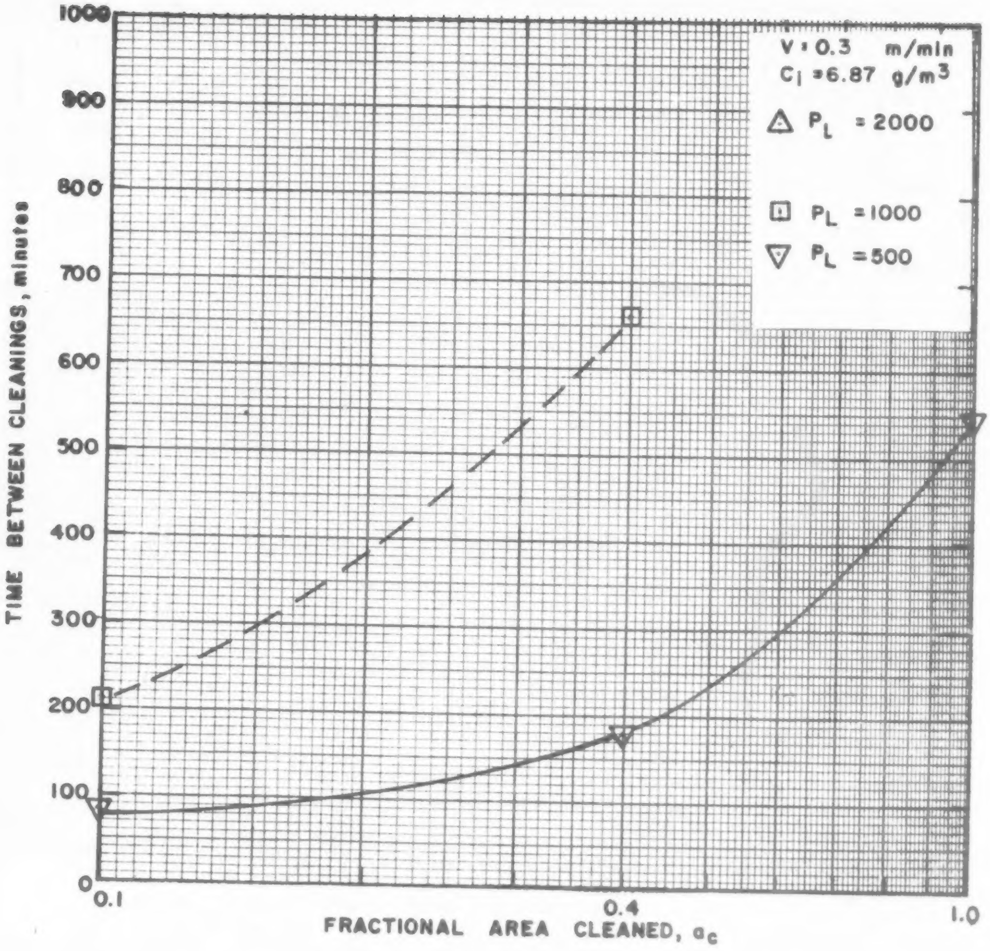

Figure 85. t_f versus a_c and P_L.

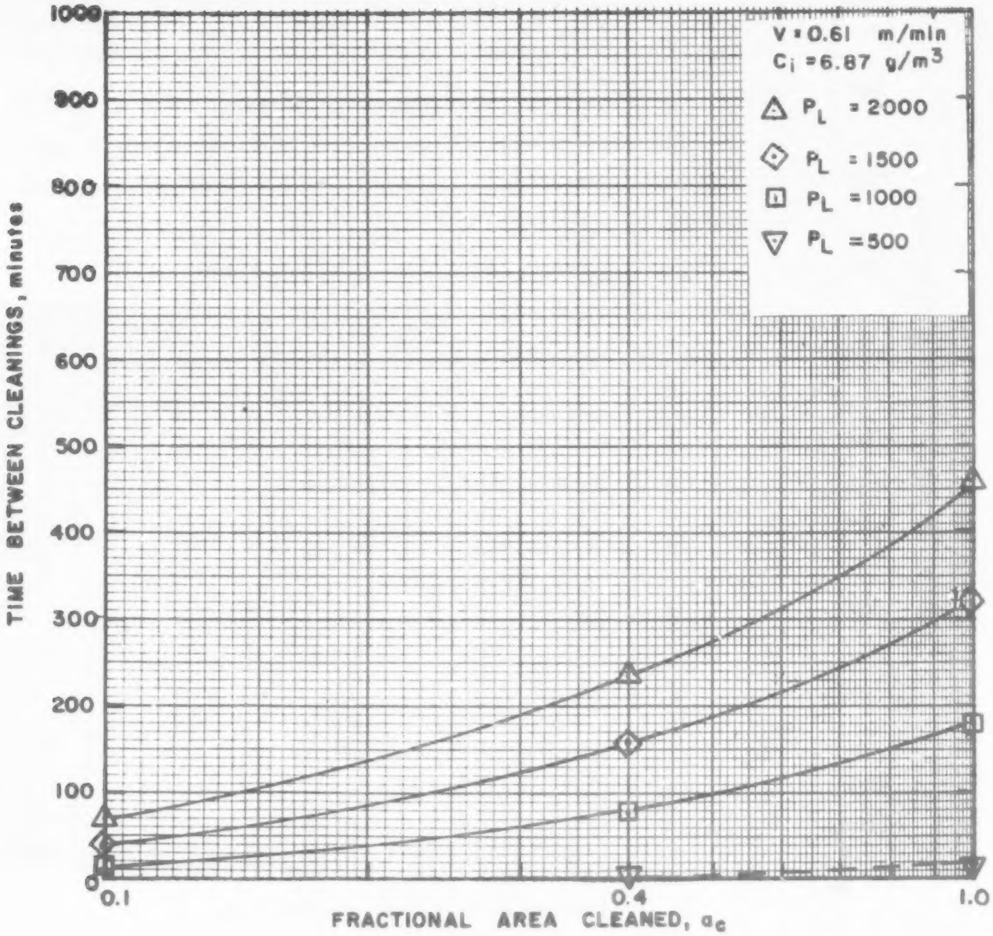

Figure 86. t_f versus a_c and P_L.

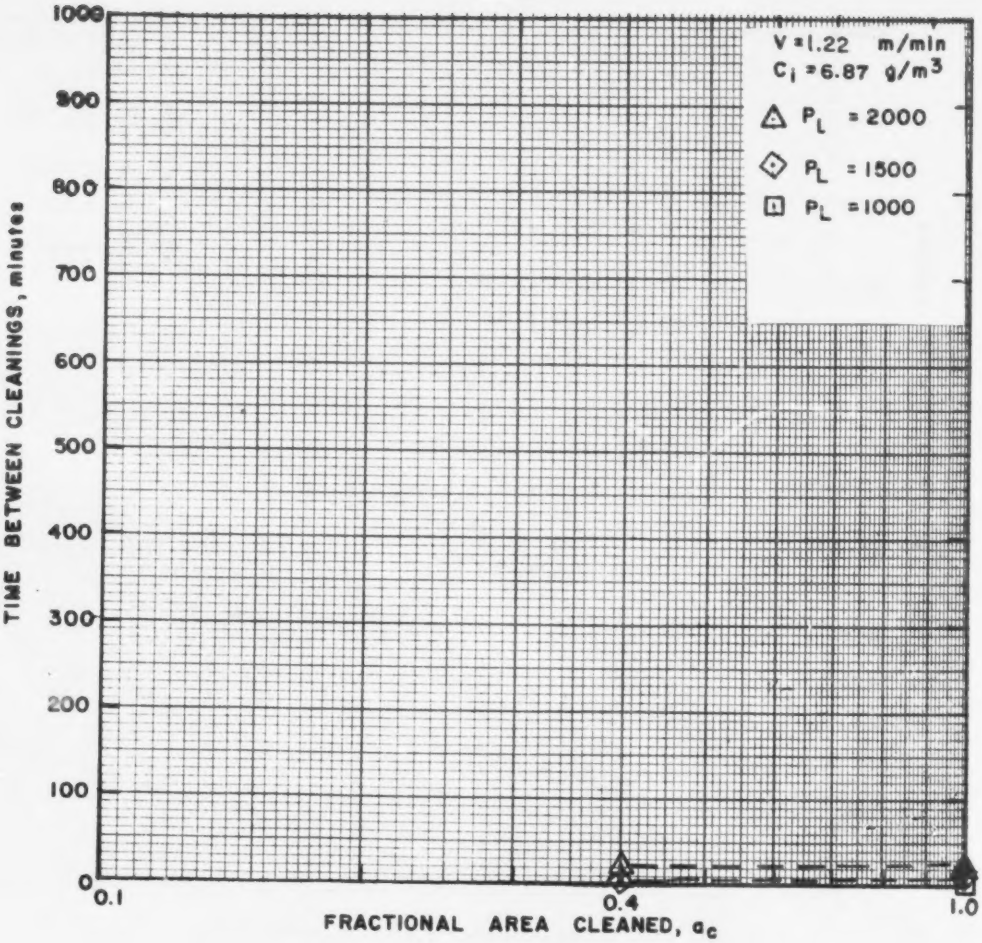

Figure 87. t_f versus a_c and P_L.

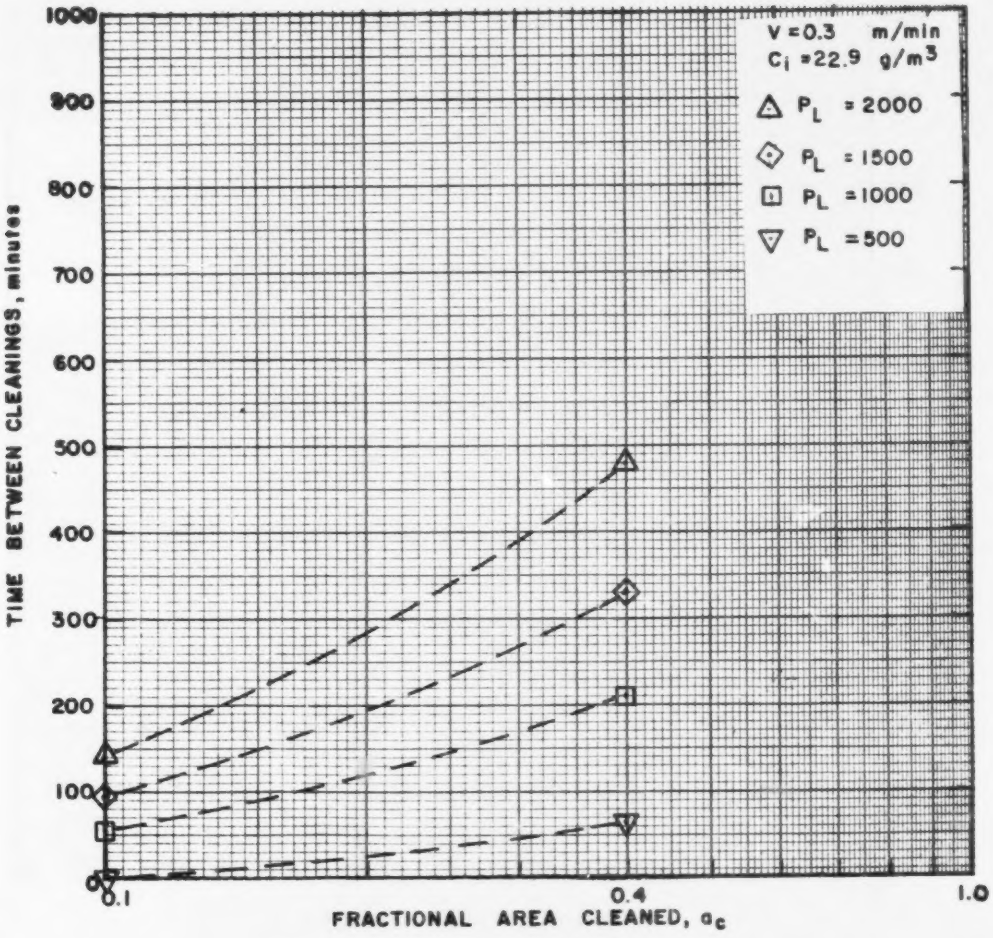

Figure 88. $\overline{P}n$ versus a_c and P_L.

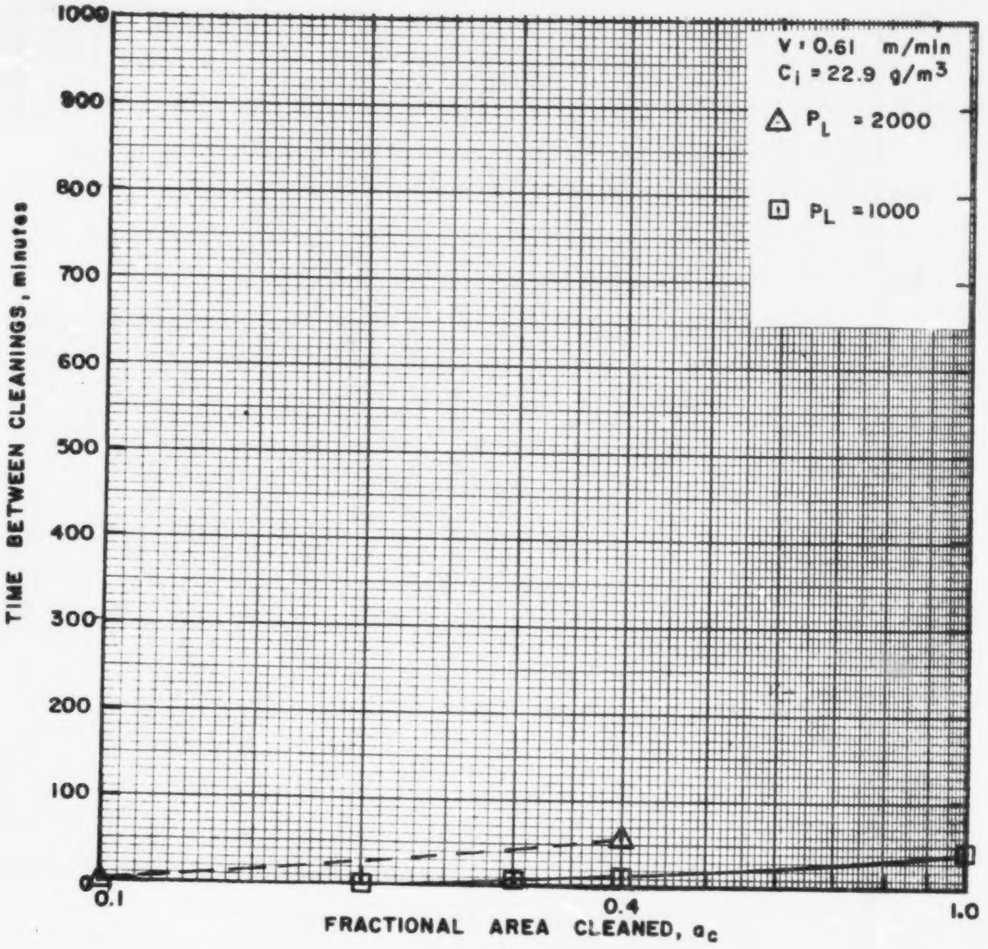

Figure 89. t_f versus a_c and P_L.

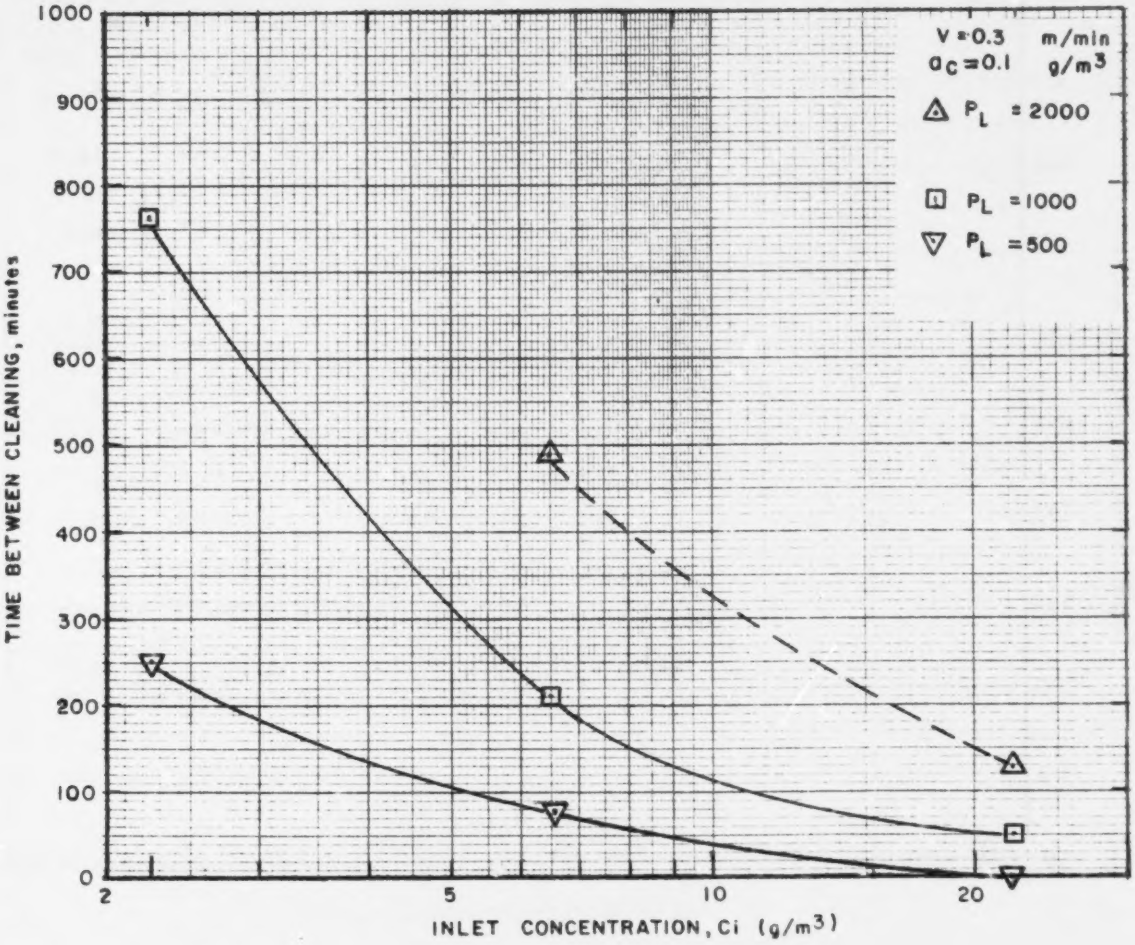

Figure 90. t_f versus C_i and P_L.

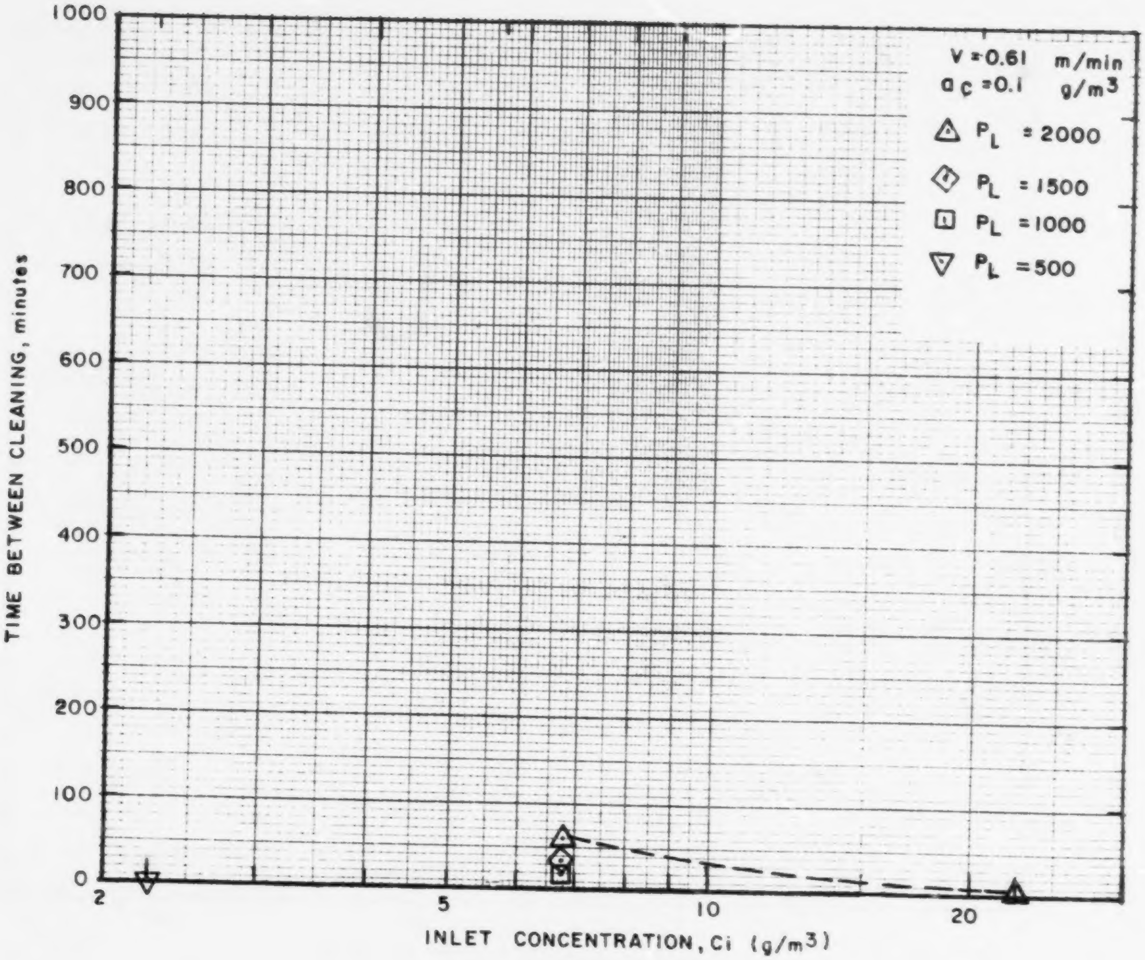

Figure 91. t_f versus C_i and P_L.

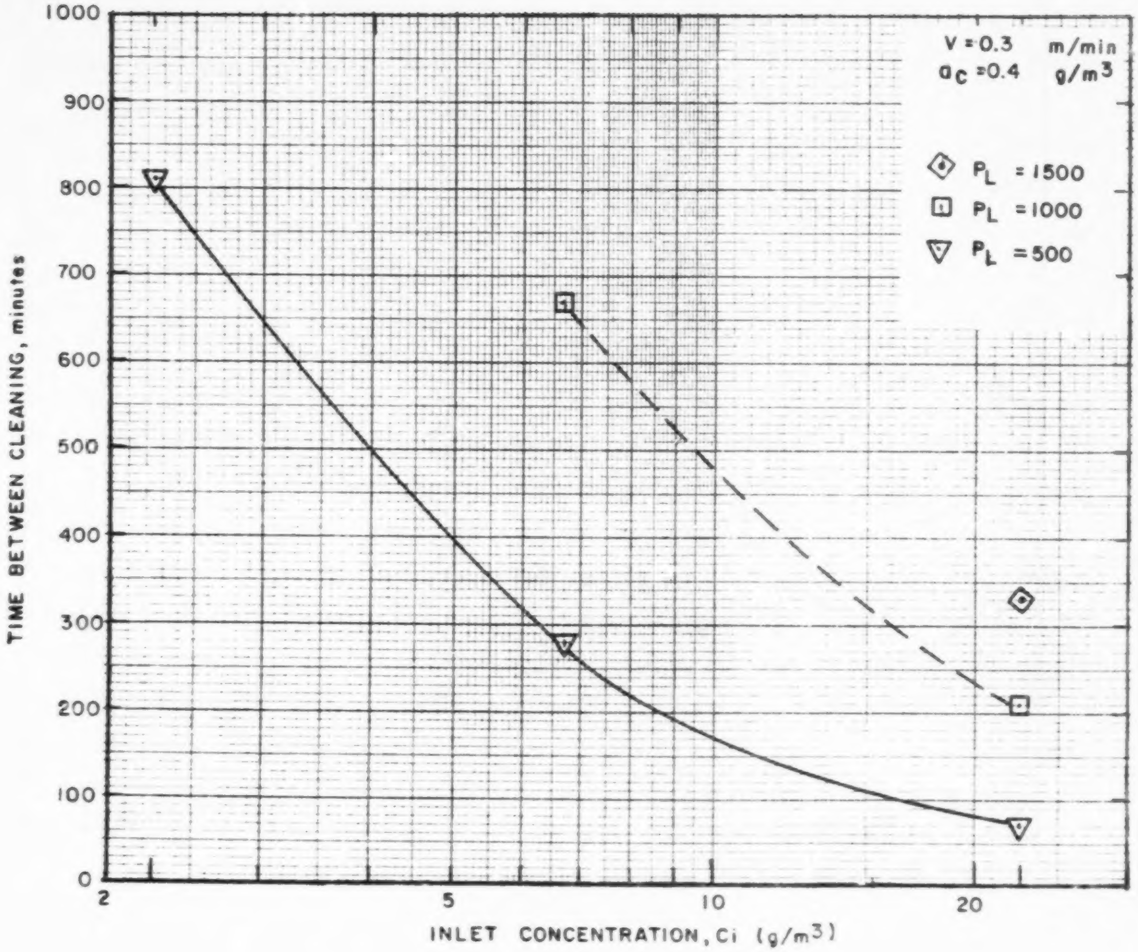

Figure 92. t_f versus C_i and P_L.

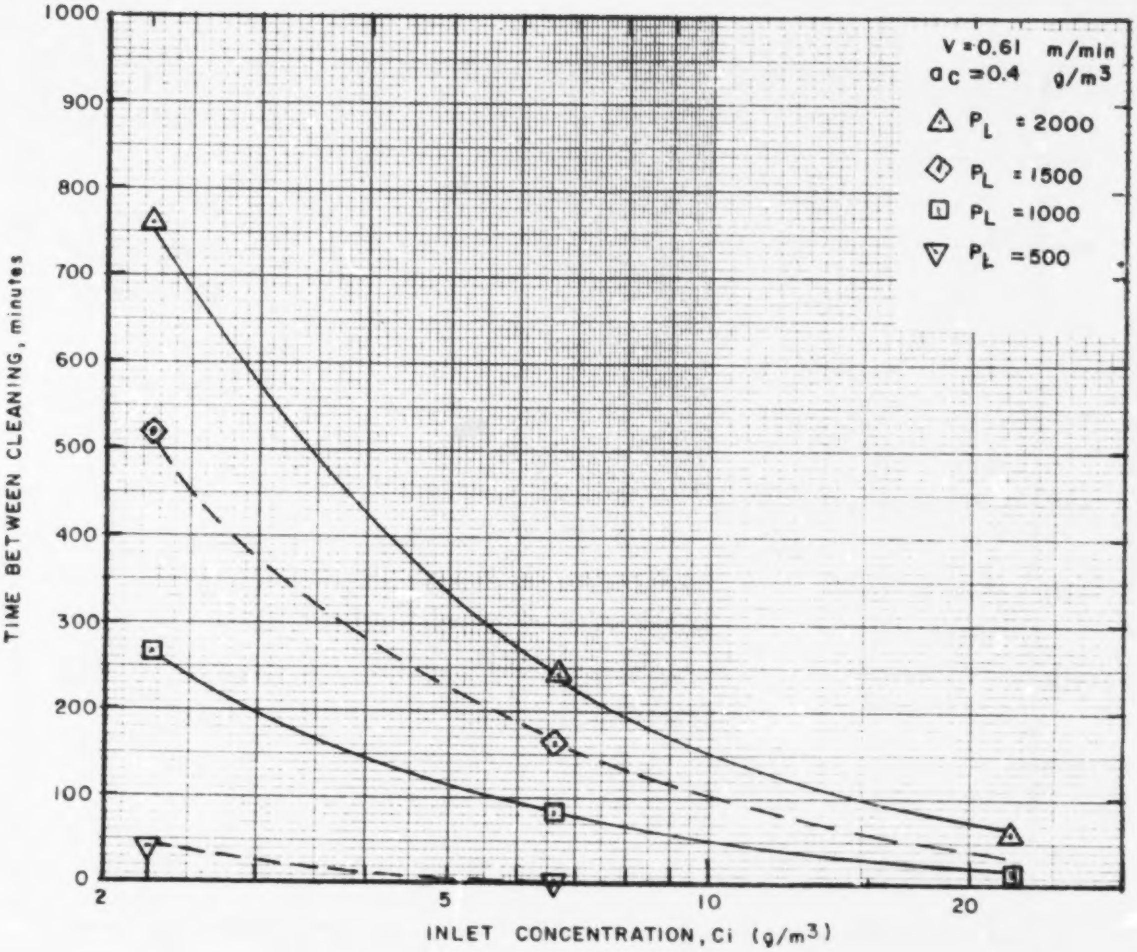

Figure 93. t_f versus C_i and P_L.

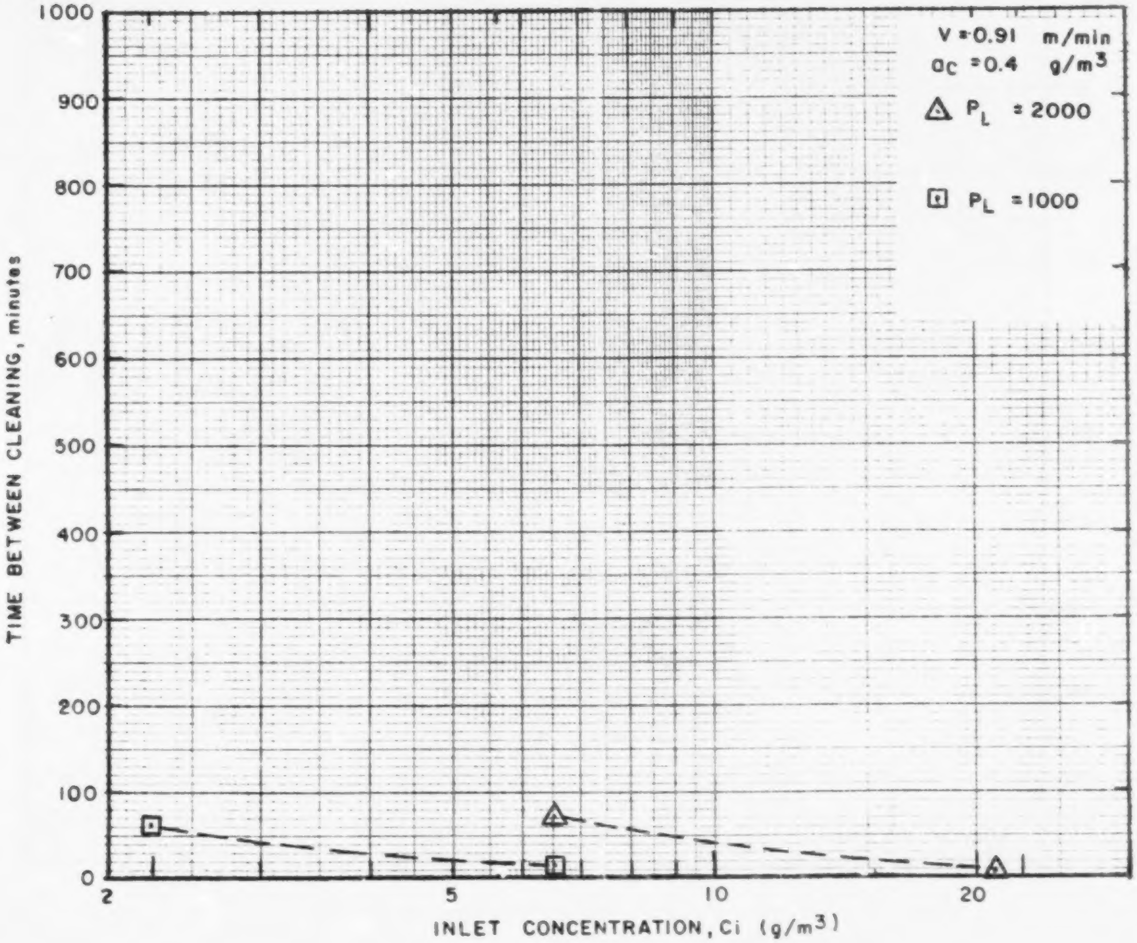

Figure 94. t_f versus C_i and P_L.

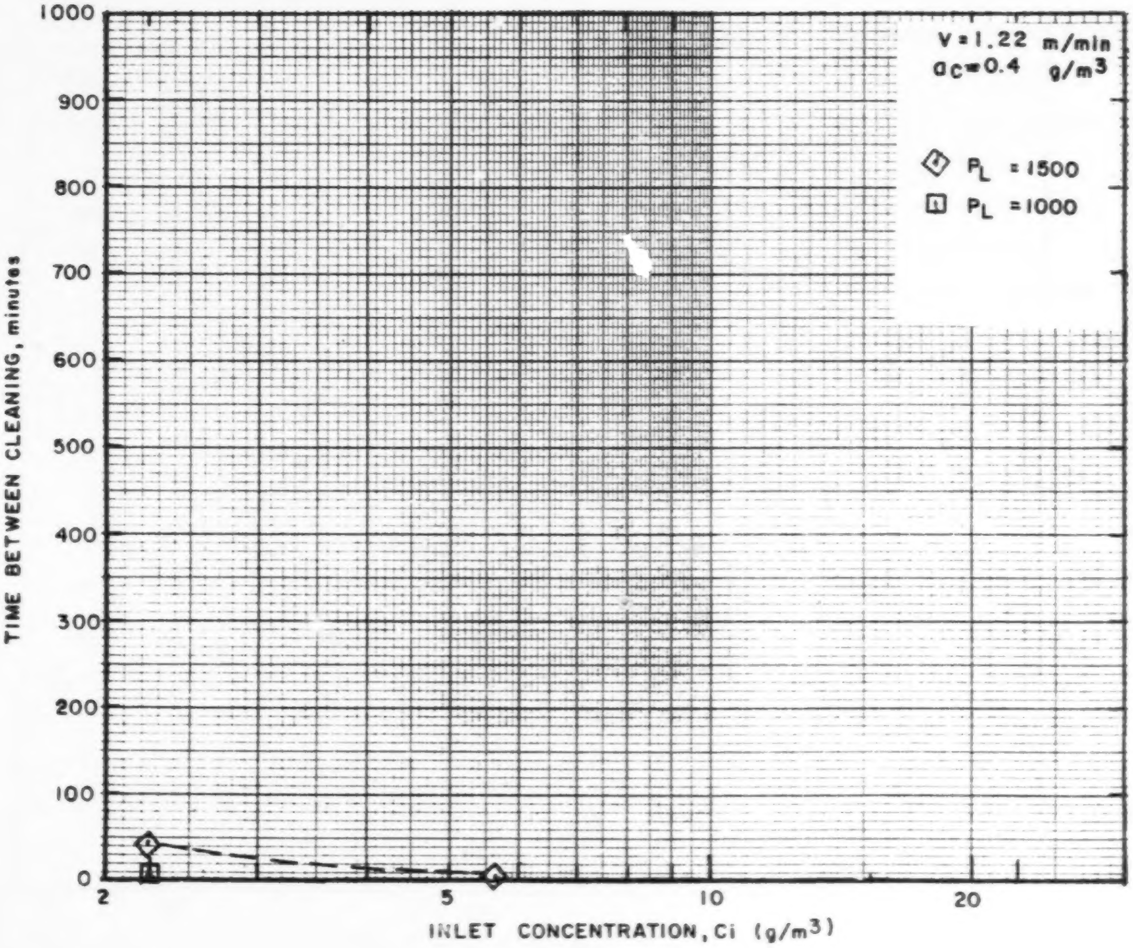

Figure 95. t_f versus C_i and P_L.

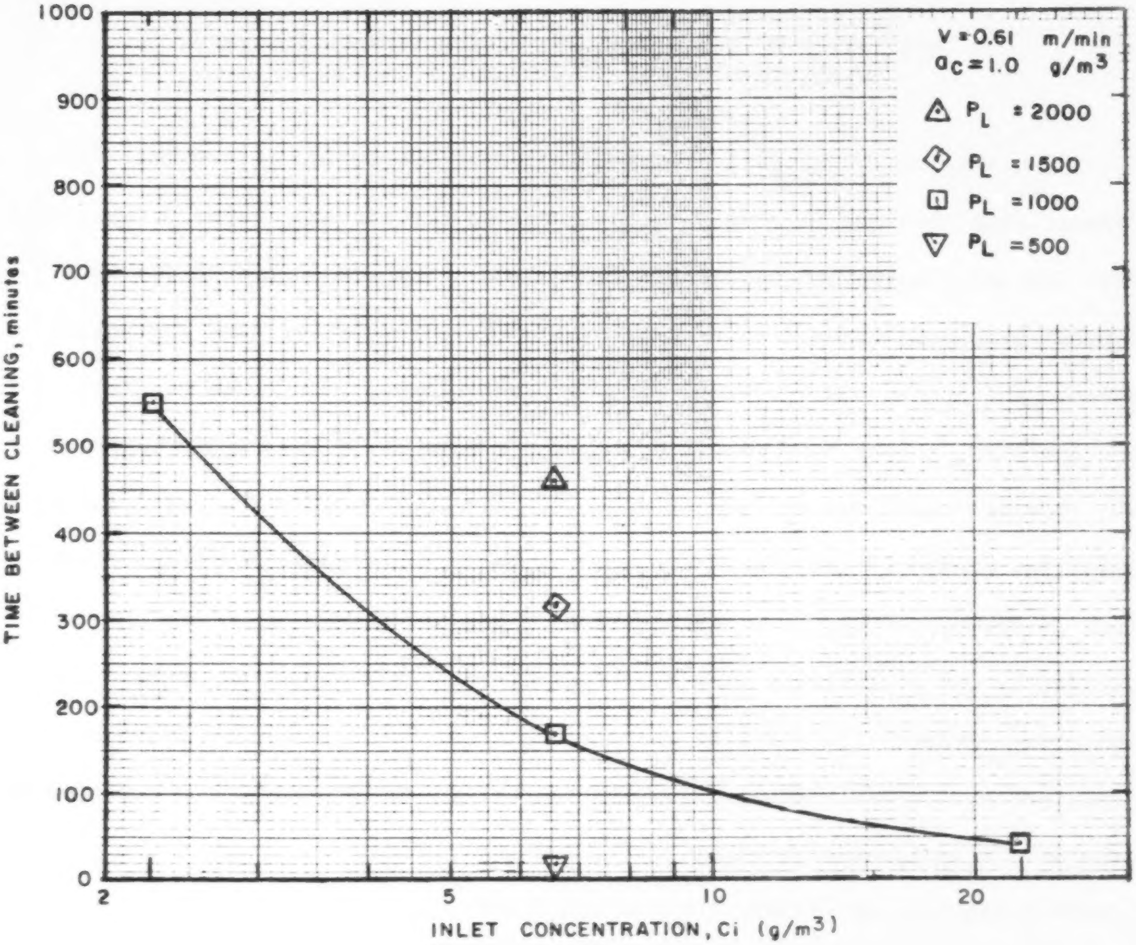

Figure 96. t_f versus C_i and P_L.

APPENDIX D

DERIVATION OF RELATIONSHIPS BETWEEN AVERAGE SYSTEM PRESSURE DROP AND SYSTEM DESIGN PARAMETERS

By examining the overall pressure drop characteristics of a fabric filter system, equations can be developed to correlate the average system pressure drop with the major operating and design parameters. Figures 97 and 98 represent typical pressure versus time traces for limiting pressure or time controlled systems and continuously cleaned systems, respectively. In order to simplify the analysis, a four compartment system was chosen for illustration purposes. The approach taken was to first resolve the total area under the curve for a specified pressure-time trace into several readily definable secondary areas such as deliniated by the bounding dotted lines. The area below the curve divided by the appropriate time differential then represents the average system operating pressure for the time range of interest. Since the two systems described here behave differently with respect to the pressure-time relationship, each one is analyzed separately.

LIMITING PRESSURE AND TIMED CYCLE SYSTEMS

The average pressure drop for the system conforming to Figure 97 can be expressed as:

$$\overline{P} = \sum_{i=1}^{n=8} a_i \Big/ t_c + t_f \qquad (40)$$

noting that t_c and t_f refer to the cleaning cycle and the noncleaning time intervals, respectively.

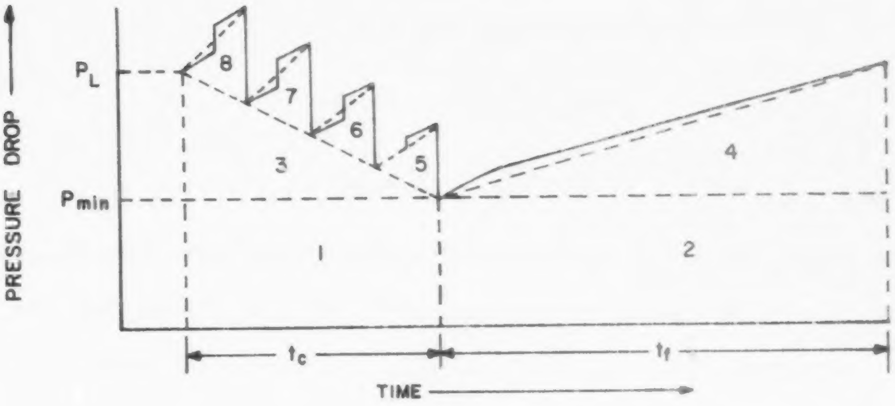
PRESSURE DROP
P_L
P_min
8
7
6
5
3
4
1
2
t_c
t_f
TIME

Figure 97. Example of pressure-time trace for limiting pressure or time controlled cleaning systems.

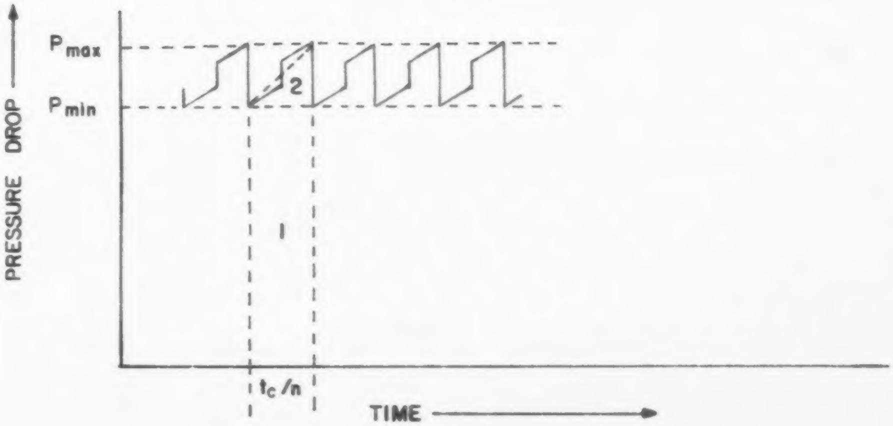
PRESSURE DROP
P_max
P_min
2
1
t_c /n
TIME

Figure 98. Example of pressure-time trace for continuously cleaned systems.

The area of sections 1 through 4

$$\Sigma\ a_1 + a_2 = P_{min}\ (t_f + t_c) \qquad (41)$$

$$a_3 = \frac{t_c}{2}\ (P_2 - P_{min}) \qquad (42)$$

$$a_4 = \frac{t_f}{2}\ (P_2 - P_{min}) \qquad (43)$$

If t_f is large, >2 hours, the assumption of a linear path from P_{min} to P_L will not cause a large error in the estimation of area 4 such that the Equation (43) approximation is acceptable. However, definition of areas 5 through 8 is more difficult since the dust loading distribution throughout the baghouse changes with time during the cleaning cycle.

To simplify the integration process for areas 5 through 8 it was first assumed that the area of each section could be approximated by a triangular element. It has been further assumed that each section (5 through 8) could be described by an average of the uppermost and lowermost areas; i.e., $(a_5 + a_8)/2$ in the present case. The base of the triangles (5 and 8) has been defined in terms of the pressure increase that takes place when any compartment is taken off line at any point during the cleaning cycle. The height of each triangle is the time interval required to clean each compartment, t_c/n.

For areas 5 and 8, respectively.

$$a_5 = \frac{t_c}{2n}\ \left[P_{min}\left(\frac{n}{n-1}\right) - P_{min}\right]$$

and

$$a_8 = \frac{t_c}{2n}\ \left[P_L\left(\frac{n}{n-1}\right) - P_L\right]$$

Thus the average area is estimated to be

$$a_{5-8} = \frac{t_c}{n(n-1)}\ \left(\frac{P_L + P_{min}}{4}\right)$$

and the total area for elements 5 through 8 becomes

$$\sum_{i=5}^{n=8\text{ to }8} a_i = \frac{t_c}{4(n-1)}\left(P_L + P_{min}\right) \qquad (44)$$

The combination of Equations (40) through (44) leads to the following expression for average pressure drop, $\bar{P}$

$$\bar{P} = 1/2\ \left(P_{min} + P_L\right)\left(1 + \frac{t_c}{2(n-1)t_c + t_f}\right) \qquad (45)$$

For any specified system design, the terms t_c and either t_f or P_L represent known quantities.

However, since a value for P_{min} will not be available, P_{min} must be defined in terms of the other system parameters. If the value for the average fabric dust loading in the baghouse is known at the point of minimum pressure loss, P_{min}, then P_{min} can be determined from:

$$P_{min} = S_E V + K_2\ W_{min} V \qquad (46)$$

The average fabric loading just after cleaning, W_{min}, can be estimated from a material balance over the cleaning cycle.

$$W_{min} = W_P' - a_c\ W_P' \qquad (47)$$

Since W_P' is the average loading during the cleaning cycle and a_c is the fractional area cleaned, the product of a_c and W_P' describes the amount of dust removed during the cleaning cycle. The average loading during cleaning can be estimated from:

$$W_P' = \frac{P_L - S_E V}{K_2 V} + \frac{C_i V t_c}{2} \qquad (48)$$

The first term on the right hand side of Equation (48) represents the average fabric loading (W_P') corresponding to a pressure level of P_L. The average amount of dust added during cleaning is represented by the second term.

Combining Equations (46) to (47) leads to the following equations for P_{min},

$$P_{min} = S_E V_i + (P_L - S_E V_i + C_i V_i^2 K_2 t_c/2)\ (1-a_c) \tag{49}$$

Depending upon the type of system (pressure or time controlled) either t_f or P_L will appear as known quantities. Since both terms appear in Equations (45) and (49), a relationship between P_L and t_f is required. A material balance over the filtration period results produces the following,

$$W_{min} + C_i V_i t_p = W_p \tag{50}$$

The term $C_i V_i t_f$ is the amount of dust added to the system over the filtration period. Thus the combination of Equations (47), (48) and (50) results in a relationship between t_f and P_L:

$$t_f = t_c\ (a_c - 1)/2 + \frac{a_c\ (P_L - S_E V_i)}{C_i K_2 V_i^2} \tag{51}$$

and rearranged:

$$P_L = \frac{K_2 C_i V_i^2}{a_c} \left| t_f + (1-a_c) t_c/2 \ + S_E V_i \right| \tag{52}$$

Since all critical parameters are now defined on the basis of known quantities, the relationship between average system pressure loss and the system's operating parameters can be developed by combining Equations (45) and (49):

$$\overline{P} = 1/2 \left[1 + \frac{1}{2(n-1)(1 + t_f/tc)} \right] \left[P_L(2-a_c) + a_c S_E V_i + (1-a_c) C_i K_2 V_i^2 t_c/2 \right] \tag{53}$$

The average pressure loss for limiting pressure systems can be estimated from Equations (51) and (53).

Timed cycle systems can be analyzed with Equations (52) and (53). Equation (51) can also serve to indicate whether or not a limiting pressure system must be in fact clean continuously. If the time between cleanings, t_f, reduces to zero then the system must clean continuously since the dust deposition rate is too high for pressure drops lower than P_L to be achieved.

CONTINUOUSLY CLEANED SYSTEMS

The approach to the analysis of continuously cleaned systems is similar to that used for limiting pressure systems. With reference to Figure 99 the average pressure drop is:

$$\overline{P} = \frac{a_1 + a_2}{t_c/n}$$

$$= \frac{P_{min} \times t_c/n + 1/2\ (P_{max} - P_{min})t_c/n}{t_c/n} \qquad (54)$$

$$= \frac{P_{max} + P_{min}}{2}$$

The area of section 2 has been approximated by a triangular section. If the increase in pressure due to added dust can be neglected over the time interval t_c/n then P_{min} and P_{max} can be related by:

$$P_{max} = \frac{n}{(n-1)}\ P_{min} \qquad (55)$$

Equation (55) describes the increase in pressure loss due to shifting the flow of n compartments through n-1 compartments when a compartment is taken off line for cleaning. A relationship for P_{min} can be found if the fabric loading distribution through the baghouse can be determined. The minimum and maximum average compartment loadings are related by:

$$W_{max} - a_c\ W_{max} = W_{min} \qquad (56)$$

and

$$W_{min} + C_i V_i t_c = W_{max} \qquad (57)$$

Equation (56) is basically a rearranged form of the relationship defining the fractional area cleaned, a_c.

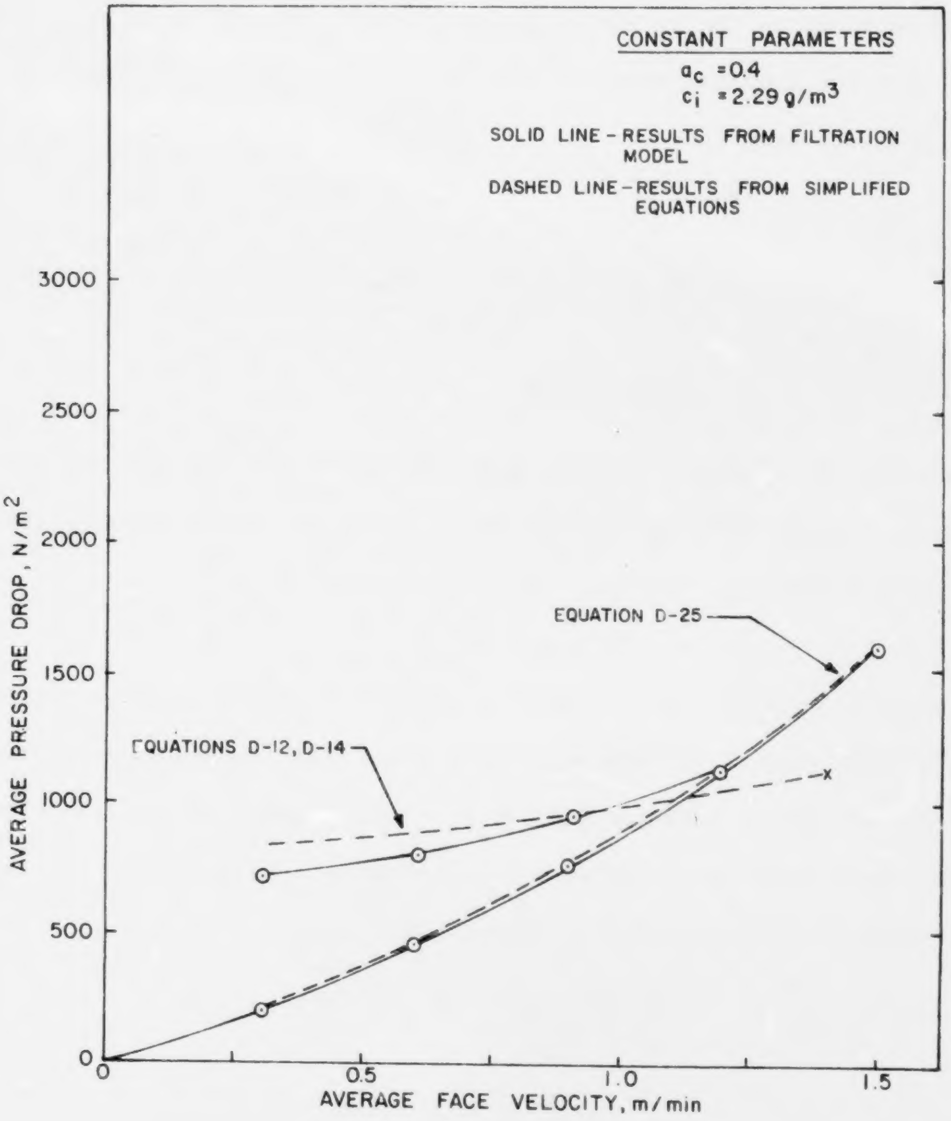

Figure 99. Estimation of average pressure drop by computer model and simplified equations.

Equation (57) describes the material balance in which the term $C_iV_it_c$ is the amount of dust added to the system during the cleaning cycle. The minimum and maximum loadings are therefore:

$$W_{min} = C_iV_it_c\ (1-a_c)/a_c \tag{58}$$

$$W_{max} = C_iV_it_c/a_c \tag{59}$$

An expression for the minimum pressure loss can now be determined by integrating the linear drag relationship over the loading distribution. If a linear loading distribution is assumed then loading varies as:

$$W = C_iV_it_c(1-a_c)/a_c + C_iV_it_c\ n/N_T \tag{60}$$

Where n denotes an arbitrary bag area and N_T is the total number of such areas on the bag surfaces. The overall system minimum drag, S_{min}, is calculated as:

$$\frac{1}{S_{min}} = \sum_{n=0}^{N_T} \frac{1/N_T}{S_E + K_2W_r} \tag{61}$$

If the loading distribution is treated as a continuous function, Equation (61) may be rewritten as,

$$\frac{1}{S_{min}} = \frac{1}{N_T} \int_{n=0}^{N_T} \frac{1}{S_E + K_2\ W} dn \tag{62}$$

Upon substituting Equation (60) for W in Equation (62) and integrating the following is obtained:

$$S_{min} = \frac{K_2C_iV_it_c}{\ln\left|1 + \dfrac{K_2C_iV_it_c}{S_E + K_2C_iV_it_c(1-a_c)/a_c}\right|} \tag{63}$$

Since $P_{min} = S_{min}\ V_i$, an expression for the average pressure loss can be obtained by combining Equations (54), (55) and (63) along with the relationship between pressure and drag.

$$\overline{P} = \frac{K_2 C_i V_i^{2} t_c \ (2n-1)(2n-2)}{\ln \left[1 + \dfrac{K_2 C_i V_i t_c}{S_E + K_2 C_i V_i t_c (1-a_c)/a_c} \right]} \tag{64}$$

Equations (51) and (40) and Equation (64) have been plotted in Figures 99, 100 and 101 for selected combinations of filter operating parameters. Also shown in the figures are the curves developed by the baghouse simulation program for the same operating parameters. The values of the parameters used in Equations (51), (53) and (64), other than those shown in Figures 99 through 101 are listed in Table 24.

TABLE 24. VALUES OF PARAMETERS USED TO GENERATE AVERAGE PRESSURE DROP VERSUS VELOCITY CURVES

Number of compartments, n = 10

Cleaning cycle time, t_c = 30 minutes

Specific resistance coefficient, K_2 = 1.322 N-min/g-m at 0.61 m/min, 150^{o}c

Effective residual drag, S_E = 529 N-min/m^3 at 150^{o}C

The specific resistance coefficient must also be corrected for velocity before entry into the equations.

With reference to Figure 99, the system described as $a_c = 0.4$ and $C_i = 2.29$, which is represented by the solid line, is the performance predicted by the baghouse model computer program. The dashed curves, which follow roughly the path of those predicted by the model were generated by Equations (51), (53) and (64). The curve predicted by Equations (51) and (53) extends beyond the lower continuous cleaning curve as indicated by the dotted line. The end point of the dotted curve is the point at which Equation (51) predicts a time between

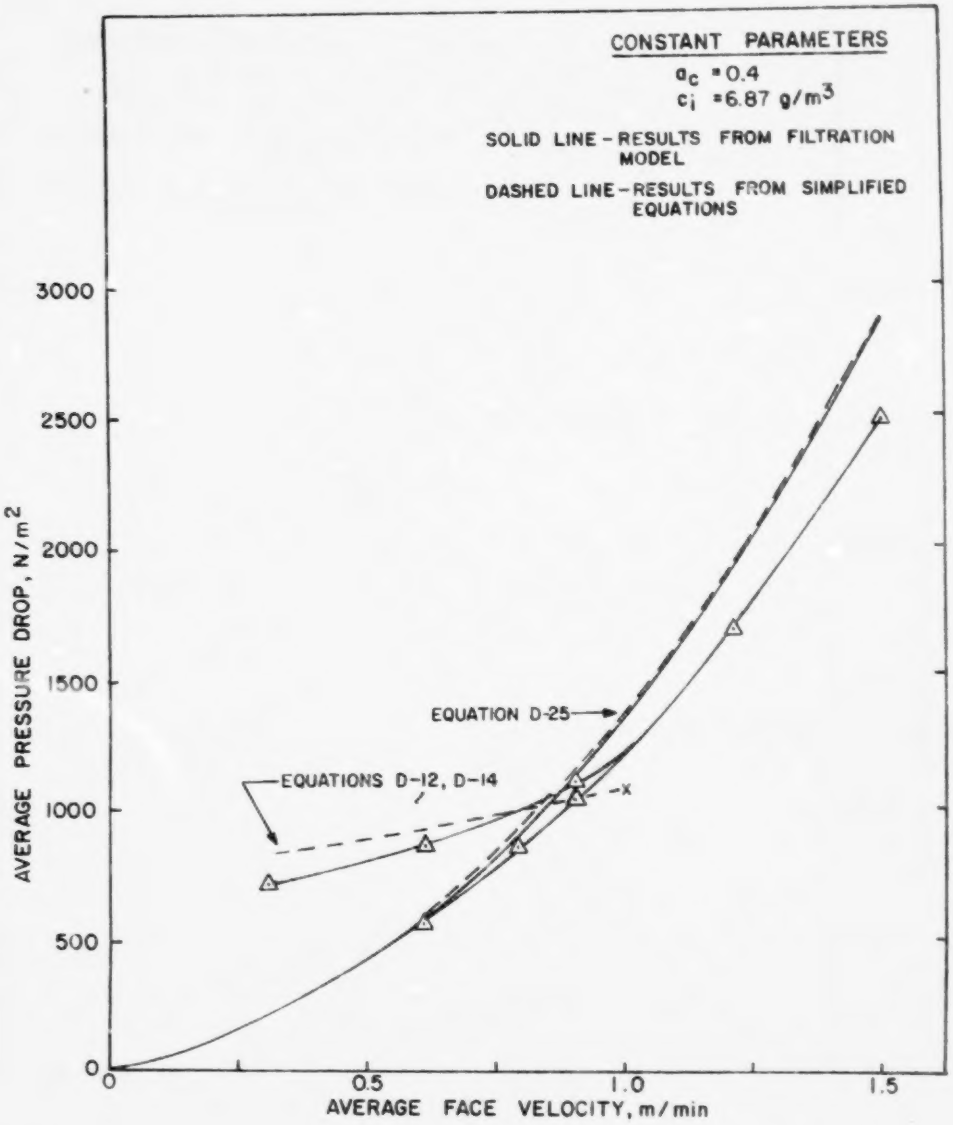

Figure 100. Estimation of average pressure drop by computer model and simplified equations.

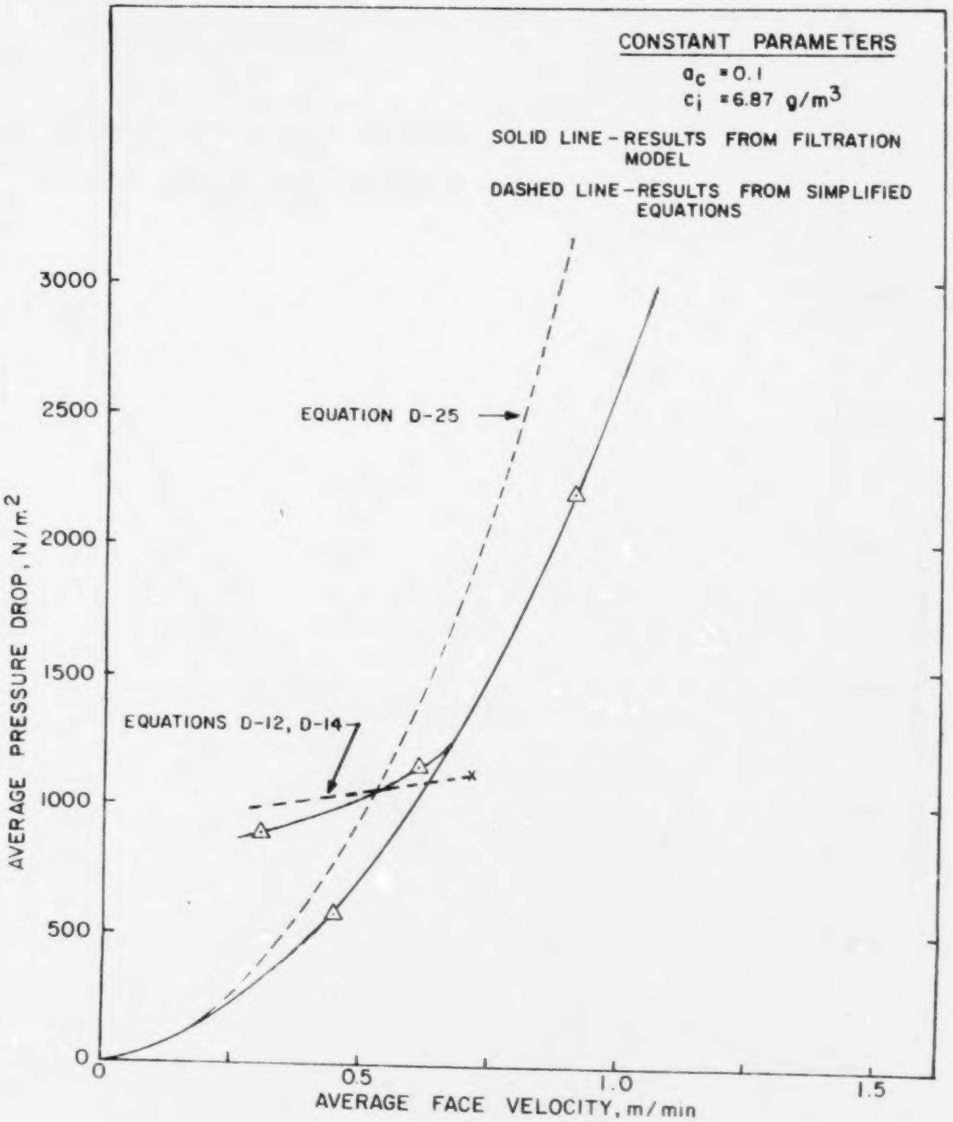

Figure 101. Estimation of average pressure drop by computer model and simplified equations.

cleanings, t_f, of zero. The actual intersection of the limiting pressure and continuous cleaning curves appears at a lower velocity, however. Performance as predicted from Equations (51) and (53) is not dependable at very low values of t_f, even though the error in pressure drop is less than about 30 percent. If the intersection of the limiting pressure and continuous cleaning curves is taken as the point of actual transition to continuous cleaning, however, then the differences in pressure drop as predicted by the model and the equations presented in this section become smaller and perhaps more flexible. Inspection of the remaining curves in Figures 99 through 101 suggests that the pressure loss estimates for the two approaches are in fair agreement considering the assumptions and simplifications used in the development of Equations (51), (53) and (64).

The equations should be used mainly to investigate the interrelationships between the various operating parameters and their combined effect on system pressure loss. The basic equations are amenable to solution by conventional pocket size calculators.